A METHODOLOGY FOR THE KINEMATIC DESIGN AND PERFORMANCE EVALUATION OF SERIAL MANIPULATORS

Farzam Ranjbaran

B.Eng. (University of Shiraz), 1986

M.A.Sc. (Concordia University), 1991

Department of Mechnical Engineering

McGill University

Montreal, Quebec, Canada

A thesis submitted to the Faculty of Graduate Studies and Research in partial fulfillment of the requirements for the degree of Doctor of Philosophy

April 1997

0-612-30367-5

Abstract

Kinematic design and performance evaluation of serial-type robotic manipulators is the main focus of this thesis with due attention being paid to redundant manipulators. The thesis provides a review of the existing contributions made to the subject, identifying those areas that can be advanced in depth or breadth and making theoretical contributions to some of these areas. The design, manufacturing and commissioning of a full-scale representative example of a redundant manipulator designed for *kinematic isotropy* is also discussed. Although various theoretical methods of analysis and characterization of the kinematic performance have been reported in the past two decades, the *kinematic architecture* of industrial manipulators has not changed very much. The design requirements for these manipulators, have been mostly driven by issues such as *kinematic simplicity* and *mechanical constructibility.* These criteria have thus led to the existence of a particular class of manipulators whose axes are either parallel or perpendicular, i.e., *orthogonal manipulators.*

It is believed that, in order to fully exploit the redundancy of the new generation of industrial manipulators, it is advantageous to consider general architectures. If improved kinematic performance can be achieved by examining novel manipulator architectures, then it becomes necessary to explore new design requirements. The aim of this thesis is to contribute to the above-mentioned exploration. In Chapter 2, the singularity and workspace of regional structures (i.e., three-axis manipulators) are discussed. Regional structures forming the positioning part of most industrial manipulators, they have been regarded as representatives of nonredundant manipulators.

Chapter 3 contains a detailed review of the proposed measures of dexterity together with an extensive discussion on the invariance properties of these indices. Chapter 4 is devoted to the investigation of the condition numbers of matrices in general, and of the Jacobian matrix of the robotic manipulators in particular. In Chapter 5, the isotropic design of redundant manipulators is discussed in detail whereby several isotropic seven-axis designs are introduced. Anthropomorphic requirements are also included where, it is shown that seven- and eight-axis manipulators cannot possess isotropy and anthropomorphism simultaneously. Optimum postures of hyperredundant manipulators are then investigated and finally, singularity distributions in the workspace of isotropic manipulators are compared to those of their nonisotropic counterparts. In Chapter 6, kinematic performance of serial manipulators is discussed from a geometric point of view. A novel measure of conditioning based on an index of isotropy, defined elsewhere, is examined in detail, and several interesting features of this measure are provided. With the aid of this measure, explicit expressions for the determination of the *characteristic length*, and the *characteristic point* are derived. In Chapter 7, the kinematic and mechanical design of a full-scale seven-axis isotropic manipulator called REDIESTRO 1 are introduced. REDIESTRO 1 was designed, manufactured and commissioned during the course of this thesis at the McGill Centre for Intelligent Machines (CIM) of McGill University.

Résumé

La conception et l'évaluation cinématiques de l'opération de manipulateurs *à chaîne cinématique ouverte simple* sont les principaux sujets abordés dans cette thèse, avec une attention particulière portée aux manipulateurs redondants. Cette thèse comporte un aperçu des contributions déjà apportées à ce domaine, identifie les sujets où de nouvelles avancées peuvent être faites, et apporte des contributions sur le plan théorique à certains d'entre eux. Finalement, la conception, la fabrication et la mise en opération d'un exemple grandeur nature d'un manipulateur redondant conçu avec une *cinématique isotrope* sont décrites. Bien que plusieurs méthodes théoriques d'analyse et de caractérisation de la performance cinématique aient été proposées depuis deux décennies, l'architecture cinématique des manipulateurs industriels disponibles n'a pas beaucoup changé. En effet, les contraintes de conception ont davantage été liées à la *simplicité cinématique* et à la *réalisation mécanique* de ces manipulateurs. Ces conditions ont donc mené à l'existence d'une classe particulière de manipulateurs dont les axes sont parallèles ou perpendiculaires, c.-à-d., des *manipulateurs orthogonaux*. Il est affirmé que, pour exploiter pleinement la redondance de la nouvelle génération de manipulateurs industriels, il est avantageux de porter attention à l'architecture générale. Si une performance accrue peut-être obtenue en utilisant des architectures différentes, il devient alors nécessaire de considérer de nouveaux critères de conception.

Dans le Chapitre 2, les singularités et l'espace de travail des manipulateurs à trois

axes sont examinés. Dans la plupart des cas, les trois premiers axes des manipulateurs industriels à poignet découplé servent à résoudre le problème du positionnement de l'organe terminal. Ces trois premiers axes peuvent donc être considérés comme exemples représentatifs de la classe des manipulateurs non-redondants. Le Chapitre 3 contient une revue détaillée des *mesures de dextérité* proposées ainsi qu'une discussion sur les propriétés *invariantes* de ces indices. Le Chapitre 4 fait l'étude du *facteur de conditionnement* des matrices en général, et de la matrice jacobienne des manipulateurs robotique en particulier. Dans le Chapitre 5, la conception de manipulateurs redondants *isotropes* est étudiée en détail et plusieurs exemples de robots isotropes à sept axes sont proposés. Des contraintes *anthropomorphiques* sont également incluses et il est montré que des manipulateurs à sept ou huit axes ne peuvent pas être isotropes et anthropomorphes simultanément. Ensuite, la posture optimale des manipulateurs *hyper-redondants* est étudiée et finalement, la distribution des singularités dans l'espace de travail des manipulateurs isotropes est comparée à celle de manipulateurs non-isotropes. Dans le Chapitre 6, la performance cinématique des manipulateurs à chaîne ouverte simple est étudiée d'un point de vue géométrique. Une nouvelle mesure du conditionnement basée sur un indice d'isotropie, défini ailleurs, est examinée en détail et plusieurs propriétés intéressantes de cette mesure sont présentées. Entre autre, cette mesure permet d'introduire les notions de *longueur* et de *point caracteristiques.* Dans le Chapitre 7, la conception cinématique et mécanique d'un manipulateur isotrope grandeur nature à sept axes nommé REDIESTRO 1 est présentée. REDIESTRO 1 a été conçu, construit et mis en opération dans le cadre de cette thèse au Centre McGill pour les Machines Intelligentes (CIM) à l'Université McGill.

Acknowledgements

I would like to express my most sincere appreciation for the academic supervision and professional guidance that my thesis adviser, Professor Jorge Angeles, has provided so generously over the course of my Ph. D. studies. Working with Professor Angeles has been, both a pleasure, and, an excellent source of experience for my academic and professional endeavours. Many others have helped me through many technical and emotional challenges that I faced while completing the thesis:

For the design and manufacturing of REDIESTRO 1, I would like to thank John Darcovich for creating the very useful Robot Visualisation System (RVS), which has been an essential tool for the kinematic design of REDIESTRO 1, as well as for other useful graphical renderings needed for my research. The valuable contributions made by Mr. Frank Bubic for the preliminary mechanical design of REDIESTRO 1 is also acknowledged. I would also like to thank Dr. Max A. González–Palacios for creating the three-dimensional CAD renderings of the link-subassemblies of REDIESTRO 1, as well as Karim Shafik for designing the DSP-based control hardware, software and data acquisition for the robot. The assistance provided by Remi Hasenohr a visiting student from Ecole Centrale de Lyon, for some of the detailed drawings of the robot is acknowledged. The skillful machining work of Mr. Fernand Picard of the Department of Mechanical Engineering at McGill University and of Mr. Serge Lemir, of the counterpart department at Ecole Polytechnique de Montréal, are highly appreciated.

For my theoretical research work, I would like to thank Professor Andres Kecskeméthy for the fruitful discussions on the subject of Chapter 6. The insight gained during discussions with Drs. Manfred Husty and John Lloyd also deserves due acknowledgement.

For the completion of the manuscript of the thesis, most thorough and valuable scrutiny of Prof. Angeles and his constructive comments are greatly appreciated. Many thanks also go to Noga Arenson for her help on the LaTeX compilation of the actuator specifications and to Yves Gonthier and Pierre Montagnier for the French translation of the abstract.

I would also like to thank my friends Mordechai Arenson, Ferhan Bulca, Kyung Sang Cho and Kourosh E. Zanganeh for their understanding and support. Other fellow students, friends and staff members of the McGill Centre for Intelligent Machines and the Department of Mechanical Engineering, particularly, Irene Cartier, and Barbara Whiston for their patience and assistance, are sincerely acknowledged. Finally, I would like to express my deepest gratitude to my family and friends, for their continuous encouragement and support during the difficult times, when the completion of the thesis seemed so distant.

Claim of Originality

The author claims the originality of the main ideas and research results presented in this thesis, the following being the most significant:

1. The characterization of the Cartesian and the joint space singularities of regional structures are presented, with the aid of the concept of *non-minimal realizations* of transfer functions of single-input/single-output (SISO) linear dynamical systems. The *uniqueness domains* of the forward kinematic maps are also discussed, and algebraic expressions that define these subregions of the manipulator joint-space are derived[1].
2. A CAD-based technique is introduced for the development of the three-dimensional graphical renderings of the Cartesian workspace.
3. With the aid of a theorem, it is shown that the class of *special* regional structures cannot change solution branches without crossing singularities.
4. Within the realm of kinematic design, comparison of singular- vs. nonsingular-posture-changing manipulators is discussed, whereby it is shown that the ability of a manipulator to change solution branch without crossing singularities is not necessarily an advantageous feature.
5. A detailed discussion on the *invariance* properties of different *dexterity measures* is provided.

[1]This methodology was independently proposed by Tsai et al., (1993) and Ranjbaran et al., (1994).

6. With the aid of a theorem, the necessary and sufficient conditions for the *isotropy* of a general rectangular matrix is presented.

7. Isotropic design of redundant manipulators is discussed in detail:

   - It is shown that isotropic seven-axis manipulators exist[2].

   - While incorporating other kinematic issues such as anthropomorphism, it is concluded that full isotropy and anthropomorphism cannot coexist for seven- and eight-axes manipulators, the latter requirements leading to *pseudoredundancy*. An illustrative example of a nine-axes robot that possesses both of the foregoing features is provided.

8. The optimum posture design of hyperredundant manipulators for isotropy is examined through an example of a 30-axis planar manipulator. It is shown that the isotropic configuration of this manipulator—to some extent—resembles a familiar posture of a cobra in an attack configuration.

9. A framework for the qualitative comparison of redundant manipulators is constructed. This framework is then utilized to compare isotropic and nonisotropic manipulators in the sense of the distribution of the singularities in their respective joint spaces. It is observed that the joint-space singularity distribution of isotropic architectures are *better* behaved than those associated with comparable nonisotropic designs.

10. A novel measure of conditioning for general matrices is introduced:

    - It is shown that this measure is a linear approximation of the normalized Frobenius-norm condition number, and, for quasiisotropic matrices, it provides a very close prediction of the condition number.

[2]Independently, Klein and Miklos (1991) also provided examples of such designs using a different approach

- For both rectangular, and square matrices, upper and lower bounds in terms of the F-norm and the 2-norm condition numbers are obtained for the proposed measure.

11. Based on this measure of conditioning, an index of manipulator conditioning is devised that is highly suited for the intended task of manipulator design.

12. Based on the differentiation of this index with respect to the normalizing length and the operation point of the end-effector, a preferred scale factor and a preferred operation point of the end-effector are obtained.

13. A full-scale seven-axis isotropic manipulator called REDIESTRO 1 was designed, manufactured and commissioned by the research work conducted under the scope of this thesis.

The above contributions have been reported partially in (Angeles et al., 1992), (Ranjbaran et al., 1992), (Tandirci et al., 1992), (González–Palacios et al., 1993), and (Ranjbaran et al., 1994; 1995; 1996).

Contents

List of Figures

List of Tables

Chapter 1

Introduction

1.1 Motivation

The mechanical performance of robotic manipulators has been the focus of extensive research work in the past two decades. Almost all of these efforts have focused on the kinematic performance or motion-transmission capabilities of mechanical manipulators and mechanisms at large. The kinetostatic duality has allowed researchers to quantify both motion- and force-transmission capabilities with a common merit figure called the *kinetostatic performance index* (IFToMM, 1991). The earliest considerations of the kinetostatic performance of mechanisms can be traced back to concepts such as the *indices of merits*, *mechanical advantage*, *pressure angle*, *transmission angle* or *angular velocity ratio*, (Shigley and Uicker, 1995). Dexterity and kinetostatic analyses of robotic manipulators is in a sense a generalization of these simple concepts in more complex settings.

Dexterity is defined by Webster as "readiness and grace in physical activity; esp: skill and ease in using the hands". This definition has thus been extended to characterize the kinematic performance of robotic manipulators, while concepts such as *service angle*, *dexterous workspace*, *dexterity measures*, *manipulability index*, *kinematic distortion*, and *measure of isotropy*, among others, have been proposed.

Notions such as *readiness*, *ease*, or *comfort* induce familiar senses in human perception. Extending these notions for characterization of the performance of mechanical devices, however, does not seem as immediate. Examples from natural articulated bodies can be found that to some extent validate the aforementioned extension. Considering the architecture of our limbs, the ratio between the length of the *humerus* (upper arm) to that of the *radius* (forearm) falls within the range of 70 to 80%. As a classical example, Leonardo Da Vinci being interested on the ratio of several parts of our limbs provided extensive anthropomorphic data, Fig. 1.1 (O'Malley and Saunders, 1983). Leonardo reported a value of five-sevenths or 71.4%, for the *radio-humerus* ratio. On the other hand, while performing manual tasks that require our

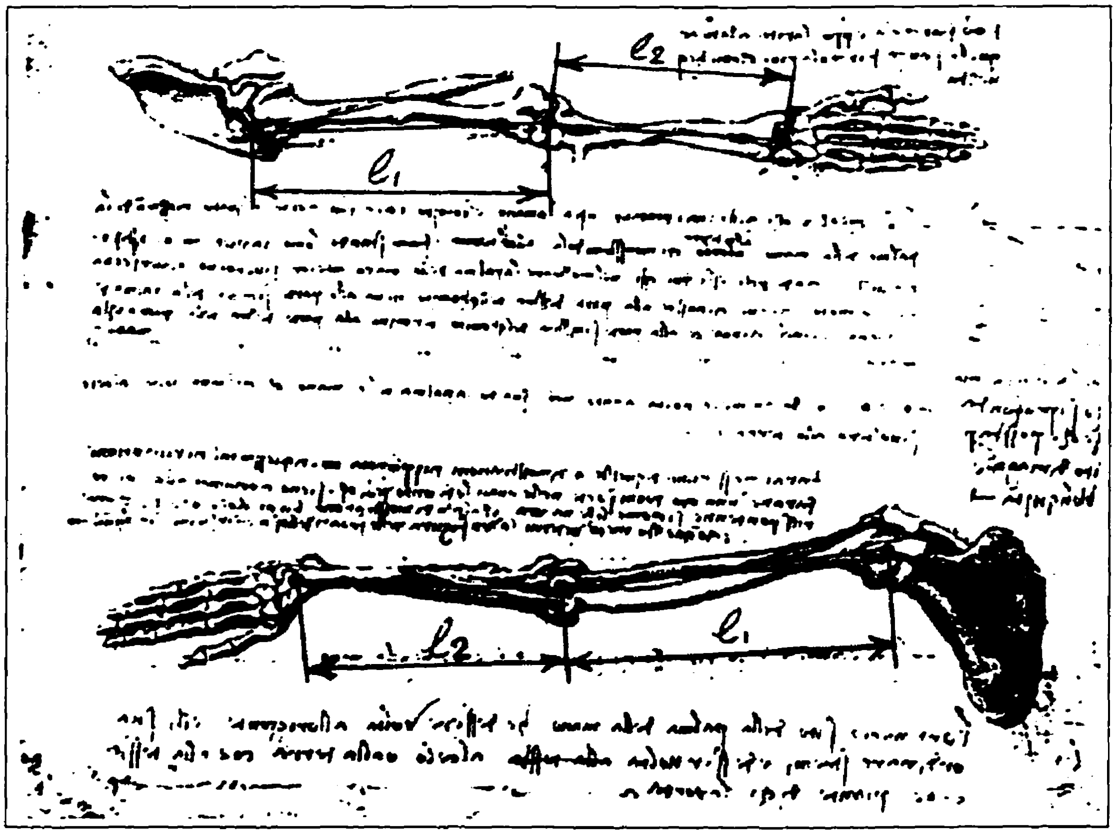

Figure 1.1: Leonardo's anthropomorphic data (O'Malley and Saunders, 1983)

highest dexterity, or similarly, while attaining *comfortable* configurations, the angle

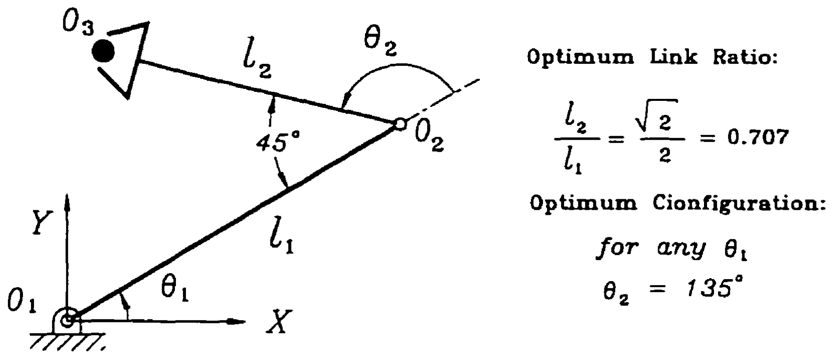

Figure 1.2: Optimum kinematic design of a 2-axis planar manipulator

made between our upper arm and our forearm tends to be an acute angle within 30 to 60 degrees. It is interesting to note that while designing planar two degrees of freedom fingers, Salisbury and Craig (1982) proposed the optimum solution shown in Fig. 1.2. The optimality criterion for this design is based on the *condition number* of the Jacobian matrix associated with the instantaneous kinematics of the manipulator. The link-length ratio for this optimum two-axis manipulator (as discussed in Chapter 4) is found to be $\sqrt{2}/2 = 0.7071$, which is not very different from Leonardo's *radio-humerus* ratio of 71.4%. Moreover, the optimum configuration of the mechanism is achieved when $\theta_2 = 45°$, i.e., the mid-range of 30° to 60°. Although this analogy is an interesting link from our familiar senses of comfort and dexterity to the characterization of the performance of mechanical manipulators, it is by no means intended here to over emphasize this similarity, for the evolution of the living articulated architectures lends itself to a spectrum of complex phenomena from different fields of science of which kinematics can only be one.

Motivated by these arguments, and by the curiosity for the existence of other natural analogies, we considered the shape of a cobra in its familiar ready-to-attack configuration. The closest candidate from mechanical manipulators to stand the comparison is the class of *hyper-redundant* or *snake-like* manipulators. As discussed in detail in

Chapter 5, an optimum configuration of a 30-jointed hyper-redundant planar manipulator based on the same optimality criterion of kinematic dexterity plus additional smoothness requirements gives rise to a solution illustrated in Fig. 1.3 (see Chapter 5 for details).

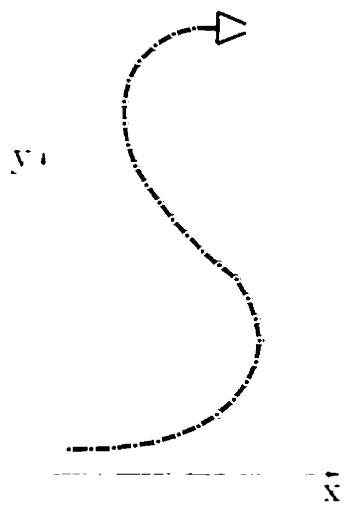

Figure 1.3: A 30-axis planar manipulator at an optimum configuration

The characterization of the performance of serial-type robotic manipulators in the sense of kinematic dexterity is the main focus of this thesis. This characterization is aimed at providing a review of the existing contributions made to subject, identifying those areas that can be advanced in depth or breath, making theoretical contributions to some of these areas, and, finally, to implementing a full-scale representative example of a manipulator designed for dexterity, specifically for kinematic isotropy.

1.2 General Background

Throughout the thesis several references are made to the notions of *manipulator architecture*, *manipulator posture*, *end-effector (EE) pose*, and *kinematic design*. The definition of these concepts, as used in the thesis, are provided below:

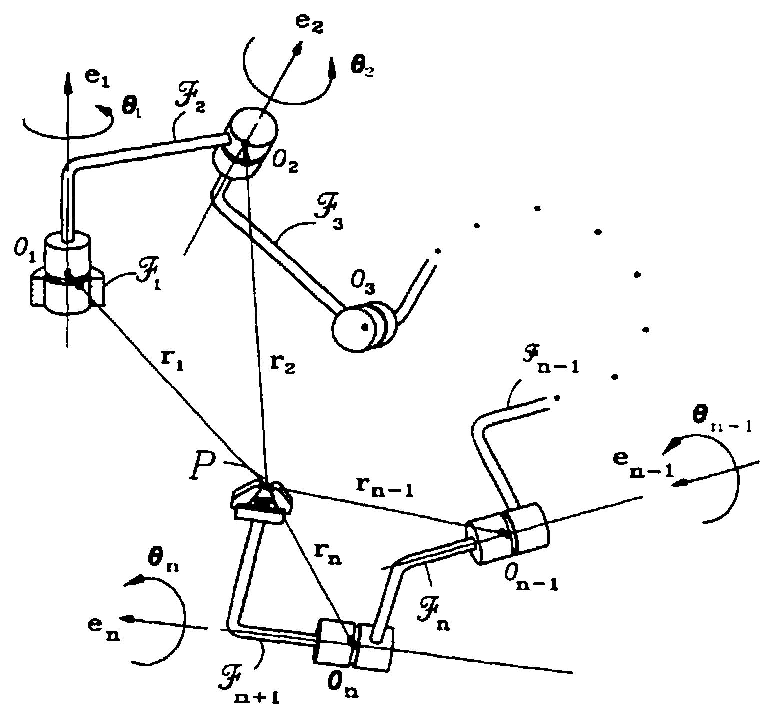

Figure 1.4: An n-revolute jointed manipulator.

- **Manipulator Architecture and Manipulator Posture** (Angeles, 1997): An n-axis manipulator has n joint variables, which are grouped in the n-dimensional vector $\boldsymbol{\theta}$, regardless of whether the joints are revolute or prismatic, and $3n$ constant parameters that define the relative position and orientation of the two joint-axes attached to a link. The latter define *architecture* of the manipulator, while the former determine its *configuration* or *posture*. Fig. 1.4 illustrates an n-axis revolute-jointed manipulator.

For the sake of completeness the definition of the Denavit and Hartenberg (DH) parameters (Denavit and Hartenberg, 1955) are provided next, as illustrated in Fig. 1.5.

Links are numbered 0, 1, ..., n, the ith pair being defined as that coupling the $(i-1)$st with the ith link, with link 0 being the fixed base. The end-effector (EE) is attached to the nth link, whose *operation point* is denoted by P. Next, a coordinate

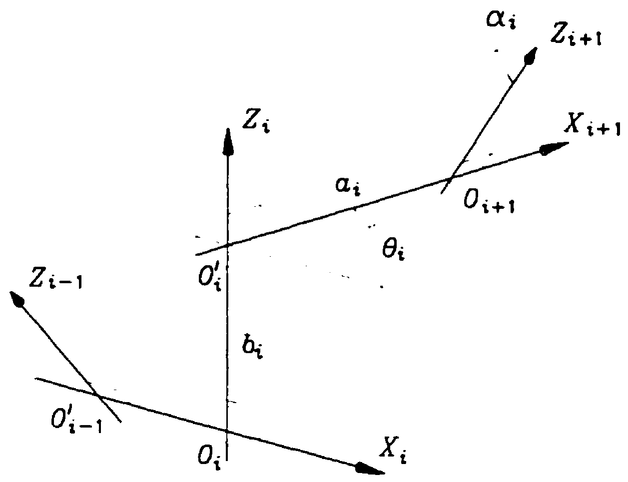

Figure 1.5: Denavit and Hartenberg parameters representation

frame is defined with origin O_i and axes X_i, Y_i, Z_i, which is attached to the $(i-1)$st link, for $i = 1, \ldots, n+1$. Furthermore, Z_i is the axis of the ith pair, X_i is defined as the common perpendicular to Z_{i-1} and Z_i, directed from the former to the latter. Moreover, the *distance* between Z_i and Z_{i+1} is defined as a_i, which is, thus, *nonnegative*. The Z_i-coordinate of the intersection O'_i of Z_i with X_{i+1} is denoted by b_i, its absolute value being the distance between X_i and X_{i+1}. The *twist angle* α_i, is the angle between Z_i and Z_{i+1} and is measured about the positive direction of X_{i+1}. Finally, θ_i is the angle between X_i and X_{i+1} and is measured about the positive direction of Z_i.

Having specified the four parameters defining each link-frame and its connection to the neighbouring ones, the position and orientation of the two consecutive frames i and $i+1$ expressed in frame i are determined from the position vector $\mathbf{a}_i$ and the rotation matrix $\mathbf{Q}_i$ as shown below:

$$\mathbf{Q}_i = \begin{bmatrix} \cos\theta_i & -\sin\theta_i \cos\alpha_i & \sin\theta_i \sin\alpha_i \\ \sin\theta_i & \cos\theta_i \cos\alpha_i & -\cos\theta_i \sin\alpha_i \\ 0 & \sin\alpha_i & \cos\alpha_i \end{bmatrix} \quad \mathbf{a}_i = \begin{bmatrix} a_i \cos\theta_i \\ a_i \sin\theta_i \\ b_i \end{bmatrix} \tag{1.1}$$

- **End-Effector Pose:** The position and orientation of the coordinate frame attached to the last link of the manipulator in the Cartesian space.
- **Kinematic Design:** Selection of the manipulator architecture.
- **Configuration Design:** Selection of the manipulator posture.

1.3 Literature Survey

1.3.1 Singularity and Workspace Analyses

Workspace and singularity analyses of robotic manipulators have been the focus of intense work in the past decade. The determination of the workspace of a general n-axis manipulator in its space of Cartesian coordinates is a formidable task, for it amounts to representing a hypersurface embedded in a six-dimensional space, studies so far having focused only on three-axis manipulators for either positioning (regional structures), e.g. (Spanos and Kohli, 1985), or orienting tasks, e.g. (Angeles, 1988; Lin and Tsai, 1991). Since a wrist-partitioned manipulator (most of the industrial manipulators in use today are wrist-partitioned) is the concatenation of a three-axis arm, i.e., *the regional structure*, and a spherical wrist that is attached to the terminal link of the arm, the workspace analysis of such manipulators can be performed by considering the positioning and orienting singularities separately.

All of the contributions made in this regard are oriented along two main tracks.

a) Determination of the workspace boundaries in the Cartesian space associated with the location of the end-effector (EE), (Spanos and Kohli, 1985; Hsu and Kohli, 1987a, 1987b; Smith, 1990; Smith and Lipkin, 1993; Ranjbaran et al., 1992). Among these contributions, only a few works include explicit algebraic expressions defining the workspace boundaries. Kohli and Hsu (1987a and b), for example, give an extensive categorization of different types of regional structures, and expressions for some examples. Also, in Ranjbaran et al. (1992), a general expression defining the singularities of the *quartic closure polynomial* that relates the Cartesian coordinates of the end-effector to one of the joint angles is derived. Smith and Lipkin (1993) obtained expressions for the foregoing surfaces through the use of conic sections. In general these expressions are of a high degree in the Cartesian coordinates of the EE. They are convenient, however, in that they can be used to trace the intersection of the workspace boundaries and any arbitrary plane cutting it. Recently, Ceccarelli (1994a, 1995, and 1996) extended the analysis and synthesis of the workspace boundaries of serial manipulators to four-, five-, and N-axis architectures, while employing toroidal geometries and the resulting envelopes when rotating a toroidal surface about a given axis.

b) Singularity analysis of the kinematic maps in the joint space using invariants of the Jacobian matrix (Borrel and Liégeois, 1986; Oblak and Kohli, 1988; Burdick, 1988; Pai and Leu, 1989; 1992; Tsai et al., 1993; Burdick, 1991; 1992; 1995; Wenger, 1992; 1996). Most of these works approach the problem by deriving a condition on the singularity of the associated Jacobian matrix. Since this matrix is an explicit function of the joint coordinates, the aforementioned condition is usually derived in the joint-coordinate space. In recent years, the behaviour of the direct kinematic maps and their singularities have been discussed with powerful tools of differential topology, e.g., Burdick (1995). The direct kinematics of the manipulators are thus regarded as smooth *manifold mappings* from the joint space to the Cartesian space. Furthermore, in Pai and Leu (1989; 1992), the concepts of *genericity* and *non-genericity* of general maps between smooth manifolds are applied to the direct kinematic maps of robotic manipulators, and thus, the notions of generic and non-generic manipulators are introduced. A more detailed investigation of genericity of the kinematic maps for three-, six-, and seven-degree-of-freedom manipulators are given in Tsai et al. (1993), where a closed form genericity test for the regional structures is derived.

As suggested by Burdick (1991), regions free of singularities in the joint space, called the *c-sheets* according to Burdick, or *aspects* according to Borrel and Liégeois

(1986), do not partition this space into the uniqueness domain of the kinematic maps. In other words, it is possible to find two inverse kinematic solutions for the same end-effector pose that lie in the same aspect. This enables the manipulator to change solution branch or posture without passing through singularities.

Wenger (1992) first introduced a method for obtaining the separating surfaces in an aspect that indeed divide the corresponding aspect into sub-regions where the kinematic map is one-to-one and onto (bijection). This gave rise to the definitions of *characteristic surfaces* and *basic components*. The characterization of the singularities of *generic* regional structures based on *homotopy classes* are further discussed in Wenger (1996).

1.3.2 Kinematic Performance

As one of the first efforts to measure the kinematic performance of manipulators, Vinogradov et al. (1971) proposed the *service angle*, as the range of joint angles allowing the end-effector to reach a specified point in space. Roth (1975) analyzed the performance of manipulators in terms of their constitutive geometries, and introduced the notions of *approach angle*, *working space*, or *zones of operation*, and coupling between position and orientation of the end-effector. Throughout the decade that followed, most of the research effort in the performance analysis of manipulators focused on the analysis and evaluation of the *reachable* and *dexterous* workspaces of serial-type manipulators, e.g., Kumar and Waldron (1981), Gupta and Roth (1982), Lee and Yang (1983), Tsai and Soni (1981), Tsai and Soni (1983), and Yang and Lai (1985).

Salisbury and Craig (1982) introduced the *condition number* of the Jacobian matrix $\mathbf{J}$, $\kappa(\mathbf{J})$ as a measure of the kinetostatic performance of a manipulator. Later on, the *manipulability* index $\mu(\mathbf{J})$ was defined, as a measure of the kinetostatic performance by Yoshikawa, as the square root of the determinant of the product of the Jacobian by its transpose (Yoshikawa, 1985). During the past ten years, different local and global dexterity measures for the kinematic design and analysis of manipulators have been proposed. Klein and Blaho (1987) related the kinematic performance to the minimum singular value σ_{min} of the Jacobian as a measure of the distance to singularities. The optimum kinematic design of 6R manipulators with given *manipulator-lengths*, for *work-volume* and *well-connectedness* of this volume was discussed by Paden and Sastry (1988). The notion of work-volume used by Paden and Sastry is intermediate between those of the *reachable* and *dextrous* workspaces. It is based on the translation-invariant volume form on the group of all rigid body motions SE(3), i.e., it is equivalent to the *volume* of the image of the underlying joint space under its forward kinematic map. In Angeles and López-Cajún (1988, 1993), a dexterity measure based on the reciprocal of the condition number was proposed, while Gosselin and Angeles (1991), proposed a global dexterity measure by integrating the variation of the reciprocal of the condition number throughout the workspace. Kinematic dexterity and *workspace volume* of robotic manipulators were discussed by Park (1991) and by Park and Brockett (1994) using *harmonic mapping theory* to introduce the notion of *kinematic distortion* as a means of quantifying dexterity. The workspace volume considered in the latter reference is based on Paden and Sastry's translation-invariant volume form on SE(3). Motion capabilities of rigid bodies attached to the end-effector of serial manipulators were quantified using the Euclidean group of rigid-body motions and its semi-Riemannian structures by Basavaraj and Duffy (1993). With the aid of the weighted distribution of the end-effector pose over the workspace, while employing probabilistic models, Singh and Rastegar (1995) discussed the global motion capabilities or the velocity-transmission characteristics of manipulators. While discussing the optimal synthesis of the three-axis manipulators, Ceccarelli (1994b) employed the sequential quadratic programming technique for optimizing the manipulator architecture based on the notion of *minimum size encumbrance* while satisfying constraints on the workspace volume.

The kinetostatic performance of tendon-driven manipulators have been discussed by Ou and Tsai (1993;1994). In these papers the effects of pulley size and routings on the kinetostatic performance of the manipulators are discussed whereby the notion of *isotropic transmission characteristics* is defined.

Recently, while analyzing *hybrid motion-and-force* control strategies, Goldenberg (1996) proposed a kinematic optimality condition for manipulators that enhances the force-and-motion couplings. This criterion simply reflects the ability of a manipulator to take on a posture at which the product of the associated Jacobian matrix by its transpose becomes a scalar multiple of the identity matrix. Although in the context of hybrid control the latter condition was found rather novel, in kinematic analysis and optimum kinematic design, however, this criterion has been referred to as the *kinematic isotropy* for a quite a few years. The effects of *actuation-schemes* of manipulators are discussed in Maton and Roth (1996). In this paper it is shown that whether the actuators are placed on the base or locally on the corresponding link, the kinematic performance of the manipulator is affected. Based on this observation a methodology is introduced for determining the optimal placement of the actuators, while concluding that placing the actuators on the base is more advantageous in terms of kinematic dexterity.

The sensitivity and robustness of the redundancy resolution schemes are also discussed in Arenson (1997), where different types of error amplifications that present themselves in the Cartesian-space tracking capabilities of the redundant manipulators are investigated through numerical examples. Moreover, a theoretical framework is introduced in Angeles et al. (1996), where the overall sensitivity of the posture of redundant manipulators with respect to the Cartesian-space trajectory changes is divided into two parts, namely, a *primary* and a *secondary* sensitivities. It is shown in this reference that the primary sensitivity that has to do with the architectural design of the manipulator is a function of the condition number of the Jacobian matrix divided by the norm of the said matrix, while the secondary matrix that has to do with the type of secondary task augmented to the primary task of following the desired trajectory, is always equal to the identity.

1.3.3 Kinematic Design

In the design of industrial serial-type manipulators only a few simplifying kinematic criteria have been considered. For nonredundant manipulators, the kinematic design has been mainly oriented towards achieving *kinematic solvability* and *manufacturing feasibility*. These criteria, in turn, have led to the existence of a particular class of manipulators whose axes are either parallel or perpendicular, i.e., orthogonal manipulators. Here, we mean by orthogonal a manipulator whose consecutive axes make angles that are multiples of 90°; for example, manipulators with spherical wrists (Pieper, 1968), or with planar two-revolute sub-chains pertain to this class. Moreover, a general classification of manipulators with simple inverse kinematics is reported in Mavroidis and Roth (1992). The associated simple inverse kinematics has been formulated by exploiting the special features, like orthogonality, of the kinematic structures of these robots. With the advent of fast and general inverse kinematics algorithms developed in the last ten years, the need for simple kinematic structures is less critical. On the other hand, parallelism and orthogonality of the axes can give rise to undesirable singularities. These singularities are manifested, for example in the rate control and kinematic calibration of these manipulators (Hayati, 1985; Bennett et al., 1992). Serving the two foregoing objectives excludes a major class of manipulators with general architectures. By exploring general manipulator architectures, one can not only improve the numerical conditioning of the manipulator kinetostatic maps, but also take into consideration other critical issues pertinent to the design and realization of the overall robotic system. Some researchers have emphasized the methodologies for the design of redundant manipulators for specific tasks or classes of tasks. In this regard, the framework of *task-based design* for *reconfigurable modular manipulators* has been introduced (Kim and Khosla, 1992a–c).

1.4 Thesis Overview

The thesis consists of seven chapters, as per the summary given given below:

1.4.1 Chapter 2: Singularity and Workspace Analyses

Two novel methods for the analysis and characterization of the singularities of serial manipulators are presented. The numerical examples provided are three-axis revolute-jointed manipulators, *regional structures.* First, the workspace boundaries are determined directly in the Cartesian space by resorting to the concept of *non-minimal realizations* of transfer functions of single-input/single-output (SISO) linear dynamical systems.

The characterization of the manipulator singularities both in the joint space and in the Cartesian space is also discussed, with the aim of determining the *uniqueness domain* of the forward kinematic maps. Here, by uniqueness domain we mean all subsets of the joint space over which the forward kinematic map is a diffeomorphism, i.e., where for each end-effector pose there is a unique inverse kinematic solution. We present an algebraic expression that defines all of the separating surfaces of the joint space for general regional structures. Furthermore, the kinematic design of regional structures in relation to *singular-* vs. *nonsingular-posture changing* architectures are discussed. A comparison of the two foregoing types of regional structures in terms of trajectory following capabilities are also discussed.

1.4.2 Chapter 3: Measuring Manipulator Dexterity

The *kinematic dexterity* of robotic manipulators is discussed and comparisons are made among different measures proposed in the past. Since the centrepiece of almost all performance measures are based on the manipulator Jacobian matrix, some features of this matrix, as applied to kinematic dexterity and workspace analysis, are discussed as well. With the aid of illustrative examples, the effects of the numerical conditioning of a matrix on the amount of error magnification upon solving an associated linear system of equations is discussed. Furthermore, the invariance properties of dexterity measures with respect to the physical units and base-and-end-effector coordinate frames is also discussed in detail.

1.4.3 Chapter 4: Condition Number as a Measure of Kinetostatic Performance

A review of some of the theoretical aspects of the theory of condition in general is included. The condition number of the Jacobian matrix as applied to manipulator dexterity assessments will then be discussed, where the two related issues of characterizing *distance to singularities* and *sensitivity of linear systems to perturbations* are given due attention. The notion of isotropic transformations and isotropic manipulators will also be reviewed, followed by a geometric interpretation of isotropy. In the last three sections of the chapter, the isotropic design of nonredundant manipulators is discussed, and some of the contributions of the thesis are introduced.

1.4.4 Chapter 5: Isotropic Design of Redundant Manipulators

The kinematic design of redundant manipulators is addressed in this chapter, the focus being the optimization of the kinematic conditioning of the manipulators of interest. It is shown in this chapter that isotropic seven-axis manipulators are possible, and structural considerations pertaining to the design of such manipulators are then discussed, while providing several illustrative examples. Kinematic isotropy is then combined with *anthropomorphic* considerations to serve the overall design requirements. It will be shown that, in principle, isotropy and anthropomorphism for seven-axis designs cannot coexist. This becomes apparent as the incorporation of anthropomorphic criteria leads to architectures whose redundancies are rather *limited* in the sense that the overall mobility of the arm is severely impaired if one of the joints is locked. In this regard the notion of *pseudoredundancy* is discussed extensively. A nine-axis isotropic design is then discussed in an attempt to combine isotropy and anthropomorphism. The isotropic design of hyperredundant planar manipulators is then discussed, whereby a 30-axis example of such designs is studied. Finally, comparative studies between isotropic and nonisotropic manipulators in the sense of workspace singularity distributions are conducted.

1.4.5 Chapter 6: A Geometric Analysis of Kinematic Isotropy

The kinematic conditioning and dexterity of general revolute-jointed manipulators are discussed from a geometric point of view. A novel measure of conditioning for general matrices is introduced. It is shown that this measure is a linear approximation to the normalized-Frobenius norm condition number and, for quasiisotropic matrices, it provides a very close prediction of the condition number. For both rectangular and square matrices, upper and lower bounds are obtained for this measure in terms of the F-norm and the 2-norm condition numbers. Based on this measure of conditioning, an index of manipulator conditioning is devised that is highly suited for the intended task of manipulator design. Moreover, this performance index is substantially less expensive to compute than other measures of kinematic conditioning, and is amenable to differentiation. Based on the differentiation of this index with respect to the normalizing length and the operation point of the end-effector, a natural scale factor and characteristic point of the end-effector are obtained. In this regard, the notions of *manipulator layout*, *layout conditioning*, *layout length* and *layout centre*, for any serial-type robotic manipulators, are introduced. Furthermore, the characteristic layout of manipulators is discussed followed by the definition of the manipulator characteristic length and characteristic point.

1.4.6 Chapter 7: REDIESTRO 1

An overview of the design and manufacturing of a redundant seven-axis manipulator with an isotropic architecture for six-dimensional Cartesian tasks is presented. This manipulator, called REDIESTRO 1, was designed, manufactured and commissioned during the course of this research at the McGill Centre for Intelligent Machines. Since its completion in 1994, REDIESTRO 1 has been serving as an experimental device for several robotics-related projects both internally in the Department of Mechanical Engineering of McGill University and in collaboration with external research groups. The base-line kinematic design of REDIESTRO 1 stems from the results discussed in Chapter 5. The design, methodology, kinematic design and mechanical design of the manipulator are reviewed and mechanical specifications of the robot are outlined.

1.4.7 Chapter 8: Concluding Remarks

A summary of the thesis is provided here, while highlighting its main contributions.

Chapter 2

Singularity and Workspace Analyses

2.1 Introduction

While characterizing the performance of robotic manipulators, workspace boundaries and singularities are of primary importance. An immense amount of research work has been reported in the past two decades, giving rise to many different concepts, approaches and techniques for the analysis of manipulator singularities and workspace. In this chapter two novel methods for the analysis and characterization of the singularities of serial manipulators are introduced. In Section 2 we deal with the representation of the workspace boundaries directly in the Cartesian space by resorting to the concept of *nonminimal realizations* of transfer functions of single-input/single-output (SISO) linear dynamical systems (Ranjbaran et al., 1992).

In Section 3, the characterization of the manipulator singularities both in the joint and the Cartesian spaces is discussed with the aim of determining the *uniqueness domain* of the forward kinematic maps. Here, by uniqueness domain we mean all subsets of the joint space over which the forward kinematic map is a diffeomorphism, i.e., where for each end-effector position there is a unique inverse kinematic solution.

We introduce an algebraic expression that defines all the separating surfaces of the joint space for general regional structures. It is believed that this result was presented for the first time in Tsai et al. (1993) and, independently, in Ranjbaran and Angeles (1994).

In Section 4, the kinematic design of regional structures in relation to *singular-* vs. *nonsingular posture-changing* architectures are discussed. A comparison of the two foregoing types of regional structures in terms of the trajectory-following capabilities are also discussed.

2.2 Cartesian-Space Singularity Analysis and Transfer Function Realization

The singularities of a manipulator can be characterized both in the joint and in the Cartesian spaces. While joint-space singularities can be readily obtained by determining the singularities of the Jacobian matrix, the Cartesian space counterpart requires analysis of the inverse kinematic functions and the way they map subsets of the Cartesian space into disjoined regions in the joint space. Tsai et al. (1993) provide a complete review of the recent developments of the singularity analysis of general manipulators.

2.2.1 Formulation

Kohli and Spanos (1985a, b) showed that singularity manifolds in the Cartesian space can be obtained by equating the discriminant of the inverse kinematic polynomial to zero. Moreover, Kohli and Hsu (1987) showed that a Jacobian singularity occurs if and only if at least two solutions of the inverse kinematics are equal. In this section we propose an alternative method for determining the singularity surfaces in the Cartesian space of the manipulator, where the inverse kinematic polynomial admits multiple roots. The proposed technique can be applied to general manipulators; if the input-output polynomial of the manipulator is available to illustrate this method, we will apply it to three-axis positioning manipulators or regional structures.

For a general 3-R manipulator, the closure polynomial is quartic (Takano, 1985). Moreover, the coefficients of this polynomial are functions of the Denavit-Hartenberg (DH) parameters (Denavit and Hartenberg, 1955) and the Cartesian coordinates of the EE. We aim at finding the boundaries of the workspace of 3-R manipulators by relating the characteristic polynomial $P_4(t)$ (Angeles, 1997) with its derivative with respect to $t \equiv \tan\theta_3/2$, $P_4'(t)$, where

$$P_4(t) = at^4 + bt^3 + ct^2 + dt + e \tag{2.1}$$

The coefficients of $P_4(t)$ are all functions of the manipulator architecture and the Cartesian coordinates of the endpoint of its third link, the inverse kinematics solutions $\{t_i\}_1^4$ being found by zeroing the foregoing polynomial. Moreover, it can be shown that, at points where at least two branches of the manipulator meet, both $P_4(t)$ and $P_4'(t)$ vanish. Therefore, it is required to obtain a relationship between the coefficients of $P_4(t)$ that would guarantee that both $P_4(t)$ and $P_4'(t)$ have at least one common root. A well-established method already exists for determining the aforementioned condition, namely *dialytic elimination* (Salmon, 1964). An alternative method is introduced here, that relies on the concepts of controllability and observability in the framework of transfer-function realizations of linear systems (Kailath, 1980).

Let $T(s)$ be the transfer function of a single-input/single-output (SISO) linear system, i.e.,

$$T(s) = \frac{N(s)}{D(s)} \tag{2.2}$$

where $N(s)$ and $D(s)$ are polynomials of degrees d and n, respectively, with $n < d$, and $D(s)$ monic, i.e., with leading coefficient equal to unity. A *realization* of $T(s)$ is a triad $\{\mathbf{A}, \mathbf{b}, \mathbf{c}\}$ where $\mathbf{A}$ is a $d \times d$ matrix and $\mathbf{b}$ and $\mathbf{c}$ are d-dimensional vectors such that the linear dynamical system given below has the transfer function $T(s)$:

$$\dot{\mathbf{x}} = \mathbf{A}\mathbf{x} + \mathbf{b}u \tag{2.3}$$

$$y = \mathbf{c}^T \mathbf{x} \tag{2.4}$$

In eqs. (2.3) and (2.4), $\mathbf{x}$ is the d-dimensional vector of state variables, while u and y are scalars denoting the single input and the single output of the system, respectively. Moreover, the transfer function of the above realization is

$$T(s) = \mathbf{c}^T(s\mathbf{1} - \mathbf{A})^{-1}\mathbf{b} \tag{2.5}$$

where $\mathbf{1}$ is the $d \times d$ identity matrix.

Associated with any dynamical system represented through the state-space equations of the form given above are the two important notions of *observability* and *controllability*. These concepts are extensively discussed in the specialized literature, e.g., (Kailath, 1980; Chen, 1984). Before recalling the formal mathematical definitions of the observability and controllability of a dynamical system, a brief physical interpretation of these concepts is in order. The evolution of the internal states of a dynamical system as a function of the control inputs to the system is governed by the physical characteristics of the system and our particular realization of its input/output behaviour. Depending on the inherent features of the realization at hand, i.e., the operator $\mathbf{A}$ and the vector $\mathbf{b}$, one may or may not be able to control the system in such a way that, in a time interval, the internal states evolve from their initial values of $\mathbf{x}_o$ to take on the desired value of $\mathbf{x}_1$. As explained in Chen (1984), *roughly speaking, controllability studies the possibility of steering the state* $\mathbf{x}$ *from the input* $\mathbf{u}$. If we are able to steer the states to a desired point through the actions of the control inputs, then, our realization of the dynamical system is said to be controllable; otherwise it is said to be uncontrollable.

Furthermore, based on the inherent properties of the realization of the dynamical system that relate its inputs to the corresponding outputs, we may or may not be able to determine the internal states of the system based on our knowledge of its input/output behaviour. An observable realization of a dynamical system is one that allows such an inference. If the estimation of the internal states from the input/output properties of the system is not possible, then the realization is said to be unobservable. In other words, *observability studies the possibility of estimating the states from the output* (Chen, 1984).

Next, the formal definitions of the observability and controllability are restated from Kailath (1980): The realization (2.3) and (2.4) is *controllable* if its $d \times d$ controllability matrix $\mathbf{C}$, defined below, is nonsingular:

$$\mathbf{C} \equiv [\mathbf{b} \quad \mathbf{Ab} \quad \cdots \quad \mathbf{A}^{n-1}\mathbf{b}] \tag{2.6}$$

Likewise, the said realization is *observable* if its $d \times d$ *observability matrix* $\mathbf{O}$ is nonsingular, with $\mathbf{O}$ defined as

$$\mathbf{O} \equiv \begin{bmatrix} \mathbf{c}^T \\ \mathbf{c}^T\mathbf{A} \\ \vdots \\ \mathbf{c}^T\mathbf{A}^{n-1} \end{bmatrix} \tag{2.7}$$

Furthermore, the above realization is *minimal* if it is both controllable and observable. The necessary and sufficient condition for $T(s)$ to be minimal is that $D(s)$ and $N(s)$ do not contain any common factor. In other words, if we derive a controllable realization for $T(s)$, then it is necessary and sufficient for that realization to be minimal that its observability matrix be of full rank. Hence, if a controllable (observable) realization is not observable (controllable), then it is not minimal, and $D(s)$ and $N(s)$ share at least one common root. A physical interpretation of the notion of minimal realization can be thought of as having simultaneous observability and controllability with the least possible number of sensors expressing the state of the system and actuators driving it.

The concept of minimal realization that in effect determines whether $T(s)$ is irreducible or reducible is now applied to the closure polynomial and its derivative with respect to its argument. Hence, if $a \neq 0$, let

$$D(s) \equiv \frac{P_4(s)}{a} = s^4 + \frac{b}{a}s^3 + \frac{c}{a}s^2 + \frac{d}{a}s + \frac{e}{a} \tag{2.8}$$

and

$$N(s) \equiv \frac{1}{a}\frac{dP_4(s)}{ds} = 4s^3 + \frac{3b}{a}s^2 + \frac{2c}{a}s + \frac{d}{a} \tag{2.9}$$

Then, the transfer function $T(s)$ takes on the form

$$T(s) = \frac{4s^3 + (3bs^2 + 2cs + d)/a}{s^4 + (bs^3 + cs^2 + ds + e)/a}. \tag{2.10}$$

A controllable realization for this transfer function can be obtained as (Kailath, 1980)

$$\mathbf{A} = \begin{bmatrix} 0 & 1 & 0 & 0 \\ 0 & 0 & 1 & 0 \\ 0 & 0 & 0 & 1 \\ -e/a & -d/a & -c/a & -b/a \end{bmatrix} \tag{2.11a}$$

$$\mathbf{b} = [0 \quad 0 \quad 0 \quad 1]^T, \qquad \mathbf{c} = [d/a \quad 2c/a \quad 3b/a \quad 4]^T. \tag{2.11b}$$

Thus, for the problem at hand, in order to obtain the workspace boundaries, it will be sufficient to make our controllable realization unobservable. Below we expand the determinant of the observability matrix $\mathbf{O}$ of the realization of eq. (2.11):

$$\begin{aligned}\det(\mathbf{O}) \equiv (&d^2c^2b^2 - 4ec^3b^2 - 4d^3b^3 + 18edcb^3 - 27e^2b^4 - 4d^2c^3a + 16ec^4a + \\ &18d^3cba - 80edc^2ba - 6ed^2b^2a + 144e^2cb^2a - 27d^4a^2 + \\ &144ed^2ca^2 - 128e^2c^2a^2 - 192e^2dba^2 + 256e^3a^3)/a^6\end{aligned} \tag{2.12}$$

The right-hand side of eq. (2.12) being a polynomial function of the Denavit-Hartenberg (DH) parameters and of the x, y and z coordinates of the endpoint, when equated

Link	a_i	b_i	α_i
1	$-\frac{2\sqrt{2}}{3}$	$-\frac{5\sqrt{3}}{9}$	$2\pi/3$
2	$\frac{2\sqrt{2}}{3}$	$-\frac{2\sqrt{3}}{9}$	$\pi/3$
3	$\frac{2\sqrt{6}}{3}$	$-\frac{4\sqrt{3}}{9}$	$\pi/2$

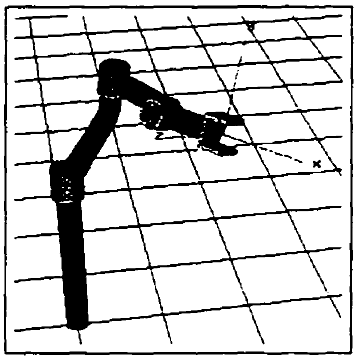

Figure 2.1: DH parameters and skeleton rendering for Example 2.1

to zero, the equation thus resulting defines the boundaries of the workspace of the manipulator under study. By utilizing Mathematica, it was observed that this polynomial is of a maximum degree in x and y, namely, 32, while it is of 16th degree in z. However, for given values of x and y, it was observed that z admits no more than four real values.

Next, we resort to a CAD-based method of constructing the workspace boundaries that result in three-dimensional renderings of the overall workspace. In doing so, we will take advantage of the symmetric nature of the workspace boundaries about the first joint axis. If, in eq. (2.12) expressed in the Cartesian space, the y coordinate is set equal to zero and the contour of the remaining equation is drawn in the X-Z plane, we will obtain the intersection of the manipulator workspace with the X-Z plane. In order to obtain the overall workspace boundaries, it is then sufficient to rotate the said intersection about the first axis.

2.2.2 Numerical Examples

For Example 2.1 we choose a 3-R manipulator formed with the first three links of the C-3 arm, an isotropic 4-axis manipulator designed at the McGill Centre for Intelligent Machines (CIM). The DH parameters and the skeleton rendering for this manipulator are shown in Fig. 2.1.

The overall workspace boundaries, for the Examples 2.1 is shown in Fig. 2.3.

Link	a_i	b_i	α_i
1	0.1	0.1	$\pi/2$
2	0.1	0.1	$-\pi/2$
3	0.1	0	$\pi/2$

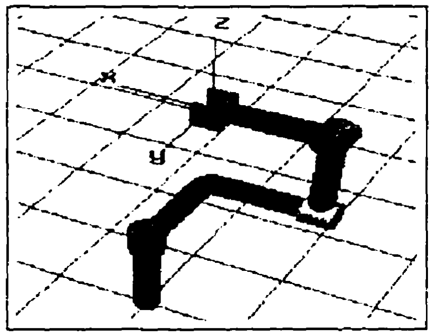

Figure 2.2: DH parameters and skeleton rendering for Example 2.2

In Example 2.2, an isotropic (for the definition of isotropic manipulators see (Chapters 3 and 4) 3–axes manipulator whose DH parameters and its skeleton rendering are shown in Fig. 2.2, is employed.

In Figure 2.4, the overall three-dimensional workspace boundaries of the isotropic 3-axes manipulator in the Cartesian space is illustrated.

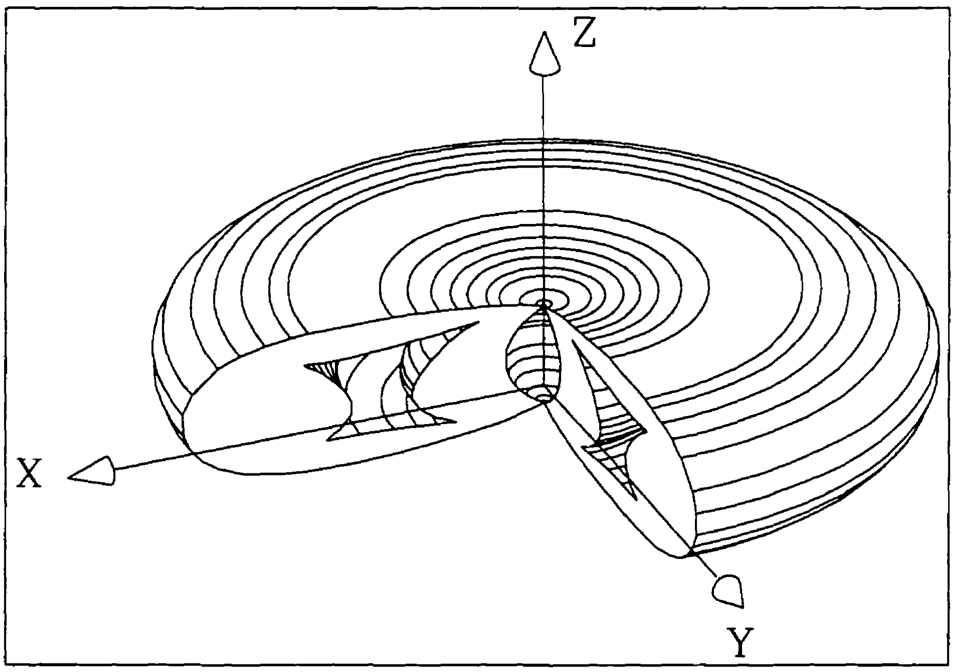

Figure 2.3: Overall workspace boundary of Example 2.1

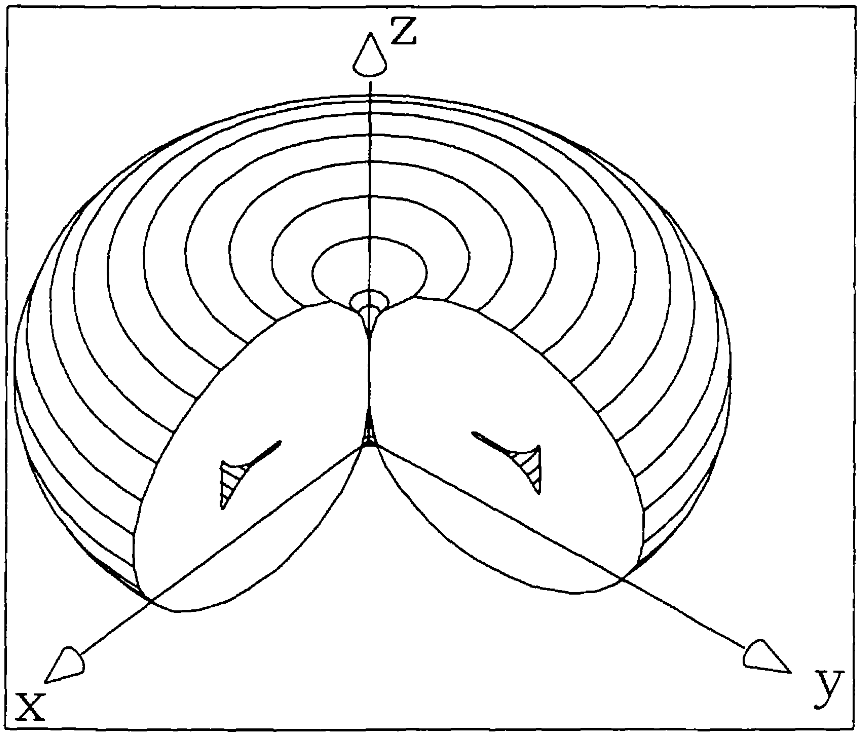

Figure 2.4: Overall workspace boundary of Example 2.2

2.3 Joint Space Singularities

For the first time, Borel and Liégeois (1986), introduced the notion of *aspects* as maximal singularity-free regions in the manipulator joint space. They argued that in each aspect $\mathcal{A}_i$ of the manipulator joint space, there is at most one inverse kinematic solution for a given end-effector pose. Although this is indeed the case for most industrial manipulators that possess simplifying architectures, it is by no means valid for general-architecture manipulators. For example, Burdick (1992) introduced a three-revolute joint manipulator, Example 2.3, whose solution branches could be connected pairwise in the joint space without crossing any singularity surface. The architecture of this manipulator is given in Fig. 2.5.

Furthermore, the notion of *configuration-space sheets*, or *c-sheets*, identical to that of Borel and Liégeois', aspects, was proposed by Burdick in the foregoing reference. Specifically a c-sheet is a maximal singularity-free region of the joint space, the image of each c-sheet under the forward kinematics being termed a *workspace-sheet* or a

Link	a_i	b_i	α_i
1	3.5	0.0	10.0°
2	6.0	1.0	75.0°
3	1.6	0.5	0.0°

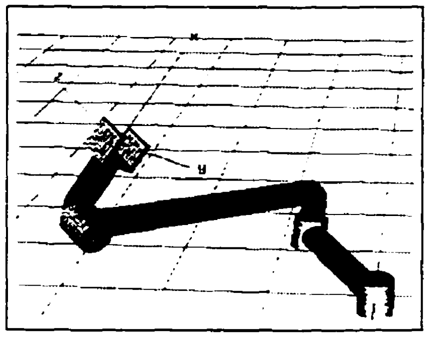

Figure 2.5: DH parameters and skeleton rendering for Example 2.3 (Burdick, 1992)

w-sheet. Depending on the number of inverse kinematic solutions, the c-sheets map on top of each other and form the w-sheets of the workspace. Burdick conducted extensive analyses of the c-sheets and the w-sheets with the aid of tools of differential topology. He showed that in one c-sheet, there can be more than one inverse solution for some points of the Cartesian space. Figures 2.6 and 2.7 depict the joint-space and the Cartesian space singularities for the latter example. Shown in Fig. 2.6 are the four inverse kinematic solutions numbered 1 to 4. These are the corresponding inverse kinematic solutions to the Cartesian point P illustrated in Fig. 2.7.

At the time, the observation that some regional structures are indeed able to change solution branch without becoming singular was found rather surprising by many researchers in the field. Wenger (1992) proposed the notion of *characteristic surfaces* as separating surfaces that divide the joint space into disjoint regions that map *diffeomorphically* into the Cartesian workspace. In (Wenger, 1992) these regions of the joint space were termed the *basic components*, and an iterative method was proposed to determine the characteristic surfaces. Other contributions to this issue followed through the works of Tsai et al. (1993), and Ranjbaran and Angeles (1994). The last two papers employed the closure equations of the manipulators to obtain algebraic expressions that define the subregions of the joint space that map diffeomorphically into their Cartesian counterparts. Despite the growing amount of research efforts on

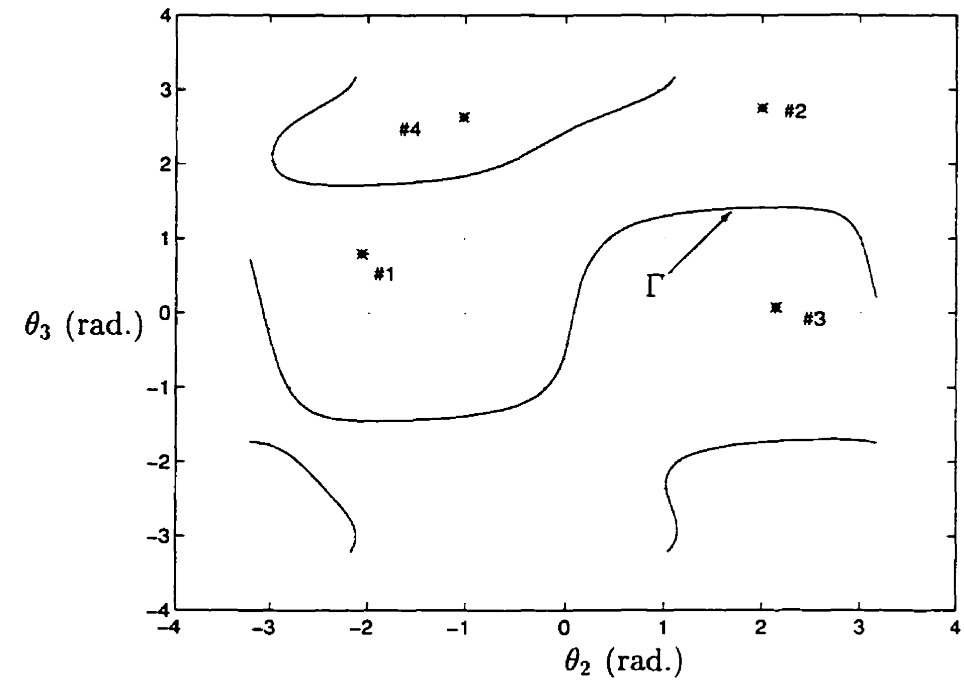

Figure 2.6: Joint space singularities for Example 2.3

singularity analysis in general, there has not been a concrete design-oriented characterization of the abilities of manipulators to change solution branch continuation with or without passing through singularities. In the following sections we will discuss this important issue in more detail, but first some preliminary definitions and tools are in order.

It is recalled that the joint space $\mathcal{J}$ of an n-revolute manipulator can be represented by an n-torus (T^n), or an n-cube whose sides are identified. Since the singularities of a manipulator are independent of the first joint angle θ_1, we can represent the joint space of a regional structure (3-revolute manipulator) conveniently by a square whose sides are identified, while θ_2 and θ_3 represent the horizontal and the vertical sides of the square. Furthermore, the Cartesian workspace of a 3-R manipulator is in $\mathbb{R}^3$, but, due to the symmetric nature of the workspace about the vertical axis, usually the z axis, for any value of θ_1, the boundaries of the workspace of the manipulator in the Cartesian space can also be represented by a square with its sides being either

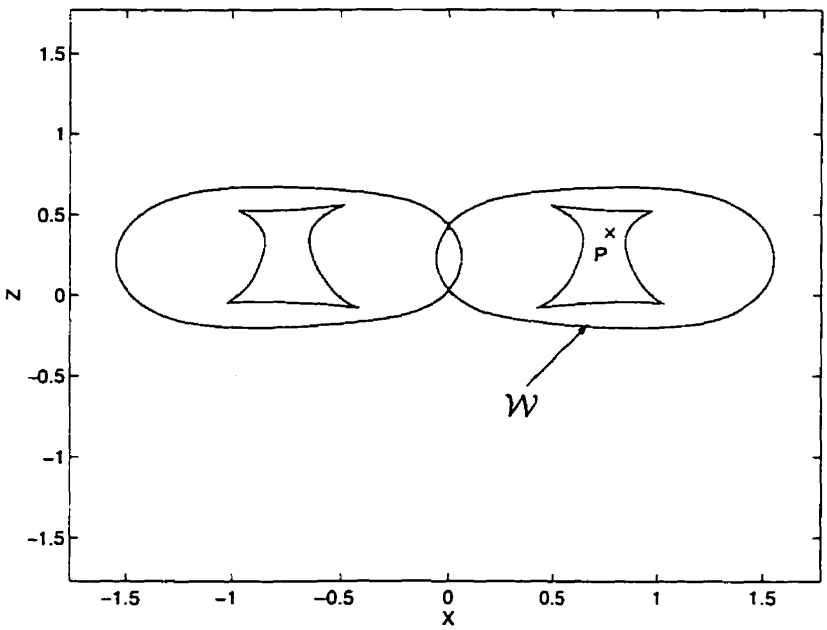

Figure 2.7: Cartesian space singularities for Example 2.3

the x and the z axes, or the y and the z axes. Let Γ denote the set of joint variables that make the Jacobian matrix $\mathbf{J}$ singular,

$$\Gamma = \{\forall \boldsymbol{\theta} \in \mathcal{J} \mid \Delta \equiv \det(\mathbf{J}) = 0\}$$

Let, moreover, the forward kinematic map of the manipulator be denoted by the vector function $\mathbf{f}$,

$$\mathbf{f} : \mathcal{J} \rightarrow \mathbb{R}^3$$

or,

$$f_1(\theta_1, \theta_2, \theta_3) \rightarrow x \tag{2.13}$$

$$f_2(\theta_1, \theta_2, \theta_3) \rightarrow y \tag{2.14}$$

$$f_3(\theta_2, \theta_3) \rightarrow z \tag{2.15}$$

while noting that f_3 is independent of θ_1. Hence, the workspace boundaries in the

Cartesian space, denoted by $\mathcal{W}$, will be

$$\mathcal{W} \equiv \mathbf{f}(\Gamma)$$

For a regional structure an alternative form for the determinant of the Jacobian matrix $\mathbf{J}$ is introduced here that is linear in the harmonic functions of sums and differences of the joint angles θ_2 and θ_3. If the manipulator is parametrized (Fig.1.5) using the DH notation, then one can obtain the following relation for the determinant of the Jacobian matrix that is obviously independent of θ_1

$$\begin{aligned}\Delta = {} & m_1 \cos\theta_2 + m_2 \cos\theta_3 + m_3 \cos(\theta_2+\theta_3) + m_4 \cos(\theta_2-\theta_3) + m_5 \cos(\theta_2+2\theta_3) + \\ & m_6 \cos(\theta_2-2\theta_3) + n_1 \sin\theta_2 + n_2 \sin\theta_3 + n_3 \sin(2\theta_3) + n_4 \sin(\theta_2+\theta_3) + \\ & n_5 \sin(\theta_2-\theta_3) + n_6 \sin(\theta_2+2\theta_3) + n_7 \sin(\theta_2-2\theta_3) \qquad (2.16)\end{aligned}$$

where m_i and n_i are constant coefficients that are functions of the architecture of the given manipulator (functions of the DH parameters). The simplified expressions for these coefficients are given in Appendix A. Representing the determinant of the Jacobian matrix in the foregoing form is more convenient than the usual expression containing the trigonometric products. In Fig. 2.8, the set of joint-space singularities Γ and its image in the Cartesian space $\mathcal{W}$ that comprise the workspace boundaries are shown for the manipulator introduced by Wenger (1992), and whose architecture is given in Fig. 2.9.

In Fig. 2.8, the four inverse kinematic solutions in the joint space are shown and numbered 1–4, while the corresponding Cartesian configuration is denoted by P. It is apparent that the joint space $\mathcal{J}$ is divided into two disjoint regions only, and not four (since the top and bottom as well as the two sides of the square are identified. This is sometimes called a *flat torus*). Hence, as can be seen in Fig. 2.8, the two solutions numbered 1 and 3 fall in one c-sheet, while solutions 2 and 4 fall in the second c-sheet. Hence, this manipulator can indeed change its solution branch from solution number 1 to solution number 3 without crossing the solid lines that represent the Jacobian singularities Γ.

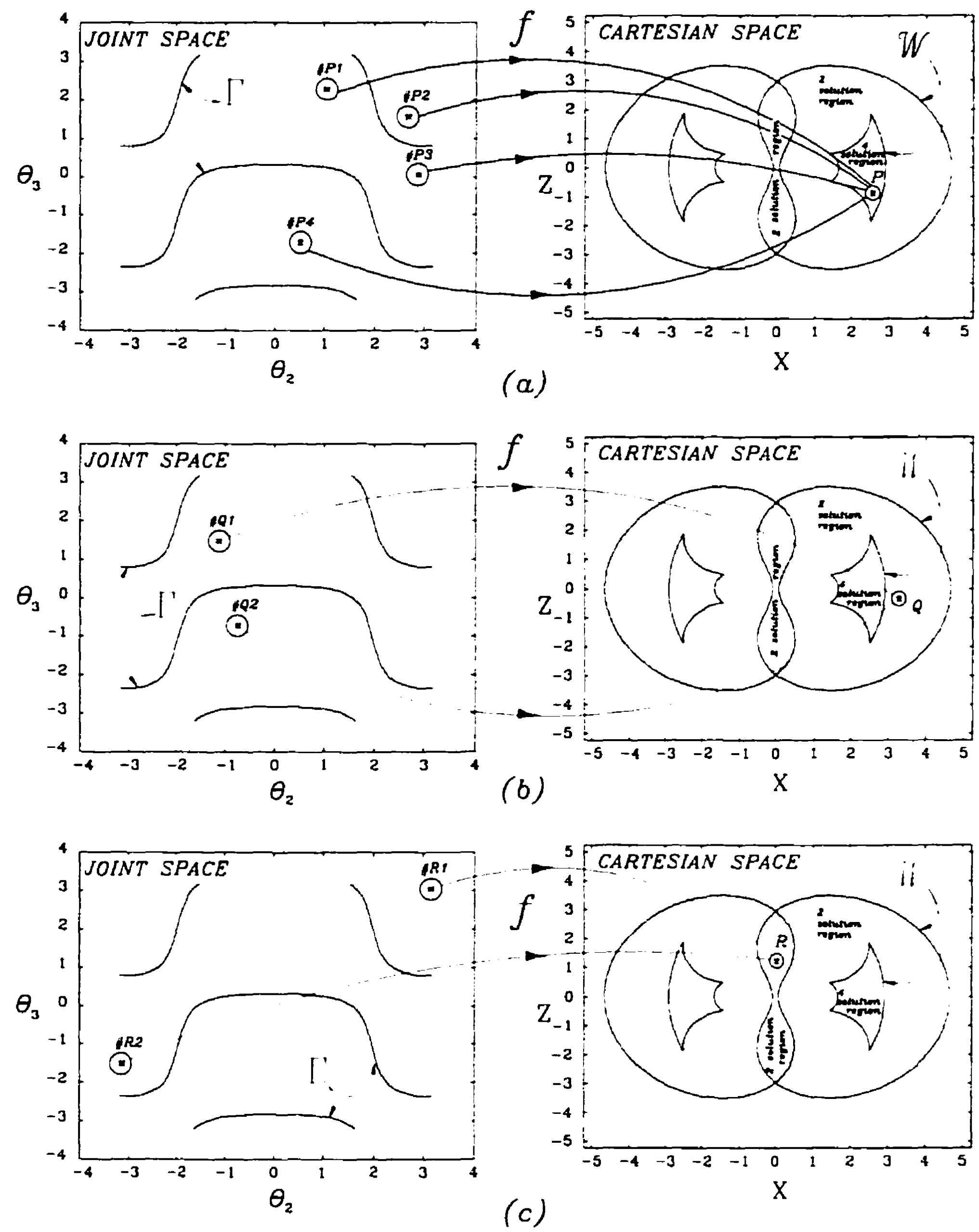

Figure 2.8: Mapping of the joint space into the Cartesian space for Example 2.4

Link	a_i	b_i	α_i
1	1.0	0.0	−90.0°
2	2.0	1.0	90.0°
3	1.5	0.0	0.0°

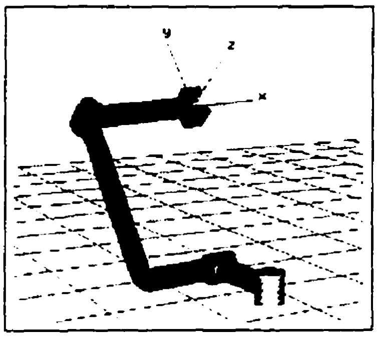

Figure 2.9: DH parameters and skeleton rendering for Example 2.4 (Wenger, 1992)

Next, with the aid of a simple example, we will shed some light on the root of the misconception mentioned before, i.e., why some regional structures can change solution branch without becoming singular. First, some fundamental definitions as well as the *inverse function theorem* are recalled:

- A map g is said to be of class C^p ($p \geq 1$), if all its pth-order partial derivatives exist and are continuous.

- A map g is a C^p diffeomorphism if g is bijective (one-to-one and onto) and both g and g^{-1} are of class C^p.

- A map g is said to be regular at a point of its domain if the Jacobian matrix of g at that point is of full rank.

- **Inverse Function Theorem** (Berger and Gostiaux, 1988): Let $\mathcal{U}$ and $\mathcal{V}$ be open subsets of Banach spaces E and F, and g be a C^p map from $\mathcal{U}$ to $\mathcal{V}$. If g is regular at a point $q_o \in \mathcal{U}$, then there exists an open neighbourhood $\mathcal{U}' \subset \mathcal{U}$ of q_o such that the restriction of g to $\mathcal{U}'$ is a C^p diffeomorphism from $\mathcal{U}'$ to $g(\mathcal{U}')$

A Simple Example

Consider the map $f : \mathbb{R}^* \times \mathbb{R} \to \mathbb{R}^2$, defined by

$$f(\rho, \theta) = (x, y) = (\rho \cos\theta, \rho \sin\theta)$$

where, $\mathbb{R}^* = \mathbb{R} - \{0\}$. It is evident that the map f is regular (nonsingular) everywhere in its domain, since $\det \mathbf{J} = \rho \neq 0$. But f is not a diffeomorphism on all of $\mathbb{R}^* \times \mathbb{R}$, i.e., there are multiple points of $\mathbb{R}^* \times \mathbb{R}$ that are mapped into the same point of $\mathbb{R}^2$, which is due to the periodicity of f in θ. That is, any two points (ρ, θ) and $(\rho, \theta + 2\pi)$ are mapped into the same point $(\rho, 0)$. However, the restriction of f to $\mathbb{R}^* \times]0, 2\pi[$ is a diffeomorphism, and thus, an invertible mapping with its inverse given by

$$f^{-1}(x, y) = (\rho, \theta) = (\sqrt{x^2 + y^2}, \tan^{-1} \frac{y}{x})$$

Extending the foregoing argument for general nonlinear maps is extremely complex. The first attempt towards answering this question for the manipulator forward kinematics is due to Wenger (1992), where an iterative technique is used to trace the pre-images of the Cartesian space singularities of the forward kinematics. In this regard the characteristic surfaces S_c of an aspect $\mathcal{A}_i$ with the boundary $\bar{\mathcal{A}}_i$, were defined by Wenger as the set of the pre-image in $\mathcal{A}_i$ of $\bar{\mathcal{A}}_i$, i.e.,

$$S_c(\mathcal{A}_i) \equiv f^{-1}(f(\bar{\mathcal{A}}_i)) \cap \mathcal{A}_i \tag{2.17}$$

Moreover, in (Wenger, 1992), disjoint subsets of an aspect in which the forward kinematic map is one-to-one and onto is termed the *basic components*.

A brief outline of the technique used by Wenger is explained below:

1. Denote by $\mathcal{A}$ the set of all points in the joint space where the Jacobian matrix is singular.
2. Find the image of $\mathcal{A}$ in the Cartesian space under the action of the forward kinematic map and denote it by $\mathcal{W}$. This set of points defines all of the workspace boundaries of the manipulator as well as internal separating surfaces in the Cartesian space.
3. Find the pre-images of the points of $\mathcal{W}$, by solving the inverse kinematic problem, and obtain four sets of points in the joint space. These sets then divide the joint space into four disjoint regions.

This method, that requires tracing each singular point of f from the joint space into the Cartesian space and back into the joint-space, is not amenable to symbolic manipulations and requires solving the forward and inverse kinematics numerous times. A contribution of this chapter is an algebraic expression that defines the internal separating surfaces explicitly. For 3R manipulators this method was reported by Ranjbaran and Angeles (1994), while the same technique in a more elaborate setting for general manipulators was discussed independently by Tsai et al. (1993). In the latter paper the internal separating surfaces are called *pseudo singularity manifolds* and the *basic components* are termed *joint-space patches.*

From eq. (2.17), it is apparent that the collection of the Jacobian singularities Γ, the boundaries of the aspects $\mathcal{A}_i$, and the internal separating surfaces, pseudo-singularities, are preimages of the workspace boundaries in the manipulator Cartesian space. The internal separating surfaces as well as the boundaries of the aspects in the manipulator joint space are the points that render the discriminant of the manipulator closure equation zero. The quartic characteristic polynomial $P_4(t)$ that relates the set of DH parameters and the set of Cartesian coordinates of the EE to one of the joint angles, i.e., $t \equiv \tan\theta_3/2$ is once again recalled see eq. (2.1):

$$P_4(t) \equiv at^4 + bt^3 + ct^2 + dt + e \tag{2.18}$$

with

$$a = 4a_1^2B^2 + \mu_1^2D^2 - 4a_1^2\mu_1^2\xi^2 \tag{2.19a}$$

$$b = 16a_1^2FB + 4\mu_1^2ED \tag{2.19b}$$

$$c = 8a_1^2BA + 2\mu_1^2DC + 16a_1^2F^2 + 4\mu_1^2E^2 - 8a_1^2\mu_1^2\xi^2 \tag{2.19c}$$

$$d = 16a_1^2FA + 4\mu_1^2EC \tag{2.19d}$$

$$e = 4a_1^2A + \mu_1^2C^2 - 4a_1^2\mu_1^2\xi^2, \tag{2.19e}$$

where,

$$\xi^2 \equiv x^2 + y^2$$

and

$$
\begin{aligned}
A &= b_2 + b_3\lambda_2 + b_4\lambda_2\lambda_3 - \lambda_1(z - b_1) - b_4\mu_2\mu_3 \\
B &= b_2 + b_3\lambda_2 + b_4\lambda_2\lambda_3 - \lambda_1(z - b_1) + b_4\mu_2\mu_3 \\
C &= a_2^2 + a_3^2 + b_2^2 + b_3^2 + b_4^2 - a_1^2 - \xi^2 - (z - b_1)^2 \\
&\quad + 2b_2b_3\lambda_2 + 2b_2b_4\lambda_2\lambda_3 + 2b_3b_4\lambda_3 + 2a_2a_3 - 2b_2b_4\mu_2\mu_3 \\
D &= a_2^2 + a_3^2 + b_2^2 + b_3^2 + b_4^2 - a_1^2 - \xi^2 - (z - b_1)^2 \\
&\quad + 2b_2b_3\lambda_2 + 2b_2b_4\lambda_2\lambda_3 + 2b_3b_4\lambda_3 - 2a_2a_3 + 2b_2b_4\mu_2\mu_3 \\
E &= 2a_3b_2\mu_2 + 2a_2b_4\mu_3, \qquad F = a_3\mu_2
\end{aligned}
$$

We can now proceed to investigate the singularities of $P_4(t)$, by searching for points where $P_4(t)$ has repeated roots (its discriminant vanishes). In the previous Section an expression in terms of the coefficients of the quartic polynomial was obtained by employing the concepts of nonminimal realizations of transfer functions. Here we use an alternative expression for these singularities which is more compact. As shown in Neumark (1965), the condition for a quartic to have repeated roots is of the following form,

$$
\begin{aligned}
h(x, y, z) &\equiv (2c^3 + 27ad^2 + 27b^2e - 9bcd - 72ace)^2 - 4(c^2 - 3bd + 12ae)^3 \\
&= 0
\end{aligned}
\tag{2.20}
$$

It has to be mentioned that if the right hand side of the foregoing equation is expanded, the same relation as given by eq. (2.12) will be obtained.

Any point in the Cartesian space of the manipulator that satisfies the foregoing relation must lie on either the workspace boundaries where two solution branches meet, or on the internal separating surfaces that divide the workspace into subregions with different degrees of accessibility, i.e., subregions with different numbers of inverse kinematic solutions.

In order to find the preimage of these surfaces in the joint space, it is noted that the coefficients a to e given by eqs. (2.19) are independent of the x and y coordinates of the end-effector, and are functions of the manipulator parameters as well as the z coordinates of the EE only. Also, the z coordinate of the end-effector is determined by θ_2 and θ_3 only, as θ_1 produces a rigid body rotation of the manipulator about the first axis. It is not difficult to show that ξ^2 appearing in eq. (2.19) is not affected by θ_1 either. Hence, all the points that satisfy eq. (2.20) can be brought back into the joint space by simply substituting for ξ^2 and z in terms of θ_2 and θ_3. If we let

$$\xi^2 \equiv f_1^2(\theta_2, \theta_3) + f_2^2(\theta_2, \theta_3) \tag{2.21}$$

$$z \equiv f_3(\theta_2, \theta_3) \tag{2.22}$$

then, eq. (2.20) can be rewritten as a function of the DH parameters as well as of θ_2 and θ_3, i.e.,

$$\begin{aligned} h_\theta(\theta_2, \theta_3) \equiv (2c_\theta^3 + 27a_\theta\, d_\theta^2 + 27\, b_\theta^2\, e_\theta - 9\, b_\theta\, c_\theta\, d_\theta - 72\, a_\theta\, c_\theta\, e_\theta)^2 - \\ 4\,(c_\theta^2 - 3\, b_\theta\, d_\theta + 12\, a_\theta e_\theta)^3 = 0 \end{aligned} \tag{2.23}$$

where, $a_\theta, b_\theta, c_\theta, d_\theta$, and e_θ are all functions of θ_2 and θ_3 only. The contours of this equation can be plotted in the plane of the second and the third joint variables. It can then be observed that the joint space is divided into four disjoint regions. In order to show the applicability of this technique, the numerical examples of the previous section are reexamined.

The complete joint-space singularities of Example 2.3 are illustrated in Fig. 2.10, where it is observed that the joint space is now divided into four disjoint regions and each solution branch is contained in one region, or *basic components*, according to Wenger (1992). For Examples 2.4, similar results are obtained and shown in Fig. 2.11.

Another interesting example of a 3R manipulator with general geometry is that given by Example 2.5, with its DH parameters given in Fig. 2.12. This architecture corresponds to the class of *nongeneric* manipulators, i.e., those manipulators whose

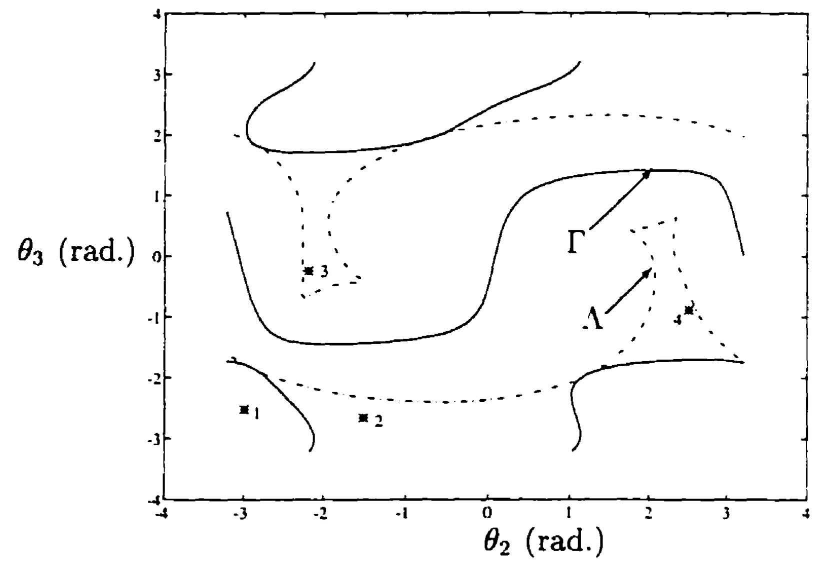

Figure 2.10: Uniqueness domains for Example 2.3

singularities in the joint space form smooth manifolds (Pai and Leu, 1989; 1992). Although most nongeneric manipulators cannot change posture without becoming singular (Burdick, 1992; 1995), the foregoing example is an exception. It satisfies the nongenericity condition of 3R manipulators proposed by Pai and Leu (1989; 1992), while it admits only two c-sheets. Burdick (1992) conjectured the existence of such regional structures.

The uniqueness domain for the foregoing example is shown in Fig. 2.13, where it is apparent that the two c-sheets contain two inverse kinematic solutions and thus the manipulator at hand is a nonsingular posture-changing, albeit nongeneric, manipulator.

Another interesting class is that of *special* manipulators with simplifying geometries. For example, consider the regional structure of the Puma 560 manipulator, as given in Fig. 2.14

It turns out that for this regional structure $h(x, y, z)$, and thus, $h_\theta(\theta_2, \theta_3)$, as given

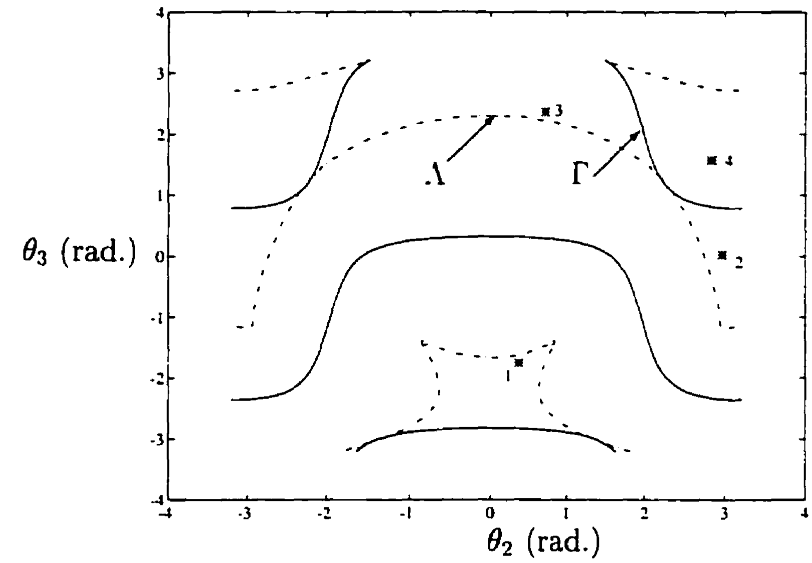

Figure 2.11: Uniqueness domains for Example 2.4

by eq. (2.23), identically vanish, the Jacobian singularity surfaces then dividing the joint space into disjoint uniqueness domains with unique inverse kinematic solutions in each region (Fig 2.15).

In fact, for all *special* manipulators, eq. (2.20) is identically satisfied, and thus we have the following proposition:

Proposition 2.1 *A regional structure cannot change solution branch without becoming singular iff the associated DH parameters of the manipulator identically satisfy eq.* (2.20) *throughout the entire workspace.*

Before proving the foregoing proposition three facts are recalled:

Fact 1 *Special* manipulators are those whose characteristic polynomials reduce to quadratic polynomials (Tsai et al., 1994)

Fact 2 Each c-sheet of a special manipulator contains one and only one inverse kinematic solution branch (Tsai et al., 1994).

Link	a_i	b_i	α_i
1	0.7576	1.5	70.703°
2	1.636	−0.1498	−33.810°
3	1.123	0.17049	88.386°

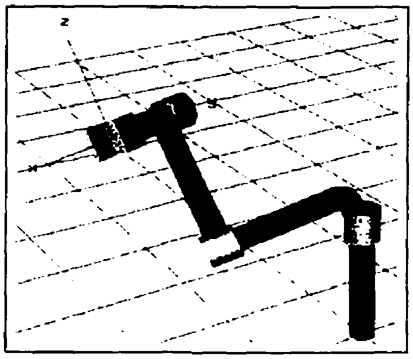

Figure 2.12: DH parameters and skeleton rendering for Example 2.5

Fact 3 Identically vanishing of the discriminant of a quartic polynomial $P_4(t)$, amounts to the existence of two double roots and a factorizing of $P_4(t)$ of the following form (Neumark, 1965):

$$P_4(t) = a\,(t^2 + \frac{b}{2a}\,t + \frac{d}{b})^2 \tag{2.24}$$

Proof:

Necessary: If for a given regional structure, $h(x, y, z)$ and, thus $h_\theta(\theta_2,\ \theta_3)$ as defined in eq. (2.20) is identically zero, then from Facts 1 and 3 follows that the manipulator is *special.* Moreover, from Fact 2 follows that in every c-sheet of the manipulator there must be only one inverse kinematic solution associated with a given Cartesian configuration. Hence, the manipulator cannot change posture without crossing the boundary of a c-sheet i.e., without crossing a singularity surface.

Sufficient: If the manipulator cannot change solution branch without crossing singularities, then, in each c-sheet there is only one inverse kinematic solution for a given Cartesian configuration; hence, from Fact 2, the manipulator has to be special, and, from Fact 1, the inverse kinematic solution must reduce to a quadratic equation. This, in turn, is equivalent to the identically vanishing of $h(x, y, z)$, and thus, of the identically vanishing of $h_\theta(\theta_2,\ \theta_3)$.

q.e.d

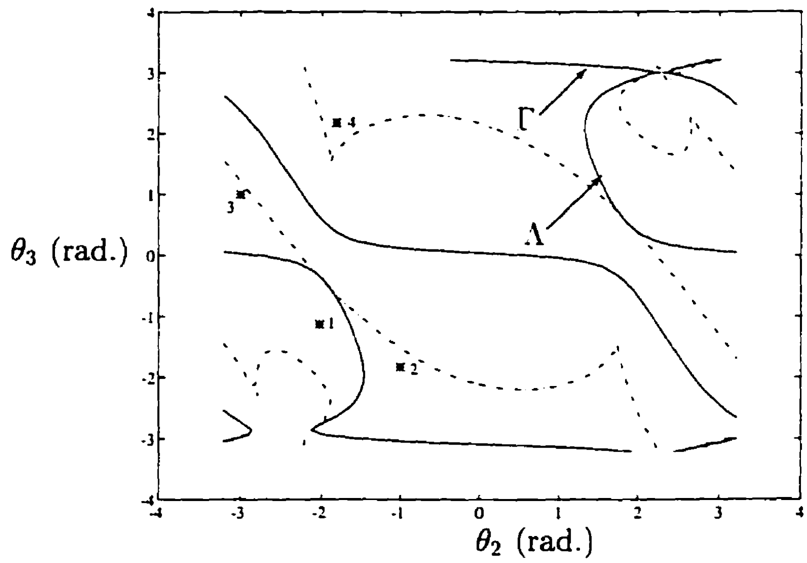

Figure 2.13: Uniqueness domains for Example 2.5

The same CAD-based technique as discussed in Section 2.2.2 is used now to obtain complete 3-dimensional renderings of the Cartesian workspaces for Examples 2.3 to 2.6, as shown in Figs. 2.16 to 2.19.

2.4 Kinematic Design and Singularity Distribution

Despite the significant amount of work and interest devoted to the characterization of the singularity and workspace analysis of regional structures, particularly with the wave ot the recent attention to those manipulators that can change solution branch continuation without crossing singularities, there seems to be a fundamental question remaining unanswered, namely *for the kinematic designer, are there any merits in making the manipulator a nonsingular posture-changing one at the expense of losing simplifying architectures?*

Link	a_i	b_i	α_i
1	0.0	0.0	$-90°$
2	4.32	1.49	$0.0°$
3	4.32	0.0	$-90°$

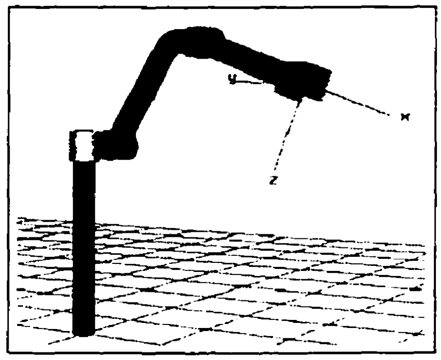

Figure 2.14: DH parameters and skeleton rendering for Example 2.6

It is a well known fact that the Jacobian singularities are undesirable while inverting the kinematics, that is, when controlling the motion of the end-effector at the Cartesian level while commanding controller actions at the joint-space level. These singularities, however, do not hinder the direct joint space control of the manipulator motions. Although a change in the posture from one solution branch to another can be beneficial in order to satisfy additional requirements, this posture-change in general cannot be a part of the Cartesian task that the manipulator is executing. Should a change of posture become necessary, the segment of the task being performed would have to come to a stop, the manipulator should then reconfigure itself to the new branch and then the execution of the next segment of the task would resume. Therefore, if branch-switching is not to be considered as an integral part of the assigned task, the controller can readily perform the change from one posture to another at the joint-space level, where Jacobian singularities do not prevent the control.

The foregoing argument suggests that despite the recent research enthusiasms towards designing nonsingular posture-changing manipulators, not much of an advantage is gained while doing so. On the contrary, as will be shown presently, these manipulators can pose kinematic disadvantages over their singular posture-changing counterparts. For the sake of comparison, let us consider the two regional structures of Examples 2.3 and 2.6 that depict, respectively, a nonsingular- and a singular

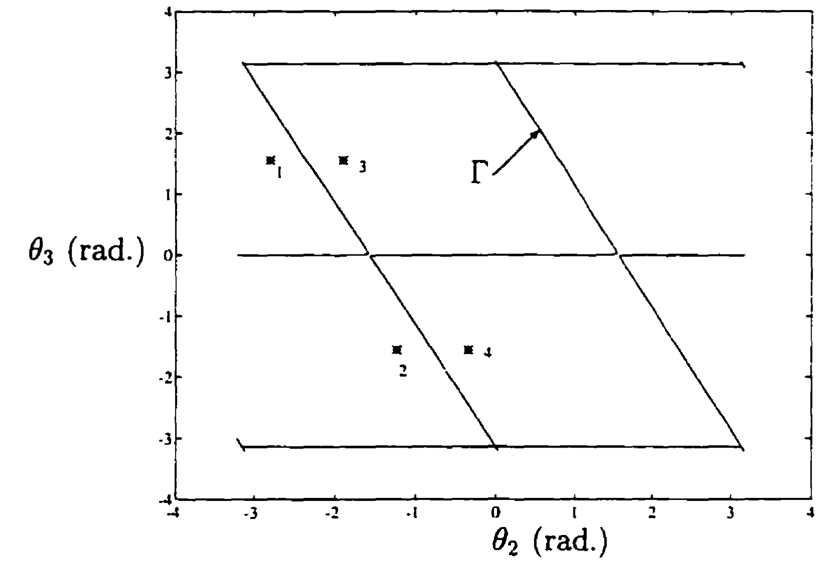

Figure 2.15: Uniqueness domains for Example 2.6

posture-changing manipulator. To make the comparison more precise, the two manipulators are normalized with respect to their maximum reach, thus attaining the same stretch. The Cartesian workspace boundaries and internal singularities of the two normalized manipulators in their Cartesian XZ planes are shown in Figs. 2.20 and 2.21, respectively. Identical Cartesian straight-line trajectories are also shown in both figures connecting points P and Q with position vectors $\mathbf{p} = [0.3, 0.0, -0.4]^T$ and $\mathbf{q} = [0.7, 0.0, 0.4]^T$, respectively.

The line PQ is then parametrized by a path parameter s such that the points $\mathbf{r}(s)$ along PQ, for $s \in (0, 1)$ are obtained from

$$\mathbf{r}(s) = \mathbf{q}\, s + (1 - s)\, \mathbf{p}, \quad s \in (0, 1)$$

The inverse kinematics of the two manipulators for the above trajectory are then solved with the four solution-branch continuations for the second joint variable θ_2 of the two manipulators shown in Figs. 2.22 and 2.23, respectively. It can be seen from Fig. 2.23 that any one of the four solution branches $\mathcal{A}_1$ to $\mathcal{A}_4$ can be chosen

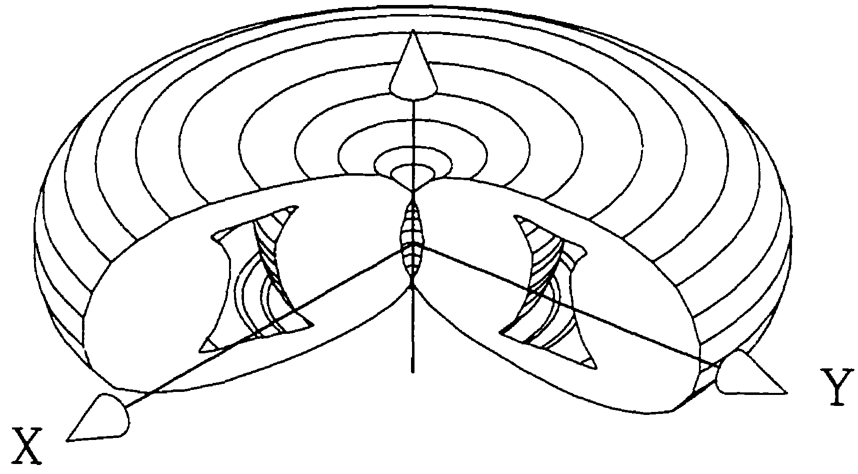

Figure 2.16: Workspace boundaries for Example 2.3

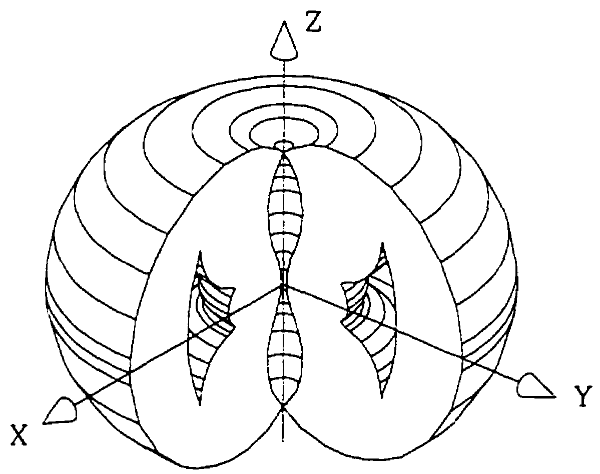

Figure 2.17: Workspace boundaries for Example 2.4

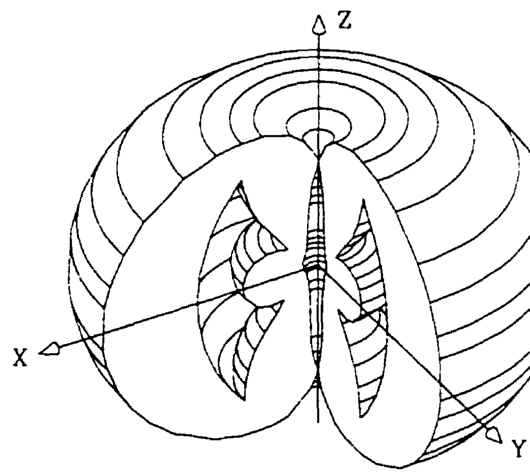

Figure 2.18: Workspace boundaries for Example 2.5

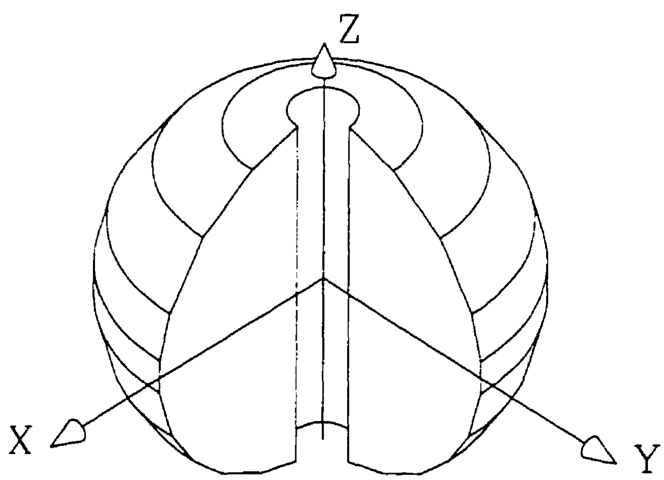

Figure 2.19: Workspace boundaries for Example 2.6

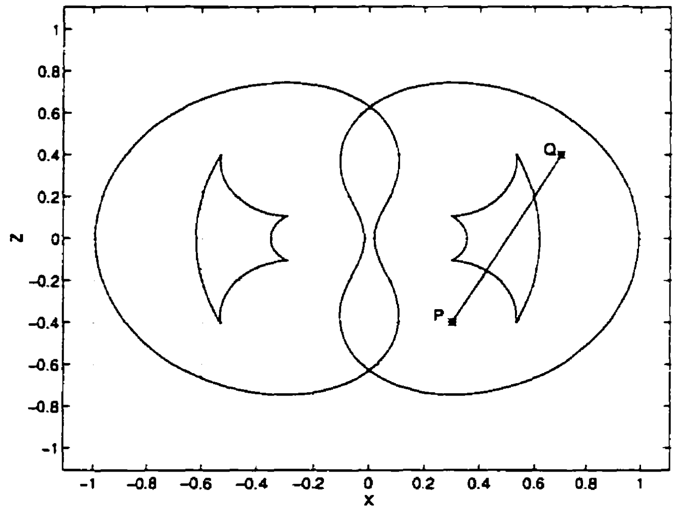

Figure 2.20: Normalized Workspace boundaries in XZ plane for Example 2.3

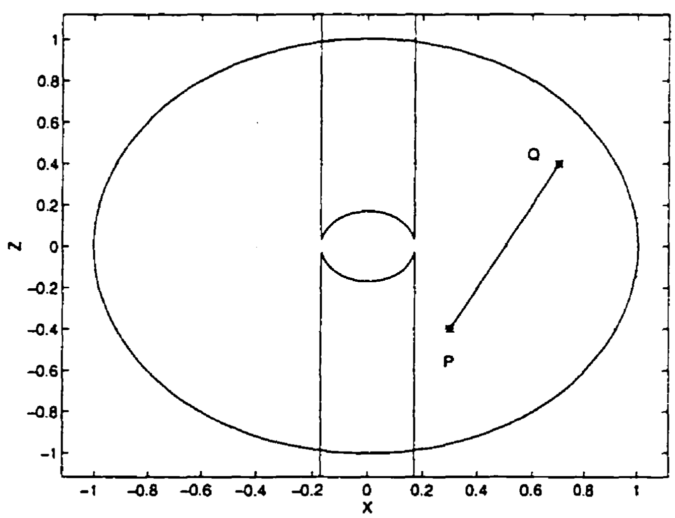

Figure 2.21: Normalized Workspace boundaries in XZ plane for Example 2.6

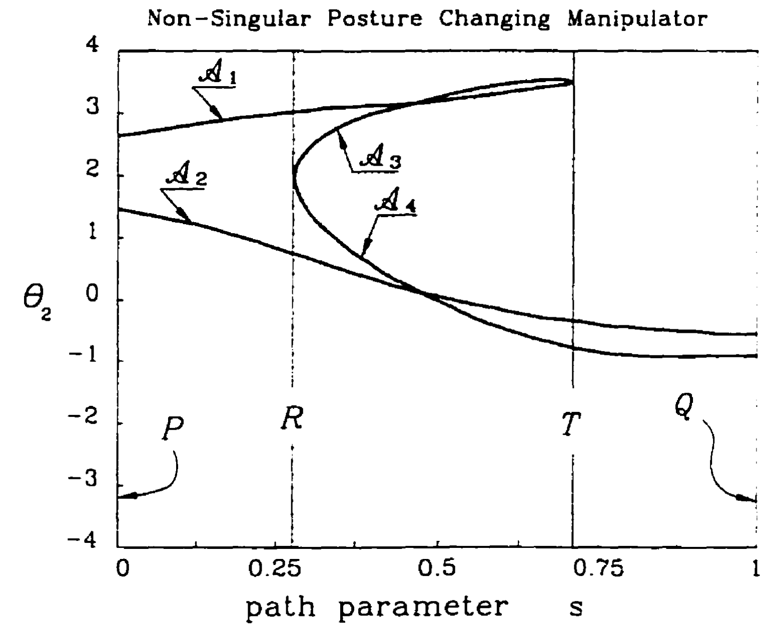

Figure 2.22: Inverse kinematics for Example 2.3 (nonsingular posture-changing)

and continuously followed from P to Q without any interruptions. Now, considering Fig. 2.22 for the nonsingular posture-changing manipulator, a much more limited situation is observed. The PQ interval is divided into three segments, namely, PR, RT and TQ. At the start of the trajectory only two solution branches $\mathcal{A}_1$ and $\mathcal{A}_2$ are available with $\mathcal{A}_1$ ending at T while $\mathcal{A}_2$ can continue to the end of the trajectory at Q. Solution branches $\mathcal{A}_3$ and $\mathcal{A}_4$ begin from R, where the associated Jacobian matrix of the manipulator is singular, as these two solution branches meet. Continuation $\mathcal{A}_3$ fails to complete the desired trajectory and ends at T, while $\mathcal{A}_4$ passes through Q. Hence, for achieving a continuous solution-branch from P to Q the manipulator is left with only one choice, namely $\mathcal{A}_2$, a disadvantage that nonsingular posture-changing nature of the manipulator can circumvent.

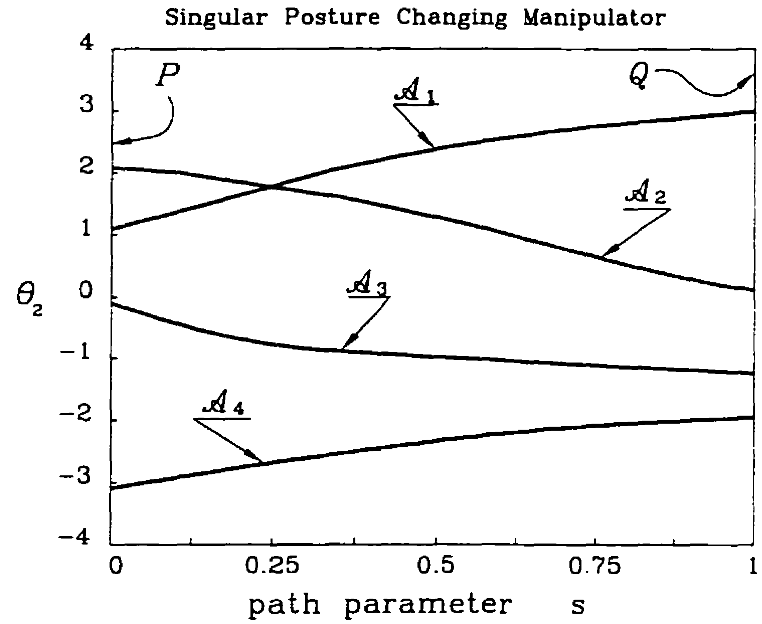

Figure 2.23: Inverse kinematics for Example 2.6 (singular posture-changing)

2.5 Conclusions

In the first part of the Chapter, singularities and workspaces of regional structures were discussed. A novel method of determining the Cartesian workspace boundaries of these structures was introduced. This technique that in effect determines the resolvent of the characteristic polynomial of the manipulator and its derivative, is based on nonminimal realization of transfer functions associated with single-input-single-output linear dynamical systems. A CAD-based scheme was also presented for three dimensional renderings of the overall Cartesian workspaces.

In the second part of the Chapter, singular and nonsingular posture-changing manipulators were discussed. First, a review of the major contributions on the subject was given. A method for determining algebraic expressions that divide the joint space into disjoint regions that contain only one inverse kinematic solution for a given Cartesian pose were provided. Finally, a critical discussion on the issue of singular-versus nonsingular posture-changing manipulators was provided that should be of interest to the kinematic designer. It was shown that designing a manipulator in such a way that it can change solution-branch without crossing any singularity does not necessarily lead to a *better* manipulator. Unless the designer is able to push the internal separating surfaces of the workspace outward close to the workspace boundaries, chances are that the manipulator will be in a much worse situation as compared to its singular posture-changing counterpart with a comparable workspace volume.

Chapter 3

Measuring Manipulator Dexterity

3.1 Introduction

In this chapter *kinematic dexterity* of robotic manipulators is discussed and comparisons are made between the different measures proposed so far. Since the centrepiece of almost all performance measures is the manipulator Jacobian matrix, some features of this matrix as applied to kinematic dexterity and workspace analysis are discussed as well. With regard to the kinetostatic performance of robotic manipulators, extensive research work has been published in the past two decades. A summary of these works is provided in Chapter 1, and a more elaborate discussion of some of these works that are relevant to this thesis will follow.

Dexterity or *gracefulness* of a mechanical hand is mainly attributed to its abilities to position and orient its end-effector *comfortably* in different *directions* (kinematic dexterity) while being able to apply forces and moments on the environment through its end-effector equally well in all directions (static dexterity). Kinematic and statics being dual to each other, most often the notion of *kinetostatics* (IFToMM, 1990) is used to quantify both kinematic and static performances.

The basis of the definition of kinetostatic dexterity in this thesis is on the following statement: A manipulator loses kinetostatic dexterity as the contribution of the motion and forces produced by one or more kinematic pair to the end-effector motion and forces is impaired due to the relative spatial placement of the joint axes. Hence, measuring dexterity amounts to assessing how *comfortably* and how *accurately* the end-effector motions and the contact forces at the Cartesian space of the manipulator can be achieved by commanding joint space motions/forces. This, in turn, boils down to the accuracy and robustness with which the relations between joint and Cartesian variables of the manipulator can be inverted. Local Cartesian- and joint-space motions and forces of the manipulator are related through the linear mapping produced by the Jacobian matrix associated with the manipulator, as reviewed below.

3.1.1 Variable Transformations in Kinematics

When dealing with motion transmission capabilities, the local behaviour of the manipulator is determined through the following linear transformation:

$$\mathbf{J}\,\dot{\mathbf{q}} = \mathbf{t} \tag{3.1}$$

For an n-axis manipulator working in an m-dimensional task space, $\mathbf{J}$ is the $m \times n$ Jacobian matrix, mapping the n-dimensional vector of joint velocities $\dot{\mathbf{q}}$ into the m-dimensional vector of Cartesian velocities $\mathbf{t}$. When the manipulator is used for both positioning and orienting tasks in the three dimensional Cartesian space, $\mathbf{t}$ is the *twist* vector of the operation point of the end-effector (EE) which is defined as:

$$\mathbf{t} \equiv \begin{bmatrix} \boldsymbol{\omega} \\ \mathbf{v} \end{bmatrix}$$

with $\mathbf{v}$ being the linear velocity vector of the operation point of the end-effector and $\boldsymbol{\omega}$ the angular velocity vector of the EE.

In order to command a desired twist to the manipulator, it is required that vector $\dot{\mathbf{q}}$ of eq. (3.1) be determined. For nonredundant manipulators, the foregoing system of equations can be inverted if $\mathbf{J}$ is non-singular, thus obtaining

$$\dot{\mathbf{q}} = \mathbf{J}^{-1}\,\mathbf{t} \tag{3.2}$$

For redundant manipulators where, the linear system of eq. (3.1) is underdetermined, the general solution to the inverse problem is given by

$$\dot{\mathbf{q}} = \mathbf{J}^{\dagger}\,\mathbf{t} + (\mathbf{1} - \mathbf{J}^{\dagger}\,\mathbf{J})\,\boldsymbol{\zeta} \tag{3.3}$$

where $\mathbf{J}^{\dagger}$ represents the *generalized inverse* of the Jacobian matrix $\mathbf{J}$ defined by

$$\mathbf{J}^{\dagger} = \mathbf{J}^{T}\,(\mathbf{J}\,\mathbf{J}^{T})^{-1}$$

and $\boldsymbol{\zeta}$ is an arbitrary vector in $\mathbb{R}^{n}$ that defines a secondary task to be satisfied in addition to the primary task of achieving the desired twist $\mathbf{t}$. The first term of eq. (3.3) represents the *minimum norm solution* of the underdetermined linear system given by eq. (3.1), while the second term represents the homogeneous solution to eq. (3.1). This term, $(\mathbf{1} - \mathbf{J}^{\dagger}\,\mathbf{J})\,\boldsymbol{\zeta}$, corresponds to the internal motion, or self-motion, of the manipulator, that gives rise to no end-effector motion. From eqs. (3.2) and (3.3), it is apparent that solving the instantaneous kinematics of the manipulator amounts to inverting either $\mathbf{J}$ or the matrix product $(\mathbf{J}\,\mathbf{J}^{T})$. In doing so, the numerical conditioning of the Jacobian matrix becomes important. Furthermore, it is the numerical conditioning of a linear transformation that determines how much magnification (distortion) will result when the vectors from the domain of the transformation are mapped into its range. In the sense of a manipulator being able to move its end-effector equally well in all directions, the characterization of the amount of distortion (maximum and minimum magnifications) that $\mathbf{J}^{\dagger}$ produces on the space of twists of the end-effector while mapping it into the space of the joint rates becomes important.

3.1.2 Variable Transformations in Statics

When dealing with static force transmission capabilities of the manipulator the situation is the converse of the kinematic motion transmission capabilities mentioned above, i.e.,

$$\mathbf{J}^{T}\,\mathbf{w} = \boldsymbol{\tau} \tag{3.4}$$

where the transpose of the Jacobian matrix maps the *wrench* $\mathbf{w}$ applied at the end-effector onto the vector of joint torques $\boldsymbol{\tau}$. Here, the six-dimensional wrench $\mathbf{w}$ represented in *axis coordinates*,[1] is defined as

$$\mathbf{w} \equiv \begin{bmatrix} \mathbf{n} \\ \mathbf{f} \end{bmatrix}$$

where $\mathbf{f}$ is the resultant external force acting at the operation point of the end-effector and $\mathbf{n}$ is the resultant external moment sustained by the EE, while $\boldsymbol{\tau}$ is the vector of joint torques. In this situation, given any desired wrench to be balanced by the manipulator, the resulting joint torque vector $\boldsymbol{\tau}$ is readily determined and no matrix inversion is needed. However, if it is required to determine the wrench acting on the end-effector from joint-torque information provided by torque sensors at the joints, that is stored in the vector $\boldsymbol{\tau}$, then, for nonredundant manipulators we have

$$\mathbf{w} = \mathbf{J}^{-T}\,\boldsymbol{\tau} \tag{3.5}$$

while, for redundant manipulators, the foregoing equation takes on the form

$$\mathbf{w} = (\mathbf{J}\,\mathbf{J}^T)^{-1}\,\mathbf{J}\,\boldsymbol{\tau} \tag{3.6}$$

In the sense of the ability to determine the wrench applied at the end-effector by the environment in different directions, the concern is the distortion (maximum and minimum magnification) that $\mathbf{J}^T$ produces as it maps the space of wrenches to that of joint torques.

3.2 Jacobian Matrix

From the foregoing sections it is apparent that the Jacobian matrix of serial-type manipulators plays an important role in quantifying kinematic and static performances. Hence, a short account of the Jacobian matrix is given next.

[1] in an alternative ray-coordinates representation of the twist the locations of forces and moments are interchanged

3.2.1 Jacobian Formulation

The Jacobian matrix of a general n-revolute manipulator takes on the form (Whitney, 1972)

$$\mathbf{J} = \begin{bmatrix} \mathbf{e}_1 & \mathbf{e}_2 & \cdots & \mathbf{e}_n \\ \mathbf{e}_1 \times \mathbf{r}_1 & \mathbf{e}_2 \times \mathbf{r}_2 & \cdots & \mathbf{e}_n \times \mathbf{r}_n \end{bmatrix} \tag{3.7}$$

where $\mathbf{e}_i$ is the unit vector parallel to the axis of the ith revolute joint and $\mathbf{r}_i$ is the vector directed from any point on the same axis to the operation point P of the end-effector, as shown in Fig. 3.1. Furthermore, the ith column of $\mathbf{J}$ comprises the *normalized Plücker coordinates* of the ith axis of the manipulator (Hunt, 1978). It is worth mentioning that the entries of the Jacobian matrix are not dimensionally homogeneous. This is apparent as the associated Jacobian $\mathbf{J}$ maps the vector of joint rates with homogeneous units of *frequency* to the vector of Cartesian velocities with mixed units of *frequency* and *velocity*. This feature will be discussed further in the forthcoming sections.

3.2.2 Jacobian Evaluation

A compact method of evaluating vectors $\mathbf{e}_i$ and $\mathbf{r}_i$ comprising the entries of the Jacobian matrix is given next (Angeles, 1997). According to the DH notation, the position and orientation of the $(i+1)$st coordinate frame attached to the ith link with respect to the ith coordinate frame attached to the $(i-1)$st link is given by $\mathbf{Q}_i$ and $\mathbf{a}_i$ respectively. Expressed in the ith coordinate frame, these items take on the forms

$$\mathbf{Q}_i = \begin{bmatrix} \cos\theta_i & -\sin\theta_i\cos\alpha_i & \sin\theta_i\sin\alpha_i \\ \sin\theta_i & \cos\theta_i\cos\alpha_i & -\cos\theta_i\sin\alpha_i \\ 0 & \sin\alpha_i & \cos\alpha_i \end{bmatrix} \quad \mathbf{a}_i = \begin{bmatrix} a_i\cos\theta_i \\ a_i\sin\theta_i \\ b_i \end{bmatrix} \tag{3.8}$$

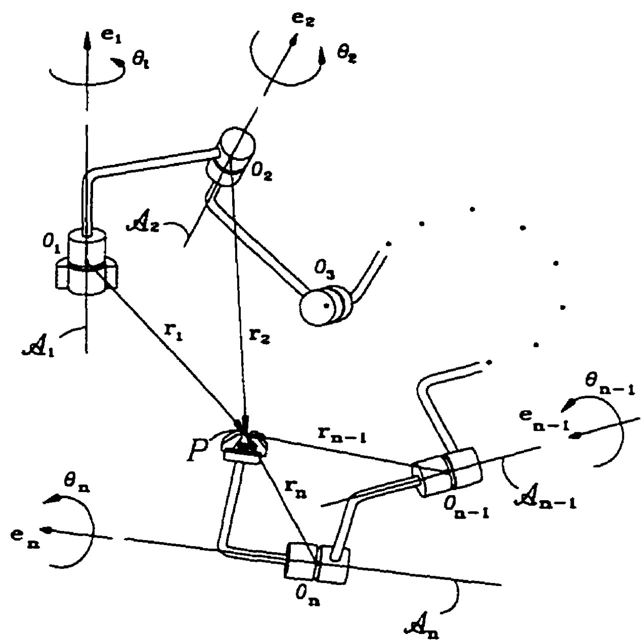

Figure 3.1: The basic notations for the Jacobian matrix

If the first joint axis of the manipulator is placed along the positive Z axis of the base frame of reference, then it can be shown that,

$$\begin{aligned} \mathbf{e}_1 &= [0 \quad 0 \quad 1]^T = \mathbf{z}^T \\ \mathbf{e}_2 &= \mathbf{Q}_1 \, \mathbf{z} \\ \mathbf{e}_3 &= \mathbf{Q}_1 \, \mathbf{Q}_2 \, \mathbf{z} \\ &\vdots \\ \mathbf{e}_n &= \mathbf{Q}_1 \, \mathbf{Q}_2 \cdots \mathbf{Q}_{n-1} \, \mathbf{z} \end{aligned}$$

the foregoing unit vectors thus being expressed in the base coordinate frame. If the frame of reference is taken as the first coordinate frame attached to the base of the robot, then the position vectors $\mathbf{r}_i$, with $i = 1, \cdots, n$ are determined from the following relations:

$$\mathbf{r}_n = \mathbf{P}_{n-1} \, \mathbf{a}_n$$

$$\begin{aligned}
\mathbf{r}_{n-1} &= \mathbf{P}_{n-2}\,\mathbf{a}_{n-1} + \mathbf{Q}_{n-1}\,\mathbf{r}_n \\
&\vdots \\
\mathbf{r}_2 &= \mathbf{P}_1\,\mathbf{a}_2 + \mathbf{Q}_2\,\mathbf{r}_3 \\
\mathbf{r}_1 &= \mathbf{P}_0\,\mathbf{a}_1 + \mathbf{Q}_1\,\mathbf{r}_2
\end{aligned}$$

where,

$$\begin{aligned}
\mathbf{P}_i &\equiv \mathbf{Q}_1\,\mathbf{Q}_2\,\mathbf{Q}_3 \cdots \mathbf{Q}_i \quad i = 1, 2, \cdots n \\
\mathbf{P}_0 &\equiv \mathbf{1}_{(3\times 3)}
\end{aligned}$$

When dealing with the Jacobian matrix, the partial derivatives of the entries of this matrix with respect to the entries of the vector of joint variables $\boldsymbol{\theta}$ are often needed. One example of this situation is when resolving the inverse kinematics at the acceleration level, where $\dot{\mathbf{J}}$ is needed. We can write

$$\dot{\mathbf{J}} = \sum_{i=1}^{n} \frac{\partial\,\mathbf{J}}{\partial\theta_i}\,\dot{\theta}_i$$

Hence, the partial derivatives of the entries of $\mathbf{J}$ with respect to $\boldsymbol{\theta}$ are needed to determine $\dot{\mathbf{J}}$. A similar situation arises when formulating an optimization problem whereby a Jacobian based performance measure is minimized, and thus, the partial derivatives of the entries of $\mathbf{J}$ with respect to the joint variables are needed.

Two very useful relations needed for determining these derivatives are given below:

$$\frac{\partial\,\mathbf{e}_j}{\partial\theta_i} = \begin{cases} \mathbf{e}_i \times \mathbf{e}_j & \text{if } i < j \\ 0 & \text{otherwise} \end{cases}$$

and

$$\frac{\partial\,\mathbf{r}_j}{\partial\theta_i} = \begin{cases} \mathbf{e}_i \times \mathbf{r}_j & \text{if } i \le j \\ \mathbf{e}_i \times \mathbf{r}_i & \text{otherwise} \end{cases}$$

3.3 Dexterity Measures

In this section, some of the main measures of conditioning and dexterity of robotic manipulators are reviewed, and comparisons between these measures are made.

3.3.1 Condition Number

Salisbury and Craig (1982) introduced the *2-norm condition number* of the Jacobian matrix as a measure of the kinetostatic performance of manipulators, i.e.,

$$\kappa(\mathbf{J}) = \frac{\sigma_{max}}{\sigma_{min}} \tag{3.9}$$

where, σ_{max} and σ_{min} are the maximum and the minimum singular values of $\mathbf{J}$, respectively. This measure was employed for an optimum design of planar positioning manipulators used for multi-fingered hands. As mentioned in Section (3.2.1), the Jacobian matrix is dimensionally inhomogeneous, and thus its singular values are also of mixed units. This makes the comparison of these numbers meaningless; in turn, this makes the condition number of the Jacobian matrix dependent on the units being used. In the following sections this feature of the condition number will be discussed in more detail; however, in a general sense, condition number quantifies the sensitivity of the Jacobian transformation with respect to directions. A detailed treatment of the condition number as applied to manipulator dexterity will also be discussed in the next chapter. Furthermore, the condition number of the Jacobian matrix depends on the location of the operation point of the end-effector whose motion is of interest. This is in contrast with some other measures to be discussed presently.

3.3.2 Manipulability

Manipulability $\mu(\mathbf{J})$ was defined as a measure of the kinetostatic performance by Yoshikawa (1985) as the square root of the determinant of the product of the Jacobian by its transpose, i.e.,

$$\mu = \sqrt{\det(\mathbf{J}\,\mathbf{J}^T)} \tag{3.10}$$

It can be shown that μ is in fact the product of the m singular values of the $m \times n$ Jacobian matrix for an n-axis manipulator, i.e,

$$\mu = \sigma_1 \sigma_2 \cdots \sigma_m$$

As shown in Angeles et al. (1992), μ as defined above is independent of the location of the operation point. Although there seems to be some disagreements among researchers on this feature as an advantage or a disadvantage, in this thesis, the aforementioned insensitivity of performance measure with respect to the location of the end-effector is considered as a disadvantage. In the following chapters a detailed discussion of the invariance features of the measure of dexterity is provided. Furthermore, it is a well-known fact that the determinant of a matrix can only be used to identify a singular matrix, and near-singularity and ill-conditioning of a matrix cannot necessarily be captured by the determinant. These facts are best illustrated with the aid of the following examples:

- for a square ($m \times m$) matrix $\mathbf{A}$, and a scalar s, we have

  $$\det(s\,\mathbf{A}) = s^m \det \mathbf{A}$$

  it is obvious that for the same matrix $\mathbf{A}$, the determinant can arbitrarily become large or small through scaling of the matrix by s.

- In the sense of kinematic inversion, and the accuracy and robustness with respect to errors, the following interesting example is provided (Tarantola, 1987). The solution of the following linear system

  $$\begin{bmatrix} 10 & 7 & 8 & 7 \\ 7 & 5 & 6 & 5 \\ 8 & 6 & 10 & 9 \\ 7 & 5 & 9 & 10 \end{bmatrix} \begin{bmatrix} x_1 \\ x_2 \\ x_3 \\ x_4 \end{bmatrix} = \begin{bmatrix} 32.0 \\ 23.0 \\ 33.0 \\ 31.0 \end{bmatrix}$$

is

$$\begin{bmatrix} x_1 \\ x_2 \\ x_3 \\ x_4 \end{bmatrix} = \begin{bmatrix} 1.0 \\ 1.0 \\ 1.0 \\ 1.0 \end{bmatrix}$$

while, with slightly perturbed data, namely,

$$\begin{bmatrix} 10 & 7 & 8 & 7 \\ 7 & 5 & 6 & 5 \\ 8 & 6 & 10 & 9 \\ 7 & 5 & 9 & 10 \end{bmatrix} \begin{bmatrix} x_1 \\ x_2 \\ x_3 \\ x_4 \end{bmatrix} = \begin{bmatrix} 32.1 \\ 22.9 \\ 33.1 \\ 30.9 \end{bmatrix}$$

the solution of the same system is

$$\begin{bmatrix} x_1 \\ x_2 \\ x_3 \\ x_4 \end{bmatrix} = \begin{bmatrix} 9.2 \\ -12.6 \\ 4.5 \\ -1.1 \end{bmatrix}$$

If the determinant were used to monitor the conditioning of the matrix above, this result would have seemed quite surprising since the determinant of this matrix is not *too small*; it is in fact equal to unity.

3.3.3 Minimum Singular Value

By comparing the condition number and the manipulability index, Klein and Blaho (1987) argued that the minimum singular value of **J** that appears in both of the aforementioned measures can be regarded as a faithful measure of accuracy and dexterity by its own right. It was argued that since the minimum singular value σ_{min} is more dominant near the singularities, it plays a more critical role when quantifying manipulator performance. It was further argued that σ_{min} forms the 2-norm of the pseudo-inverse part of eq. (3.3) and can be used as an upper bound on required joint velocities, i.e.,

$$||\dot{\mathbf{q}}|| \leq (1/\sigma_{min})\, ||\mathbf{t}||$$

It can be shown that σ_{min} is the minimum magnification that $\mathbf{J}$ can produce while mapping $\dot{\mathbf{q}}$ to the twist of the end-effector. The minimum singular value is also dependent on the location of the operation point of the end-effector. Although σ_{min} can be regarded as an important performance measure for monitoring the behaviour of the redundancy resolution schemes and rate controls, it will not be as applicable to the optimum kinematic design and global performance quantifications, since by itself $\sigma_{min}(= \|\mathbf{J}^{-1}\|)$ does not quantify *distance* to singularity; neither does it carry information about the maximum magnification that $\mathbf{J}$ can produce.

3.3.4 The Kinematic Conditioning Index

Based on the condition number of the manipulator Jacobian matrix, a global measure of dexterity called *the kinematic conditioning index*, or KCI, was introduced by Angeles and López-Cajún (1988, 1993). They argue that a conditioning measure should be unique and configuration independent; therefore, they proposed to find the minimum over all manipulator configurations of the condition number, i.e..

$$\kappa_m = \min_{\boldsymbol{\theta}} \kappa(\mathbf{J})$$

where $\boldsymbol{\theta}$ represents the set of joint variables that affect κ. The kinematic conditioning index KCI is thus defined as,

$$KCI \equiv \frac{100}{\kappa_m}\%$$

the KCI ranging between 0% and 100%, as the condition number ranges from infinity (singularities of the Jacobian) to its minimum value of unity (isotropy of the Jacobian). As shown in the following sections, since the reciprocal of the (p-norm) condition number of a matrix measures the p-norm distance of the matrix from the closest set of singular matrices, KCI, is in fact, a percentage of such a distance.

3.3.5 The Global Conditioning Index

A global performance index for optimization of manipulator architectures was proposed in Gosselin and Angeles (1991). This measure, called the Global Conditioning Index (GCI) is defined as the mean value of the variations of the reciprocal of the condition number throughout the workspace, i.e.,

$$GCI = \frac{\int_{\mathcal{W}}(\frac{1}{\kappa})\, dW}{\int_{\mathcal{W}} dW}$$

where κ is the condition number, $\mathcal{W}$ the manipulator workspace, and dW the volume element on $\mathcal{W}$. In the aforementioned reference, the GCI was used for the globally optimum design of a two-axis planar manipulator. It is quite interesting to note that the optimal solution for global conditioning turned out to be the one found by Salisbury and Craig (1982) while locally optimizing the condition number. The equivalence of the local and global conditioning for the planar two-axis manipulator was shown in Gosselin and Angeles by directly carrying out the double integration in the joint space of the robot. Extending this technique to the spatial case is a formidable task, but it should be used to investigate whether this appealing feature extends to spatial manipulators as well or not.

3.3.6 Physical Workspace

Motion capabilities of rigid bodies attached to the end-effector of serial manipulators were quantified using the Euclidean group of rigid-body motions and its semi-Riemannian structures by Basavaraj and Duffy (1993). In this reference, the measure derived is called *the physical workspace* of the manipulator, while emphasis has been placed on the invariance of this measure with respect to the location of the fixed and moving frames, type and number of joints, and the scaling of the manipulator. It can be shown that this volume form is the square root of the determinant of the product $\mathbf{J}\,\mathbf{J}^T$, where, $\mathbf{J}$ is the Jacobian matrix of the manipulator with its last link excluded.

3.3.7 Kinematic Distortion

Park and Brockett (1994) made use of the left-invariant metric of SE(3) to quantify the amount of *distortion* that the forward kinematic map

$$f : \mathcal{N} \rightarrow \mathcal{W}$$

produces while mapping the joint space $\mathcal{N}$ into the manipulator workspace $\mathcal{W}$. Using the left-invariance nature of that metric, this dexterity measure is invariant with respect to base-coordinate changes, but it does depend on the end-effector coordinate changes. The integral of the distortion measure over the entire workspace produces an indication of how distorted or "non-flat", the workspace of the robot is, but it does not quantify local dexterity. The *distortion density* is defined as

$$d(f) = \frac{1}{2}\mathrm{tr}(\mathbf{J}^T \, \mathbf{G} \, \mathbf{J} \, \mathbf{H}^{-1})$$

while the *global kinematic distortion* is defined as

$$D(f) = \int_N d(f) \, \Omega_N \tag{3.11}$$

with $\mathbf{H}$ and $\mathbf{G}$ defined as the Riemannian metrics on $\mathcal{N}$ and $\mathcal{W}$, respectively. Moreover, Ω_N is the volume element in $\mathcal{N}$ induced from its metric $\mathbf{H}$. Clearly, $d(f)$ being a function of $\mathbf{J}$ only, and not of $\mathbf{J}^{-1}$, it does not quantify the local invertibility of $\mathbf{J}$, and thus, neither does $d(f)$ quantify the local dexterity of the manipulator at hand.

3.4 Invariance Properties of Dexterity Measures

The issue of the invariance properties of the dexterity measures has been the subject of numerous research papers, e.g., Paden and Sastry (1988), Li (1990), Dotty et al. (1992), Basavaraj and Duffy (1993), and Park and Brockett (1994).

These research works are mainly concerned with invariance of dexterity measures with respect to units, the base and the moving coordinate frames.

3.4.1 Invariance with Respect to Physical Units

It is usually required that a performance measure that is used for comparison of different systems be independent of the physical units used. For example, the performance of a robot should not change if one switches from the *SI* to the *Imperial System* of units. The entries of the Jacobian matrix having mixed dimensions, the set of singular values of $\mathbf{J}$ are also of mixed units. In order to overcome this inhomogeneity, normalizing lengths have been introduced to make the Jacobian dimensionally homogeneous, e.g., (Angeles and López-Cajún 1988; 1993). This is achieved by dividing the last three rows of the matrix by a *characteristic length* associated with the manipulator. If we denote this normalizing length by L then the normalized Jacobian matrix—hereafter denoted by $\bar{\mathbf{J}}$—takes on the form,

$$\bar{\mathbf{J}} = \begin{bmatrix} \mathbf{e}_1 & \mathbf{e}_2 & \cdots & \mathbf{e}_n \\ \frac{1}{L}\mathbf{e}_1 \times \mathbf{r}_1 & \frac{1}{L}\mathbf{e}_2 \times \mathbf{r}_2 & \cdots & \frac{1}{L}\mathbf{e}_n \times \mathbf{r}_n \end{bmatrix} \tag{3.12}$$

There has been some discussion and criticism on the choice of this characteristic length, its physical interpretations and its invariance with respect to coordinate frames in the literature, e.g. (Dotty et al., 1992). In the following chapters we will provide a normalizing length that has a geometrical interpretation, and that is unique for a given manipulator and independent of the choice of coordinate frame.

3.4.2 Invariance with Respect to the Base and Moving Coordinate Frames

The invariance of a physically meaningful performance measure on the choice of the base coordinate frame is imperative and all of the proposed measures conform with this requirement. What is not immediate is the dependence of a dexterity measure on the choice of the moving coordinate frame attached to the end-effector. As discussed by Park and Brockett (1994), the underlying common ground for invariance features of dexterity measures lies in that the group of rigid-body motions, SE(3), does not possess a *bi-invariant* (or *translation-invariant*) induced Riemannian metric, while it does admit a *left translation-invariant* Riemannian metric as well as a bi-invariant volume form.

Paden and Sastry (1988) argue that a measure of *work-volume* that is based on the bi-invariant volume form of SE(3) should be considered to quantify the performance of manipulators, since such a measure does not depend on the size of the hand attached to the robot. They argued that such a measure will be useful in designing general-purpose manipulators, *disregarding* the size or shape of the end-effector needed for specific tasks. The same volume form is used for introducing the *physical workspace* by Basavaraj and Duffy (1993)[2].

In comparing *condition number*, the *manipulability*, and the *minimum singular value*, Li (1990) argued that the condition number and the minimum singular value of the Jacobian matrix depend on the size of the hand, i.e., the location of the *operation point* P, of the end-effector. By operation point it is meant a point of the end-effector on which the Jacobian definition is based[3]. Furthermore, as a proponent of translation-invariant dexterity measures, Li argues that, if the dexterity measure used is not translation-invariant, then there will exist preferred robot postures by this measure, for different end-effector points; this, he maintains, is *inconsistent* and undesirable. It is then concluded that, since the Jacobian determinant is independent of the location of the operation point, the determinant-based manipulability index μ is preferred over the condition number, while measuring the performance of a robotic arm.

The kinematic distortion introduced by Park and Brockett (1994) is also based on the left-invariant metric, and thus, is invariant with respect to base-coordinate changes, but it does depend on end-effector coordinate changes.

Based on these views, it seems that there is a subtle but fundamental disagreement

[2]The authors were apparently not aware of the extensive work of Paden and Sastry in 1988, in using the volume form of SE(3).

[3]The operation point P defined here is not to be confused with the *operating point* that was used in Li (1990) to denote the posture of the robot specified by its set of joint variables.

among researchers in defining manipulator dexterity. On the one hand, for example, Paden and Sastry (1988), Basavaraj and Duffy (1993), and Li (1990) believe that the end-effector of a robot should be excluded while analyzing the kinetostatic performance of the manipulator. More specifically, they argue that a faithful performance measure for the manipulator should be *insensitive* to the location of any operation point of the end-effector. On the other hand, approaches such as those of Park and Brockett (1994), Singh and Rastegar (1995), Tandirci et al. (1992), regard the end-effector as an integral element of the manipulator, because it is with the use of this device that any manipulator task is performed. In other words, if the size of the end-effector can affect the dexterity, why exclude its effects in the analysis and design?

In summary, there currently exist two views on how manipulator dexterity should be defined, namely,

(**a**) Manipulator performance should be quantified without considering either the end-effector or any of its points.

(**b**) The operation point, or a preferred point of the end-effector whose motion is of interest, should be regarded as an intrinsic element of the manipulator, and thus, its effects on dexterity of the arm should be considered.

As a means of combining these two approaches, one can ask the questions below:

- Is there a preferred point of the end-effector, in measuring manipulator dexterity and accuracy, that could be used to relate joint rates with the end-effector twist?

In this thesis, both (**b**) and the above question are addressed by introducing a method of determining a preferred point of the end-effector with respect to which the Jacobian matrix is optimally conditioned. Also introduced in this thesis is a method for determining a preferred posture of the manipulator that is useful for task-placement or manipulator-placement (Chapter 6).

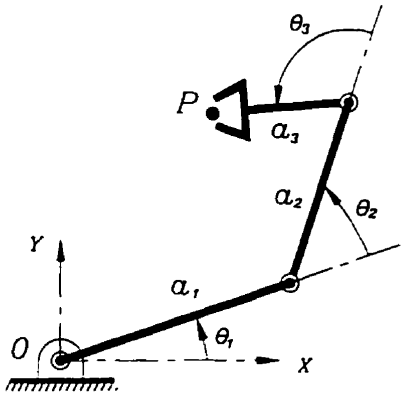

Figure 3.2: Planar 3R manipulator for positioning-and-orienting tasks

3.4.3 Illustrative Examples

The effects of the location of the operation point on the dexterity and reachability of robotic manipulators are further examined through three simple examples: First, let us consider planar manipulators for positioning-and-orienting tasks, Fig. 3.2. In Fig. 3.3, two manipulators are shown, together with their corresponding reachable, dextrous, and physical workspaces. Precise definitions of reachable and dextrous workspaces are available in Paden and Sastry (1988), while the physical workspace is discussed in Basavaraj and Duffy (1993). If the end-effector is not considered as an intrinsic element of the manipulator, then the two manipulators shown in Figs. 3.3*a* and 3.3*b* are to be considered identical. That is, in the sense of the operation-point-invariant workspace measure such as the physical workspace, denoted by $\mathcal{W}_P$, the two manipulators are one and the same. However, in the sense of reachable and dextrous workspaces, denoted by $\mathcal{W}_D$ and $\mathcal{W}_R$, they are quite different. Although the invariance of $\mathcal{W}_P$ in the group of planar motions is a theoretically attractive feature, for any practical application of the two robots shown in Figs. 3.2, changing the end-effector size has a direct effect on both the dexterity and the reachability of the manipulator. If this effect is not considered at the design stage, it will have to be taken into account when a task is planned, or when an end-effector is to be designed for the task.

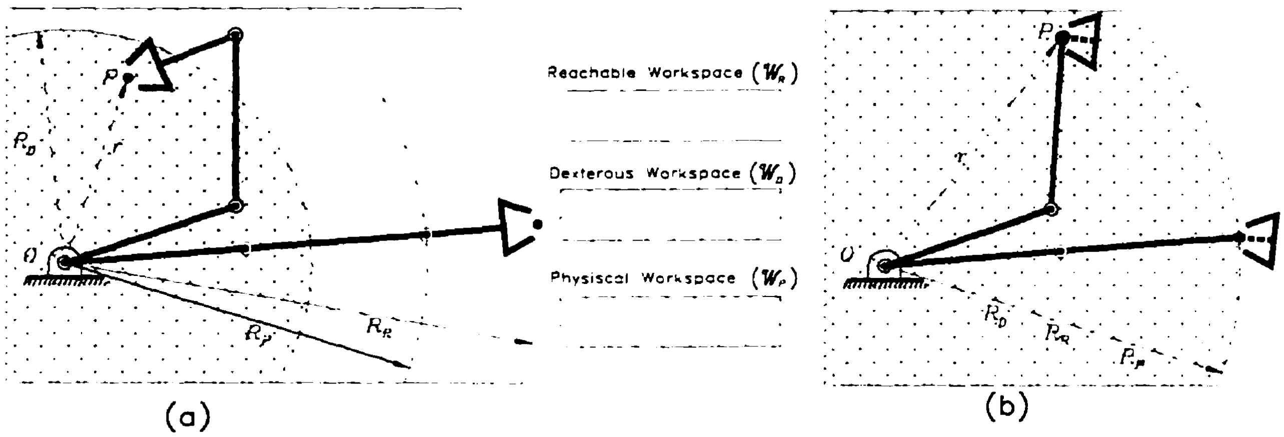

Figure 3.3: Reachable, dextrous and physical workspaces of a manipulator with two different end-effectors

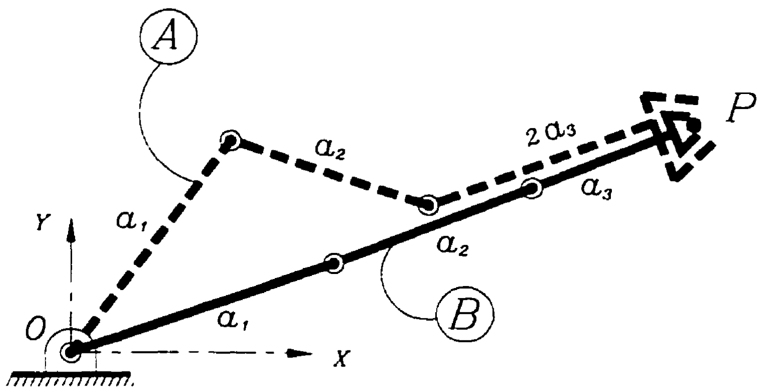

Figure 3.4: Comparison of identical manipulators in the sense of invariant volume measures

As a second example, let us compare the two manipulators A and B shown in Fig. 3.4. Once again, these manipulators are equivalent in the sense of invariant volume measures. However, if the anchor point O of the robot as well as point P, at which the robot is to perform a positioning and orienting task, are given by the task, then it is apparent that the two robots A and B behave very differently for this application. Indeed, manipulator A is at a relatively dextrous posture, while manipulator B is at its clumsiest configuration possible, where neither accuracy nor dexterity is within reach.

As a third example, consider the natural motor activities of human beings. From every day experience we can appreciate that, as we interact with our environment by means of tools of different sizes and shapes, we learn how to manipulate each of these objects in a rather *comfortable* (preferred) posture. We know how to adjust our postures if we are forced to play ping-pong with a racket whose handle is unusually long, or, if we are to draw or write with a long pencil, holding it from the far end. Despite the ability of making the foregoing adjustments, one will play a very different ping-pong game with the long racket, from one with a normal-size racket. Likewise, the quality of the hand-writing achieved with a long pencil will be significantly influenced by the location at which we hold the pencil.

As will be shown in Chapter 6, a manipulator has a uniquely defined preferred point of operation at which it achieves maximum dexterity. By characterizing robot performance as its dexterity with respect to this preferred point, one obtains an intrinsic measure of manipulator performance that is independent of the actual hand geometry. In contrast to translation-invariant measures, this intrinsic performance measure also quantifies the "distance" of a robot from critical points, and tells the designer where to place the tool in order to attain an optimum performance. Thus, it is believed that this kind of performance measure is more practical for robot work-cell design than those measures in which the aforementioned influences are filtered out.

3.5 Conclusions

In this chapter, a detailed review of the proposed dexterity measures for robot manipulators was provided. Basic properties of some of these measures were discussed, and comparisons were made. Particular attention was given to the invariance properties of these measures with respect to physical units and with respect to the base and moving coordinates frames of the manipulator. Although invariance with respect to physical units, and base-coordinate frames are well agreed upon by all contributors to the subject, there seems to be two opposing views on the requirement of the invariance of the dexterity measures with respect to the reference point (the operation point) of the end-effector. With the aid of several examples it was proposed that a faithful measure of kinetostatic dexterity should take advantage of the effects of the operation point.

Chapter 4

Condition Number as a Measure of Kinetostatic Performance

4.1 Introduction

Having established the main features of different dexterity measures in the previous Chapter, the attention of the thesis will be focused on the condition number of the manipulator Jacobian matrix in this chapter. The condition number of the Jacobian matrix, as applied to manipulator dexterity assessments, is discussed in detail. The notion of isotropic transformations and isotropic manipulators will also be reviewed. Geometric interpretations of isotropy of linear transformations will then be provided. In the last three sections of the Chapter, the isotropic design of nonredundant manipulators is discussed, where some of the contributions of the thesis are discussed, namely a geometric interpretation of the isotropy of 2-R planar manipulators. It will also be shown that although the Frobenius-norm condition number is a smooth function of the joint variables, the two-norm condition number is not smooth at the isotropic point.

4.2 Condition Numbers

Almost all of the measures of dexterity share the same common ground: losing dexterity and approaching a singularity (of the Jacobian matrix) are closely related phenomena. To quantify the dexterity in this context—recalling that the Jacobian matrix associated with the manipulator is the linear transformation mapping the vector of joint rates into the *twist* of the end-effector—we primarily have to monitor how *far* the Jacobian matrix is from a singularity.

4.2.1 Condition Number and Distance to Singularity

One of the most important features of the condition number of linear transformations is that it quantifies *distance* to the closest singularities. Strictly speaking, the p-norm condition number of an $n \times n$ matrix $\mathbf{A}$, or, $\kappa_p(\mathbf{A})$, measures the relative p-norm distance from $\mathbf{A}$ to the set of singular matrices (Golub and Van Loan, 1989), i.e,

$$\frac{1}{\kappa_p(\mathbf{A})} = \min_{\mathbf{E}} \frac{\|\mathbf{E}\|_p}{\|\mathbf{A}\|_p}$$

$$\text{subject to}: \quad \det(\mathbf{A} + \mathbf{E}) = 0$$

Once again, the *distance* from a matrix to the set of singularities cannot be captured by its determinant, as shown by the following two examples taken from (Golub and Van Loan, 1989): The matrix $\mathbf{B}_n$ defined by

$$\mathbf{B}_n \equiv \begin{bmatrix} 1 & -1 & \cdots & -1 \\ 0 & 1 & \cdots & -1 \\ \vdots & \vdots & \ddots & \vdots \\ 0 & 1 & \cdots & -1 \end{bmatrix} \in \mathbb{R}^{n\times n} \tag{4.1}$$

belongs to the unimodular groups, i.e., its determinant is identity , whereas $\kappa_\infty(\mathbf{B}_n) = n\,2^{n-1}$. Also, for

$$\mathbf{D}_n = \mathrm{diag}(10^{-1}, \cdots, 10^{-1}) \in \mathbb{R}^{n\times n} \tag{4.2}$$

we have, $\kappa_p(\mathbf{D}_n) = 1$, although $\det(\mathbf{D}_n) = 10^{-n}$. Hence, it is concluded that the condition number of the Jacobian matrix is the best suited tool for measuring the distance of the manipulator configuration (locally represented by its Jacobian matrix) to the closest singular configuration.

4.2.2 Condition Number and Sensitivity of Linear Systems to Perturbations

Besides characterizing distance to singularities, the condition number of a matrix defines bounds on the error magnifications while solving linear systems of equations. In fact, the basic definition of the condition number has naturally evolved while analyzing the sensitivity of linear systems (Golub and Van Loan, 1989; Watkins, 1991).

- Square Matrices: (nonredundant manipulators)

For nonredundant manipulators, if $\dot{\mathbf{q}}$ is the exact solution of the non-singular instantaneous kinematics equation

$$\mathbf{J}\,\dot{\mathbf{q}} = \mathbf{t}$$

then, for a perturbed system,

$$(\mathbf{J} + \delta\mathbf{J})\,(\dot{\mathbf{q}} + \delta\dot{\mathbf{q}}) = (\mathbf{t} + \delta\mathbf{t}), \tag{4.3}$$

It can be shown that the relative error in the solution, $||\delta\dot{\mathbf{q}}||/||\dot{\mathbf{q}}||$, due to relative errors $||\delta\mathbf{J}||/||\mathbf{J}||$ and $||\delta\mathbf{t}||/||\mathbf{t}||$ in the data, is bounded by the following inequality

$$\frac{||\delta\dot{\mathbf{q}}||}{||\dot{\mathbf{q}}||} \leq \kappa(\mathbf{J})\,(\frac{||\delta\mathbf{J}||}{||\mathbf{J}||} + \frac{||\delta\mathbf{t}||}{||\mathbf{t}||}) + O(\epsilon^2) \tag{4.4}$$

with $O(\epsilon^2)$ denoting higher order error terms.

- Underdetermined Systems: (instantaneous kinematics of redundant manipulators)

In this case, we have $\mathbf{J} \in \mathbb{R}^{m \times n}$ with $m \leq n$. Assuming that $\mathbf{J}$ is of full rank, and $\delta\mathbf{J}$ is the perturbation of $\mathbf{J}$, with $\delta\mathbf{t}$ being the perturbation of $\mathbf{t}$, then the relative errors in $\mathbf{J}$ and $\mathbf{t}$ are denoted by,

$$\epsilon_J \equiv \frac{||\delta\mathbf{J}||}{\mathbf{J}} \quad \epsilon_{\mathbf{t}} \equiv \frac{||\delta\mathbf{t}||}{\mathbf{t}}, \tag{4.5}$$

respectively. Now, if

$$\epsilon = \max\{\epsilon_J, \epsilon_{\mathbf{t}}\} < \sigma_{max}(\mathbf{J})$$

Then,

$$\frac{||\delta\mathbf{t}||_2}{||\mathbf{t}||_2} \leq \kappa_2(\mathbf{J})(\epsilon_J \min\{2, n-m+1\} + \epsilon_{\mathbf{t}}) + O(\epsilon^2) \tag{4.6}$$

- Overdetermined Systems: (statics of redundant manipulators)

The static variable transformation for redundant manipulators that leads to an overdetermined system of equations is first recalled:

$$\mathbf{J}^T\mathbf{w} = \boldsymbol{\tau}$$

In this situation, $\mathbf{J}^T \in \mathbb{R}^{n \times m}$, $\boldsymbol{\tau} \in \mathbb{R}^n$, and $\mathbf{w} \in \mathbb{R}^m$. In general, the foregoing equation does not have any exact solution, however, there is always one approximate solution in the least squares sense. It has been shown (Golub and Van Loan, 1989) that if the data are perturbed such that

$$(\mathbf{J}^T + \delta\mathbf{J}^T)(\mathbf{w} + \delta\mathbf{w}) = (\boldsymbol{\tau} + \delta\boldsymbol{\tau})$$

then the perturbed least-square solution to the foregoing equation verifies the following inequality

$$\frac{||\delta\mathbf{w}||}{\mathbf{w}} \leq \epsilon\{\frac{2\kappa_2(\mathbf{J})}{\cos(\theta)} + \tan(\theta)\,\kappa_2^2(\mathbf{J})\} + O(\epsilon^2) \tag{4.7}$$

where θ, (with $0 \leq \theta \leq \pi/2$), is the angle made between the vector of data $\boldsymbol{\tau}$ and the range of $\mathbf{J}^T$. Furthermore, we have

$$\epsilon \equiv \max\{\frac{||\delta\mathbf{J}||_2}{||\mathbf{J}||_2}, \frac{||\delta\boldsymbol{\tau}||_2}{||\boldsymbol{\tau}||_2}\} \leq \frac{\sigma_{max}}{\sigma_{min}}$$

and

$$\sin(\theta) = \frac{\|\mathbf{J}^T \mathbf{w}_0 - \boldsymbol{\tau}\|_2}{\|\boldsymbol{\tau}\|_2} \neq 1$$

with $\mathbf{w}_0$, the least-square solution being defined as,

$$\mathbf{w}_0 = (\mathbf{J}\,\mathbf{J}^T)^{-1}\,\mathbf{J}\,\boldsymbol{\tau}$$

An interesting observation on the foregoing characterization of the sensitivity of the detemined, underdetermined and overdetermined systems of linear equations is the fact that, for *zero-residual* cases, i.e., the determined and the underdetermined systems, the sensitivity is linear in $\kappa_2(\mathbf{J})$, whereas for the *nonzero-residual* problems such as the overdetermined system, the sensitiviety is a function of the square of the condition number.

In the context of manipulator kinetostatic, the foregoing sensitivity analysis is reflected through the sensitivity and robustness with respect to which the the kinematic and static relations are resolved. Numerical examples that underline the aforementioned sensitivity and robustness while resolving the redundancy of positioning manipulators are examined in Arenson (1997). Furthermore, a theoretical investigation of the sensitivity of redundant manipulators postures with respect to changes in the Cartesian trajectories is discussed in Angeles et al. (1996), where the overall sensitivity is shown to be independent of the particular secondary tasks that are usually augmented to the main desired task and is only a function of the condition number of the associated Jacobian matrix devided by the norm of this matrix.

Having identified manipulator dexterity and accuracy with the condition number of $\mathbf{J}$, we have, on the one hand, *ill-conditioning* and singularities of $\mathbf{J}$ and, on the other hand, *well-conditioning* and *isotropy* of $\mathbf{J}$. It is recalled that isotropic matrices are those whose condition numbers attain the minimum value of unity.

A discussion of the *theory of condition* associated with general transformations is given by Rice (1966), while the condition number of matrices is discussed in detail in the specialised literature, e.g., in Golub and Van Loan (1989). For square matrices $\mathbf{A} \in \mathbb{R}^{m\times m}$, we have:

$$\kappa_p(\mathbf{A}) = ||\mathbf{A}||_p \, ||\mathbf{A}^{-1}||_p \tag{4.8}$$

Clearly, κ is norm-dependent, but, any two condition numbers $\kappa_\alpha(\cdot)$ and $\kappa_\beta(\cdot)$ on $\mathbb{R}^{m\times m}$, are equivalent in that constants c_1 and c_2 can be found for which

$$c_1\, \kappa_\alpha(\mathbf{A}) \leq \kappa_\beta(\mathbf{A}) \leq c_2\, \kappa_\alpha(\mathbf{A}) \quad \mathbf{A} \in \mathbb{R}^{m\times m}.$$

4.3 Matrix Norms

In this section some of the basic definitions and properties of matrix norms are reviewed (Golub and Van Loan, 1989; Watkins, 1991; Householder, 1964). A matrix norm $||\cdot||$ is a function that assigns to each of its matrix argument $(\cdot)$ a real number called the norm of the matrix, with the following three properties: For all $\mathbf{A}$, $\mathbf{B} \in \mathbb{R}^{m\times n}$, and $\alpha \in \mathbb{R}$,

$$(i) \quad ||\mathbf{A}|| > 0, \text{if} \mathbf{A} \neq \mathbf{0} \tag{4.9a}$$

$$(ii) \quad ||\alpha\, \mathbf{A}|| = |\, \alpha \,|\; ||\mathbf{A}|| \tag{4.9b}$$

$$(iii) \quad ||\mathbf{A} + \mathbf{B}|| \leq ||\mathbf{A}|| + ||\mathbf{B}|| \tag{4.9c}$$

Any real-valued matrix function satisfying the foregoing three properties is considered a matrix norm. A fourth property, called the *consistency* property, which is a generalization of the *Cauchy-Schwartz* inequality for matrices (Householder, 1964), is also defined, i.e.,

$$||\mathbf{A}\, \mathbf{B}|| \leq ||\mathbf{A}||\, ||\mathbf{B}|| \tag{4.10}$$

Not all matrix norms are consistent; however, the F-norm (the matrix Euclidean norm) is a consistent norm. As explained in Householder (1964), the notion of consistency stems from the relations between the matrix norms and vector norms. That is, if any matrix norm $||\mathbf{A}||$ and any vector norm $||\mathbf{x}||$ satisfy the following inequality

$$||\mathbf{A}\, \mathbf{x}|| \leq ||\mathbf{A}||\, ||\mathbf{x}||$$

then the two norms are said to be consistent. For example, the vector Euclidean norm and the matrix Euclidean norm (also called the Frobenius norm) are consistent.

- The Frobenius norm $\|\cdot\|_F$ is defined by:

$$\|\mathbf{A}\|_F = \sqrt{\mathrm{tr}(\mathbf{A}\,\mathbf{A}^T)} = \sqrt{\sum_{i=1}^{m}\sum_{j=1}^{n} a_{ij}^2} \tag{4.11}$$

where tr$(\cdot)$ is the trace of its matrix argument. Moreover, in general, not any matrix norm qualifies as an upper bound for the matrix when regarded as a linear transformation (Householder, 1964). The Frobenius norm of a matrix, as defined above, is one such example. Although the least upper bound of the $m \times m$ identity transformation is equal to one, i.e., $\mathrm{lub}(\mathbf{I}_{m\times m}) = 1$, from the foregoing definition of the Frobenius norm follows that $\|\mathbf{I}_{m\times m}\|_F = m^{\frac{1}{2}}$. In this thesis a normalized form of the Frobenius norm will be used so that the norm of the identity matrices will be the identity, regardless of their dimensions. This is achieved at the expense of violating the consistency property of the Frobenius-norm.

- The normalized-Frobenius norm $\|\cdot\|_{\hat{F}}$ is defined by:

$$\|\mathbf{A}\|_{\hat{F}} = \sqrt{\frac{1}{k}\,\mathrm{tr}(\mathbf{A}\,\mathbf{A}^T)} \tag{4.12}$$

with $k \equiv \min\{m, n\}$. Hence,

$$\|\mathbf{A}\|_{\hat{F}} = k^{-\frac{1}{2}}\|\mathbf{A}\|_F \tag{4.13}$$

As shown presently, the normalized F-norm is no longer a consistent norm. This is demonstrated by proving the following inequality, which is indeed the reverse of the consistency inequality given by (4.10) with $\mathbf{B}$ being replaced by $\mathbf{A}^T$:

$$\|\mathbf{A}\,\mathbf{A}^T\|_{\hat{F}} > \|\mathbf{A}\|_{\hat{F}}\,\|\mathbf{A}^T\|_{\hat{F}} = \|\mathbf{A}\|_{\hat{F}}^2$$

Let

$$\mathbf{u} \equiv [a_1 \quad a_2 \quad \cdots \quad a_m]^T \in \mathbb{R}^m, \quad \text{and} \quad \mathbf{v} \equiv [1 \quad 1 \quad \cdots \quad 1]^T \in \mathbb{R}^m$$

then, from the Cauchy-Schwartz inequality for the Euclidean norms of vectors, we have

$$\mathbf{u}^T \mathbf{v} \leq ||\mathbf{u}|| \, ||\mathbf{v}||$$

or

$$(a_1 + a_2 + \cdots a_m) \leq \sqrt{m\,(a_1^2 + a_2^2 + \cdots a_m^2)}$$

Now, if a_i is considered to be the ith eigenvalue of the matrix product $\mathbf{A}\,\mathbf{A}^T$, then the foregoing inequality can be rewritten as

$$\mathrm{tr}(\mathbf{A}\,\mathbf{A}^T) \leq \sqrt{k\,\mathrm{tr}[(\mathbf{A}\,\mathbf{A}^T)^2]},$$

or

$$\frac{1}{k}\,\mathrm{tr}(\mathbf{A}\,\mathbf{A}^T) \leq \sqrt{\frac{1}{k}\,\mathrm{tr}[(\mathbf{A}\,\mathbf{A}^T)^2]}$$

hence,

$$||\mathbf{A}||_{\bar{F}}^2 = ||\mathbf{A}||_{\bar{F}}\,||\mathbf{A}^T||_{\bar{F}} \leq ||\mathbf{A}\,\mathbf{A}^T||_{\bar{F}} \tag{4.14}$$

which is the reverse of the consistency property, thereby proving that the $\bar{F}$-norm is not a consistent norm.

The foregoing inequality will be employed in Chapter 6 when a novel measure of conditioning is introduced.

- Every vector p-norm on $\mathbb{R}^n$ can be used to define a matrix norm on $\mathbb{R}^{m\times n}$ by,

$$||\mathbf{A}||_p = \max_{\mathbf{x}\neq 0} \frac{||\mathbf{A}\,\mathbf{x}||_p}{||\mathbf{x}||_p}$$

the geometric interpretation of $||\mathbf{A}||_p$ thus defined is that it characterizes the maximum magnification that the matrix $\mathbf{A}$ will produce when mapping a vector $\mathbf{x} \in \mathbb{R}^n$ to its image $\mathbf{y} \in \mathbb{R}^m$. Moreover, for square matrices $\mathbf{A} \in \mathbb{R}^{n\times n}$, we have

$$||\mathbf{A}||_p = \frac{1}{||\mathbf{A}^{-1}||_p}$$

□ The one-norm, defined for $p = 1$, is

$$||\mathbf{A}||_1 = \max_{1\leq j\leq n} \sum_{i=1}^{m} |\, a_{ij}\,|$$

□ The infinity-norm, defined for $p = \infty$, is in turn,

$$\|\mathbf{A}\|_\infty = \max_{1 \le i \le m} \sum_{j=1}^{n} | a_{ij} |$$

- Some of the important properties of matrix norms are

$$\|\mathbf{A}\|_2 \le \|\mathbf{A}\|_F \le \sqrt{n}\,\|\mathbf{A}\|_2 \tag{4.15a}$$
$$\frac{1}{\sqrt{m}}\,\|\mathbf{A}\|_2 \le \|\mathbf{A}\|_{\hat{F}} \le \sqrt{\frac{n}{m}}\,\|\mathbf{A}\|_2 \tag{4.15b}$$
$$\max_{i,j} | a_{ij} | \le \|\mathbf{A}\|_2 \le \sqrt{m\,n}\,\max_{i,j} | a_{ij} | \tag{4.15c}$$
$$\frac{1}{\sqrt{n}}\|\mathbf{A}\|_\infty \le \|\mathbf{A}\|_2 \le \sqrt{m}\|\mathbf{A}\|_\infty \tag{4.15d}$$
$$\frac{1}{\sqrt{m}}\|\mathbf{A}\|_1 \le \|\mathbf{A}\|_2 \le \sqrt{n}\|\mathbf{A}\|_1 \tag{4.15e}$$

4.4 Matrix Condition Numbers

From eq. (4.8), which is the basic definition of the matrix condition number, the 2-norm and the F-norm condition numbers, κ_2 and κ_F for $m \times m$ square matrices, take on the forms

$$\kappa_2(\mathbf{A}) = \frac{\sigma_{max}}{\sigma_{min}} = \sqrt{\frac{\lambda_{max}}{\lambda_{min}}} \tag{4.16}$$

and

$$\kappa_F(\mathbf{A}) = \sqrt{\mathrm{tr}(\mathbf{A}\,\mathbf{A}^T)\,\mathrm{tr}[(\mathbf{A}\,\mathbf{A}^T)]^{-1}} \tag{4.17}$$

σ_{max} and σ_{min} being, respectively, the maximum and the minimum singular values of $\mathbf{A}$, λ_{max} and λ_{min} being the maximum and minimum eigenvalues of $\mathbf{A}\,\mathbf{A}^T$, respectively. From the definition of the normalized-Frobenius norm, it follows that

$$\kappa_{\hat{F}}(\mathbf{A}) = \frac{1}{m}\sqrt{\mathrm{tr}(\mathbf{A}\,\mathbf{A}^T)\,\mathrm{tr}[(\mathbf{A}\,\mathbf{A}^T)]^{-1}} \tag{4.18}$$

Hence,

$$\kappa_F = \sqrt{m}\,\kappa_{\hat{F}} \tag{4.19}$$

For a rectangular matrix $\mathbf{A} \in \mathbb{R}^{m \times n}$ we can rewrite eq. (4.8) as,

$$\kappa(\mathbf{A}) = \|\mathbf{A}\| \, \|\mathbf{A}^{\dagger}\| \tag{4.20}$$

where, $\mathbf{A}^{\dagger}$ is any appropriate generalized inverse of $\mathbf{A}$. It will be shown presently that using the generalized inverse, eq. (4.18) can be applied to general rectangular matrices as well as to square matrices.

- overdetermined systems: $\mathbf{A} \in \mathbb{R}^{n \times m}$ with $m \leq n$,

$$\begin{aligned}
\kappa_{\hat{F}}(\mathbf{A}) &= \|\mathbf{A}\|_{\hat{F}} \, \|(\mathbf{A}^T \mathbf{A})^{-1} \mathbf{A}^T\|_{\hat{F}} \\
\kappa_{\hat{F}}(\mathbf{A}) &= \sqrt{\frac{1}{m}\mathrm{tr}\,(\mathbf{A}\,\mathbf{A}^T)} \sqrt{\frac{1}{m}\mathrm{tr}[(\mathbf{A}^T \mathbf{A})^{-1} \mathbf{A}^T \mathbf{A} (\mathbf{A}^T \mathbf{A})^{-1}]} \\
\kappa_{F} &= \frac{1}{m}\sqrt{\mathrm{tr}(\mathbf{A}\,\mathbf{A}^T)\,\mathrm{tr}[(\mathbf{A}\,\mathbf{A}^T)^{-1}]}
\end{aligned} \tag{4.21}$$

  which is the same expression as that of eq. (4.18) given for square matrices.

- underdetermined systems: $m \leq n$,

$$\begin{aligned}
\kappa_{\hat{F}}(\mathbf{A}) &= \|\mathbf{A}\|_{\hat{F}} \, \|\mathbf{A}^T (\mathbf{A}\,\mathbf{A}^T)^{-1}\|_{\hat{F}} \\
\kappa_{\hat{F}}(\mathbf{A}) &= \sqrt{\frac{1}{m}\mathrm{tr}(\mathbf{A}\,\mathbf{A}^T)} \sqrt{\frac{1}{m}\mathrm{tr}[\mathbf{A}^T (\mathbf{A}\,\mathbf{A}^T)^{-1} (\mathbf{A}\,\mathbf{A}^T)^{-1} \mathbf{A}]} \\
\kappa_{F} &= \frac{1}{m}\sqrt{\mathrm{tr}(\mathbf{A}\,\mathbf{A}^T)\,\mathrm{tr}[(\mathbf{A}\,\mathbf{A}^T)^{-1}]}
\end{aligned} \tag{4.22}$$

The foregoing equation is also the same as eq. (4.18) given for square matrices. Some other useful properties of condition numbers in general are:

$$\kappa(\mathbf{A}) = \kappa(\mathbf{A}^{-1}), \quad \text{independent of the norm used} \tag{4.23a}$$

$$\kappa(\mathbf{A}) = \kappa(\mathbf{A}^T), \quad \text{for F- or 2-norms} \tag{4.23b}$$

$$\kappa_{\infty}(\mathbf{A}) = \kappa_1(\mathbf{A}^T) \tag{4.23c}$$

$$\kappa_2(\mathbf{A}\,\mathbf{A}^T) = \kappa_2^2(\mathbf{A}) \tag{4.23d}$$

$$\kappa_F(\mathbf{A}\,\mathbf{A}^T) \leq \kappa_F^2(\mathbf{A}), \quad \text{consistency of } \|\cdot\|_F \tag{4.23e}$$

$$\kappa_{\hat{F}}(\mathbf{A}\,\mathbf{A}^T) \geq \kappa_{\hat{F}}^2(\mathbf{A}), \quad \text{inconsistency of } \|\cdot\|_{\hat{F}} \tag{4.23f}$$

The proofs for the identities (4.23a) to (4.23e) can be found in specialized literature, e.g., Golub and Van Loan (1989).

4.5 Kinematic Isotropy

In the foregoing sections we argued that the condition number of a matrix $\kappa(\mathbf{A})$, with $\mathbf{A} \in \mathbb{R}^{m\times n}$, is a useful measure for quantifying distance to singularity and error magnifications in solving overdetermined ($m > n$), determined ($m = n$), and underdetermined ($m < n$) linear systems associated with $\mathbf{A}$. In this section the concept of *isotropy* as applied to general real matrices; the notion of *kinematic isotropy* of manipulators is discussed as well. Having reviewed important features of isotropic matrices, we will then discuss kinematic isotropy and isotropic manipulators.

4.5.1 Matrix Isotropy

First the concept of isotropy for matrices is recalled. Isotropic matrices are those with a minimum condition number of unity. On the one hand, as $\mathbf{A}$ becomes ill-conditioned, its distance to singularity, defined as $1/\kappa(\mathbf{A})$ approaches zero, while the error magnification factor $\kappa(\mathbf{A})$ approaches infinity. On the other hand, as $\mathbf{A}$ approaches isotropy, its distance to singularity approaches a maximum value of one, while the error magnification approaches its minimum value of zero. It is apparent that as $\mathbf{A}$ approaches a singularity, its minimum singular value σ_{min} vanishes, i.e.,

$$\begin{aligned} \sigma_{min}(\mathbf{A}) \to 0 \quad &\Rightarrow \quad \kappa_2(\mathbf{A}) \to \infty \\ \sigma_{min}(\mathbf{A}) \to \sigma_{max}(\mathbf{A}) \quad &\Rightarrow \quad \kappa_2(\mathbf{A}) \to 1 \end{aligned} \tag{4.24}$$

Hence, for the 2-norm condition number to become one, all singular values of $\mathbf{A}$ must become identical. Furthermore, recalling eq.(4.18), the normalized Frobenius norm condition number is of the form

$$\kappa_{\bar{F}}(\mathbf{A}) = \frac{1}{m}\sqrt{\mathrm{tr}(\mathbf{A}\,\mathbf{A}^T)\,\mathrm{tr}[(\mathbf{A}\,\mathbf{A}^T)^{-1}]} \tag{4.25}$$

Denoting by $\{\sigma_i\}_1^m$ the ordered set of singular values of $\mathbf{A}$, with $\sigma_1 \equiv \sigma_{min}$ and $\sigma_m \equiv \sigma_{max}$, we have

$$\mathrm{tr}(\mathbf{A}\,\mathbf{A}^T) = \sigma_1 + \sigma_2 + \cdots + \sigma_m$$
$$\mathrm{tr}[(\mathbf{A}\,\mathbf{A}^T)^{-1}] = \frac{1}{\sigma_1} + \frac{1}{\sigma_2} + \cdots + \frac{1}{\sigma_m}$$

from the foregoing equations following that

$$\begin{aligned} \sigma_1(\mathbf{A}) \to 0 \quad &\Rightarrow \quad \kappa_{\bar{F}}(\mathbf{A}) \to \infty \\ \sigma_i(\mathbf{A}) \to \sigma \neq 0 \quad (\forall\, i = 1, 2, \cdots m), \quad &\Rightarrow \quad \kappa_{\bar{F}}(\mathbf{A}) \to 1 \end{aligned}$$

where σ is the common singular value of $\mathbf{A}$. Thus, for $\mathbf{A}$ to become isotropic its m singular values should be identical, or, equivalently, the m eigenvalues of the product $\mathbf{A}\,\mathbf{A}^T$ should be identical. From the foregoing basic definition of isotropic matrices, the following theorem can be stated:

Theorem 4.1

The full-rank matrix $\mathbf{A} \in \mathbb{R}^{m\times n}$ $(m \leq n)$ *is isotropic* if and only if $\mathbf{A}\,\mathbf{A}^T = \sigma^2\,\mathbf{1}$, *where* σ *is the common singular value of* $\mathbf{A}$, *and* $\mathbf{1}$ *is the* $m \times m$ *identity matrix.*

Proof: The matrix product $\mathbf{A}\,\mathbf{A}^T \in \mathbb{R}^{m\times m}$ being symmetric, it can be diagonalized in the form

$$\mathbf{A}\,\mathbf{A}^T = \mathbf{Q}\,\boldsymbol{\Lambda}\,\mathbf{Q}^T$$

with $\boldsymbol{\Lambda} \equiv \mathrm{diag}\,(\lambda_1, \lambda_2, \cdots \lambda_m)$, and $\mathbf{Q}$ orthogonal. From the isotropy of $\mathbf{A}$, it follows that $\lambda_1 = \lambda_2 = \cdots \lambda_m = \lambda$, and hence,

$$\mathbf{A}\,\mathbf{A}^T = \mathbf{Q}\,(\lambda\mathbf{1})\,\mathbf{Q}^T = \lambda\,\mathbf{1} = \sigma^2\,\mathbf{1}$$

where the orthogonality of $\mathbf{Q}$, and the definition of singular value were used.

Let

$$\mathbf{A}\,\mathbf{A}^T = \sigma^2\,\mathbf{1} = \lambda\,\mathbf{1}$$

Since the matrix product $\mathbf{A}\,\mathbf{A}^T$ is diagonal, its diagonal entries are its m eigenvalues, i.e.,

$$\lambda\,\mathbf{1} = \begin{bmatrix} \lambda_1 & 0 & \cdots & 0 \\ 0 & \lambda_2 & \cdots & 0 \\ \vdots & \vdots & \ddots & \cdots \\ 0 & 0 & \cdots & \lambda_m \end{bmatrix}$$

Hence, $\lambda_1 = \lambda_2 = \cdots = \lambda_m = \lambda$

q.e.d

Corollary 1: From the foregoing Theorem, it follows that the rows of the product $\mathbf{A}\,\mathbf{A}^T$ are mutually perpendicular, and have the same Euclidean norm which is equal to σ, the common singular value of $\mathbf{A}$.

Corollary 2: If $\mathbf{A}$ is square and of full rank, then the isotropy condition can be equally written as

$$\mathbf{A}^T\,\mathbf{A} = \sigma^2\,\mathbf{1} \tag{4.26}$$

thereby making both columns and rows of of $\mathbf{A}$ mutually perpendicular. Equation (4.26) can be obtained directly from the main isotropy condition given above, i.e.,

$$\begin{aligned} \mathbf{A}\,\mathbf{A}^T &= \sigma^2\,\mathbf{1} \\ \mathbf{A}^T &= \sigma^2\,\mathbf{A}^{-1} \\ \mathbf{A}^T\,\mathbf{A} &= \sigma^2\,\mathbf{A}^{-1}\,\mathbf{A} = \sigma^2\,\mathbf{1} \end{aligned}$$

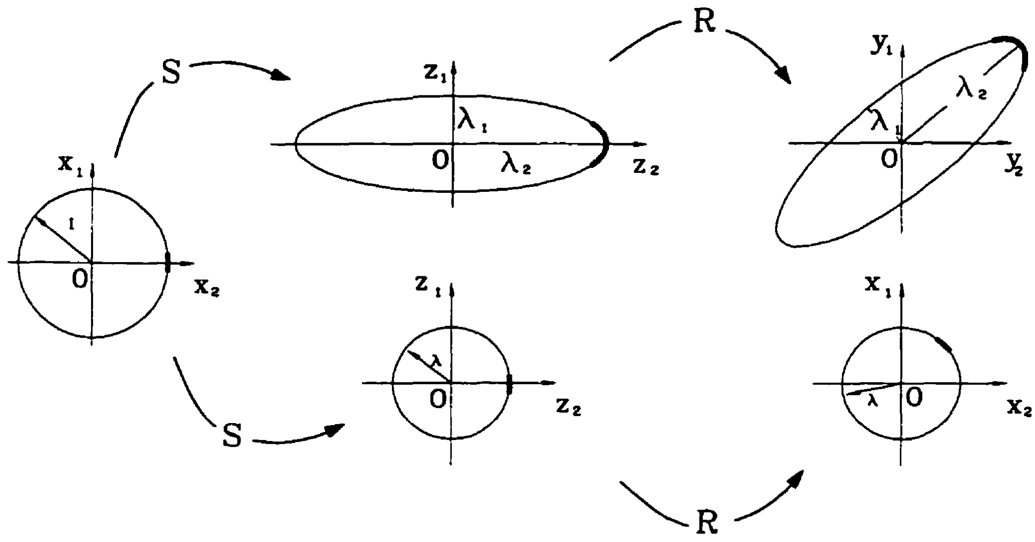

Figure 4.1: Geometrical interpretation of isotropy

4.5.2 Geometric Interpretations

The linear transformation $\mathbf{A} \in \mathbb{R}^{m \times n}$ maps vectors $\mathbf{x}$ from its domain i.e., $\mathbb{R}^n$ into vectors $\mathbf{y}$ in its range $\mathbb{R}^m$. Depending on the numerical conditioning of $\mathbf{A}$ and the orientation of the vector $\mathbf{x}$ being mapped, $\mathbf{x}$ can undergo various degrees of distortion. However, if $\mathbf{A}$ is isotropic, then no distortion would result, since $\mathbf{A}$ maps a unit sphere into another unit sphere either of a smaller or larger radius. This is best illustrated by examining the mapping induced by a square and positive-definite 2×2 matrix $\mathbf{A}$.

$$\mathbf{y} = \mathbf{A}\,\mathbf{x}$$

Applying the *polar decomposition* to $\mathbf{A}$, we have

$$\mathbf{A} = \mathbf{R}\,\mathbf{S}$$

Thus,

$$\mathbf{y} = \mathbf{R}\,\mathbf{z}$$

$$\mathbf{z} \equiv \mathbf{S}\,\mathbf{x}$$

where $\mathbf{R}$ is orthogonal and $\mathbf{S}$ is symmetric and positive-semidefinite. The mapping induced by $\mathbf{A}$ is now characterized by first mapping the unit circle under $\mathbf{S}$ into an ellipse. This distortion is followed by the mapping of the orthogonal matrix $\mathbf{R}$ that does not produce any distortion and only rotates the ellipse into its final position. It is apparent that the larger the ratio between the two positive eigenvalues of $\mathbf{S}$, the higher the eccentricity of the ellipse. However, when $\mathbf{A}$ is isotropic, it induces the most uniform magnification and the shape of the unit circle is not affected (Fig 4.1). The same geometrical interpretation can be extended to rectangular matrices as well. For instance, if $\mathbf{A} \in \mathbb{R}^{m\times n}$, then one can apply the QR factorizing (Strang, 1988) to $\mathbf{A}$ and obtain

$$\mathbf{A} = \mathbf{Q}\begin{bmatrix}\mathbf{U}\\ \mathbf{0}\end{bmatrix}$$

where $\mathbf{Q} \in \mathbb{R}^{m\times m}$ is orthogonal, $\mathbf{U} \in \mathbb{R}^{n\times n}$ is upper triangular and $\mathbf{0}$ is the $(m-n)\times n$ zero matrix. Now, the same argument can be applied to the square matrix $\mathbf{U}$.

Another interesting feature of an isotropic matrix is that its generalized inverse can be determined by one single scalar inversion, e.g.,

$$\begin{aligned}\mathbf{A}^{\dagger} &= \mathbf{A}^T(\mathbf{A}\mathbf{A}^T)^{-1} = \frac{1}{\sigma^2}\mathbf{A}^T \quad \text{if} \quad m < n\\ \mathbf{A}^{\dagger} &= (\mathbf{A}^T\mathbf{A})^{-1}\mathbf{A}^T = \frac{1}{\sigma^2}\mathbf{A}^T \quad \text{if} \quad m > n\end{aligned}$$

4.6 Isotropic Manipulators

Having discussed the notion of isotropic matrices in general, the concepts of kinetostatic isotropy and isotropic manipulators are now discussed.

Definition 4.1

Kinetostatic Isotropy *is defined as the ability of a manipulator to produce motions and forces with an accuracy that is insensitive to the direction in which these* *motions and forces are applied.* In our motor activities, we regard those postures as most "comfortable" when our motion-and-force transmission abilities are direction-independent.

Definition 4.2

Isotropic Manipulators *are those whose normalized Jacobian matrix is isotropic in at least one point in their workspace.*

Fact 1: Not all manipulators are isotropic; in fact, most manipulators are not isotropic.

Fact 2: An isotropic n-R serial-type manipulator has at least a circle of isotropic configurations in its joint space. This follows from the fact that the rotation of the first joint of the manipulator, which results in a rigid-body rotation of the whole arm, would rotate the isotropic point through a whole circle[1]

Fact 3: The kinematic isotropy of a manipulator is the result of a particular choice of the set of DH parameters defining the manipulator architecture.

Fact 4: A manipulator that cannot attain an isotropic posture is called nonisotropic.

4.7 Isotropic Design of Manipulators

The optimum kinematic design of serial-type nonredundant manipulators for isotropy is discussed in this section, while the design of redundant manipulators for kinematic isotropy is the subject of the following three Chapters. For both redundant and nonredundant manipulator designs, two main design strategies can be outlined, namely, *Jacobian synthesis* (González–Palacios, 1993), and *Non-linear optimization.* In Jacobian synthesis, first an isotropic matrix of appropriate dimension and structure is constructed from which the set of DH parameters is then extracted (Klein and Miklos, 1991). Nonlinear optimisations and solving sets of nonlinear equations

[1]Here we are assuming ideal joints with no physical limits

can also be used to obtain the set of DH parameters. In this chapter, a simple example of the isotropic design of planar 2-R manipulators is introduced using the direct differentiation of the condition number. Although this problem was solved as the first example of an isotropic manipulator by Salisbury and Craig (1982), its inclusion here is meant to provide some additional algebraic and geometric insights. In the following chapters nonlinear optimization is used to provide isotropic designs of redundant manipulators.

To this end, the isotropy condition for the Jacobian matrix of a general n-axis manipulator, as per Theorem 4.1, is recalled, while denoting the $3 \times n$ upper block of $\mathbf{J}$ by $\mathbf{E}$, and its $3 \times n$ lower block by $\mathbf{S}$, i.e.,

$$\mathbf{J} = \begin{bmatrix} \mathbf{e}_1 & \mathbf{e}_2 & \cdots & \mathbf{e}_n \\ \mathbf{e}_1 \times \mathbf{r}_1 & \mathbf{e}_2 \times \mathbf{r}_2 & \cdots & \mathbf{e}_n \times \mathbf{r}_n \end{bmatrix} = \begin{bmatrix} \mathbf{E} \\ \mathbf{S} \end{bmatrix} \tag{4.27}$$

If the normalized Jacobian matrix $\mathbf{J}$ is introduced the isotropy condition takes on the form

$$\bar{\mathbf{J}}\,\bar{\mathbf{J}}^T = \begin{bmatrix} \mathbf{E}\,\mathbf{E}^T & \frac{1}{L}\mathbf{E}\,\mathbf{S}^T \\ \frac{1}{L}\mathbf{S}\,\mathbf{E}^T & \frac{1}{L^2}\mathbf{S}\,\mathbf{S}^T \end{bmatrix} = \sigma^2\,\mathbf{1} \tag{4.28}$$

Thus, isotropic design amounts to determining the constant and the variable sets of DH parameters in such a way that the foregoing condition is satisfied.

4.7.1 A Simple Example

In this subsection the isotropic design of planar two-axis manipulators is discussed through directly differentiating the condition number of the Jacobian matrix. Since the condition number is a complicated function of the entries of its matrix argument, for general matrices this method is not feasible. However, since geometric insight can be gained through direct differentiation of the condition number, this simple example is discussed here. Some new contributions that are byproducts of this exercise are also introduced.

The Jacobian matrix of the general 2-R manipulator shown in Fig. 4.2 takes on the form

$$\mathbf{J} = \begin{bmatrix} -l_1\,s_1 - l_2\,s_{12} & -l_2\,s_{12} \\ l_1\,c_1 + l_2\,c_{12} & l_2\,c_{12} \end{bmatrix} \tag{4.29}$$

where l_i and θ_i are, respectively, the ith link length, and the ith joint variable, while $c_i \equiv \cos\theta_i$, $s_i \equiv \sin\theta_i$for $i = 1, 2$, $c_{12} \equiv \cos(\theta_1 + \theta_2)$, and $s_{12} \equiv \sin(\theta_1 + \theta_2)$. It can be shown that

$$\tau \equiv \mathrm{tr}(\mathbf{J}\,\mathbf{J}^T) = l_1^2 + 2\,l_2^2 + 2\,l_1\,l_2\,\cos\theta_2 \tag{4.30}$$

and

$$\delta \equiv \det(\mathbf{J}\,\mathbf{J}^T) = l_1^2\,l_2^2\,\sin^2\theta_2 \tag{4.31}$$

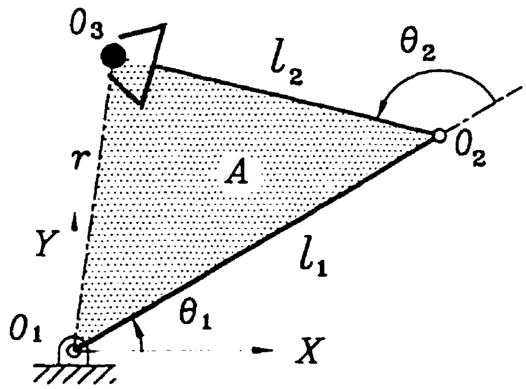

Figure 4.2: Planar 2-axes manipulator

Moreover, the inverse of $\mathbf{J}$ is readily determined, as

$$\mathbf{J}^{-1} = \frac{1}{\det(\mathbf{J})}\begin{bmatrix} l_2\,c_{12} & l_2\,s_{12} \\ -l_1\,c_1 - l_2\,c_{12} & -l_1\,s_1 - l_2\,s_{12} \end{bmatrix} \tag{4.32}$$

with $\det(\mathbf{J}) = l_1\, l_2 \sin\theta_2 = \sqrt{\delta}$, and

$$(\mathbf{J}\,\mathbf{J}^T)^{-1} = \frac{1}{\delta}\begin{bmatrix} l_2^2 & -l_1^2 - l_1\, l_2 \cos\theta_2 \\ -l_1^2 - l_1\, l_2 \cos\theta_2 & l_1^2 + l_2^2 + 2\, l_1\, l_2 \cos\theta_2 \end{bmatrix} \tag{4.33}$$

Hence,

$$\mathrm{tr}[(\mathbf{J}\,\mathbf{J}^T)^{-1}] = \frac{l_1^2 + 2\, l_2^2 + 2\, l_1\, l_2 \cos\theta_2}{l_1^2\, l_2^2 \sin^2\theta_2} = \frac{\mathrm{tr}(\mathbf{J}\,\mathbf{J}^T)}{\det(\mathbf{J}\,\mathbf{J}^T)} = \frac{\tau}{\delta} \tag{4.34}$$

Thus,

$$\kappa_{\bar{F}}^2(\mathbf{J}) \equiv \frac{1}{4}\,\mathrm{tr}(\mathbf{J}\,\mathbf{J}^T)\,\mathrm{tr}[(\mathbf{J}\,\mathbf{J}^T)^{-1}] = \frac{\mathrm{tr}^2(\mathbf{J}\mathbf{J}^T)}{4\det(\mathbf{J}\mathbf{J}^T)} = \frac{\tau^2}{4\,\delta} \tag{4.35}$$

noting that both $\mathrm{tr}(\mathbf{J}\mathbf{J}^T)$ and $\det(\mathbf{J}\mathbf{J}^T)$ are positive, we obtain

$$\kappa_{\bar{F}}(\mathbf{J}) = \frac{\mathrm{tr}(\mathbf{J}\mathbf{J}^T)}{2\sqrt{\det\mathbf{J}\mathbf{J}^T}} = \frac{\tau}{2\sqrt{\delta}} \tag{4.36}$$

The isotropy of $\mathbf{J}$ requires that $\kappa_{\bar{F}}(\mathbf{J}) = 1$, or

$$\tau = 2\sqrt{\delta} \tag{4.37}$$

Substituting eqs. (4.30) and (4.31) in the foregoing equation yields the expression shown below:

$$l_1^2 + 2\, l_2^2 + 2\, l_1\, l_2 \cos\theta_2 - 2\, l_1\, l_2 \sin\theta_2 = 0$$

With the usual half-angle substitution ($t_2 \equiv \tan\theta_2/2$) for $\cos\theta_2$ and $\sin\theta_2$ in the foregoing equation, a quadratic equation in t_2 is obtained, namely,

$$(l_1^2 + 2\, l_2^2 - 2\, l_1\, l_2)\, t_2^2 - 4\, l_1\, l_2\, t_2 + (l_1^2 + 2\, l_2^2 + 2\, l_1\, l_2) = 0 \tag{4.38}$$

with its two roots being given by

$$t_2 = \frac{2\, l_1\, l_2 \pm \sqrt{-(l_1^2 - 2\, l_2^2)^2}}{l_1^2 + 2\, l_2^2 - 2\, l_2^2 - 2\, l_1\, l_2}$$

Therefore, the only possibility for the existence of a real solution is

$$l_1^2 = 2\, l_2^2 \quad \text{or} \quad s \equiv \frac{l_2}{l_1} = \frac{\sqrt{2}}{2}$$

Hence, the isotropy of $\mathbf{J}$ is attained at

$$t_2 = \tan\theta_2/2 = \sqrt{2}+1$$

or

$$\theta_2^* = \pm\frac{3\,\pi}{4}$$

where * denotes isotropy. We conclude that, up to a scale factor s, there exist only one isotropic planar manipulator for positioning tasks. This solution is, in fact, that found by Salisbury and Craig (1982).

Next, it is shown that $\kappa_{\bar{F}}$ thus defined is smooth everywhere, its derivative vanishing only at the isotropic configuration θ_2^*. By differentiating both sides of eq. (4.35) with respect to θ_2, while recalling that $\delta \equiv \det(\mathbf{J}\mathbf{J}^T)$ and $\tau \equiv \mathrm{tr}(\mathbf{J}\mathbf{J}^T)$, we obtain

$$2\,\kappa_{\bar{F}}\,\frac{d\,\kappa_{\bar{F}}}{d\theta_2} = \frac{d}{d\,\theta_2}\left(\frac{\tau^2}{4\,\delta}\right) = \frac{8\,\delta\,\tau\,\tau' - 4\,\tau^2\,\delta'}{16\,\delta^2} \tag{4.39}$$

The foregoing derivative exists for all nonsingular configurations ($\delta \neq 0$). This derivative is evaluated at θ_2^* next, while noting from eqs. (4.30) and (4.31) that

$$\tau(\theta_2^*) = 1, \quad \text{and} \quad \tau' \equiv \left.\frac{d\,\tau}{d\,\theta_2}\right|_{\theta^*} = -2\,l_1\,l_2\,\sin\theta_2^* = \pm\,1 \tag{4.40}$$

and

$$\delta(\theta_2^*) = \frac{1}{4}, \quad \text{and} \quad \delta' \equiv \left.\frac{d\,\delta}{d\,\theta_2}\right|_{\theta^*} = 2\,l_1^2\,l_2^2\,\sin\theta_2^*\,\cos\theta_2^* = \pm\,\frac{1}{2} \tag{4.41}$$

Next we will show that unlike the smooth behaviour of the F-norm condition number around isotropy, the 2-norm condition number does not exhibit the same smoothness at the isotropic point. To this end, the characteristic polynomial of the 2 by 2 matrix $\mathbf{J}\mathbf{J}^T$ can be written as

$$\lambda^2 - \tau\,\lambda + \delta = 0 \tag{4.42}$$

where, as before, $\tau = \mathrm{tr}(\mathbf{J}\mathbf{J}^T)$, $\delta = \det(\mathbf{J}\mathbf{J}^T)$, and λ is an eigenvalue of $\mathbf{J}\,\mathbf{J}^T$. Moreover, since $\mathbf{J}\,\mathbf{J}^T$ is positive-definite, for all nonsingular configurations, the foregoing quadratic equation always admits two real and positive roots, namely,

$$\lambda_{max} = \frac{1}{2}(\tau + \sqrt{\tau^2 - 4\,\delta}), \quad \text{and} \quad \lambda_{min} = \frac{1}{2}(\tau - \sqrt{\tau^2 - 4\,\delta}) \tag{4.43}$$

At the isotropic configuration $\theta_2 = \theta_2^*$, $\kappa_2 = 1$, and the two eigenvalues are identical. Thus, the condition for the existence of repeated roots for the characteristic polynomial is examined, i.e.,

$$\tau^2 - 4\,\delta = 0$$

thus

$$\tau = 2\sqrt{\delta}$$

which is the same condition as that obtained before for $\kappa_{\bar{F}} = 1$, with the repeated eigenvalues being,

$$\lambda_0 \equiv \lambda_{max}(\theta_2^*) = \lambda_{min}(\theta_2^*) = \frac{\tau(\theta_2^*)}{2}$$

After some simplifications, $\kappa_2(\mathbf{J})$ takes on the form

$$\kappa_2(\mathbf{J}) = \frac{\tau + \sqrt{\tau^2 - 4\,\delta}}{2\sqrt{\delta}} \tag{4.44}$$

The variation of κ_2 and $\kappa_{\bar{F}}$ with respect to θ_2 in its entire domain is shown in Fig. 4.3, while in Fig. 4.4, the latter quantities are plotted around one of the isotropic configurations, namely, $\theta_2^* = \frac{3\pi}{4}$. From these figures, it is apparent that, although, $\kappa_{\bar{F}}$ is smooth at the isotropic point, κ_2 is not. A proof of this result is provided in Appendix B. The significance of this observation may be recognized while implementing the optimization methods used for both analysis and design of isotropic manipulator.

4.8 Algebraic and Geometric Discussions

As a byproduct, we can obtain an interesting relationship between $\kappa_{\bar{F}}(\mathbf{J})$ and $\kappa_2(\mathbf{J})$ for 2×2 matrices, namely,

$$\kappa_2 = \kappa_{\bar{F}} + \sqrt{\kappa_{\bar{F}}^2 - 1}$$

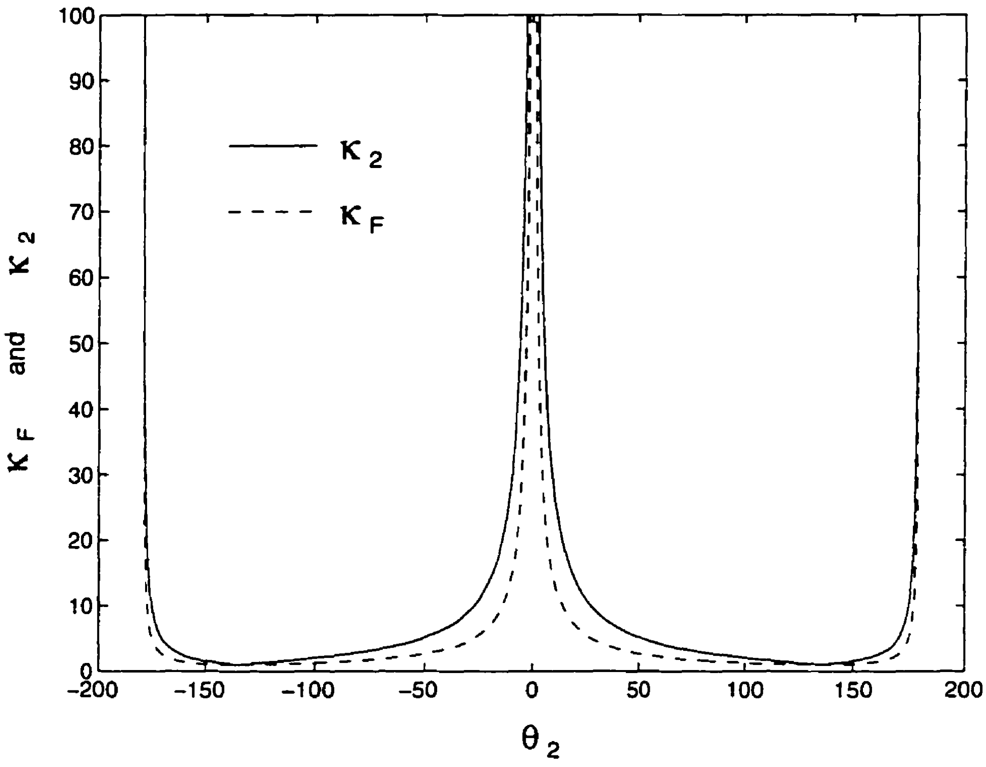

Figure 4.3: Variations of the 2-norm and Frobenious-norm condition numbers for 2R planar manipulator

The geometric interpretations of τ, δ, and the isotropy condition for planar 2R manipulators are discussed next. Using eqs. (4.30) and (4.31), and referring to Fig. 4.2, the relationships below follow:

$$\tau = \mathrm{tr}(\mathbf{J}\mathbf{J}^{\mathrm{T}}) = l_1^2 + 2\,l_2^2 + 2\,l_1\,l_2\cos\theta_2 = r^2 + l_2^2 \tag{4.45}$$

$$\delta = \det(\mathbf{J}\mathbf{J}^T) = l_1^2\,l_2^2\,\sin^2\theta_2 = 4\,A^2 \tag{4.46}$$

where r is the distance from the origin to the end-effector, and A is the area of the triangle $O_1\,O_2\,O_3$ formed by the manipulator. Moreover, we recall that both $\kappa_{\bar{F}}$ and κ_2, gave rise to the same isotropy condition, i.e.,

$$\tau = 2\sqrt{\delta}$$

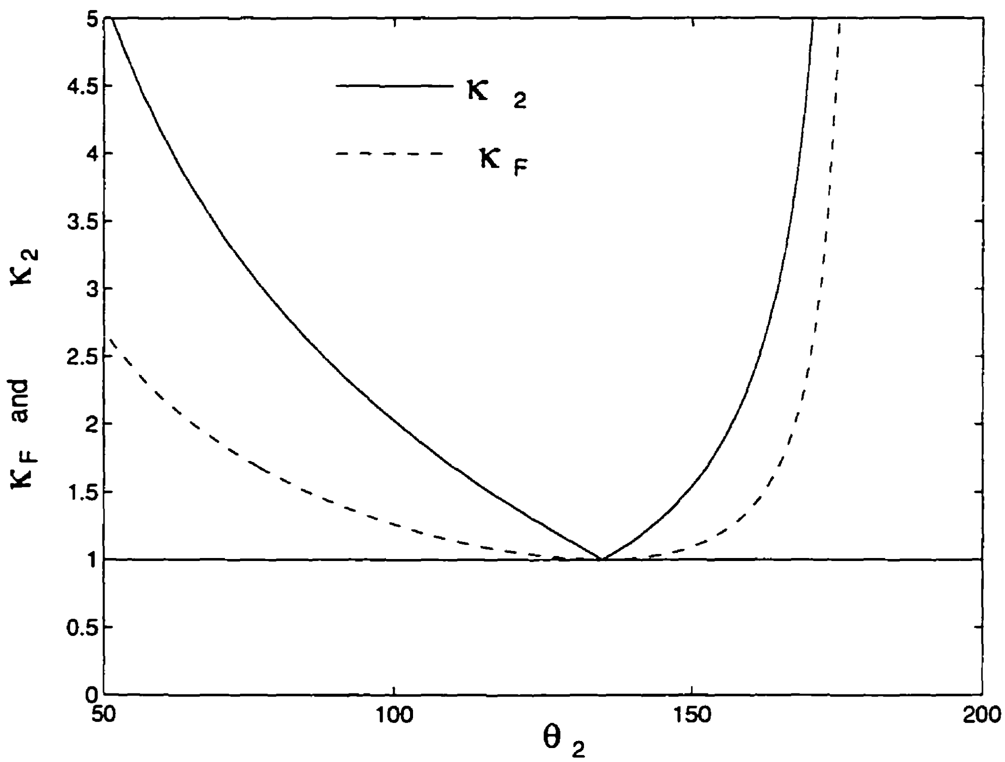

Figure 4.4: Variations of the 2-norm and Frobenious-norm condition numbers for 2R planar manipulator around the isotropic point

This condition can be rewritten as shown below:

$$r_{\mathrm{rms}}^2 \equiv \frac{r^2 + l_2^2}{4} = A$$

or,

$$\frac{r_{\mathrm{rms}}^2}{A} = 1$$

By examining the foregoing condition, as well as eqs. (4.36) and (4.44), a geometric interpretation of the isotropy condition for this simple example is observed, namely, to achieve isotropy it is required to decrease the rms value of the aforementioned distances from the operation point to the two joint axis while increasing the area occupied by the triangle formed by the manipulator. This, in turn, means that, at the isotropic configuration, the square of the rms value of the distances from the end-effector to the axes of the manipulator scaled by the area of the triangle formed by these axes in the plane of the manipulator is equal to the identity. For this simple example it also turns out that the operation point of the EE is equidistant from the two axes.

4.9 Conclusions

The condition numbers of matrices were reviewed in detail. Since the condition number is norm-dependent, some of the important features of matrix norms were also discussed. As applied to kinetostatic performance, the condition number of the Jacobian matrix was argued to be a useful tool as it both quantifies the distance to the set of singularities of the Jacobian (i.e., poor dexterity, and ill-conditioning) and characterizes the robustness of the kinematic inversion with respect to manufacturing and sensing errors. Isotropic manipulators were then defined as those whose Jacobian matrices can attain a minimum condition number of unity. A necessary and sufficient condition for isotropic designs was provided, while highlighting some algebraic and geometric interpretations of isotropy. A categorization of different kinematic designs of manipulator was proposed, namely, *Jacobian synthesis* and *nonlinear optimization*. The simple problem of isotropic design of planar 2-R manipulators was revisited using the direct differentiation of the condition numbers. In doing so, additional geometric and algebraic insights were obtained; it was shown that the 2-norm condition number is not a smooth function of the set of joint variables. Although this was proven only for 2×2 matrices,this is a feature of any $m \times n$ matrices.

Chapter 5

Isotropic Designs of Redundant Manipulators

5.1 Introduction

The kinematic design of redundant manipulators is addressed in this chapter. As explained in Chapter 4, two main design methodologies can be employed for the kinematic design of manipulators. As discussed in Chapter 1, the kinematic structure of a serial manipulator is represented by the set of Denavit and Hartenberg (DH) parameters. This set can be considered as the union of a set $\mathcal{F}$ which contains all the parameters of the manipulator that do not change with the manipulator configuration and the set $\mathcal{Q}$ that contains the joint variables that define the configuration of a given manipulator, i.e.,

$$\mathcal{P} \equiv \mathcal{F} \cup \mathcal{Q}$$

with

$$\mathcal{F} \equiv \{a_1, a_2, \cdots a_n, b_2, \cdots b_n, \alpha_1, \alpha_2, \cdots \alpha_n\}$$
$$\mathcal{Q} \equiv \{q_2, \cdots, q_n\}$$

with n being the number of a and b of the manipulator. It should be noted that the first joint variable q_1 as well as the first joint offset distance b_1 are absent in the foregoing sets. This is because these two parameters produce rigid-body motions of the manipulator as a whole. In other words, any choice of these two parameters can always be accommodated by the rotation and translation of the base coordinate frame of the manipulator. Furthermore, referring to Section (3.2.2), it is apparent that neither the unit vector $\mathbf{e}_i$ nor the vector $\mathbf{r}_i$ for $i = 1, 2, \cdots n$, depend on the last offset angle α_n. Hence any function of the Jacobian matrix including its condition number will be independent of α_n. The geometric explanation for this feature is once again the independence of any intrinsic kinematic property of the manipulator on the orientation of the moving frame attached to the end-effector. The total number of design parameters k that includes the entries of both $\mathcal{F}$ and $\mathcal{Q}$ is thus given by the relation

$$k = 4n - 3$$

For example, the number of parameters required for the kinematic design of a seven-axis manipulator is 25. It will be shown here that isotropic seven-axis manipulators are possible, and structural considerations pertaining to the design of such manipulators will then be discussed while providing several illustrative examples. Kinematic isotropy and *anthropomorphism* will then be combined to serve as an augmented set of design requirements. It will be shown that in principle, isotropy and anthropomorphism for seven-axis designs cannot coexist, as the incorporation of the latter requirements leads to *pseudoredundant* architectures that can loose more than one degree of freedom if the motion of one of their joints is lost. A nine-axis isotropic design will then be introduced in an attempt to combine isotropy and anthropomorphism. The isotropic design of hyperredundant planar manipulators will then be discussed, whereby a 30-axis example of such designs will be introduced. Finally, comparative studies between isotropic and nonisotropic manipulators in the sense of workspace singularity distributions will be conducted.

5.2 Isotropic Design of Seven-Axis Manipulators

We adopt here the condition number of the Jacobian matrix discussed in Chapters 3 and 4 as the main criterion for the design of redundant manipulators. It will be shown that since the design problem at hand reduces to an underdetermined system of m nonlinear equations in n unknowns, with $m < n$, there is in general an infinity of solutions for isotropic seven-axis robots. Additional design requirements can thus be incorporated to reduce the dimension of the solution set, while achieving other functional considerations. Recall that the normalized 6×7 Jacobian matrix of a seven-axis manipulator takes on the form

$$\bar{\mathbf{J}} = \begin{bmatrix} \mathbf{e}_1 & \mathbf{e}_2 & \cdots & \mathbf{e}_7 \\ \frac{1}{L}\mathbf{e}_1 \times \mathbf{r}_1 & \frac{1}{L}\mathbf{e}_2 \times \mathbf{r}_2 & \cdots & \frac{1}{L}\mathbf{e}_7 \times \mathbf{r}_7 \end{bmatrix} = \begin{bmatrix} \mathbf{E} \\ \frac{1}{L}\mathbf{S} \end{bmatrix} \tag{5.1}$$

while the isotropy condition, as given by eq. (4.28), is expressed by

$$\bar{\mathbf{J}}\,\bar{\mathbf{J}}^T = \begin{bmatrix} \mathbf{E}\,\mathbf{E}^T & \frac{1}{L}\mathbf{E}\,\mathbf{S}^T \\ \frac{1}{L}\mathbf{S}\,\mathbf{E}^T & \frac{1}{L^2}\mathbf{S}\,\mathbf{S}^T \end{bmatrix} = \sigma^2 \begin{bmatrix} \mathbf{1} & \mathbf{O} \\ \mathbf{O} & \mathbf{1} \end{bmatrix} \tag{5.2}$$

with $\mathbf{1}$ and $\mathbf{O}$, respectively, denoting the 3×3 identity and the zero matrices. The foregoing main relation gives rise to three matrix equations, i.e.,

$$\mathbf{E}\,\mathbf{E}^T = \sigma^2\,\mathbf{1} \tag{5.3a}$$

$$\mathbf{E}\,\mathbf{S}^T = \mathbf{O} \tag{5.3b}$$

$$\frac{1}{L^2}\mathbf{S}\,\mathbf{S}^T = \sigma^2\,\mathbf{1} \tag{5.3c}$$

The foregoing matrix equations amount to 21 independent scalar equations to be satisfied by 25 elements of $\mathcal{P}$ plus the two parameters L and σ. However, as will become apparent presently, the last two parameters can be determined explicitly from eqs. (5.3). Indeed, upon equating the trace of both sides of eq. (5.3a), we obtain

$$\mathrm{tr}(\mathbf{E}\,\mathbf{E}^T) = \mathrm{tr}(\sum_1^n \mathbf{e}_i\,\mathbf{e}_i^T) = 3\,\sigma^2$$

On the other hand,

$$\mathrm{tr}(\sum_1^n \mathbf{e}_i\,\mathbf{e}_i^T) = \sum_1^n \mathbf{e}_i^T\,\mathbf{e}_i = n$$

where we used the normality of vectors $\{\mathbf{e}_i\}_1^n$. Therefore,

$$\sigma = \sqrt{n/3} \tag{5.4}$$

This means that the common singular value of the Jacobian matrix of an isotropic manipulator at the isotropic configuration is a function only of the number n of degrees of freedom of the manipulator. Moreover, by equating the trace of both sides of eq. (5.3c), we have

$$\mathrm{tr}(\frac{1}{L^2}\mathbf{S}\,\mathbf{S}^T) = \frac{1}{L}\,\mathrm{tr}[\sum_1^n(\mathbf{e}_i \times \mathbf{r}_i)\,(\mathbf{e}_i \times \mathbf{r}_i)^T]$$

On the other hand,

$$\mathrm{tr}[\sum_1^n(\mathbf{e}_i \times \mathbf{r}_i)\,(\mathbf{e}_i \times \mathbf{r}_i)^T] = \sum_1^n(\mathbf{e}_i \times \mathbf{r}_i)^T\,(\mathbf{e}_i \times \mathbf{r}_i) = \sum_1^n ||\mathbf{e}_i \times \mathbf{r}_i||^2$$

Hence,

$$L^2 = \frac{\sum_1^n ||\mathbf{e}_i \times \mathbf{r}_i||^2}{n} \tag{5.5}$$

As shown below, the terms $||\mathbf{e}_i \times \mathbf{r}_i||$, with $i = 1, 2, \cdots n$, appearing in the right-hand side of the foregoing equation are, in fact, the distances from the operation point P to the n joint axes. Referring to Fig 5.1 the following vector equation can be verified

$$\mathbf{r}_i + \mathbf{d}_i = (\mathbf{r}_i \cdot \mathbf{e}_i)\,\mathbf{e}_i$$

or

$$\mathbf{d}_i \cdot \mathbf{d}_i = ||\mathbf{d}_i||^2 = (\mathbf{r}_i \cdot \mathbf{r}_i) - (\mathbf{r}_i \cdot \mathbf{e}_i)^2$$

Thus,

$$||\mathbf{d}_i||^2 = (\mathbf{e}_i \times \mathbf{r}_i) \cdot (\mathbf{e}_i \times \mathbf{r}_i) = ||\mathbf{e}_i \times \mathbf{r}_i||^2$$

A second interesting geometrical attribute of kinematic isotropy for both positioning and orienting tasks stems from the condition on vanishing of the off-diagonal blocks in eq. (5.3b), namely, $\mathbf{E}\,\mathbf{S}^T = \mathbf{0}$. This condition gives rise to the following result.

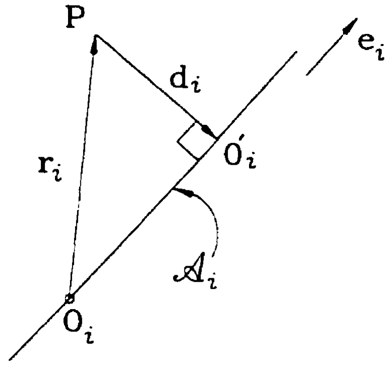

Figure 5.1: Projection of the operation point onto the ith axis

Theorem 5.1

Let O_i' be the foot of the perpendicular to the kth axis $\mathcal{A}_i$ from the operation point P (Fig. 5.1). The operation point of an isotropic manipulator, in its isotropic posture, is the centroid of the set $\{ O_i' \}_1^n$.

Proof: From the condition given by eq. (5.3b) i.e., $\mathbf{E}\mathbf{S}^T = \mathbf{O}$, we have that

$$\sum_1^n \mathbf{e}_i \, (\mathbf{e}_i \times \mathbf{r}_i)^T = \mathbf{O}$$

If we take the axial vector (Leigh, 1968) of the two sides of the foregoing matrix equation, we obtain

$$\sum_1^n \mathbf{e}_i \times (\mathbf{e}_i \times \mathbf{r}_i) = \mathbf{0}$$

which can be rewritten as

$$\sum_1^n \mathbf{E}_i^2 \mathbf{r}_i = \mathbf{0}$$

where $\mathbf{E}_i$ is the cross-product matrix of $\mathbf{e}_i$. Moreover, $\mathbf{E}_i^2$ is expanded as

$$\mathbf{E}_i^2 = -(\mathbf{1} - \mathbf{e}_i \, \mathbf{e}_i^T)$$

and hence, the foregoing equation leads to

$$\sum_1^n (\mathbf{1} - \mathbf{e}_i \mathbf{e}_i^T) \, \mathbf{r}_i = \mathbf{0}$$

But matrix $\mathbf{e}_i\mathbf{e}_i^T$ maps $\mathbf{r}_i$ into the transverse component of $\mathbf{r}_i$ along $\mathbf{e}_i$, i.e., along $\mathcal{A}_i$. That is, $(\mathbf{1} - \mathbf{e}_i\mathbf{e}_i^T)\,\mathbf{r}_i$ denotes the vector connecting O_i' with P.

q. e. d.

5.3 Methodology

Two main approaches are followed in using the set of isotropy conditions, namely, the system of 21 nonlinear equations for the 25 unknowns derived above. The first approach is based on the optimization of a cost function over the 25 unknown parameters subject to the isotropy conditions. In the second approach, the number of design variables will be reduced to 21 upon assigning four of the 25 unknown parameters based on functional conditions, thereby deriving a system of 21 nonlinear equations in 21 unknowns.

5.3.1 The Kinematic Optimization Approach

The first approach is based on determining the design variables by optimizing a cost function that penalizes the violation of eqs. (5.3). The first candidate for the cost function is apparently the condition number itself. However, because of the complexity of the evaluation of the condition number, not to speak of its gradient, other cost functions should be considered. To this end, an objective function z is defined as the *distance* of a *design*, given by the 25-dimensional vector $\mathbf{x}$ of design variables, to isotropy, the distance being defined in terms of the Frobenius norm. We thus define a matrix $\mathbf{M}$ as

$$\mathbf{M} \equiv \mathbf{J}\mathbf{J}^T - \sigma^2\mathbf{1} \tag{5.6}$$

Matrix $\mathbf{M}$ is thus a measure of how different the Jacobian matrix is from an isotropic matrix. Hence, we have an unconstrained optimization problem, namely,

$$z \equiv \sqrt{\mathrm{Tr}(\mathbf{M}\mathbf{M}^T)} \;\rightarrow\; \min_{\mathbf{x}} \tag{5.7}$$

However, a solution for $\mathbf{x}$ may very well include a link length a_i that is negative. Since a_i is defined as a positive quantity that represents the *distance* between two consecutive axes, it seems that one needs to add constraints to the foregoing problem, in order to limit the search domain of $\{a_i\}_1^n$ to positive values only. Instead of doing so, however, if any of the resulting a_i turns out to be negative, its absolute value can be used while making the simple adjustments of the other parameters such that the relative position and orientation of the two consecutive joint axes remains unchanged. We do this using Algorithm 5.1.

Algorithm 5.1 :

For $k = 1, \cdots, n-1$, do

if $a_k < 0$, then,

$a_k \leftarrow |a_k|$

$\alpha_{k-1} \leftarrow |\alpha_{k-1}|$

$\theta_k \leftarrow \theta_k - \pi$

$\theta_{k+1} \leftarrow \theta_{k+1} - \pi$

endif

Enddo

For $k = n$, do

if $a_n < 0$, then,

$a_n \leftarrow |a_n|$

$\alpha_{n-1} \leftarrow |\alpha_{n-1}|$

$\theta_n \leftarrow \theta_n - \pi$

endif

Enddo

Link i	a_i	b_i	α_i(deg)	θ_i(deg)
1	0.1154	0	104.6285	180.0000
2	1.5704	-0.0483	-86.3539	40.1118
3	0.1756	1.0226	60.6524	30.5779
4	1.0499	-0.7054	108.6141	-105.7290
5	0.9094	-0.0104	-110.1435	-69.0636
6	0.0053	-0.0614	-107.3289	146.9810
7	0.4810	0.8844	0	33.5665
$L = 0.7502$ $\kappa = 1.0$				

Table 5.1: DH parameters for the fully isotropic architecture: Design 1

Numerical Examples: Design 1

As an illustrative example for the approach discussed above, the *Matlab* function *fmins* was used for solving the foregoing minimization problem. The objective function was chosen to be norm of the 21-dimensional vector function $\mathbf{f}(\mathbf{x})$, with $\mathbf{x}$ containing 25 entries of the set $\mathcal{P}$ plus the characteristic length L, and the 21 components of $\mathbf{f}(\mathbf{x})$ being the 21 distinct scalar components of matrix $\mathbf{M}$ defined in eq. (5.6). The results obtained for this design are given in Table 5.1.

These DH parameters produce a configuration whose Jacobian matrix is isotropic, with its singular values being identical and equal to $\sqrt{7/3}$. For this isotropic design, eq. (5.5) yields the same value for L as the one obtained with *fmins* (Table 5.1). Furthermore, Fig. 5.2 depicts a 3-dimensional rendering of this manipulator in its isotropic posture.

5.3.2 Kinematic Design via Nonlinear-Equation Solving

The second approach for solving our design problem is by means of functional constraints. For functional reasons, some of the entries of the set $\mathbf{x}$ can be fixed a priori, thus reducing the dimension of the design space. By preassigning five unknowns, a determined system of nonlinear equations can be obtained whose solutions are computed numerically.

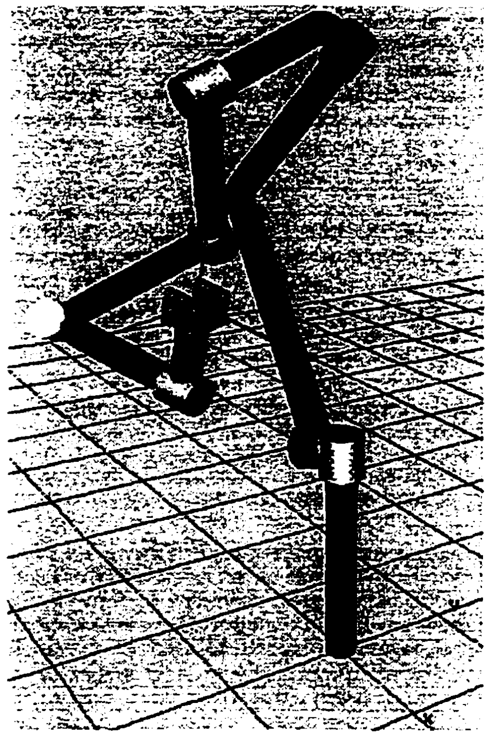

Figure 5.2: Fully isotropic seven-axis manipulator: Design 1

Numerical Example: Design 2

As an illustrative example for the second approach, the number of design variables was reduced to 21 as explained next. From a structural viewpoint, it is advantageous to concentrate as much mass of the arm as possible close to the manipulator base. This would enhance the dynamic performance and the structural rigidity of the manipulator. It is thus attempted to obtain an alternative design by preassigning values to five of the components of $\mathbf{x}$, thus obtaining a system of 21 nonlinear equations in 21 unknowns. Moreover, we set a_1, a_3, a_5, b_2 and b_4 all equal to zero, which is intended to bring the first three moving axes, and hence, their motors, close to the first, fixed, axis. Elimination of these five parameters from the design vector $\mathbf{x}$ results in a system of 21 nonlinear equations in 21 unknowns, which can be solved numerically. The subroutine *fsolve* of *Matlab*, that is based on Newton-Raphson method,

Link i	a_i	b_i	α_i(deg)	θ_i(deg)
1	0	0	-62.7126	0
2	0.0239	0	-11.0926	35.0924
3	0	0.1760	106.6820	62.7137
4	2.2620	0	72.8709	117.7082
5	0	-1.8796	55.8331	-24.6355
6	0.0738	3.2468	62.8430	-2.3164
7	1.2060	-1.4819	0	225.4504
$L = 1.0444 \quad \kappa = 1.0$				

Table 5.2: DH parameters for the fully isotropic architecture: Design 2

was employed for solving the said system of nonlinear equations. The results obtained for this design are given in Table 5.2, while the corresponding manipulator in its isotropic configuration is shown in Fig. 5.3. The associated Jacobian matrix for this configuration can be shown to have a condition number of unity. Similar to the previous example, eq. (5.5) results in the same value for L as the one obtained with *fsolve*. The DH parameters of this example (Design 2), serves as a baseline design for the final kinematic design of REDIESTRO 1, as discussed in Chapter 7.
From Fig. 5.3 it can be observed that, by having the first four joints concentrated very close to the manipulator base, the mass of the corresponding links and actuators will be less imposing on the power requirements.

5.3.3 Anthropomorphic Considerations

Anthropomorphic manipulators are those that resemble the human upper limbs. This often requires compact articulations with zero offset distances and intersecting axes. For example, concatenations of three concurrent joint axes forming parts of our limbs are observed, e.g., in the shoulder and the wrist articulations of our upper limbs. In order to aim for anthropomorphism during the kinematic design process, it is thus necessary to set some of the DH parameters equal to zero in such a way that the aforementioned concurrency is achieved. As depicted in Fig. 5.4, in order to have the origins of the two consecutive revolute joints R_i and R_{i+1} coincide, it is required

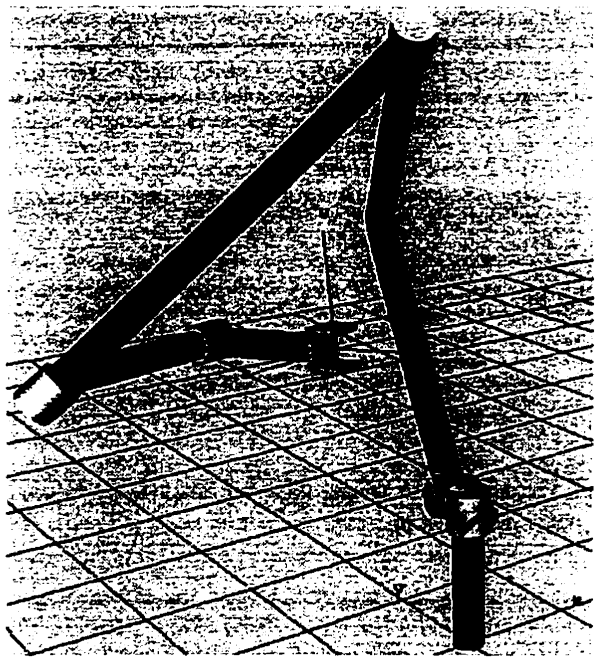

Figure 5.3: Fully isotropic seven-axis manipulator: Design 2

to assign $a_i = b_{i+1} = 0$. Furthermore, if the orthogonality of the intersecting joint axes is also required, a third condition, $\alpha_i = 90°$, would have to be incorporated. For a seven-axis robot, three anthropomorphic architectures are considered here, namely,

(A) 3R-3R-R
(B) 3R-R-3R
(C) 3R-2R-2R

The first two architectures of the foregoing set have two triads of coinciding revolute joints, each triad being consecutively concurrent, the last one having one set of three coinciding joints as well as two sets of two coincident ones. It is apparent that anthropomorphic requirements thus deigned can be achieved at the expense of the overall mobility of the manipulators and to some extent at the expense of the kinematic dexterity. In fact, the existence of any two three-R modules in a seven-axis design gives rise to an architecture that is termed here *pseudoredundant*. The reason for this terminology becomes clear through a simple example. If the fourth revolute

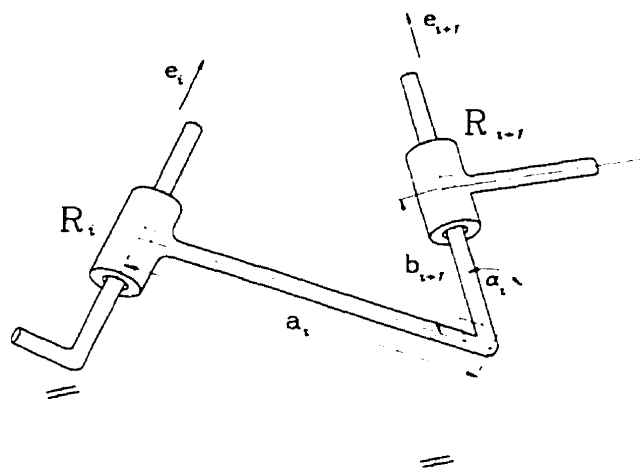

Figure 5.4: Consecutive ith and $i+1$st revolute joints

joint of the 3R-R-3R design is locked, one would expect to be left with a six-axis manipulator having a full mobility of six degrees of freedom. It is apparent that this is not the case, for the operation point is constrained to lie in a sphere centred at the shoulder, and of radius equal to the distance between the shoulder and the wrist centres.

The anthropomorphic conditions proposed above give rise to the following design requirements:

Numerical Example: Design A, 3R-3R-R

For this case one must have

$$a_1 = b_2 = 0, \quad a_4 = b_5 = 0$$

$$a_2 = b_3 = 0, \quad a_5 = b_6 = 0$$

Having preassigned values to the eight foregoing design parameters, one is left with a *pseudoredundant manipulator*, with only 18 nonzero design variables to satisfy 21 equations, thereby obtaining an overdetermined system of nonlinear equations. Since, in general, one cannot expect a solution to exist for this overdetermined system, it is concluded that isotropic manipulators with two 3R modules cannot exist. By preassigning zero values to eight of the design variables, namely, $a_1, a_2, a_4, a_5, b_2, b_3, b_5$, and b_6, a nonlinear optimization problem is formulated. The aforementioned subroutine *fmins* was used to find the least-square approximation of this nonlinear overdetermined system. The solution obtained is given in Table 5.3, while the corresponding Jacobian matrix has a condition number of 1.3845. Figure 5.5 shows a 3-dimensional rendering of this design. It can be seen

Link i	a_i	b_i	α_i(deg)	θ_i(deg)
1	0	0	-77.8800	0
2	0	0	-80.1659	259.9013
3	1.5045	0	55.4774	3.6829
4	0	1.7420	95.4346	-108.8578
5	0	0	-93.0426	-87.9244
6	2.0629	0	188.9605	-101.4668
7	1.3420	0.0089	0	-145.6447
$L = 1.0002$ $\kappa = 1.3845$				

Table 5.3: DH parameters for Design (A), 3R-3R-R

that this solution, as compared to the previous alternatives, has a closer resemblance to the human arm architecture than the previous fully isotropic examples. Obviously, this is achieved through a trade-off by a small increase in the magnitude of the condition number and an impairment on the overall redundancy of the arm. Therefore, this manipulator is not isotropic. Notice that the CI of this manipulator is 72.4%. For this example, since $\mathbf{J}$ is not isotropic, we cannot expect to obtain L by means of eq.(5.5).

Numerical Example: Design B, 3R-R-3R

For the isotropic design of the second pseudoredundant architecture, i.e., a 3R-R-3R architecture, it is required to have

$$a_1 = b_2 = 0, \quad a_5 = b_6 = 0$$

$$a_2 = b_3 = 0, \quad a_6 = b_7 = 0$$

The DH parameters for Design B is illustrated in Table 5.3.3, while the rendering of this anthropomorphic, but nonisotropic architecture, is given in Fig. 5.6.

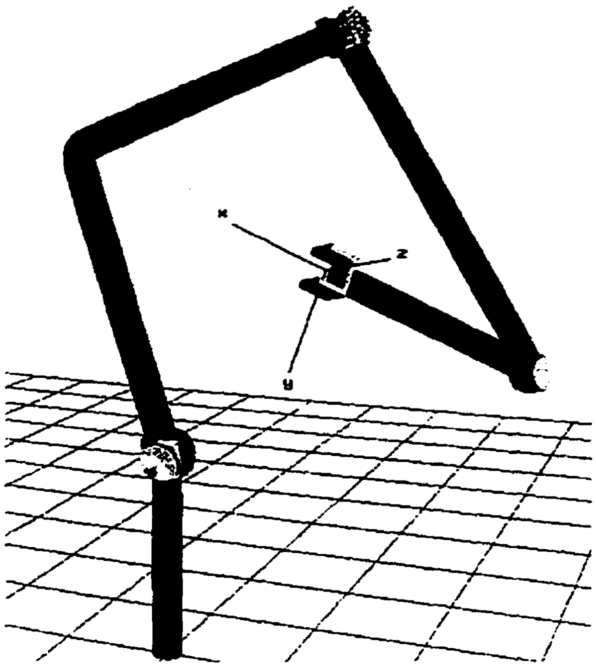

Figure 5.5: Quasi-isotropic anthropomorphic architecture: Design (A), 3R-3R-R

Numerical Example: Design C, 3R-2R-2R

Finally, for the design of the 3R-2R-2R architecture, the set of DH parameters should satisfy the conditions given below:

$$a_1 = b_2 = 0, \quad a_4 = b_5 = 0$$

$$a_2 = b_3 = 0, \quad a_6 = b_7 = 0$$

The DH parameters for this design are given in Table 5.3.3, while its graphical rendering is illustrated in Fig. 5.7.

Numerical Example: Design D, Nine-axis fully isotropic anthropomorphic manipulator

For the sake of completeness, the kinematic design of a fully isotropic anthropomorphic manipulator is discussed next. From the foregoing discussions it is apparent

Link i	a_i	b_i	α_i(deg)	θ_i(deg)
1	0	0	68.4246	0
2	0	0	-77.6089	-81.247
3	1.3353	0	132.0783	50.5267
4	1.2304	0.0977	-120.0623	-105.2396
5	0	-0.1854	93.5111	80.4914
6	0	0	-84.3166	-82.1153
7	0.6798	0.6575	0	63.0681
$L = 1.1658 \quad \kappa = 1.4432$				

Table 5.4: DH parameters for Design (B), 3R-R-3R

Link i	a_i	b_i	α_i(deg)	θ_i(deg)
1	0	0	-67.2917	0
2	0	0	133.6988	-2.4689
3	1.4323	0	159.6295	161.9426
4	0	-0.4111	-93.3292	53.1595
5	1.4440	0	-90.9870	137.8626
6	0	1.1185	80.8763	32.3106
7	1.1380	0	0	-150.4670
$L = 0.8706 \quad \kappa = 1.4623$				

Table 5.5: DH parameters for Design (C), 3R-2R-2R

that isotropy and anthropomorphism cannot be achieved simultaneously for seven-axis robots, since the latter requirements often lead to pseudoredundancy. It is thus required to increase the number of degrees of freedom of the robot. In order to obtain such a design it is required to have at least 21 unknowns to satisfy the 21 isotropy conditions on the Jacobian matrix. If an eight-axis robot is considered, the number of design variables will be:

$$\begin{aligned} k &= 32 \quad \text{(total number of DH parameters)} \\ &- 3 \quad (b_1, \theta_1, \alpha_7) \\ &- 12 \quad \text{(condition for the three 3R modules)} \\ &= 17 < 21. \end{aligned}$$

Therefore, eight-axis manipulators with three 3R modules do not possess enough number of design variables either. A nine-axis manipulator with three modules of

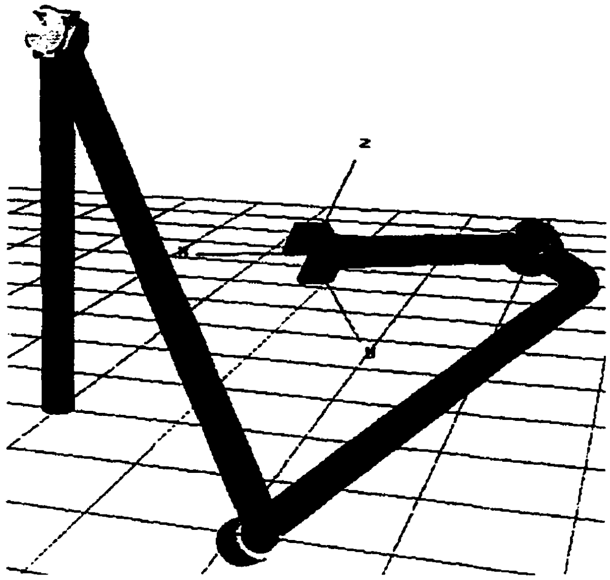

Figure 5.6: Quasi-isotropic anthropomorphic architecture: Design (B), 3R-R-3R

three concurrent axes is examined next. The number of design parameters k for this class of manipulators is:

$$\begin{aligned} k &= 36 \quad \text{(total number of DH parameters)} \\ &- 3 \quad (b_1, \theta_1, \alpha_7) \\ &- 12 \quad \text{(condition for the three 3R modules)} \\ &= 21 \end{aligned}$$

Having established 21 unknowns, the design problem can now be formulated as a set of nonlinear equations. The results obtained from *fsolve* are given in Table 5.6, while the graphical rendering of this manipulator is presented in Fig 5.8.

5.4 Hyperredundancy and Isotropy

The notion of *hyperredundant* manipulators has been used for those manipulators with a significant number of degrees of redundancy (Chirikjian and Burdick, 1993,

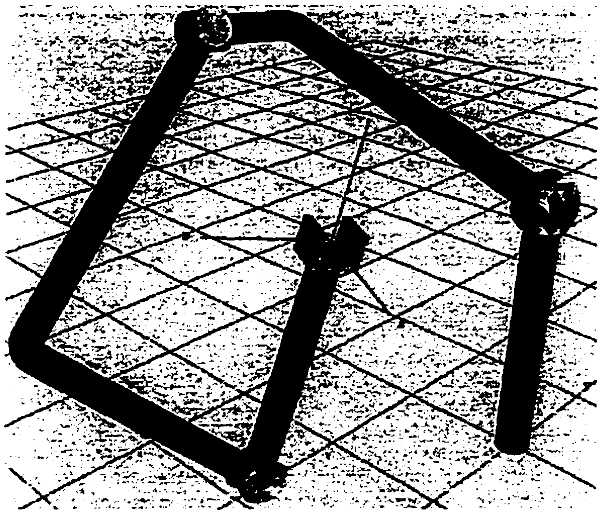

Figure 5.7: Quasi-isotropic anthropomorphic architecture: Design (C), 3R-2R-2R

1994). In this section, kinematic isotropy, as applied to hyperredundant planar (snake-like) architectures, is discussed. It will be shown that the isotropic posture of these manipulators indeed resembles to some extent the familiar shape of a cobra in an attack pose. Although the shape of comfortable/dextrous configurations attained by living articulated bodies is the outcome of complex natural interactions, and it is by no means intended here to overemphasize kinetostatic dexterity as a determining factor in shaping these configurations, it is interesting to note that by aiming at optimum kinetostatic postures (i.e., isotropy), such familiar configurations are obtained.

5.4.1 Formulation

The schematic drawing of a typical hyper-redundant planar manipulator for both positioning and orienting is shown in Fig 5.9. The forward kinematics of this manipulator takes on the form

$$\phi = \theta_1 + \theta_2 + \cdots + \theta_n \tag{5.11a}$$

Link i	a_i	b_i	α_i(deg)	θ_i(deg)
1	0	0	59.3517	0
2	0	0	90.0	90.0
3	0.7559	0	-90.0	60.6483
4	0	-0.3478	120.6483	90.0
5	0	0	-90.0	90.0
6	0.7559	0	90.0	60.6483
7	0	0.3478	-120.6483	90.0
8	0	0	90.0	90.0
9	0.4804	0	0	65.941
$L = 0.3397$ $\kappa = 1.00000$				

Table 5.6: Fully-isotropic anthropomorphic nine-axis manipulator: Design D, 3R-3R-3R

$$x = a_1 \cos\theta_1 + a_2 \cos(\theta_1 + \theta_2) + \cdots + a_n \cos(\theta_1 + \theta_2 + \cdots \theta_n) \tag{5.11b}$$

$$y = a_1 \sin\theta_1 + a_2 \sin(\theta_1 + \theta_2) + \cdots + a_n \sin(\theta_1 + \theta_2 + \cdots \theta_n) \tag{5.11c}$$

where ϕ is the orientation of the last link, with x and y being the Cartesian coordinates of the operation point, attached to the last link. If the manipulator is considered for positioning tasks only, the forward kinematics reduces to the last two of the foregoing three equations (eqs. 5.11b, and 5.11c). The instantaneous forward kinematics of hyper-redundant manipulators is of the from shown below.

$$\mathbf{J}\,\dot{\boldsymbol{\theta}} = \dot{\mathbf{x}} \tag{5.12}$$

where, in general $\mathbf{J}$, the $(3 \times n)$ Jacobian matrix associated with the manipulator takes on the form

$$\mathbf{J} = \begin{bmatrix} 1 & 1 & \cdots & 1 \\ -(s_1 + s_{12} \cdots + s_{12\cdots n}) & -(s_{12} \cdots + s_{12\cdots n}) & \cdots & -s_{12\cdots n} \\ (c_1 + c_{12} \cdots + c_{12\cdots n}) & (c_{12} \cdots + c_{12\cdots n}) & \cdots & c_{12\cdots n} \end{bmatrix} \tag{5.13}$$

with $\dot{\boldsymbol{\theta}}$, the n-dimensional vector of joint rates, defined as

$$\dot{\boldsymbol{\theta}} \equiv \begin{bmatrix} \dot{\theta}_1 \\ \dot{\theta}_2 \\ \vdots \\ \dot{\theta}_n \end{bmatrix} \tag{5.14}$$

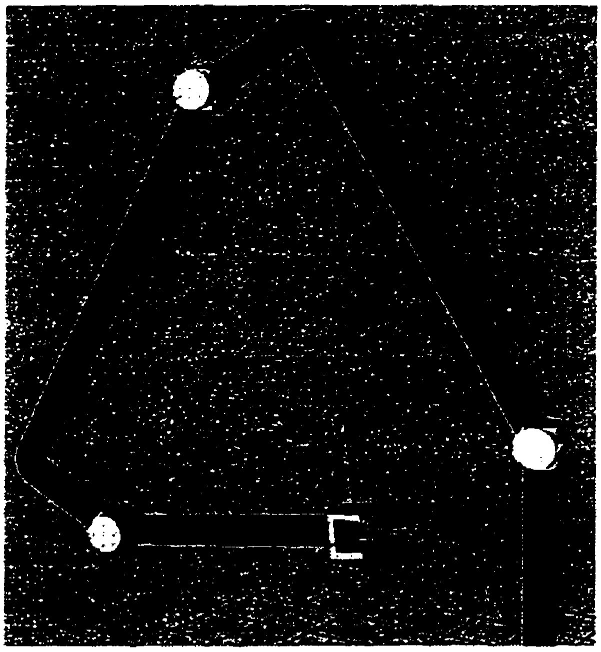

Figure 5.8: Fully-isotropic anthropomorphic nine-axis manipulator. Design D, 3R-3R-3R

with $\dot{\mathbf{x}}$, the *three*-dimensional vector of Cartesian velocities of the end-effector being defined, in turn, as

$$\dot{\mathbf{x}} \equiv \begin{bmatrix} \dot{\phi} \\ \dot{x} \\ \dot{y} \end{bmatrix} \tag{5.15}$$

In the foregoing equations it was assumed that $a_1 = a_2 \cdots = a_n = 1$, with,

$$s_1 \equiv \sin\theta_1, \quad c_1 \equiv \cos\theta_1$$

$$s_{12} \equiv \sin(\theta_1 + \theta_2), \quad c_{12} \equiv \cos(\theta_1 + \theta_2)$$

$$\vdots$$

$$s_{12\cdots j} \equiv \sin(\theta_1 + \theta_2 \cdots + \theta_j), \quad c_{12\cdots j} \equiv \cos(\theta_1 + \theta_2 \cdots \theta_j)$$

The link lengths of the manipulator having been chosen a priori, isotropic *architecture* design will have no relevance for this manipulator; however, it is desired to obtain an optimum *configuration* of the manipulator in the sense of kinematic isotropy.

Hence, the problem reduces to minimizing the condition number of the Jacobian matrix over the set of joint variables $\dot{\boldsymbol{\theta}}$. After formulating an optimization problem similar to those of the previous sections, it becomes apparent that possibly due to the large number of trigonometric sums and products involved, the convergence of the problem to an optimal solution is not adequate. However, by performing some simple algebraic manipulations on the definition of the Jacobian matrix, and reducing the number of the said sums and products, the convergence of the problem can be significantly improved. These simplifications are explained next. Equation (5.12) can be rewritten as

$$\mathbf{J}\,\mathbf{U}\,\mathbf{U}^{-1}\dot{\boldsymbol{\theta}} = \dot{\mathbf{x}} \tag{5.16}$$

with the nonsingular permutation matrix U and its inverse $\mathbf{U}^{-1}$ being defined as,

$$\mathbf{U} \equiv \begin{bmatrix} 1 & 0 & 0 & 0 & \cdots & 0 \\ -1 & 1 & 0 & 0 & \cdots & 0 \\ 0 & -1 & 1 & 0 & \cdots & 0 \\ 0 & 0 & -1 & 1 & \cdots & 0 \\ \vdots & \vdots & \vdots & \vdots & \ddots & \vdots \\ 0 & 0 & 0 & 0 & \cdots & 1 \end{bmatrix}, \quad \mathbf{U}^{-1} \equiv \begin{bmatrix} 1 & 0 & 0 & 0 & \cdots & 0 \\ 1 & 1 & 0 & 0 & \cdots & 0 \\ 1 & 1 & 1 & 0 & \cdots & 0 \\ 1 & 1 & 1 & 1 & \cdots & 0 \\ \vdots & \vdots & \vdots & \vdots & \vdots & \ddots \\ 1 & 1 & 1 & 1 & \cdots & 1 \end{bmatrix} \tag{5.17}$$

respectively. Now the modified version of eq. (5.12), takes on the form

$$\mathbf{J}_a\,\dot{\boldsymbol{\alpha}} = \dot{\mathbf{x}} \tag{5.18}$$

with

$$\mathbf{J}_a \equiv \mathbf{J}\,\mathbf{U}^{-1} = \begin{bmatrix} 0 & 0 & 0 & \cdots & 1 \\ -s_1 & -s_{12} & -s_{123} & \cdots & -s_{12\cdots n} \\ c_1 & c_{12} & c_{123} & \cdots & c_{12\cdots n} \end{bmatrix} \tag{5.19}$$

and

$$\dot{\boldsymbol{\alpha}} = \begin{bmatrix} \dot{\alpha}_1 \\ \dot{\alpha}_2 \\ \dot{\alpha}_3 \\ \vdots \\ \dot{\alpha}_n \end{bmatrix} \equiv \mathbf{U}^{-1}\dot{\boldsymbol{\theta}} = \begin{bmatrix} \dot{\theta}_1 \\ \dot{\theta}_1 + \dot{\theta}_2 \\ \dot{\theta}_1 + \dot{\theta}_2 + \dot{\theta}_3 \\ \vdots \\ \dot{\theta}_1 + \dot{\theta}_2 \cdots + \dot{\theta}_n \end{bmatrix} \tag{5.20}$$

A geometric interpretation of the foregoing algebraic manipulation is that the Jacobian matrix of the system of equations expressed by (5.12) maps the vector of *relative* joint rates $\dot{\boldsymbol{\theta}}$ to the Cartesian velocity vector $\dot{\mathbf{x}}$, while $\mathbf{J}_a$ appearing in eq. (5.18) transforms the vector of *absolute* joint rates $\dot{\boldsymbol{\theta}}_a$ to $\dot{\mathbf{x}}$. The ith relative joint rate $\dot{\theta}_i$ is defined as the angular displacement of the ith link with respect to the $(i-1)$st link, with 0 denoting the base. The ith absolute joint rate, $\dot{\alpha}_i = \sum_1^i \dot{\theta}_i$, is, in turn, defined as the angular displacement of the ith link with respect to the base. Once the absolute joint rates are obtained from the reduced system, the relative joint rates can be readily determined using the equation given below:

$$\dot{\boldsymbol{\theta}} = \mathbf{U}^{-1}\,\dot{\boldsymbol{\alpha}}.$$

Another interpretation of the absolute joint variables used here was recently considered by Maton and Roth (1996), while relating the *schemes of actuation* to the kinematic performance of planar manipulators. By the schemes of actuation it is meant the way in which each joint is driven, that is, whether locally by an actuator attached directly to the link, or remotely by placing the actuator on the base. The absolute angles mentioned before are in fact the joint variables associated with the case of all actuators being installed at the base while assuming identical transmission ratios. Maton and Roth showed that for a 2-R planar manipulator accurate positioning—particularly at larger manipulator reaches—the ground-based actuation is preferred over the manipulator with locally-driven joints. During the numerical optimization of the example given below, this conclusion was clearly observed.

Further simplification of the Jacobian matrix can be achieved if positioning manipulators are considered only. Although the Jacobian is reduced to that of positioning tasks only, it is still possible to achieve a desired orientation for the last link at the isotropic configuration. This is possible since the number of optimization parameters at hand is quite large, and also because the orientation ϕ of the last link is simply the nth absolute joint coordinate. Having reduced the system to that of positioning

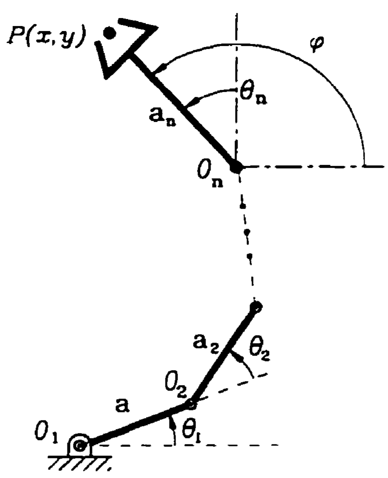

Figure 5.9: Hyper-redundant planar manipulators

tasks only, one obtains

$$\mathbf{J}_a \equiv \mathbf{J}\,\mathbf{U}^{-1} = \begin{bmatrix} -s_1 & -s_{12} & -s_{123} & \cdots & -s_{12\cdots n} \\ c_1 & c_{12} & c_{123} & \cdots & c_{12\cdots n} \end{bmatrix} \tag{5.21}$$

Hence, the isotropy condition on $\mathbf{J}_a$ takes on a very simple form, i.e.,

$$\mathbf{J}_a\mathbf{J}_a^T = \begin{bmatrix} \sum_1^n \sin^2\alpha_i & -\sum_1^n \sin\alpha_i\,\cos\alpha_i \\ -\sum_1^n \cos\alpha_i\,\sin\alpha_i & \sum_1^n \cos^2\alpha_i \end{bmatrix} = \begin{bmatrix} \sigma^2 & 0 \\ 0 & \sigma^2 \end{bmatrix} \tag{5.22}$$

whereby, the common singular value of $\mathbf{J}_a$ is readily determined by equating the trace of both sides of eq. (5.22), i.e.,

$$\sigma = \sqrt{\frac{n}{2}}$$

5.4.2 Numerical Example: 30-Axis Planar Manipulator

As a representative example for the isotropic configuring of hyperredundant manipulators, a planar 30-dof robot for positioning tasks is considered. The minimization routine *fmins* is once again used to find one optimum solution $\boldsymbol{\theta}^*$ at which the condition number of the Jacobian matrix is unity, and where the additional constraints listed below are also satisfied. All of the required scalar objective functions are grouped together as entries of a vector $\mathbf{z}$ whose Euclidean norm is minimized using the *Nelder and Mead* search technique implemented by *fmins*, i.e.,

$$\boldsymbol{\theta}^{*} = \min_{\boldsymbol{\theta}}(\mathbf{z}^T \mathbf{W} \mathbf{z}) \tag{5.23}$$

with $\mathbf{W}$ being a weighting matrix of the appropriate dimension.

Objectives

- Condition number minimization:

$$z_1 \equiv \kappa(\mathbf{J}_a) \rightarrow \min$$

- It is required that at any configuration, the first two links remain horizontal, i.e.,

$$z_2 \equiv \theta_1 \rightarrow \min$$

$$z_3 \equiv \theta_2 \rightarrow \min$$

- At an isotropic configuration it is required that the last link also remains horizontal, i.e.,

$$z_4 = \phi = \sum_1^n \theta_i \rightarrow \min$$

- As the last constraint, it is required that the norm of the vector of joint variables $\boldsymbol{\theta}$ at an isotropic configuration be a minimum. This additional constraint results in a smoother shape of the manipulator at the isotropic configuration. An alternative but computationally more intensive way of ensuring a smooth shape is to minimize the second difference between the value of each joint i to that of $i+1$. This condition which is in some sense a measure of the curvature of the manipulator, was also studied, but it was decided that the computational burden that it creates outweighs the improved smoothness of the manipulator backbone. Hence, the last additional constraint was chosen to be

$$z_5 \equiv \|\boldsymbol{\theta}\| \rightarrow \min$$

The vector $\mathbf{z}$ containing the scalar objective functions of eq. (5.23) takes on the form,

$$\mathbf{z} = \begin{bmatrix} z_1 \\ z_2 \\ z_3 \\ z_4 \\ z_5 \end{bmatrix}$$

The initial guess for the joint-variable vector was chosen to be a set of very small random numbers. These were small values for each joint just enough to bring the Jacobian out of the singularity of the configuration at which all joint variables are zero. The evolution of the shape of the manipulator during the optimization procedure is shown in Fig. 5.10, a graphical rendering of this 30-axis manipulator at an isotropic posture being illustrated in Fig. 5.11. The condition number of the Jacobian matrix at this configuration is equal to unity, and, as can bee seen, the joint coordinates are such that the manipulator has a very smooth shape.

5.5 Kinematic Isotropy and Singularity Distribution

In this Section a comparative analysis of isotropic versus nonisotropic manipulators is made. The basis of the comparison is the distribution of the set of singularities of the manipulators throughout the joint-space. In general, comparing two manipulators for any functional purpose is not a clear task. The framework in which a fair comparison can find meaning should thus be laid down first. The main objective of this section is to provide a framework for the comparison of redundant manipulators in the sense of kinematic dexterity and singularity distributions.

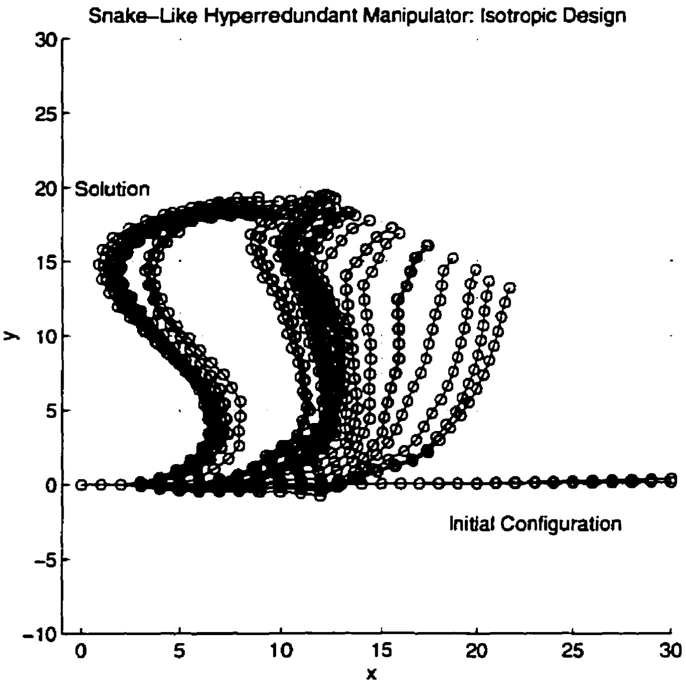

Figure 5.10: Condition number minimization of a snake-like manipulator

As explained in the previous chapters, the reciprocal of the p-norm condition number of the Jacobian matrix $\mathbf{J}$ represents the p-norm *distance* from $\mathbf{J}$ to the sets of singular matrices. Hence, in an absolute sense, isotropic matrices lie farthest from their singularities. This feature by itself is quite attractive; however, one may pose the question of how the variation of the condition number and, thus, the kinematic dexterity of an isotropic manipulator behaves throughout the entire workspace, or throughout the joint-space. Alternatively, although an isotropic manipulator at the isotropic configuration attains the largest possible distance to the singularities of $\mathbf{J}$, the mean-value of the variations of the condition number is compared to that of a nonisotropic manipulator. Obviously, the first issue to be addressed before attempting to answer the foregoing question is how two manipulators can be compared without comparing *apples* and *oranges*. Some of the factors considered here while comparing two manipulators are listed below:

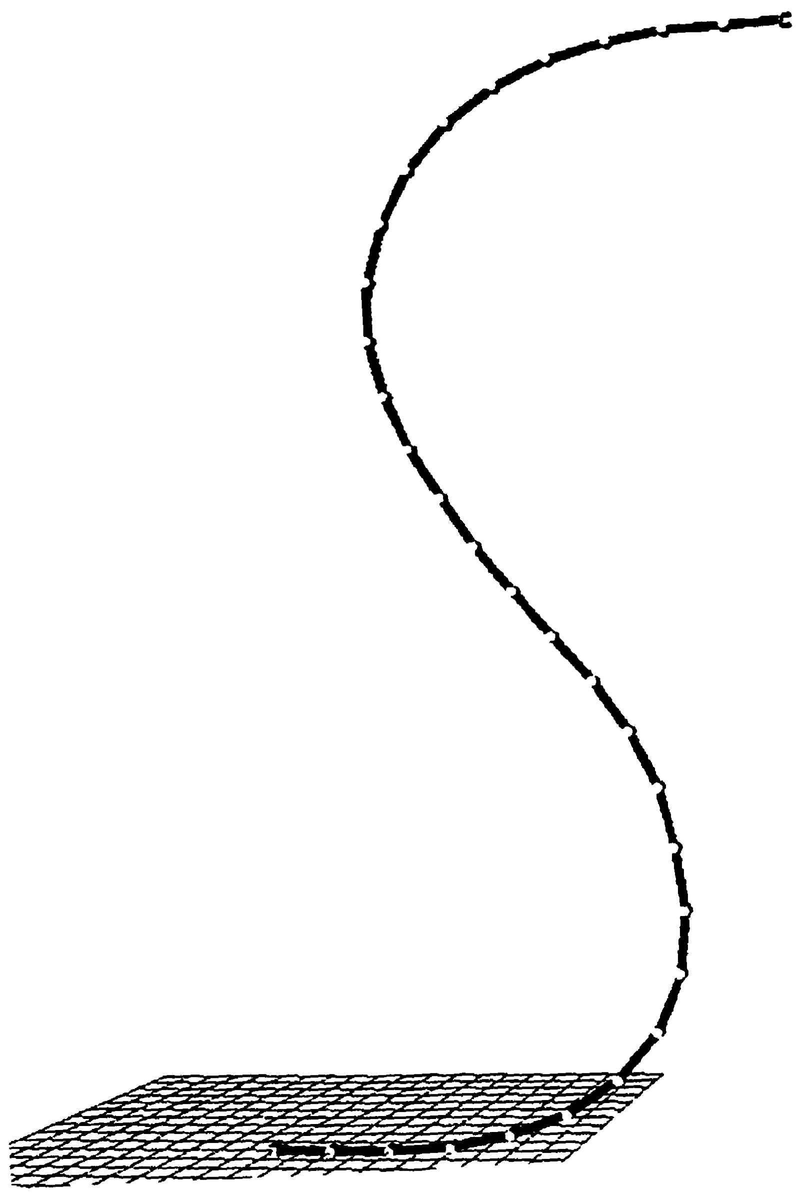

Figure 5.11: Graphical rendering of a 30-axis isotropic manipulator

Link i	a_{i-1} m	b_i m	α_{i-1}(deg)	θ_i(deg)
1	0.0	0	0.0	θ_1
2	-0.12319	0	-90.0	θ_2
3	0.10795	0.05461	90.0	θ_3
4	-0.07938	0	-90.0	θ_4
5	0.07938	0.05461	90.0	θ_5
6	-0.0492	0	-90.0	θ_6
7	0.0492	0	90.0	θ_7

Table 5.7: DH parameters of the Robotics Research K1207 Manipulator

(a) Identical degrees of freedom.

(b) Compatibility in the *size* of the manipulators.

(c) Compatibility in the configuration of the manipulators.

To satisfy requirement (a) given above, as a representative example, a redundant seven-axis and isotropic manipulator is compared with a seven-axis redundant, but nonisotropic manipulator. The isotropic manipulator used for this example is the manipulator introduced in Section 5.2 and whose DH parameters are given in Table 5.2 (Design no. 2, illustrated in Fig. 5.3). The nonisotropic manipulator to be compared against the isotropic one is the Robotics Research K1207 (Farrell et al., 1990; Seraji et al., 1993). The DH parameters of this manipulator as given in the foregoing references, are shown in Table 5.5.

As mentioned in Section 5.3, the a_i parameters are defined as link lengths and should be allowed to take on positive values only. Hence, the equivalent set of DH parameters that does not contain negative link lengths is first evaluated. Moreover, in order to satisfy the size-compatibility condition (b), it is required to normalize the link-lengths and offsets of the two manipulators. To this end a normalizing length that is intrinsic to the manipulators should be employed. The characteristic length L, as defined in Section 5.3, is used, and the link lengths a_i as well as the link offsets b_i are divided by L. Although, other choices for this normalizing length exist such as, the *maximum reach*, or the largest link-length of the manipulator, the characteristic length is used

Link i	a_i m	b_i m	α_i(deg)	θ_i(deg)
1	0.12319	0	90.0	θ_1
2	0.10795	0	90.0	43.2274
3	0.07938	0.05461	90.0	179.9416
4	0.07938	0	90.0	50.1589
5	0.0492	0.05461	90.0	180.0129
6	0.0492	0.0	90.0	19.5556
7	0.0	0.01778	90.0	0.2436
$L = 0.2554108$ m $\kappa_{min} = 1.7004$				

Table 5.8: DH parameters of the Robotics Research K1207 Manipulator (with positive link-lengths)

because it also minimizes the condition number. The characteristic length of K1207-RR was found to be 0.2554108 m. In order to satisfy requirement (c) mentioned above, the minimization routines discussed before were used to obtain a configuration of the two manipulators at which the condition number of the associated Jacobian matrix is a minimum. The modified set of DH parameters according to the convention employed in this thesis for the K1207 manipulator at its optimum configuration, together with the associated characteristic length, are given in Table 5.8.

The graphical skeleton rendering of K1207 at its optimally-conditioned configuration where the condition number of the Jacobian matrix attains a minimum of 1.7004, is shown in Fig. 5.12. It is interesting to note that although K1207 is not designed for kinematic isotropy, its minimum condition number is not very far from unity; however, as will be shown presently, even such a small deviation from isotropy results in a relatively significant difference on its singularity distribution.

Having established the three compatibility requirements, the reciprocal of the condition numbers of the two manipulators are then minimized starting from their respective optimal-dexterity configurations towards their closest singularities. The same minimization routine *fmins* is used for both cases, while the intermediate variations of the reciprocal of the condition number is recorded. As the two manipulators move away from their optimum configurations towards their nearest singularity, the condition number is plotted against the number of iterations toward singularity (Fig. 5.13).

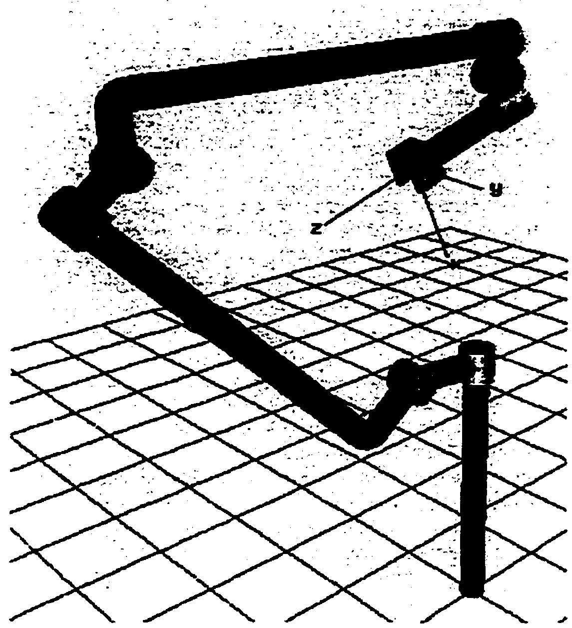

Figure 5.12: Skeleton-rendering of the Robotics Research K1207 manipulator at its optimum-dexterity configuration

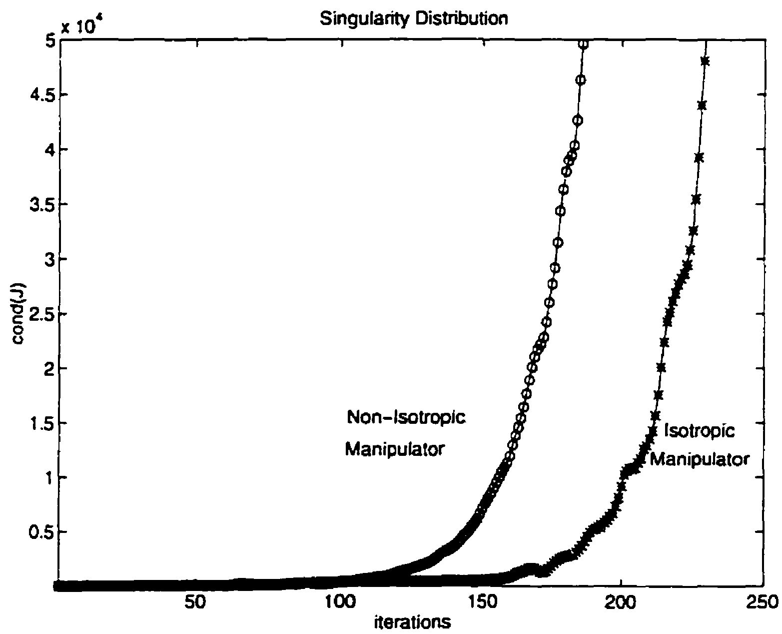

Figure 5.13: Comparison of isotropic and nonisotropic manipulators

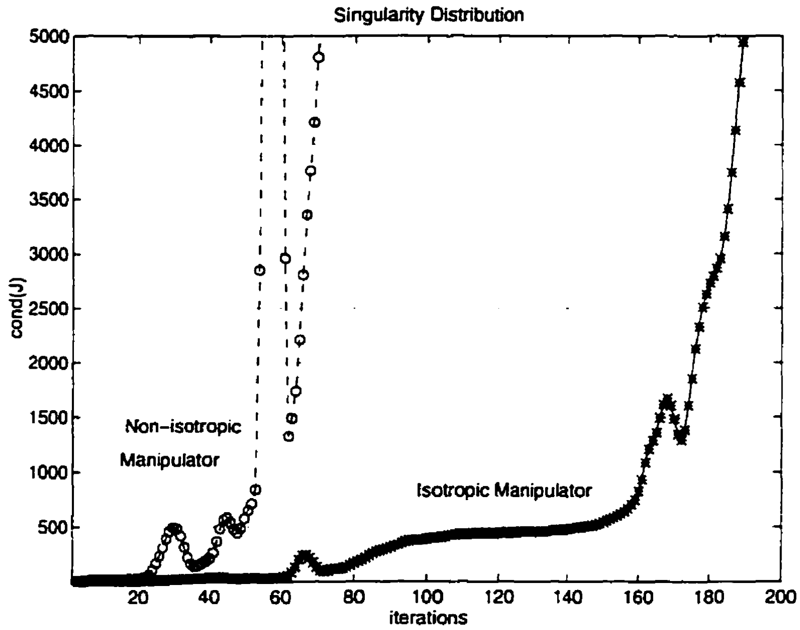

Figure 5.14: Comparison of isotropic and nonisotropic manipulators

It can be seen from Fig. 5.13 that the variation of the condition number for the isotropic manipulator stays flat for a larger number of iterations when compared to the nonisotropic arm. The same pattern was observed while repeating this comparison for other nonisotropic or quasiisotropic manipulators discussed in this chapter. As a second representative example, the anthropomorphic 3R-3R-R manipulator of Fig. 5.5 and Table 5.3 was compared with the isotropic arm introduced as Design No. 2. The results of this comparison are shown in Fig. 5.14. The condition number of the nonisotropic design used in the second example at its optimum-dexterity configuration is only 1.3845; however, a dramatic change in the variation of the condition number as compared to that of the isotropic arm can be observed in Fig. 5.14.

5.6 Conclusions

The emphasis of this Chapter was mainly on the application of kinetostatic performance indices in the design of seven-axis, revolute-coupled manipulators. Three different optimum solution approached were studied: first, a nonlinear minimization problem was solved, which, in effect, rendered the Jacobian matrix fully isotropic; next, it was argued that, despite the fully isotropic nature of the first solution, some of its structural features could be improved. This led to preassigning some of the parameters defining the structure of the manipulator, which in turn resulted in a system of 21 nonlinear equations in 21 unknowns. As a second approach, the DH parameters of an isotropic manipulator were then obtained by solving the said system of nonlinear equations. In order to make the manipulator structure anthropomorphic, further constraints were imposed, which led to three alternative designs, namely, 3R-3R-R, 3R-R-3R, and 3R-2R-2R. First, it was argued that the existence of two 3-R modules in the architecture of seven-axis designs leads to *pseudoredundancy*. Hence, it was shown that isotropy and anthropomorphism for seven-axis and eight-axis manipulators cannot coexist. An example of a nine-axis fully isotropic design was obtained.

Isotropic configuration design of hyperredundant planar manipulators was then discussed, where a method of simplifying the computational requirement of the optimization problem at hand was provided. The isotropic configuration of a 30-axis planar robot in the presence of additional functional requirements was determined. This design led to a familiar configuration that to some extent resembles the configuration of a cobra in an attack posture.

In the last part of the chapter, a comparative analysis of the effects of kinematic isotropy on the distribution of the joint-space singularities was included. Within the framework of this analysis, isotropic and nonisotropic designs were compared. The results of these comparisons provided a graphical confirmation for the role of kinematic isotropy on the nature of the joint-space singularities.

Chapter 6

A Geometric Analysis of Kinematic Isotropy

6.1 Introduction

In this Chapter, the kinematic conditioning and dexterity of general revolute-jointed manipulators are discussed from a geometric point of view. Furthermore, based on a previously reported *measure of isotropy* (Kim and Khosla, 1991), a novel measure of conditioning for general matrices is introduced. It is shown that this measure is a linear approximation to the normalized Frobenius-norm (F-norm) condition number; for quasiisotropic matrices, it provides a very close prediction of the condition number. For both rectangular and square matrices, upper and lower bounds are obtained for this measure in terms of the F-norm and the 2-norm condition numbers. Based on this measure of conditioning, a measure of manipulator conditioning is devised that is highly suited for the intended task of manipulator design. Moreover, this performance index is substantially less expensive to compute than other measures of kinematic conditioning; is amenable to optimization using gradient methods, rather than with purely direct-search methods, which are much costlier. Based on a gradient technique for the minimization of this index with respect to the normalizing length and the operation point of the end-effector, a preferred normalizing length and a preferred operation point of the end-effector are obtained. In this regard the notions of *manipulator layout*, *layout conditioning*, *layout length* and *layout centre* for any serial-type robotic manipulators are introduced. Furthermore, the characteristic layout of manipulators are discussed followed by discussions on the characteristic length and the characteristic point. Several illustrative examples are provided for determining the optimum layout of both redundant and nonredundant industrial manipulators.

6.2 A Novel Kinematic Performance Measure

In this section, a novel *measure of conditioning*, denoted by $\tilde{\kappa}_{\tilde{F}}$ for general square and rectangular matrices, is derived. Based on this conditioning measure, a performance measure called the *layout conditioning* is then introduced. This measure is significantly less complex to compute as compared to any usual p-norm or F-norm condition numbers. The characterization of this measure and a comparison of its predictions with the 2-norm and the F-norm condition numbers are discussed. Moreover, it is shown that this measure of conditioning is bounded from below by the normalized F-norm condition number and by the mth power of the 2-norm condition number from above, with m being the dimension of the task space of the manipulator (e.g., $m = 6$ for the most general tasks). A significantly reduced complexity of the proposed measure allows the use of symbolic computations, thereby gaining more geometric insight into characterizing the kinematic performance of serial manipulators.

6.2.1 Derivations

An estimate of the reciprocal of the condition number, based on the geometric and algebraic means of the singular values of the matrix, was introduced by Kim and

Khosla (1991) as

$$\Delta \equiv \frac{1}{\tilde{\kappa}} \tag{6.1}$$

where

$$\tilde{\kappa} \equiv \frac{\mathrm{tr}(\mathbf{A}\mathbf{A}^T)}{m\,[\det(\mathbf{A}\mathbf{A}^T)]^{\frac{1}{m}}} = \frac{\sigma_1^2 + \sigma_2^2 + \cdots + \sigma_m^2}{m\,(\sigma_1^2\,\sigma_2^2\,\cdots\,\sigma_m^2)^{\frac{1}{m}}} \tag{6.2}$$

Motivated by the foregoing heuristic definition of $\tilde{\kappa}$, an expression that for quasi-isotropic matrices[1] represents an approximation of the condition number is introduced. In fact, it will be shown that this index arises naturally while determining the first-order approximation of the $\bar{F}$-norm condition number of $\mathbf{A}$. In order to derive an estimate of the condition number of a general $m \times n$ matrix $\mathbf{A}$, with $m \le n$, the definition of $\kappa_{\bar{F}}$ is recalled,

$$\kappa_{\bar{F}}^2 = \frac{1}{m^2}\mathrm{tr}(\mathbf{B})\,\mathrm{tr}(\mathbf{B}^{-1}) \tag{6.3}$$

with $\mathbf{B} \equiv \mathbf{A}\mathbf{A}^T$. From the Cayley-Hamilton theorem, we have

$$\mathbf{B}^{-1} = \frac{-1}{C_m}\left(\mathbf{B}^{m-1} + C_1\mathbf{B}^{m-2} + \cdots + C_r\mathbf{B}^{m-r-1} + \cdots + C_{m-1}\,\mathbf{1}_m\right) \tag{6.4}$$

where $\mathbf{1}_m$ is the $m \times m$ identity matrix, and $\{C_i\}_1^m$ is the set of coefficients of the characteristic polynomial $P_m(\lambda)$ of $\mathbf{B}$. These coefficients are given by (Finkbeiner, 1966):

$$\begin{aligned}
C_1 &\equiv -\mathrm{tr}(\mathbf{B}) \\
C_2 &\equiv -\frac{1}{2}[C_1\,\mathrm{tr}(\mathbf{B}) + \mathrm{tr}(\mathbf{B}^2)] \\
C_3 &\equiv -\frac{1}{3}[C_2\,\mathrm{tr}(\mathbf{B}) + C_1\,\mathrm{tr}(\mathbf{B}^2) + \mathrm{tr}(\mathbf{B}^3)] \\
&\vdots \\
C_m &\equiv -\frac{1}{m}[C_{m-1}\,\mathrm{tr}(\mathbf{B}) + C_{m-2}\,\mathrm{tr}(\mathbf{B}^2) + C_{m-3}\mathrm{tr}(\mathbf{B}^3) + \cdots C_1\,\mathrm{tr}(\mathbf{B}^{m-1}) + \mathrm{tr}(\mathbf{B}^m)]
\end{aligned}$$

Furthermore, it is known that,

$$C_m = (-1)^m \det(\mathbf{B}) \tag{6.5}$$

[1]a matrix is called quasiisotropic if its condition number is $O(1)$

Equating the trace of both sides of eq.(6.4) yields

$$\mathrm{tr}(\mathbf{B}^{-1}) = \frac{-1}{C_m}\left(\mathrm{tr}(\mathbf{B}^{m-1}) + C_1\,\mathrm{tr}(\mathbf{B}^{m-2}) + \cdots + C_r\,\mathrm{tr}(\mathbf{B}^{m-r-1}) + \cdots + m\,C_{m-1}\right) \quad (6.6)$$

Now, if a real positive number λ_o approximates the set of eigenvalues $\{\lambda_i\}_1^m$, of $\mathbf{B}$, up to the first order, namely,

$$\lambda_i = \lambda_o + \delta\,\lambda_i, \quad \delta << 1, \quad i = 1, 2, \cdots m \quad (6.7)$$

then, the expressions below are readily verified:

$$\mathrm{tr}(\mathbf{B}) = m\,\lambda_o + \epsilon \quad (6.8)$$

$$\mathrm{tr}^k(\mathbf{B}) = m^{k-1}\,\lambda_o^{k-1}(m\,\lambda_o + k\,\epsilon) + O(\epsilon^2) \quad (6.9)$$

$$\mathrm{tr}(\mathbf{B}^k) = \lambda_o^{k-1}\,(m\,\lambda_o + k\,\epsilon) + O(\epsilon^2) \quad (6.10)$$

where

$$\epsilon \equiv \sum_{i=1}^{m} \delta\lambda_i.$$

Using these identities, the expressions for $\{C_i\}_1^m$ can be obtained as shown below

$$C_1 = -(m\,\lambda_o + \epsilon) \quad (6.11)$$

$$C_2 = \frac{1}{2!}\,\lambda_o\,(m-1)\,(m\,\lambda_o + 2\,\epsilon) + O(\epsilon^2)$$

$$C_3 = -\frac{1}{3!}\,\lambda_o^2\,(m-1)\,(m-2)\,(m\,\lambda_o + 3\,\epsilon) + O(\epsilon^2)$$

$$\vdots$$

$$C_k = \frac{(-1)^k}{k!}\,\lambda_o^{k-1}\,\frac{m!}{m\,(m-k)!}\,(m\,\lambda_o + k\,\epsilon) + O(\epsilon^2)$$

$$\vdots$$

$$C_{m-1} = (-1)^{m-1}\lambda_o^{m-2}\,[m\,\lambda_o + (m-1)\,\epsilon] + O(\epsilon^2)$$

$$C_m = (-1)^m\,\det\mathbf{B} = (-1)^m\lambda_o^{m-1}\,(\lambda_o + \epsilon) + O(\epsilon^2) \quad (6.12)$$

Substituting for $\{C_i\}_1^m$ from the foregoing equations in eq.(6.6) and simplifying up to the first order results in

$$\mathrm{tr}(\mathbf{B}^{-1}) = \frac{m\,\lambda_o + (m-1)\,\epsilon}{\lambda_o\,(\lambda_o + \epsilon)}\,[1 - m + \frac{m(m-1)}{2!} - \frac{m(m-1)(m-2)}{3!} + \cdots$$

$$+ (-1)^k\,\frac{m(m-1)(m-2)\cdots(m-k-1)}{k!} + \cdots + (-1)^{m-1}\,m] + O(\epsilon^2)$$

By adding and subtracting $(-1)^m$ to the terms enclosed in square brackets in the right-hand side of the foregoing equation, it follows that

$$\mathrm{tr}(\mathbf{B}^{-1}) = \frac{m\,\lambda_o + (m-1)\,\epsilon}{(-1)^m\,\lambda_o\,(\lambda_o+\epsilon)}\,[\sum_0^m B_i - (-1)^m] + O(\epsilon^2) \tag{6.13}$$

where, $\{B_i\}_0^m$ are the binomial coefficients for an expansion of the form $(X-1)^m$; hence,

$$\sum_{i=0}^m B_i = 0$$

Therefore,

$$\mathrm{tr}(\mathbf{B}^{-1}) = \frac{m\,\lambda_o + (m-1)\,\epsilon}{\lambda_o\,(\lambda_o+\epsilon)} + O(\epsilon^2) \tag{6.14}$$

or

$$\mathrm{tr}(\mathbf{B}^{-1}) = \frac{m^{m-2}\,\lambda_o^{m-2}\,[m\,\lambda_o + (m-1)\,\epsilon]}{m^{m-2}\,\lambda_o^{m-1}\,(\lambda_o+\epsilon)} + O(\epsilon^2) \tag{6.15}$$

Furthermore, by making use of eqs. (6.8), and (6.12), the foregoing expression can be written as

$$\mathrm{tr}(\mathbf{B}^{-1}) = \frac{\mathrm{tr}^{m-1}(\mathbf{B})}{m^{m-2}\,\det(\mathbf{B})} + O(\epsilon^2) \tag{6.16}$$

Finally, by substituting the foregoing expression in eq.(6.3), while neglecting the higher-order terms $O(\epsilon^2)$, the first-order approximation of the $\bar{F}$-norm condition number denoted by $\tilde{\kappa}_F$, is obtained as

$$\tilde{\kappa}_F = \sqrt{\frac{\mathrm{tr}^m(\mathbf{B})}{m^m\,\det(\mathbf{B})}} \approx \kappa_F. \tag{6.17}$$

Hence, it turns out that the proposed first-order estimate, henceforth called the *conditioning measure* is, in fact, the square root of the mth power of the reciprocal of the measure proposed in Kim and Khosla (1991), i.e.,

$$\tilde{\kappa}_F^2(\mathbf{A}) \equiv \frac{\mathrm{tr}^m(\mathbf{A}\mathbf{A}^T)}{m^m\,\det(\mathbf{A}\mathbf{A}^T)} = \tilde{\kappa}^m \tag{6.18}$$

From eq.(6.18), it is apparent that $\tilde{\kappa} = \tilde{\kappa}_F^{2/m}$, and, as shown in the numerical example below, $\tilde{\kappa}_F^{2/m}$ predicts κ more accurately than $\tilde{\kappa}$.

6.2.2 Features of $\tilde{\kappa}_F$

The conditioning measure $\tilde{\kappa}_F$ obtained above can be regarded as an estimate of the condition number for general matrices (Ranjbaran et al., 1996). In this section several useful features of $\tilde{\kappa}_F$, as applied to kinematic dexterity, are highlighted, that make this index an attractive alternative for the characterization of kinematic dexterity.

Comparison of $\tilde{\kappa}_F$ vs. the 2-Norm and the F-Norm Condition Numbers

Comparisons of κ_2, κ_F, $\tilde{\kappa}$ and $\tilde{\kappa}_F$ are shown in Figs. 6.1 and 6.2 for a planar 3R manipulator, with $l_1 = l_2 = 1$, $l_3 = \sqrt{3}/3$, as functions of the second joint variable θ_2, while the comparison of the reciprocal of these numbers is plotted in Fig. 6.3. From the three foregoing diagrams it is clear that $\tilde{\kappa}_F$ follows κ_2 more closely. At lower condition numbers, the difference may not seem significant; however, by examining this difference near the singular posture, a substantial improvement is gained by using $\tilde{\kappa}_F$. For example, at $\theta_2 = 179.95°$, where the 2-norm condition number κ_2 is about 2000, and the Frobenius-norm condition number κ_F is 808, the two estimates are $\tilde{\kappa} = 99.3$, and $\tilde{\kappa}_F = 989.4$. This shows an improvement of an order of magnitude if $\tilde{\kappa}_F$ is used. It should be apparent that, for larger values of m, the improvement will be even more significant. Henceforth, we will make use of $\tilde{\kappa}_F$ throughout the rest of this chapter. It has to be emphasized that the isotropic design of manipulators can now be conducted by using $\tilde{\kappa}_F$ instead of other complex measures such as κ_2. This is possible, since $\tilde{\kappa}_F$ attains a minimum of unity at the isotropic configuration, similar to other condition numbers.

The foregoing numerical characterizations are more rigorously underlined next, where it is shown that the conditioning measure $\tilde{\kappa}_F(\bar{\mathbf{J}})$ is bounded by $\kappa_{\bar{F}}$ from below and by κ_2^m from above. The proof for $m \times m$ matrices that was first reported in Ranjbaran et al., (1996), is provided first, followed by the proof for general $m \times n$ matrices.

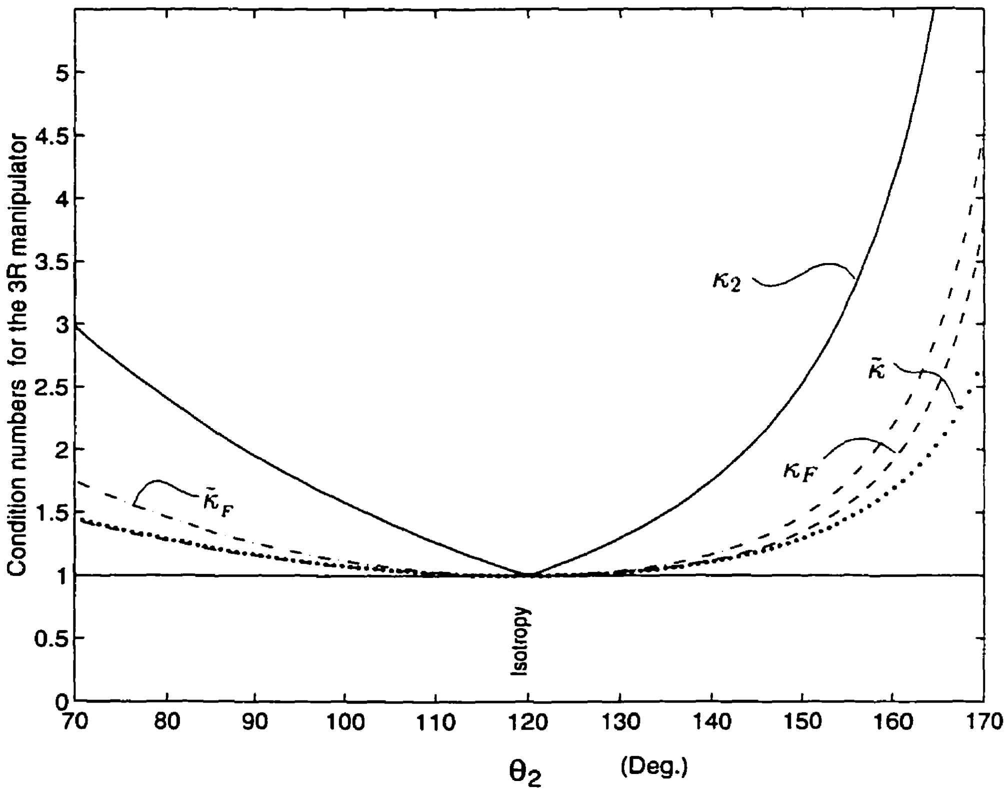

Figure 6.1: Comparison of the condition numbers

Theorem 6.1

The conditioning measure of an $m \times m$ matrix, $\tilde{\kappa}_F(\mathbf{B})$ is bounded by the normalized Frobenius norm from below and by the mth power of the 2-norm condition number from above, i.e,

$$\kappa_{\bar{F}}(\mathbf{B}) \leq \tilde{\kappa}_F(\mathbf{B}) \leq \kappa_2^m(\mathbf{B}) \tag{6.19}$$

Proof:

- Lower bound:

In order to prove the existence of the lower bound in the foregoing statement for square matrices, we recall Richter's Theorem (Householder, 1964; Mirsky, 1956), stating that the Frobenius norm of the adjoint of any $m \times m$ matrix $\mathbf{A}$ verifies the inequality given below:

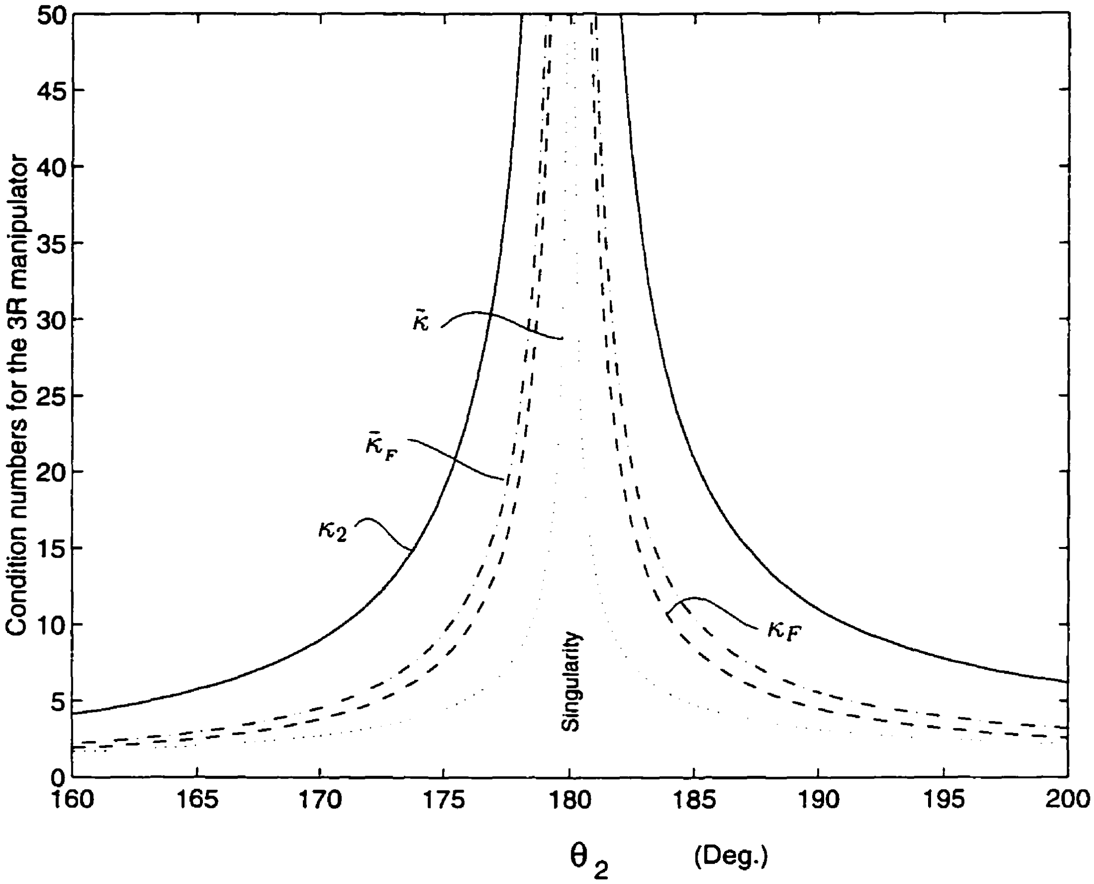

Figure 6.2: Comparison of the condition numbers near singular posture

$$\|\mathrm{adj}(\mathbf{B})\|_F \leq m^{-(m-2)/2}\,\|\mathbf{B}\|_F^{m-1} \tag{6.20}$$

with equality if and only if $m \leq 2$ or if $\mathbf{B}$ is isotropic. If $\mathbf{B}$ is nonsingular, one can divide both sides of the foregoing inequality by $|\det(\mathbf{B})|$. Furthermore, if those two sides are multiplied by $\|\mathbf{B}\|_F$, the following relation is obtained:

$$\|\mathbf{B}\|_F\,\|\mathbf{B}^{-1}\|_F \leq \frac{\|\mathbf{B}\|_F^m}{m^{(m-2/)2}\,|\det(\mathbf{B})|} \tag{6.21}$$

Now, substituting for $\|\cdot\|_F$ in the foregoing inequality from the inequality of eq.(4.19) results in

$$\sqrt{m^2}\,\|\mathbf{B}\|_{\hat{F}}\,\|\mathbf{B}^{-1}\|_{\hat{F}} \leq \frac{\sqrt{m^m}\,\|\mathbf{B}\|_{\hat{F}}^m}{m^{(m-2)/2}\,|\det(\mathbf{B})|} \tag{6.22}$$

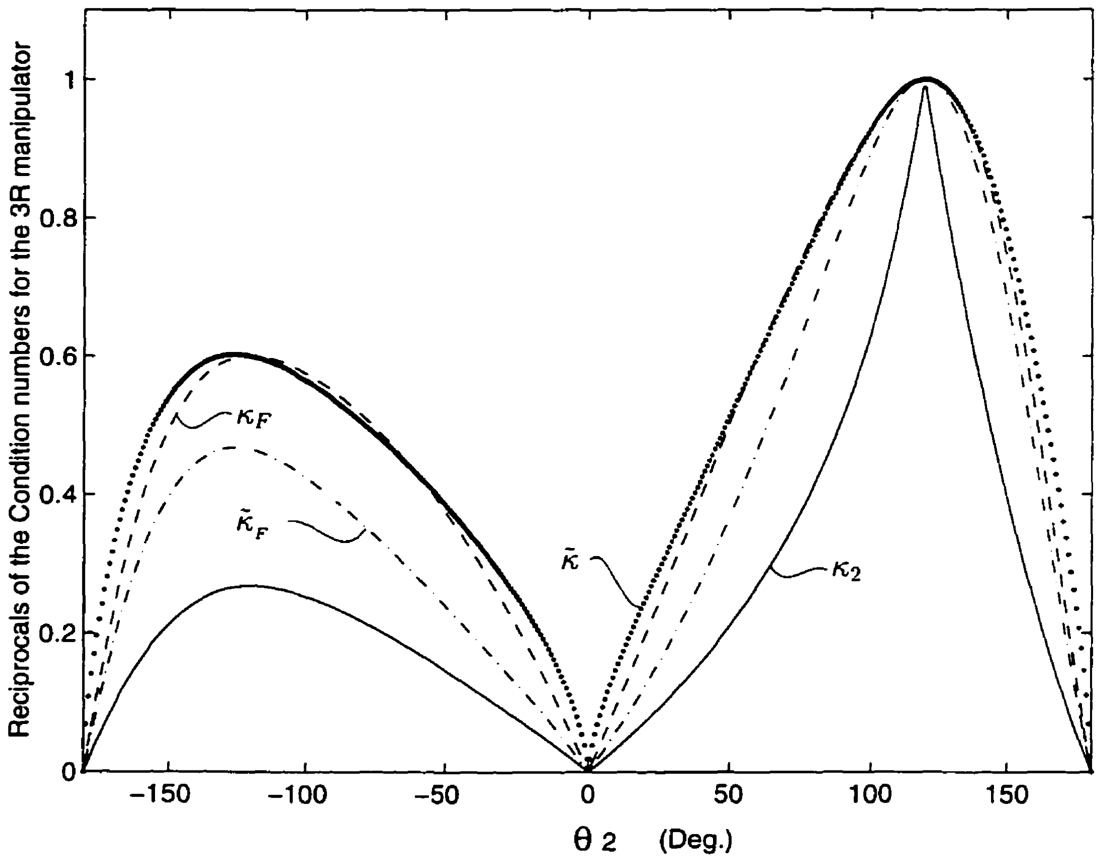

Figure 6.3: Comparison of the reciprocal of the condition numbers

or

$$\|\mathbf{B}\|_{\bar{F}}\,\|\mathbf{B}^{-1}\|_{\bar{F}} \leq \frac{\|\mathbf{B}\|_{\bar{F}}^{m}}{\sqrt{\det(\mathbf{B}\,\mathbf{B}^T)}} \tag{6.23}$$

Hence,

$$\|\mathbf{B}\|_{\bar{F}}\,\|\mathbf{B}^{-1}\|_{\bar{F}} = \kappa_{\bar{F}} \leq \sqrt{\frac{\mathrm{tr}^m\,(\mathbf{B}\,\mathbf{B}^T)}{m^m\,\det(\mathbf{B}\,\mathbf{B}^T)}} \tag{6.24}$$

the lower bound for $\tilde{\kappa}_F$ thus turning out to be the normalized Frobenius-norm condition number, with equality holding only when $\mathbf{B}$ is isotropic or when $m = 2$. Hence,

$$\kappa_{\bar{F}}(\mathbf{B}) \leq \tilde{\kappa}_F(\mathbf{B}) \tag{6.25}$$

- Upper bound:

In order to obtain an upper bound for $\tilde{\kappa}_F$, a theorem relating the *harmonic*, *arithmetic* and *geometric* means for a set of m positive real numbers is first recalled (Mitrinovic, 1970). Let $0 < a_1 < a_2, \cdots, < a_m$, and define the harmonic mean $H(a)$, the arithmetic mean $A(a)$, and the geometric mean $G(a)$ of these numbers, respectively, as

$$H(a) = \frac{m}{\frac{1}{a_1} + \frac{1}{a_2} + \cdots + \frac{1}{a_m}} \tag{6.26a}$$

$$A(a) = \frac{a_1 + a_2 + \cdots a_m}{m} \tag{6.26b}$$

$$G(a) = (a_1\, a_2\, \cdots\, a_m)^{\frac{1}{m}} \tag{6.26c}$$

Then,

$$a_1 \leq H(a) \leq G(a) \leq A(a) \leq a_m \tag{6.27}$$

Now, if $\{a_i\}_1^m$ is the set of eigenvalues of the matrix product $\mathbf{B}\,\mathbf{B}^T$, with $\sqrt{a_i}$ being the corresponding singular value of $\mathbf{B}$, then $\{1/a_i\}_1^m$ is the set of eigenvalues of $(\mathbf{B}\,\mathbf{B}^T)^{-1}$. Hence, by making use of inequality (6.27) and its inverse, one can extract the two inequalities given below

$$a_m \geq \frac{\mathrm{tr}(\mathbf{B}\,\mathbf{B}^T)}{m}, \qquad \frac{1}{a_1} \geq \frac{1}{[\det(\mathbf{B}\,\mathbf{B}^T)]^{\frac{1}{m}}} \tag{6.28}$$

Therefore,

$$\frac{a_m}{a_1} \geq \frac{\mathrm{tr}(\mathbf{B}\,\mathbf{B}^T)}{m\,[\det(\mathbf{B}\,\mathbf{B}^T)]^{\frac{1}{m}}} \tag{6.29}$$

Recalling the definition of the 2-norm condition number as the ratio of the largest singular value of $\mathbf{A}$ to its smallest one, the foregoing inequality takes on the form

$$\kappa_2 \geq \sqrt{\frac{\mathrm{tr}(\mathbf{B}\,\mathbf{B}^T)}{m\,[\det(\mathbf{B}\,\mathbf{B}^T)]^{\frac{1}{m}}}} = \tilde{\kappa}_F^{\frac{1}{m}} \tag{6.30}$$

The upper and the lower bounds of $\tilde{\kappa}_F$ are thus obtained as given by inequalities (6.25) and (6.30), namely,

$$\kappa_{\bar{F}}(\mathbf{B}) \leq \tilde{\kappa}_F(\mathbf{B}) \leq \kappa_2^m(\mathbf{B}) \tag{6.31}$$

q.e.d

- Rectangular Matrices $\mathbf{A} \in \mathbb{R}^{m \times n}$:

The proof of the foregoing theorem for the existence of the upper bound can immediately be extended to rectangular matrices since no reference was made to any features of square matrices. Hence, the upper bound as given above applies directly to rectangular matrices as well. With the following theorem, it will also be shown that the same lower bound can be obtained for $\tilde{\kappa}_F$. First, it is noted that a smaller lower bound may be obtained immediately, as shown below.

Let $\mathbf{B} \equiv \mathbf{A}\,\mathbf{A}^T$ and rewrite the relation given by eq.(6.25) for the square matrix $\mathbf{B}$ as

$$\kappa_{\hat{F}}(\mathbf{B}) = \kappa_{\hat{F}}(\mathbf{A}\,\mathbf{A}^T) \leq \sqrt{\frac{\mathrm{tr}^m\,[(\mathbf{A}\,\mathbf{A}^T)^2]}{m^m\,\det^2(\mathbf{A}\,\mathbf{A}^T)}} \tag{6.32}$$

next, we recall inequality (4.14), i.e.,

$$\kappa_{\hat{F}}(\mathbf{A}\,\mathbf{A}^T) \geq \kappa_{\hat{F}}(\mathbf{A})\,\kappa_{\hat{F}}(\mathbf{A}^T) = \kappa_{\hat{F}}^2(\mathbf{A}) \tag{6.33}$$

Making use of the foregoing relation, the inequality (6.32) can be rewritten as

$$\kappa_{\hat{F}}^2(\mathbf{A}) \leq \sqrt{\frac{\mathrm{tr}^{2m}\,(\mathbf{A}\,\mathbf{A}^T)}{m^m\,\det^2(\mathbf{A}\,\mathbf{A}^T)}}$$

or

$$\kappa_{\hat{F}}(\mathbf{A}) \leq \sqrt{\frac{\mathrm{tr}^m\,(\mathbf{A}\,\mathbf{A}^T)}{m^{\frac{m}{2}}\,\det(\mathbf{A}\,\mathbf{A}^T)}}$$

Hence,

$$\frac{1}{m^{\frac{m}{4}}}\,\kappa_{\hat{F}}(\mathbf{A}) \leq \sqrt{\frac{\mathrm{tr}^m\,(\mathbf{A}\,\mathbf{A}^T)}{m^m\,\det(\mathbf{A}\,\mathbf{A}^T)}}$$

which provides a smaller lower bound for $\tilde{\kappa}_F$. After performing extensive numerical tests and comparisons between $\kappa_{\hat{F}}(\mathbf{A})$ and $\tilde{\kappa}_F(\mathbf{A})$, it became apparent that the same lower bound as obtained for square matrices should exist for rectangular matrices as well. The theorem below is indeed a validation of this numerical observation.

Theorem 6.2

The conditioning measure of the full-rank $m \times n$ matrix, denoted by $\tilde{\kappa}_F(\mathbf{A})$ is bounded by the normalized Frobenius norm from below and by the mth power of the 2-norm condition number from above, i.e,

$$\kappa_{\bar{F}}(\mathbf{A}) \leq \tilde{\kappa}_F(\mathbf{A}) \leq \kappa_2^m(\mathbf{A}) \tag{6.34}$$

Proof:

- Lower bound:

We start with an inequality concerning the *elementary symmetric functions* $\mathcal{S}_k$ of a set of positive numbers $A = \{a_1, a_2 \cdots a_m\}$ (Hardy et al., 1934; Mirsky, 1956), where

$$\mathcal{S}_1 = a_1 + a_2 + \cdots a_m \tag{6.35}$$

$$\mathcal{S}_2 = a_1\, a_2 + a_1\, a_3 + \cdots a_{m-1}\, a_m \tag{6.36}$$

$$\vdots \tag{6.37}$$

$$\mathcal{S}_{m-1} = a_2\, a_3 \cdots a_m + a_1\, a_3 \cdots a_m + \cdots + a_1\, a_2 \cdots a_{m-1} \tag{6.38}$$

$$\mathcal{S}_m = a_1\, a_2 \cdots a_m \tag{6.39}$$

Then, as shown in the aforementioned references the inequality given below can be derived:

$$\mathcal{S}_{m-1} \leq m^{-(m-2)}\, \mathcal{S}_1^{(m-1)}$$

that is,

$$a_2\, a_3 \cdots a_m + a_1\, a_3 \cdots a_m + \cdots + a_1\, a_2 \cdots a_{m-1} \leq m^{-(m-2)}\, (a_1 + a_2 + \cdots + a_m)^{(m-1)}$$

Dividing both sides of the foregoing inequality by nonzero $\mathcal{S}_m$, the following inequality is obtained,

$$\frac{1}{a_1} + \frac{1}{a_2} + \cdots + \frac{1}{a_m} \leq m^{-(m-2)}\, \frac{(a_1 + a_2 + \cdots + a_m)^{(m-1)}}{a_1\, a_2 \cdots a_m} \tag{6.40}$$

Now, let a_i be the ith eigenvalue of the matrix product $\mathbf{A}\,\mathbf{A}^T$. Hence, the foregoing inequality takes on the form

$$\mathrm{tr}[(\mathbf{A}\,\mathbf{A}^T)^{-1}] \leq \frac{\mathrm{tr}^{(m-1)}(\mathbf{A}\,\mathbf{A}^T)}{m^{(m-2)}\,\det(\mathbf{A}\,\mathbf{A}^T)}$$

Multiplying both sides of the foregoing inequality by $\frac{1}{m^2}\,\mathrm{tr}(\mathbf{A}\,\mathbf{A}^T)$ and making use of eq.(4.18) one can obtain the result shown below:

$$\kappa_{\hat{F}}^2 = \frac{1}{m^2}\,\mathrm{tr}[(\mathbf{A}\,\mathbf{A}^T)^{-1}]\,\mathrm{tr}(\mathbf{A}\,\mathbf{A}^T) \leq \frac{\mathrm{tr}^m(\mathbf{A}\,\mathbf{A}^T)}{m^m\,\det(\mathbf{A}\,\mathbf{A})} = \tilde{\kappa}_F^2 \tag{6.41}$$

Hence, the same lower bound is now obtained for $\tilde{\kappa}_F$, i.e.,

$$\kappa_{\hat{F}} \leq \tilde{\kappa}_F \tag{6.42}$$

- Upper bound:

Provided already for the proof of the upper bound given in Theorem 6.1.

q.e.d

In terms of the set of eigenvalues of the matrix product $\mathbf{A}\,\mathbf{A}^T$, i.e., $\{a_i\}_1^m$, and the ordering of the minimum, maximum, and the three different types of means of this set explained before, eqs. (6.26), one can observe an interesting comparison given below.

Knowing that

$$a_1 \leq H(a) \leq G(a) \leq A(a) \leq a_m$$

we have

$$\kappa_2 = (\frac{a_m}{a_1})^{\frac{1}{2}} \tag{6.43}$$

$$\kappa_F = m\,[\frac{A(a)}{H(a)}]^{\frac{1}{2}} \tag{6.44}$$

$$\kappa_{\hat{F}} = [\frac{A(a)}{H(a)}]^{\frac{1}{2}} \tag{6.45}$$

$$\tilde{\kappa}_F = [\frac{A(a)}{G(a)}]^{\frac{m}{2}} \tag{6.46}$$

We thus, conclude that $\tilde{\kappa}_F$ being a function of the trace and the determinant only, $\tilde{\kappa}_F$ can be considered as a useful tool for both design and control of serial-type robotic manipulators. For control purposes, at lower condition numbers, $\tilde{\kappa}_F$ can be used directly, while, at high condition numbers, say around m^m, $(\tilde{\kappa}_F)^{\frac{1}{m}}$ can be employed instead. Furthermore, it can be readily shown that, at the isotropic configuration, where all singular values of $\mathbf{A}$ are identical, $\tilde{\kappa}_F$ attains a minimum value of unity, similar to other definitions of the condition number.

Having discussed the merits of $\tilde{\kappa}_F(\mathbf{A})$, one can proceed and exploit its simple form and derive geometrical insights into manipulator kinematic dexterity. First, we will need the definitions given below:

Definition 6.1 *A layout $\mathcal{L}$ of a manipulator is a set of lines $\{\mathcal{A}_i\}_1^n$, with line $\mathcal{A}_i$ representing the axis of the ith revolute joint of the given manipulator (Fig. 6.4).*

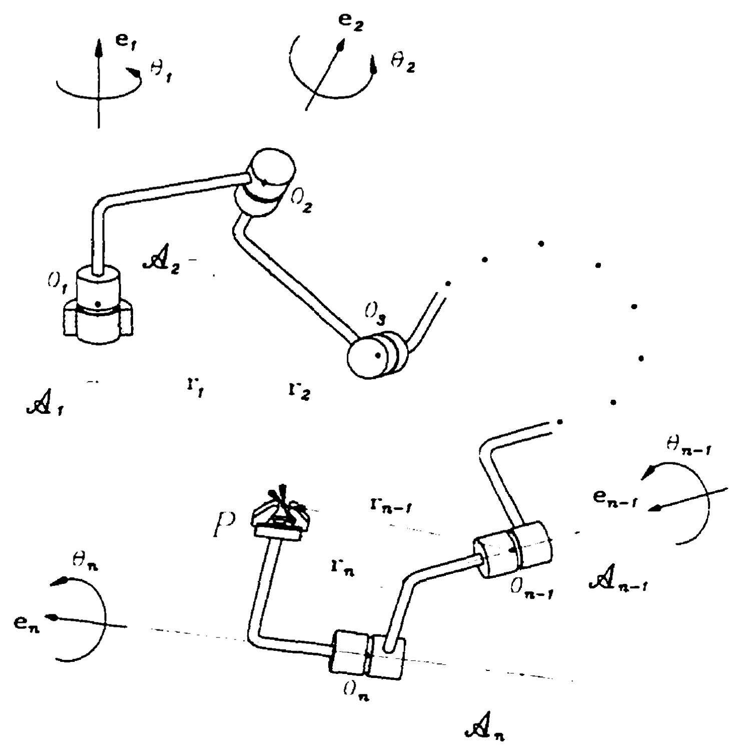

Figure 6.4: Axis-layout of a serial manipulator

Remark 1: Only the *relative* layout of the axes is important. A layout is thus fully specified by the set $\{\theta_i\}_2^n$, for a given manipulator architecture.

Definition 6.2 *The operation point P of the manipulator is the point of the last link of the manipulator whose linear velocity is of interest, the Jacobian matrix being evaluated with respect to P. This point has the position vector* $\mathbf{p}$.

Definition 6.3 *For a given layout $\mathcal{L}$, the rms value of the distances $\{d_i\}_1^n$ from all axes to the operation point P is called the* layout length $L_{\mathcal{L}}$.

Definition 6.4 *Let $\mathbf{J}$ be the Jacobian matrix of a given manipulator with a given posture of layout $\mathcal{L}$. The layout normal Jacobian $\bar{\mathbf{J}}$ is defined as*

$$\bar{\mathbf{J}} \equiv \begin{bmatrix} \mathbf{E} \\ \frac{1}{L_{\mathcal{L}}}\mathbf{S} \end{bmatrix} = \begin{bmatrix} \mathbf{e}_1 & \cdots & \mathbf{e}_n \\ \frac{1}{L_{\mathcal{L}}}\mathbf{e}_1 \times \mathbf{r}_1 & \cdots & \frac{1}{L_{\mathcal{L}}}\mathbf{e}_n \times \mathbf{r}_n \end{bmatrix} \tag{6.47}$$

Definition 6.5 *For a given manipulator, at a given posture of layout $\mathcal{L}$, the* layout conditioning $\kappa_{\mathcal{L}} \equiv \tilde{\kappa}_F(\bar{J})$ *is defined as*

$$\kappa_{\mathcal{L}} \equiv \sqrt{\frac{\mathrm{tr}^m(\bar{\mathbf{J}}\,\bar{\mathbf{J}}^T)}{m^m\ \det(\bar{\mathbf{J}}\,\bar{\mathbf{J}}^T)}} \tag{6.48}$$

Remark 2: $\kappa_{\mathcal{L}} = \kappa_{\mathcal{L}}(\theta_2, \cdots, \theta_n, L_{\mathcal{L}}, \mathbf{p})$

Remark 3: The layout length $L_{\mathcal{L}}$ minimizes the layout conditioning $\kappa_{\mathcal{L}}$ of any layout $\mathcal{L}$ (see Section 6.3.1.

Definition 6.6 *The point $P_{\mathcal{L}}$ with respect to which the layout conditioning $\kappa_{\mathcal{L}}$ is a minimum is the layout centre.*

Definition 6.7 *The characteristic layout of a manipulator, $\mathcal{L}_c$, is the manipulator layout at which $\kappa_{\mathcal{L}}$ is a minimum.*

Definition 6.8 *The characteristic length L_c of a manipulator, is the layout length determined at the characteristic layout.*

Remark 4: $L_c = L_c(\theta_2, \cdots, \theta_n)$

Definition 6.9 *The characteristic point P_c of a manipulator is the layout centre associated with the characteristic layout.*

6.3 Determination of the Layout Length and the Layout Centre

6.3.1 Layout Length

As discussed in Chapters 3–5, when considering the overall Jacobian matrix for both positioning and orienting tasks, normalizing the last three rows of $\mathbf{J}$ is essential, for the singular values of $\mathbf{J}$ have different units and, thus, cannot be compared. Although scaling the manipulator Jacobian is a relatively new idea in the context of robotics, on the one hand, it lends itself to a broader notion of *equilibration* and *scaling* in the context of numerical analysis of linear systems, (e.g., Glob and Van Loan, 1989; Kahan, 1966). As discussed in Kahan (1966), a systematic approach to defining the scaling factors that render the matrix well conditioned is an open question. In this chapter, we show that for any nonsingular manipulator Jacobian matrix, explicit formulas for L_C can be obtained that minimize $\kappa_{\bar{F}}(\bar{\mathbf{J}})$ and $\bar{\kappa}_F(\bar{\mathbf{J}})$. On the other hand, within the framework of the group of rigid body motions SE(3), one can define the Riemannian metric $\mathbf{G}$, on the manipulator workspace, as (Park and Brockett, 1994)

$$\mathbf{G} \equiv \mathrm{Diag}[\,1 \quad 1 \quad 1 \quad \tfrac{1}{L_C} \quad \tfrac{1}{L_C} \quad \tfrac{1}{L_C}\,]$$

Minimizing $\kappa_{\bar{F}}$

In this section we resort to directly minimizing $\kappa_{\bar{F}}^2$ as a function of the layout length L_C, for any given set of joint variables $\boldsymbol{\theta}$, and for a given location of the operation point P of the end-effector. Let

$$\kappa_{\bar{F}}^2 = \frac{1}{m^2}\mathrm{tr}(\bar{\mathbf{A}})\,\mathrm{tr}(\bar{\mathbf{A}}^{-1})$$

where

$$\bar{\mathbf{A}} \equiv \bar{\mathbf{J}}\,\bar{\mathbf{J}}^T = \begin{bmatrix} \mathbf{E}\,\mathbf{E}^T & \frac{1}{L_C}\mathbf{E}\,\mathbf{S}^T \\ \frac{1}{L_C}\mathbf{S}\,\mathbf{E}^T & \frac{1}{L_C^2}\mathbf{S}\,\mathbf{S}^T \end{bmatrix}$$

with $\mathbf{E}$ and $\mathbf{S}$ defined in eq.(5.1). The condition for a stationary value of $\kappa_{\bar{F}}$ in terms of $L_{\mathcal{C}}$ is

$$\frac{\partial \kappa_F^2}{\partial L_p} \equiv \frac{\partial \mathrm{tr}(\bar{\mathbf{A}})}{\partial L_{\mathcal{C}}} \mathrm{tr}(\bar{\mathbf{A}}^{-1}) + \mathrm{tr}(\bar{\mathbf{A}}) \frac{\partial \mathrm{tr}(\bar{\mathbf{A}}^{-1})}{\partial L_{\mathcal{C}}} = 0 \tag{6.49}$$

Moreover,

$$\mathrm{tr}(\bar{\mathbf{A}}) = \mathrm{tr}(\bar{\mathbf{J}}\,\bar{\mathbf{J}}^T) = \mathrm{tr}(\mathbf{E}\,\mathbf{E}^T) + \frac{1}{L_{\mathcal{C}}^2}\mathrm{tr}(\mathbf{S}\,\mathbf{S}^T) \tag{6.50}$$

In order to obtain $\mathrm{tr}[(\bar{\mathbf{J}}\,\bar{\mathbf{J}}^T)^{-1}]$, matrix $\bar{\mathbf{A}}^{-1}$ is block-partitioned in the form

$$\bar{\mathbf{A}}^{-1} = (\bar{\mathbf{J}}\,\bar{\mathbf{J}}^T)^{-1} \equiv \begin{bmatrix} \mathbf{B}_{11} & \mathbf{B}_{12} \\ \mathbf{B}_{21} & \mathbf{B}_{22} \end{bmatrix} \tag{6.51}$$

explicit expressions for the foregoing blocks being available in the literature (Householder, 1964); Thus,

$$\mathrm{tr}[(\bar{\mathbf{J}}\,\bar{\mathbf{J}}^T)^{-1}] = \mathrm{tr}(\mathbf{B}_{11}) + \mathrm{tr}(\mathbf{B}_{22}) \tag{6.52}$$

Moreover, the diagonal blocks of $\bar{\mathbf{A}}^{-1}$ are

$$\mathbf{B}_{11} \equiv [\mathbf{E}\,\mathbf{E}^T - \mathbf{E}\,\mathbf{S}^T\,(\mathbf{S}\,\mathbf{S}^T)^{-1}\,\mathbf{S}\,\mathbf{E}^T]^{-1} \tag{6.53}$$

$$\mathbf{B}_{22} \equiv [\frac{1}{L_{\mathcal{C}}^2}\mathbf{S}\,\mathbf{S}^T - \frac{1}{L_{\mathcal{C}}^2}\mathbf{S}\,\mathbf{E}^T\,(\mathbf{E}\,\mathbf{E}^T)^{-1}\,\mathbf{E}\,\mathbf{S}^T]^{-1} \tag{6.54}$$

Hence,

$$\begin{aligned} \mathrm{tr}(\bar{\mathbf{J}}\,\bar{\mathbf{J}}^T)^{-1} &= \mathrm{tr}\,[\mathbf{E}\,\mathbf{E}^T - \mathbf{E}\,\mathbf{S}^T\,(\mathbf{S}\,\mathbf{S}^T)^{-1}\,\mathbf{S}\,\mathbf{E}^T]^{-1} \\ &+ \frac{1}{L_{\mathcal{C}}^2}\mathrm{tr}[\mathbf{S}\,\mathbf{S}^T - \mathbf{S}\,\mathbf{E}^T\,(\mathbf{E}\,\mathbf{E}^T)^{-1}\,\mathbf{E}\,\mathbf{S}^T]^{-1} \end{aligned} \tag{6.55}$$

Substituting eqs.(6.55) and (6.50), into eq.(6.49) leads to a unique solution for the fourth power of the layout length $L_{\mathcal{C}}$, namely,

$$L_{\mathcal{C}}^4 = \frac{\mathrm{tr}(\mathbf{S}\,\mathbf{S}^T)\,\mathrm{tr}\,[\mathbf{E}\,\mathbf{E}^T - \mathbf{E}\,\mathbf{S}^T\,(\mathbf{S}\,\mathbf{S}^T)^{-1}\,\mathbf{S}\,\mathbf{E}^T]^{-1}}{\mathrm{tr}(\mathbf{E}\,\mathbf{E}^T)\,\mathrm{tr}\,[\mathbf{S}\,\mathbf{S}^T - \mathbf{S}\,\mathbf{E}^T\,(\mathbf{E}\,\mathbf{E}^T)^{-1}\,\mathbf{E}\,\mathbf{S}^T]^{-1}} \tag{6.56}$$

Furthermore, recalling that $\mathrm{tr}(\mathbf{S}\,\mathbf{S}^T) = \sum_1^n \|\mathbf{e}_k \times \mathbf{r}_k\|^2$, and that $\mathrm{tr}(\mathbf{E}\,\mathbf{E}^T) = n$, it follows that

$$L_{\mathcal{C}}^4 = \frac{\sum_1^n \|\mathbf{e}_k \times \mathbf{r}_k\|^2\,\mathrm{tr}\,[\mathbf{E}\,\mathbf{E}^T - \mathbf{E}\,\mathbf{S}^T\,(\mathbf{S}\,\mathbf{S}^T)^{-1}\,\mathbf{S}\,\mathbf{E}^T]^{-1}}{n\,\mathrm{tr}\,[\mathbf{S}\,\mathbf{S}^T - \mathbf{S}\,\mathbf{E}^T\,(\mathbf{E}\,\mathbf{E}^T)^{-1}\,\mathbf{E}\,\mathbf{S}^T]^{-1}} \tag{6.57}$$

L_C, as given above, minimizes the normalized F-norm condition number $\kappa_{\hat{F}}$ of any nonsingular posture of the manipulator. which, in turn, leads to a unique expression for the layout length itself, under the condition that this length be real and positive. The manipulator characteristic length L_c is, then, defined as that L_C that is evaluated at the characteristic layout. The presence of four matrix inversions in the foregoing expression should not be considered as a deterrent, since, at the characteristic layout, all these matrices are best conditioned.

Furthermore, if the manipulator at hand is isotropic, then the expression given by eq.(6.57) becomes that given by eq.(5.5). This can be shown by noting that, at the isotropic posture, $\mathbf{E}\,\mathbf{S}^T = \mathbf{O}$, $\mathrm{tr}(\mathbf{E}\,\mathbf{E}^T)^{-1} = 1/\mathrm{tr}(\mathbf{E}\,\mathbf{E}^T)$, and $\mathrm{tr}(\mathbf{S}\,\mathbf{S}^T)^{-1} = 1/\mathrm{tr}(\mathbf{S}\,\mathbf{S}^T)$, with $\mathbf{O}$ denoting the 3×3 zero matrix.

As shown below, if the layout conditioning $\tilde{\kappa}_F$ is minimized instead of $\kappa_{\hat{F}}$, then the same expression for the layout length of isotropic manipulators will be obtained.

Minimizing $\tilde{\kappa}_F$

Here it will be shown how the conditioning measure $\tilde{\kappa}_F$ is used to derive an expression for the layout length of both isotropic and nonisotropic general manipulators. Rewriting the isotropy condition for the normalized Jacobian matrix as

$$\bar{\mathbf{J}}\bar{\mathbf{J}}^T = \begin{bmatrix} \sum_1^n \mathbf{e}_k \mathbf{e}_k^T & \frac{1}{L}\sum_1^n \mathbf{e}_k(\mathbf{e}_k \times \mathbf{r}_k)^T \\ \frac{1}{L}\sum_1^n \mathbf{e}_k(\mathbf{e}_k \times \mathbf{r}_k)^T & \frac{1}{L^2}\sum_1^n (\mathbf{e}_k \times \mathbf{r}_k)(\mathbf{e}_k \times \mathbf{r}_k)^T \end{bmatrix} = \sigma^2 \mathbf{1}_6 \tag{6.58}$$

we obtain

$$\det(\bar{\mathbf{J}}\bar{\mathbf{J}}^T) = \frac{\det(\mathbf{J}\mathbf{J}^T)}{L_C^6} \tag{6.59}$$

and

$$\mathrm{tr}(\bar{\mathbf{J}}\bar{\mathbf{J}}^T) \equiv \mathrm{tr}(\sum_1^n \mathbf{e}_k \mathbf{e}_k^T) + \frac{1}{L^2}\mathrm{tr}[\sum_1^n (\mathbf{e}_k \times \mathbf{r}_k)(\mathbf{e}_k \times \mathbf{r}_k)^T] \tag{6.60}$$

$$\mathrm{tr}(\bar{\mathbf{J}}\bar{\mathbf{J}}^T) = n + \frac{\sum_1^n \|\mathbf{e}_k \times \mathbf{r}_k\|^2}{L_C^2} \tag{6.61}$$

Hence,

$$\tilde{\kappa}_F^2 = \frac{[nL_{\mathcal{L}}^2 + \sum_1^n \|\mathbf{e}_k \times \mathbf{r}_k\|^2]^6}{6^6\, L_{\mathcal{L}}^2\, \det(\mathbf{J}\,\mathbf{J}^T)} \tag{6.62}$$

Next, in order to find $L_{\mathcal{L}}$ so as to minimize $\tilde{\kappa}_F$, the derivative $\partial\tilde{\kappa}_F^2/\partial\tilde{L}$ is equated to zero, which yields an expression for L^2 as shown below:

$$L^2 = \frac{\sum_1^n \|\mathbf{e}_k \times \mathbf{r}_k\|^2}{n} \tag{6.63}$$

which is the same as the characteristic length L for an isotropic n-axis manipulator for positioning and orienting tasks obtained in Chapter 4, and is equal to the rms value of the distances of the operation point to the joint axes. The merits of the layout length, as defined above, go beyond the realm of dimensional consistency, for it can be used as a very useful normalizing tool when comparing manipulators for dexterity and workspace volume in the process of optimum kinematic design.

6.3.2 Layout Centre

In this section we derive an expression for the position vector of the layout centre $P_{\mathcal{L}}$ of the end-effector at which $\kappa_{\mathcal{L}}$ associated with the layout of the manipulator attains a minimum value when compared with any other point of the end-effector.

First, the Jacobian transfer formula (Angeles et al., 1992) relating the Jacobian matrix $\bar{\mathbf{J}}_P$ associated with point P, to the Jacobian matrix $\bar{\mathbf{J}}_O$ associated with a point O, of the end-effector, is recalled:

$$\bar{\mathbf{J}}_P = \mathbf{U}_{OP}\bar{\mathbf{J}}_O$$

with matrix $\mathbf{U}_{OP}$ defined as

$$\mathbf{U}_{OP} \equiv \begin{bmatrix} \mathbf{1}_3 & \mathbf{0} \\ -\mathbf{P} & \mathbf{1}_3 \end{bmatrix}$$

where $\mathbf{1}_3$ and $\mathbf{O}$ are the 3×3 identity and zero matrices, respectively. Moreover, $\mathbf{P}$ is the cross-product matrix of vector $\mathbf{p}$, directed from O to P, that is, given any vector $\mathbf{q}$, we have,

$$\mathbf{P}\,\mathbf{q} = \mathbf{p} \times \mathbf{q} \tag{6.64}$$

It is required to minimize $\kappa_{\mathcal{L}}$ over the set of points of the end-effector, of position vector $\mathbf{p}$, and for a given nonsingular manipulator axis-layout denoted by $\boldsymbol{\theta}$, namely,

$$\min_{\mathbf{p}} \kappa_{\mathcal{L}}(\boldsymbol{\theta}, L_{\mathcal{C}}, \mathbf{p}_p)$$

where,

$$\kappa_{\mathcal{L}}(\mathbf{J}_P) = \sqrt{\frac{\mathrm{tr}^m[(\bar{\mathbf{J}}_P \bar{\mathbf{J}}_P^T)]}{m^m \det(\bar{\mathbf{J}}_P \bar{\mathbf{J}}_P^T)}}$$

Moreover,

$$\bar{\mathbf{J}}_P \bar{\mathbf{J}}_P^T = \mathbf{U}_{OP} \bar{\mathbf{J}}_O \bar{\mathbf{J}}_O^T \mathbf{U}_{OP}^T = \begin{bmatrix} \mathbf{E}\mathbf{E}^T & \frac{1}{L}\mathbf{E}(\mathbf{S}-\mathbf{P}\mathbf{E})^T \\ \frac{1}{L}(\mathbf{S}-\mathbf{P}\mathbf{E})\mathbf{E}^T & \frac{1}{L^2}(\mathbf{S}-\mathbf{P}\mathbf{E})(\mathbf{S}-\mathbf{P}\mathbf{E})^T \end{bmatrix} \tag{6.65}$$

where $\mathbf{S}$ is evaluated with respect to point O. Clearly,

$$\det(\bar{\mathbf{J}}_P \bar{\mathbf{J}}_P^T) = \det(\bar{\mathbf{J}}_O \bar{\mathbf{J}}_O^T) \tag{6.66}$$

which means that any determinant-based measure is insensitive to a change of the operation point. Thus, in light of eq.(6.66), the optimality condition for $\kappa_{\mathcal{L}}$ in terms of $\mathbf{p}_p$ reduces to that of $\mathrm{tr}^m[(\bar{\mathbf{J}}_P \bar{\mathbf{J}}_P^T)]$, i.e.,

$$\frac{\partial \mathrm{tr}^m[(\bar{\mathbf{J}}_P \bar{\mathbf{J}}_P^T)]}{\partial \mathbf{p}} = \mathbf{0}$$

which leads to the optimality condition for the distortion density of the forward kinematics, as discussed in Park and Brockett (1994), i.e.,

$$\frac{\partial \mathrm{tr}(\bar{\mathbf{J}}_P \bar{\mathbf{J}}_P^T)}{\partial \mathbf{p}} = \mathbf{0} \tag{6.67}$$

With the aid of eq.(6.65), the foregoing condition can be expressed as

$$\frac{\partial \mathrm{tr}(\bar{\mathbf{J}}_P \bar{\mathbf{J}}_P^T)}{\partial \mathbf{p}} = \frac{2}{L_{\mathcal{C}}^2}\frac{\partial \mathrm{tr}(\mathbf{P}\mathbf{E}\mathbf{S}^T)}{\partial \mathbf{p}} - \frac{1}{L_{\mathcal{C}}^2}\frac{\partial \mathrm{tr}(\mathbf{P}\mathbf{E}\mathbf{E}^T\mathbf{P}^T)}{\partial \mathbf{p}} = 0 \tag{6.68}$$

It turns out that the optimality condition for the layout center is independent of the choice of normalizing length $L_{\mathcal{C}}$. In order to further expand the latter expression, two identities whose derivations are given, respectively, in Appendix C, and in Angeles (1997), are introduced next. Let $\mathbf{A}$ and $\mathbf{B}$ be 3×3 matrices, with $\mathbf{B}$ skew-symmetric; then,

$$\mathrm{tr}(\mathbf{B}\,\mathbf{A}\,\mathbf{B}^T) = \mathbf{b}^T\,\mathbf{b}\,\mathrm{tr}(\mathbf{A}) - \frac{1}{2}\mathbf{b}^T\,(\mathbf{A}+\mathbf{A}^T)\,\mathbf{b} \tag{6.69a}$$

$$\mathrm{tr}(\mathbf{B}\,\mathbf{A}) = 2\,\mathbf{b}^T\,\mathrm{vect}(\mathbf{A}^T) = -2\,\mathbf{b}^T\,\mathrm{vect}(\mathbf{A}) \tag{6.69b}$$

where

$$\mathbf{b} \equiv \mathrm{vect}(\mathbf{B}) = -\mathrm{vect}(\mathbf{B}^T)$$

and the operator vect$(\cdot)$ represents the *axial vector* of its matrix argument, as defined in Leigh (1968). The axial vector of any 3×3 matrix $\mathbf{B}$ has the following property

$$[\mathrm{vect}(\mathbf{B})] \times \mathbf{a} \equiv \bar{\mathbf{B}}\,\mathbf{a} = \frac{1}{2}(\mathbf{B}-\mathbf{B}^T)\,\mathbf{a}$$

where, $\bar{\mathbf{B}}$ is the skew-symmetric part of the *Cartesian decomposition* of any matrix $\mathbf{B}$. If additionally, $\tilde{\mathbf{B}}$ denotes the corresponding symmetric part, then we have (Leigh, 1968)

$$\mathbf{B} = \tilde{\mathbf{B}} + \bar{\mathbf{B}}$$

with

$$\tilde{\mathbf{B}} \equiv \frac{1}{2}(\mathbf{B}+\mathbf{B}^T), \quad \bar{\mathbf{B}} \equiv \frac{1}{2}(\mathbf{B}-\mathbf{B}^T)$$

Now, if the right-hand side terms in eq.(6.68) are expanded, while making use of the identities given above, we have

$$\frac{\partial \mathrm{tr}(\mathbf{P}\,\mathbf{E}\,\mathbf{S}^T)}{\partial \mathbf{p}} = 2\,\mathrm{vect}(\mathbf{S}\,\mathbf{E}^T) \tag{6.70}$$

and

$$\begin{aligned}\frac{\partial \mathrm{tr}(\mathbf{P}\,\mathbf{E}\,\mathbf{E}^T\,\mathbf{P}^T)}{\partial \mathbf{p}} &= 2\,\mathbf{p}_p\,\mathrm{tr}(\mathbf{E}\,\mathbf{E}^T) - 2\,\mathbf{E}\,\mathbf{E}^T\,\mathbf{p}_p \\ &= 2\,[\mathrm{tr}(\mathbf{E}\,\mathbf{E}^T)\,\mathbf{1}_3 - \mathbf{E}\,\mathbf{E}^T]\,\mathbf{p}_p \\ &= 2\,(n\,\mathbf{1}_3 - \mathbf{E}\,\mathbf{E}^T)\,\mathbf{p}_p \end{aligned} \tag{6.71}$$

Finally, by substituting the two foregoing equations into eq.(6.68), we can solve for the position vector $\mathbf{p}_p$ of the layout center P_p that minimizes $\tilde{\kappa}_F$ for any nonsingular layout of the manipulator, namely,

$$\mathbf{p}_c = 2\,(\mathbf{E}\,\mathbf{E}^T - n\,\mathbf{1})^{-1}\,\mathrm{vect}(\mathbf{E}\,\mathbf{S}^T) \tag{6.72}$$

The manipulator characteristic point P_c is then obtained by evaluating the layout center $\mathbf{p}_{\mathcal{L}}$ at the characteristic layout. Hence, using the DH notation while expressing vector $\mathbf{p}_{\mathcal{L}}$ in the $(n-1)$st coordinate frame attached to the $(n-1)$st link, we have

$$\mathbf{p}_c \equiv \begin{bmatrix} p_x \\ p_y \\ p_z \end{bmatrix} = \begin{bmatrix} a_n \cos\theta_n \\ a_n \sin\theta_n \\ b_n \end{bmatrix} \tag{6.73}$$

thus,

$$a_n = \sqrt{p_x^2 + p_y^2} \tag{6.74a}$$

$$b_n = p_z \tag{6.74b}$$

$$\theta_n = \arctan\left(\frac{p_y}{p_x}\right) \tag{6.74c}$$

6.4 Determination of the Characteristic Layout

Having obtained explicit expressions for the layout length $L_{\mathcal{L}}$, and the layout center $\mathbf{p}_{\mathcal{L}}$, the optimization problem for determining the characteristic layout defined by the set of joint variables $\boldsymbol{\theta}_c$ is formulated as

$$\min_{\{\theta_i\}_2^{n-1}} \kappa_{\mathcal{L}}(\{\theta_i\}_2^{n-1}, \theta_n, L_{\mathcal{L}}, \mathbf{p}_{\mathcal{L}}) \tag{6.75}$$

But

$$L_{\mathcal{L}} = \sqrt{\frac{\sum_1^n \|\mathbf{e}_k \times \mathbf{r}_k\|^2}{n}} \tag{6.76a}$$

$$\mathbf{p}_{\mathcal{L}} = 2\,(\mathbf{E}\,\mathbf{E}^T - n\,\mathbf{I}_3)^{-1}\,\mathrm{vect}(\mathbf{E}\,\mathbf{S}^T) \tag{6.76b}$$

$$\theta_n = \arctan\,(\frac{p_y}{p_x}) \tag{6.76c}$$

Therefore, the characteristic layout turns out to be only a function of θ_2 to θ_{n-1}, i.e.,

$$\min_{\{\theta_i\}_2^{n-1}} \kappa_{\mathcal{L}}(\{\theta_i\}_2^{n-1}) \Longrightarrow \boldsymbol{\theta}_c \tag{6.77}$$

In light of the foregoing formulation, it is apparent that the dimension of the vector of design variables is reduced from $n+2$ to $n-2$, and that these variables are now of the same nature, i.e., all are joint variables. Moreover, at each iteration with the current set of joint variables both L_C and $\mathbf{p}_C$ are explicitly evaluated. Hence, at the last iteration, when the final solution $\boldsymbol{\theta}_c$ is obtained for the characteristic layout, the associated layout length and the layout centre will become the manipulator characteristic length L_c and the manipulator characteristic point $\mathbf{p}_c$, respectively. The latter quantities are indeed intrinsic to the manipulator and do not depend on the physical shape of the end-effector, although they should be taken into account when designing end-effectors.

6.5 Examples

In this section the manipulator characteristic length L_c, the manipulator characteristic point $\mathbf{p}_c$, and the characteristic layout $\boldsymbol{\theta}_c$ of some six-axis manipulators as well as a redundant seven-axis manipulator are determined.

6.5.1 Nonredundant Manipulators

Here we examine industrial manipulators such as the Yaskawa Aid 810, the Puma 560, the Fanuc Arc Mate, the Asea IRB 6/2, as well as an isotropic six-axis research manipulator. The optimization toolbox of Matlab was once again used to implement the minimization problem given by (6.75), and eqs. (6.76).

As the first example, the six-axis isotropic manipulator called DIESTRO, whose complete design is discussed in (Williams, Angeles, and Bulca, 1993) shown in Fig. 6.5, is considered.

As discussed in the latter reference, DIESTRO being isotropic, admits a set of isotropic postures or characteristic layouts that are represented by,

$$\boldsymbol{\theta}_c = \frac{1}{2}\,[\theta_1 \quad \pi \quad -\pi \quad \pi \quad -\pi \quad 2\pi]^T .$$

Next, for the sake of comparison, it is assumed that the DH parameters of this manipulator are given without the knowledge that they correspond to an isotropic

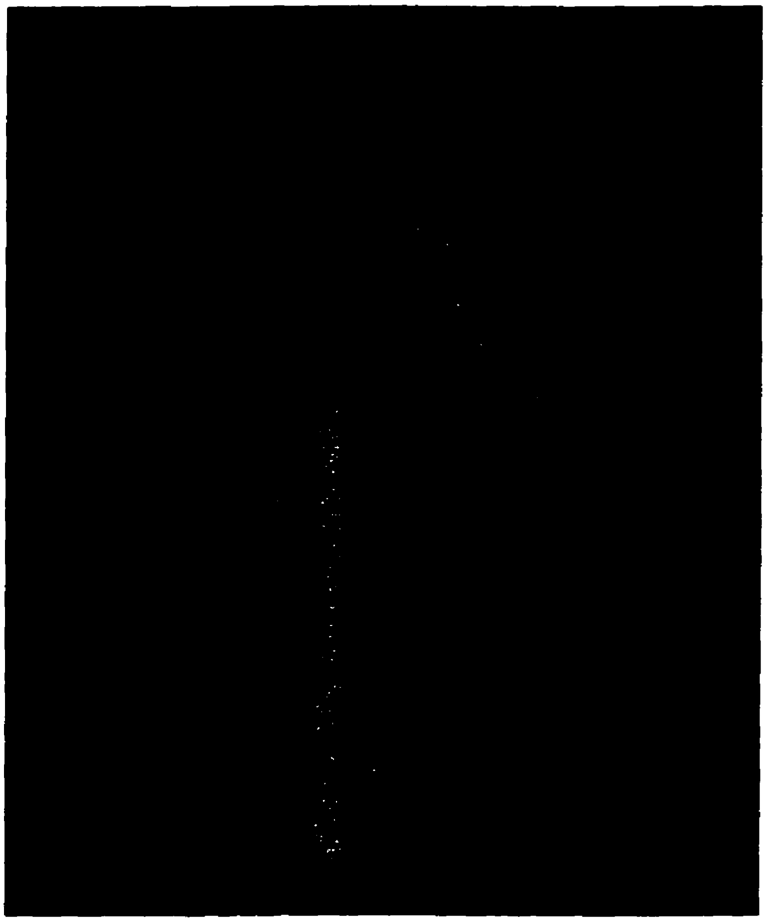

Figure 6.5: DIESTRO: A six-axis isotropic manipulator

manipulator, and thus, we aim at finding the characteristic layout as well as the associated manipulator characteristic point $\mathbf{p}_c$ and the manipulator characteristic length L_c. Starting with several randomly generated initial guesses for the design parameters $\{\theta\}_2^6$, the algorithm mentioned before consistently converged to the isotropic posture. One of these examples is summarized in Table 6.1.

Next, the characteristic layout of four nonisotropic industrial manipulators, together with their corresponding manipulator characteristic points and lengths are determined. The numerical results of these examples are summarized in Table 6.1, which, interestingly, shows that the dexterity based on the condition number as defined here, of industrial manipulators can be substantially enhanced by a proper choice of

Manipulator	θ_2 (deg)	θ_3 (deg)	θ_4 (deg)	θ_5 (deg)	θ_6 (deg)	L_c (mm)	a_6 (mm)	b_6 (mm)	$\kappa_{\bar{F}}$
DIESTRO	90.0	-90.0	90.0	-90.0	180.0	100.0	100.0	100.0	1.000
Yaskawa	-93.45	-24.18	181.46	-117.0	-8.68	410.09	367.94	-443.18	1.0663
Puma 560	-76.0	25.30	-23.80	69.13	-2.97	223.76	154.22	-229.3	1.0633
Fanuc	88.33	-28.32	-42.03	61.63	-21.48	559.46	518.92	-587.20	1.0737
Asea IRB	-268.23	204.34	-20.74	61.76	-170.91	283.2	561.0	308.13	1.0739

Table 6.1: Numerical results

the operation point.

Furthermore, the graphical renderings of these manipulators with both their original end-effectors and their end-effectors modified based on the location of the associated manipulator characteristic points at their characteristic layout, are shown in Figs. 6.6–6.9.

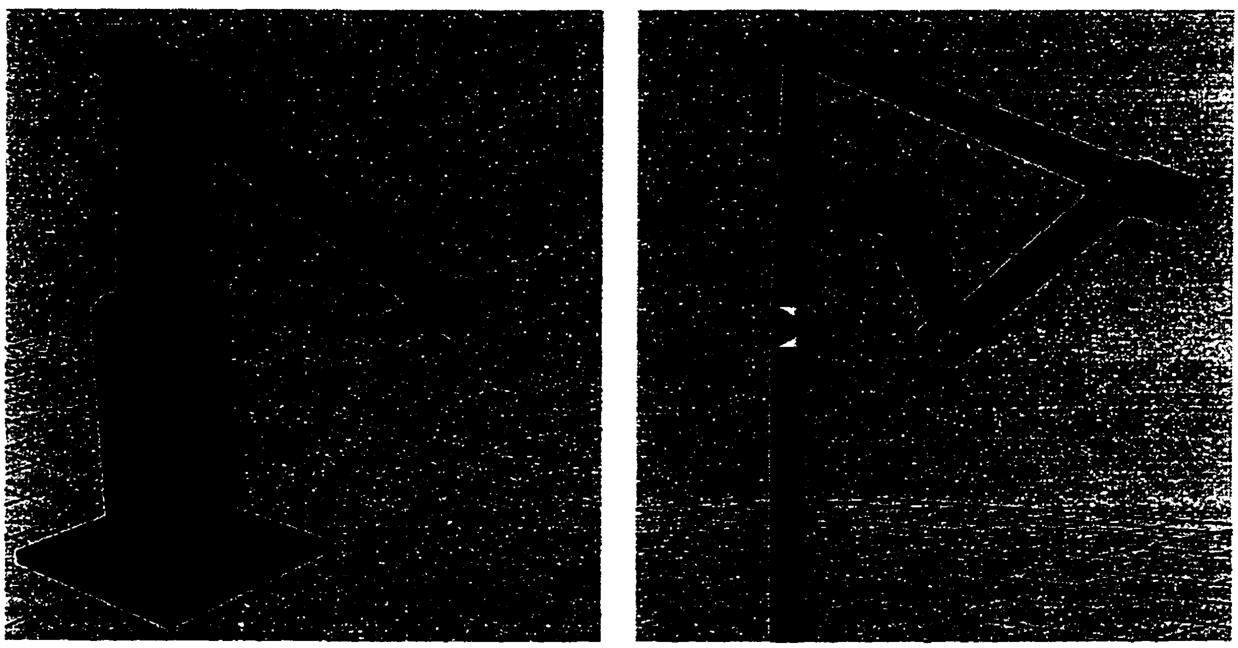

(a) (b)

Figure 6.6: Yaskawa Aid 810 at the characteristic layout: (a) Full rendering with original end-effector, (b) skeleton rendering with modified end-effector

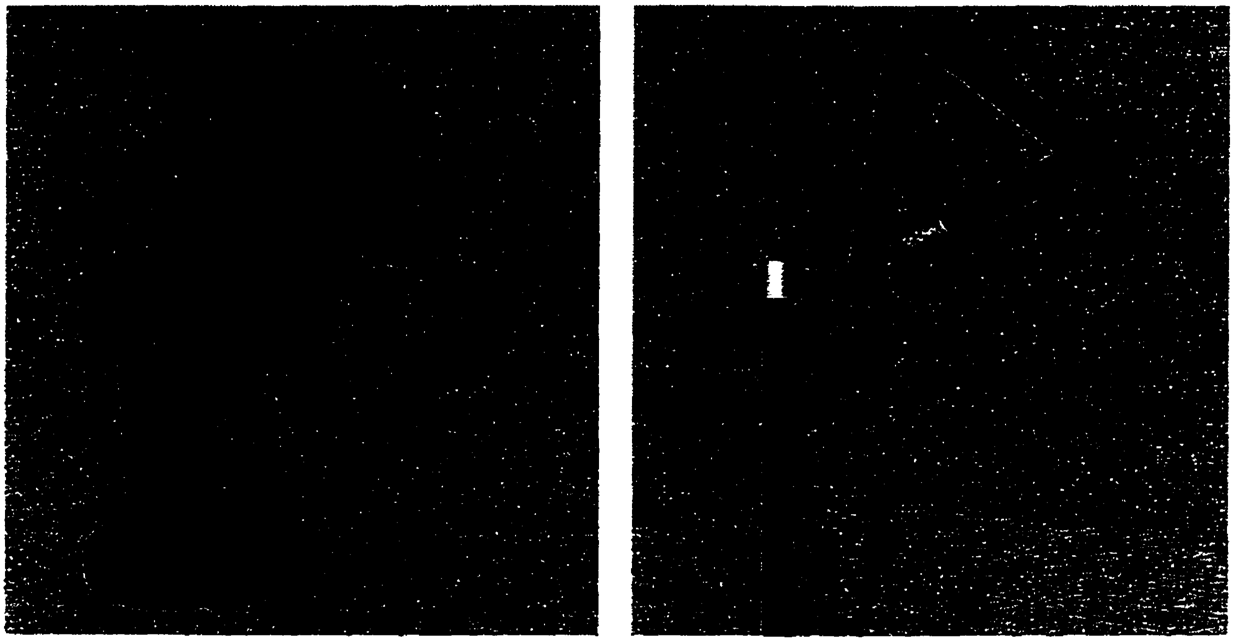

(a) (b)

Figure 6.7: Puma-560 at the characteristic layout: (a) Full rendering with original end-effector, (b) skeleton rendering with the characteristic point

6.5.2 A Redundant Industrial Manipulator

In order to demonstrate the effectiveness of the technique presented in this chapter for redundant manipulators, an industrial redundant[2] manipulator is examined here. For this purpose, we consider the dextrous seven-axis Sarcos manipulator manufactured by Sarcos Research Corporation (Jacobsen et al., 1990; Smith et al., 1992). The DH parameters of this anthropomorphic arm with two 3R modules are given in Table 6.2, while a drawing depicting its architecture is shown in Fig. 6.10.

Optimum posture design with the original operation point

The last link length $a_7 = 0.21\ m$, as given in Table 6.2, defines the location of the operation point of the end-effector. Using this operation point, the characteristic layout of the arm is then determined by minimizing the condition number over the

[2]According to the arguments presented in Chapter 5, this manipulator is considered pseudoredundant, because, by locking one of its joints, say the elbow joint, the manipulator will lose more than one degree of freedom.

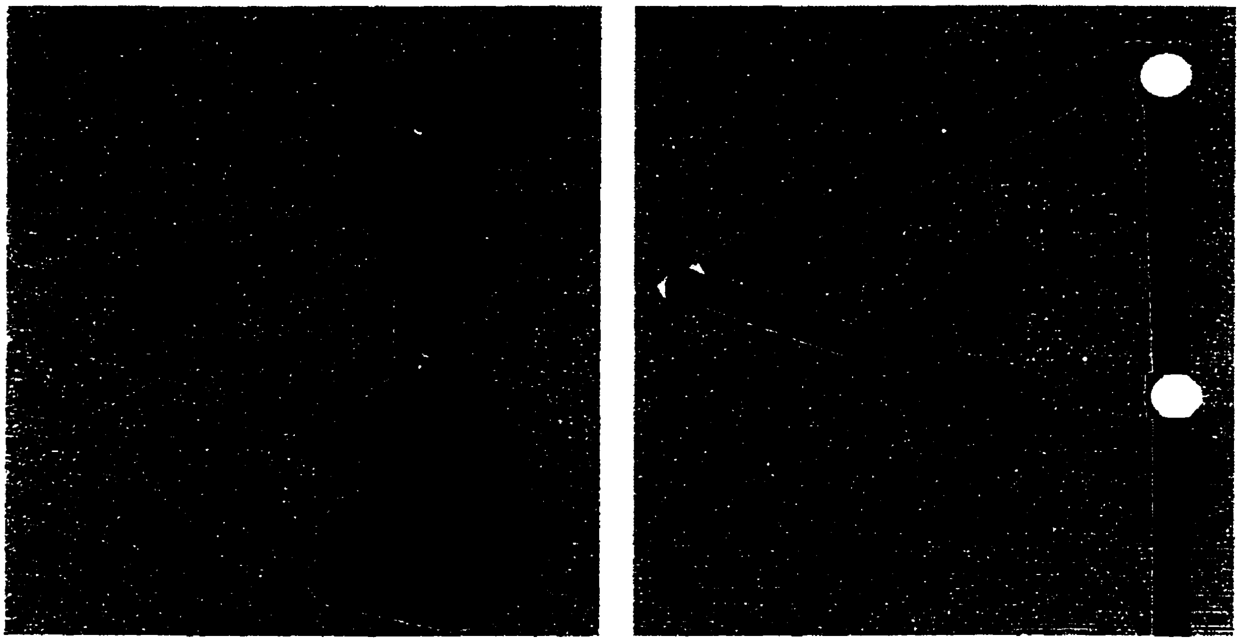

(a) (b)

Figure 6.8: Fanuc Arc Mate at the characteristic layout: (a) Full rendering with original end-effector, (b) skeleton rendering with the characteristic point

set of joint variables $\{\boldsymbol{\theta}\}_2^7$. With the aid of *fmins*, the optimum joint variable vector $\boldsymbol{\theta}_c$, defining the characteristic layout of the arm, and the characteristic length L_c of the manipulator are obtained after 825 iterations as shown below:

$$\boldsymbol{\theta}_c = [\theta_1 \quad -90.043^\circ \quad 80.773^\circ \quad -105.461^\circ \quad 89.975^\circ \quad -89.861^\circ \quad -37.845^\circ]^T,$$
$$L_c = 0.1815 \;\; \mathrm{m} \tag{6.78}$$

Link i	a_i m	b_i m	α_i (deg)	θ_i
1	0.0	0.0	90.0	θ_1
2	0.0	0.0	-90.0	θ_2
3	0.0	0.355	90.0	θ_3
4	0.0	0.0	-90.0	θ_4
5	0.0	0.230	90.0	θ_5
6	0.0	0.0	-90.0	θ_6
7	0.21	0.0	0.0	θ_7

Table 6.2: DH parameters for the Sarcos manipulator

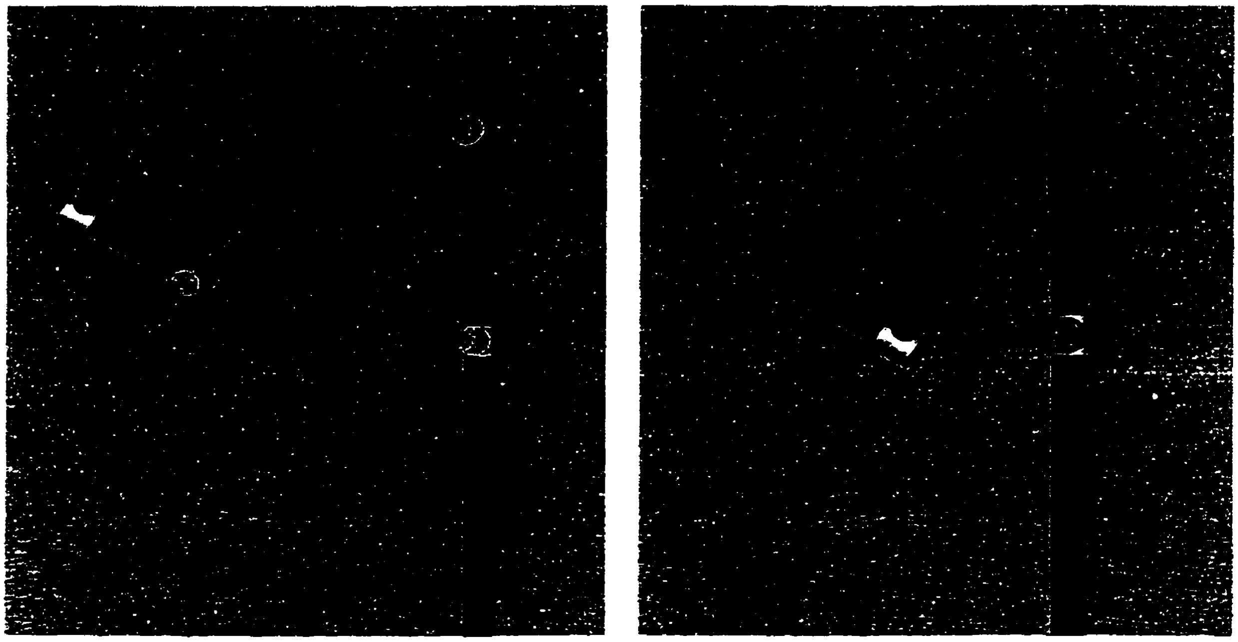

(a) (b)

Figure 6.9: Asea IRB 6/2 at the characteristic layout: (a) skeleton rendering with original manipulator, (b) skeleton rendering with the characteristic point

At this configuration we have $\tilde{\kappa}_F = 1.2430$, $\kappa_{\hat{F}} = 1.0733$, and $\kappa_2 = 1.5867$,. The foregoing minimum value of the 2-norm condition number—which is in the same range as the optimum condition numbers obtained for the three pseudoredundant manipulators introduced in Chapter 5—corresponds to a Conditioning Index (CI) of 63%. If the optimization of the dexterity of the manipulator had been included as part of the kinematic design requirements determining the architecture of the manipulator at hand, a higher CI for the manipulator could have been obtained, which will become apparent in the remaining of this section.

Optimum posture design while modifying the operation point

Next, the characteristic layout specified by the set $\{\boldsymbol{\theta}_c\}_2^6$, as well as the manipulator characteristic length L_c, and its characteristic point $\mathbf{p}_c$, are determined by eqs. (6.76). That is, a new location of the operation point is sought, in order to improve the layout

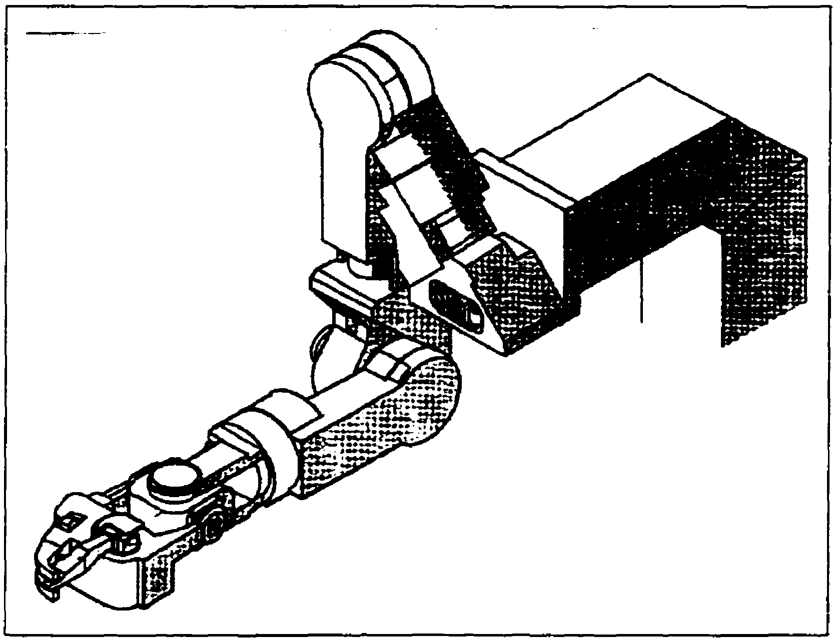

Figure 6.10: Seven-axis Dextrous SRC Arm (Sarcos Research Corporation, 1993)

conditioning of the arm, namely,

$$\boldsymbol{\theta}_c = [\,\theta_1 \quad 96.979^\circ \quad 0.006^\circ \quad -115.829^\circ \quad 0.0^\circ \quad 75.029^\circ\,]^T,$$
$$L_c = 0.1626 \ \ \text{m}$$
$$\mathbf{p}_c = [\,-0.0987 \quad 0.0 \quad -0.1595\,]^T \ \ \text{m}$$

Hence, the last link length, offset and joint variable are readily determined from eqs. (6.74), i.e.,

$$a_7 = 0.0987 \ \ \text{m}$$
$$b_7 = -0.1595 \ \ \text{m}$$
$$\theta_7 = 180.0^\circ$$

For the minimization of $\tilde{\kappa}_F$, *fmins* was once again used and the results were obtained after 413 iterations. The layout conditioning $\tilde{\kappa}_F$, normalized F-norm condition number $\kappa_{\hat{F}}$, and the 2-norm condition number of the Jacobian matrix at the characteristic layout were found to be $\tilde{\kappa}_F = 1.1251$, $\kappa_{\tilde{F}} = 1.0390$, and $\kappa_2 = 1.4295$, with a Condition Index (CI) of 70%. The skeleton rendering of this manipulator with its new end-effector is shown in Fig. 6.11[3].

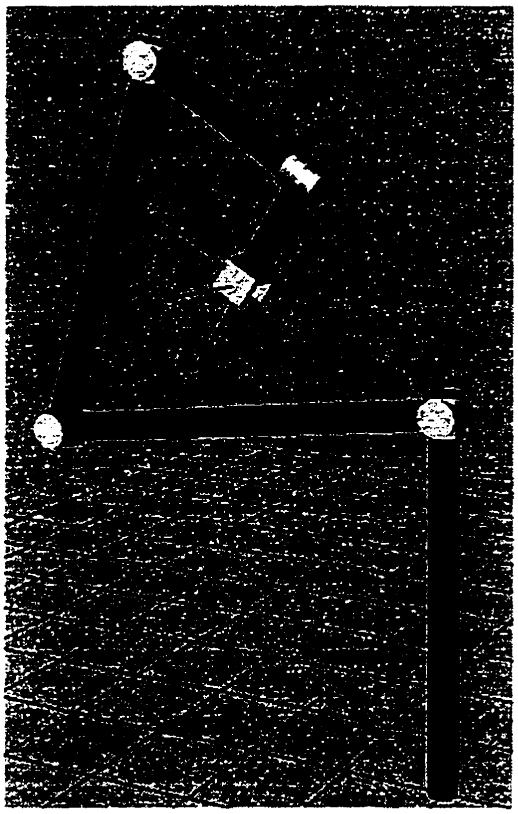

Figure 6.11: Skeleton rendering of Sarcos arm at the characteristic layout

For the sake of comparison from a computational point of view, the foregoing results are compared with an alternative formulation where all the nine unknowns are grouped into a vector of design variables and found directly through the optimization of the condition number. Using *fmins*, after 2189 iterations the results shown below were obtained:

$$\boldsymbol{\theta}_c = [\,\theta_1 \quad -64.074^\circ \quad 76.232^\circ \quad -121.198^\circ \quad 14.490^\circ \quad 44.651^\circ \quad -238.648^\circ\,]^T,$$

[3]Note that the first joint axis of the manipulator in the real setup makes an angle of 45° with the vertical axis; the default direction for the first joint under RVS is vertical.

$$L_c = 0.1744 \ \ \text{m}$$

$$\mathbf{p}_c = [\,1.6542 \quad 1.0932 \quad 1.3301\,]^T \ \ \text{m}$$

The layout conditioning $\tilde{\kappa}_F$, normalized F-norm condition number $\kappa_{\hat{F}}$, and the 2-norm condition number of the Jacobian matrix for this layout were found to be $\tilde{\kappa}_F = 1.3301$, $\kappa_{\hat{F}} = 1.0932$, and $\kappa_2 = 1.6542$, with a Condition Index (CI) of about 60%.

It is interesting to note that, by directly minimizing the condition number over the set of nine mixed variables mentioned above, as compared to the method presented earlier in this chapter where $\tilde{\kappa}_F$ is minimized over the set of five joint variables $\{\theta_i\}_2^6$ only, a much slower convergence, with more than five times the number of iterations, occurs. Moreover, computationally, each iteration of the former method where the 2-norm condition number needs to be evaluated is significantly more expensive than the latter, which only needs the computations of the trace and the determinant. It should also be noted that, once again, the *pseudoredundancy* of this anthropomorphic design leads to a non-isotropic design, i.e., isotropy is not possible.

6.6 Conclusions

Motivated by a measure of isotropy introduced by Kim and Khosla (1991), an alternative dexterity measure $\tilde{\kappa}_F$ was devised. This measure is significantly simpler to evaluate than any other condition number-based indices. Moreover, this measure is a function of the trace and the determinant of the matrix at hand, thus allowing for its symbolic differentiation. It was shown that $\tilde{\kappa}_F$ arises naturally when a linear approximation of the normalized Frobenius-norm condition number $\kappa_{\hat{F}}$ is determined. The upper and lower bounds of $\tilde{\kappa}_F$ were obtained for both square and rectangular matrices. The lower bound was found to be the normalized Frobenius-norm while the upper bound the mth power of the 2-norm condition number. The kinematic dexterity of serial manipulators was then discussed based on the notions of *manipulator layout* $\mathcal{L}$, *layout length* $L_{\mathcal{L}}$, *layout conditioning* $\kappa_{\mathcal{L}} \equiv \tilde{\kappa}_F$, and *layout center* $P_{\mathcal{L}}$. By directly minimizing $\kappa_{\hat{F}}$ over the set of all normalizing lengths of the Jacobian matrix, an explicit expression for the layout length was derived. Similarly, an explicit expression for the position vector of the operation point of the last link that renders $\kappa_{\hat{F}}$ a minimum was obtained. The characteristic layout of the manipulator was defined as a layout whose conditioning $\kappa_{\mathcal{L}}$ is a minimum. The concepts of manipulator characteristic length and characteristic point were then defined as the layout length and centre evaluated at the characteristic layout. Numerical examples of some industrial manipulators were chosen to illustrate the significance of these concepts. Significant improvements on the number of iterations and convergence of the optimization problem were achieved when compared with the minimization of condition numbers that makes no use of the layout length and layout centre.

Chapter 7

REDIESTRO 1

7.1 Introduction

In this chapter an overview of the design and manufacturing of a redundant seven-axis manipulator with an isotropic architecture for six-dimensional Cartesian tasks is reported. This manipulator, which is named REDIESTRO 1 (REDundant, Isotropically Enhanced, Seven-Turning-pair RObot) was designed, manufactured and implemented at the McGill Centre for Intelligent Machines (Ranjbaran et al., 1995). Since its completion in 1994, REDIESTRO 1 has been serving as an experimental platform for several robotics-related projects both internally in the department of Mechanical Engineering of McGill University and in collaboration with external research groups, (Seyfferth and Angeles, 1995; Canadair DSD, 1994, 1997; Shadpey et al., 1996). REDIESTRO 1 is currently located at the Robotics Laboratories of the Department of Electrical and Computer Engineering of Concordia University, where it is being used for the STEAR-5 Phase III[1] Project conducted by Bombardier Inc., Canadair Defence Systems Division (DSD), and the two universities, Concordia and McGill, as contracted by the Canadian Space Agency. In phase II of STEAR-5, REDIESTRO 1 was used to implement Trajectory Planning and Object Avoidance (TPOA) schemes

[1]Strategic TEchnologies in Automation and Robotics

developed for redundant manipulators. During phase III of the same project, currently under way, hybrid position-and-force and impedance control techniques are being successfully applied to REDIESTRO 1 for tasks such as surface cleaning and insertion and removal of mating objects such as Orbital Replacement Units (ORU) type objects.

7.2 Design Methodology

The kinematic design of nonredundant manipulators, has been mainly oriented towards achieving *kinematic solvability* and *manufacturing feasibility*. These criteria, in turn, have led to the existence of a particular class of manipulators whose axes are either parallel or perpendicular, i.e., orthogonal manipulators. Here, we mean by orthogonal a manipulator whose consecutive axes make angles that are multiples of 90°; for example, most industrial manipulators with spherical wrists; or with planar two-revolute subchains are of the aforementioned type. A general classification of manipulators with simple inverse kinematics is reported in (Mavroidis and Roth, 1992). The associated simple inverse kinematics has been formulated by exploiting special features, like orthogonality, of the kinematic structures of these robots. With the advent of fast and general inverse kinematics algorithms developed in the last ten years, however, the need for simple kinematic structures is less dominant. On the other hand, parallelism and orthogonality of the axes can give rise to undesirable singularities. These singularities are manifested, for example in the rate control and kinematic calibration of these manipulators (Hayati, 1982; Bennett et al., 1992), Serving the two foregoing objectives excludes a major class of manipulators with general architectures. By exploring general manipulator architectures, one cannot only improve the numerical conditioning of the manipulator kinetostatic maps, but also take into consideration other critical issues pertinent to the design and realization of the overall robotic systems.

For the case of redundant manipulators, general design criteria have been proposed.

For example, Hollerbach (1985) outlined the following features as guidelines for the design of these manipulators:

- Elimination of internal singularities;
- Optimization of workspace;
- Kinematic simplicity;
- Mechanical constructibility

It is apparent that the foregoing criteria highlight critical issues for the design of *general* redundant manipulators. Some researchers have emphasized methodologies for the design of redundant manipulators for specific tasks or classes of tasks. In this regard, the framework of *task-based design* for *reconfigurable modular manipulators* has been introduced (Kim and Khosla, 1991, 1992a–c). In the design of REDIESTRO 1, we have been mainly concerned with kinematic conditioning and isotropy. Thus, the main issue determining the architecture of REDIESTRO 1, defined by its Denavit-Hartenberg (DH) parameters, was the optimization of its kinematic conditioning. In Chapter 5, the kinematic design of redundant manipulators for isotropy was discussed in detail. It was shown that this criterion led not to one set of DH parameters, but rather to a manifold of these sets, which allowed the incorporation of further requirements. In addition to the design criteria listed above, issues such as maximum reach, structural behaviour, link-motor collision considerations, and functionality properties were considered. These requirements, in turn, allowed the determination of the link shapes and the selection of actuators. In the following sections, the overall strategy based on the integration of different aspects and stages of the design process is discussed and heuristic design rules are provided.

The major design activities undertaken from the start of the project to the preparation of the shop drawings of REDIESTRO 1 are listed below:

1. Kinematic design

2. Preliminary mechanical design
3. Detailed mechanical design
4. Three-dimensional rendering and animation
5. Redundancy resolution and kinematic simulation

Items 1–4 will be discussed in detail presently, while item 5 has been the main contribution of Concordia University to the realization of the REDIESTRO 1 work-cell. The activities mentioned above have been integrated into a hierarchical framework that consists of three different iterative loops at different levels. The flow diagram shown in Fig. 7.1 depicts these activities and the corresponding loops.

The innermost loop consists of the *kinematic design* and *skeleton rendering* of the resulting architectures. Numerical optimization techniques were utilized for the kinematic design, whereby a set of different isotropic seven-axes manipulators was obtained. Three-dimensional visualization of the corresponding models in the form of simple skeleton renderings were then analyzed and additional structural requirements were imposed to narrow down the selection set. As a result of this loop, a first candidate was chosen and the corresponding normalized HD parameters were identified.

The second loop includes the *kinematic* and *preliminary mechanical design*. At this stage, based on the requirements on the volume of the workspace and maximum reach, the candidate manipulator was scaled,. A preliminary mechanical analysis based on required performance characteristics of the manipulator was then performed and the actuators were selected. Furthermore, a preliminary layout of the links and placement of the actuators was also outlined. Functionality of the design and actuator placements required further constraints on the DH parameters. This demand was achieved by imposing additional constraints on the kinematic optimization schemes, whereby the final scaled DH parameters were determined.

The final design loop consists of the *detailed mechanical design*, *detailed three-dimensional* *renderings* and *animation*. In this loop, with the given DH parameters and actuator specifications, the detailed mechanical design of the links was performed. Issues such as workspace requirements, ranges of motion of each joint and collision of the link-actuator subassemblies were set forth as final design requirements. These issues were analyzed using detailed three-dimensional renderings of the assembled manipulator and thus, the required modifications on the shape and geometry of the link subassemblies were made.

7.3 Kinematic Design

The methods of isotropic design discussed in Chapter 5, were employed as the kinematic design tool. The first candidate design emerging from the first design loop is the second isotropic design introduced in Chapter 5, Design 2. Recall that the additional design requirements set out for Design 2 were mainly to concentrate as much of the manipulator mass as possible close to the first axis. The skeleton rendering of this design is once again shown in Figure 7.2 for quick reference.

7.4 Preliminary Mechanical Design

At this level, primarily an overall kinematic performance for the manipulator is specified, actuators are selected, and a rudimentary design of the manipulator is performed. Any final minor modifications or refinements of the kinematic architecture are made at this stage.

1. Scaling of the manipulator:

   First, It is necessary to bring the candidate architecture into its full-scale dimensions. To do this it is required that the manipulator should have a reach of 1.0 m when all joint angles are zero. Based on this yardstick, the candidate manipulator is scaled as given in Table 7.1.

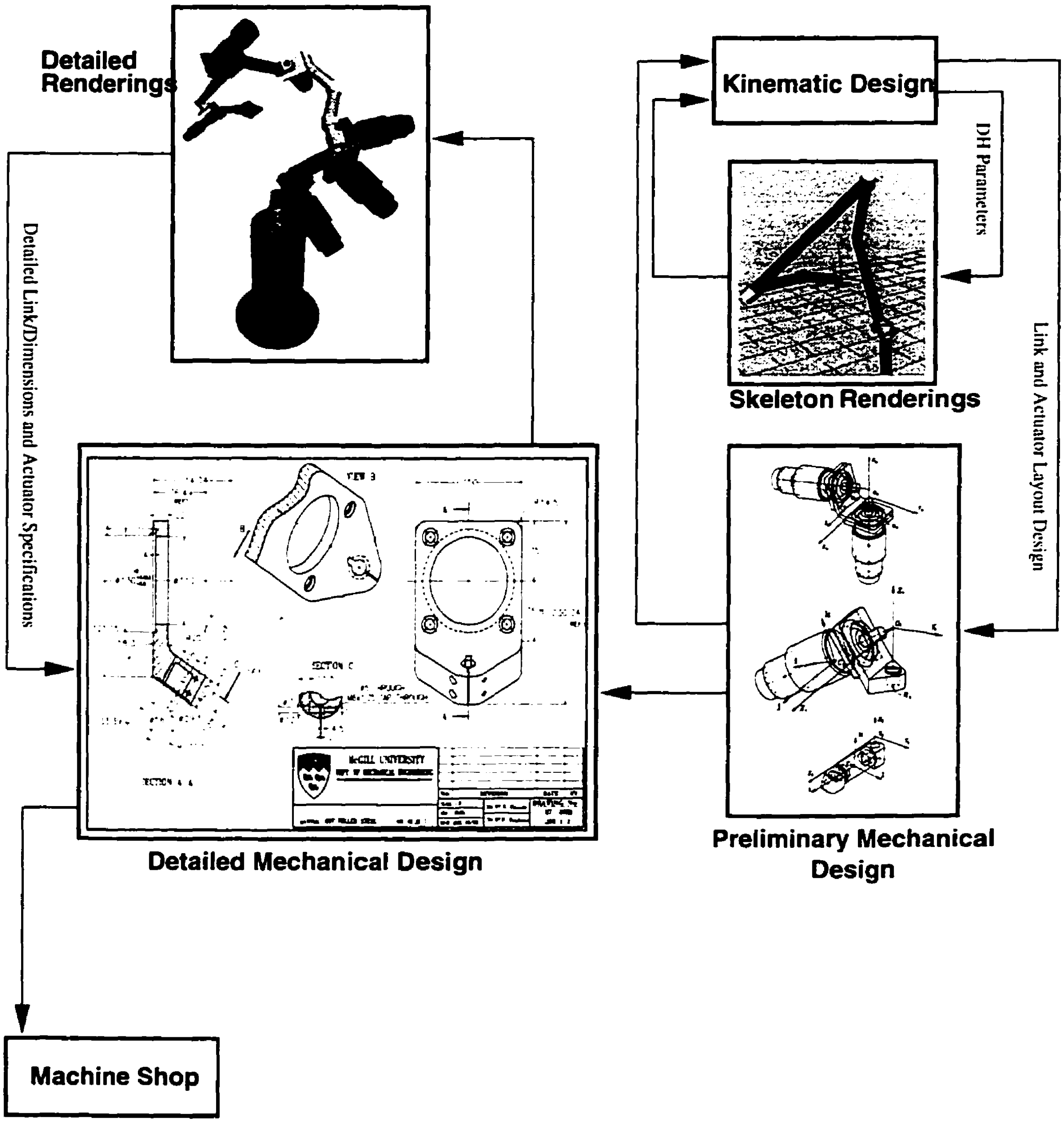

Figure 7.1: Flow Diagram of the Design Methodology

Link i	a_i (mm)	b_i (mm)	α_i (deg)	θ_i (deg)
1	0	0	-62.71	0
2	6.7	0	-11.10	35.10
3	0	49.4	106.68	62.71
4	634.4	0	72.87	117.71
5	0	-527.1	55.83	-24.63
6	20.7	910.6	62.84	-2.32
7	338.2	-415.6	0	225.45
Characteristic Length = 292.921 mm				
Reach at Zero Configuration = 1000 mm				
Maximum Reach = 1866.05 mm				

Table 7.1: Scaled parameters of the candidate manipulator

Link axis No.		1	2	3	4	5	6	7
Nominal payload distance	m	1.0	1.06	1.06	1.04	0.53	0.52	0.34
Max. joint velocity	s^{-1}	1.0	0.8	0.8	0.8	1.65	1.65	1.65
Time to travel 90°	s	1.57	1.96	1.96	1.96	0.95	0.95	0.95
Payload linear velocity	m/s	1.0	0.85	0.85	0.83	0.87	0.86	0.56
Min. average ang. acc.	s^{-2}	9.81	7.40	6.94	6.60	11.10	10.38	14.41
Average payload g-factor	g	1.0	0.8	0.75	0.70	0.60	0.55	0.50
Max. acceleration time	s	0.1	0.1	0.11	0.12	0.15	0.16	0.11
Drive output speed	rpm	9.55	7.64	7.64	7.65	15.7	15.7	15.7

Table 7.2: Design specifications for angular velocities and accelerations

2. Preliminary performance specifications:

   The overall preliminary design specifications for velocities and accelerations of different links are given in Table 7.2. Based on these requirements, the preliminary selection of the actuators was made. For all seven drives, DC servo-motors equipped with harmonic drives, incremental encoders and electro-magnetic brakes were selected.

3. Preliminary design of the link subassemblies:

   At this stage a rudimentary layout of the link shapes and actuator placement are made, and the conceptual design of the corresponding subassemblies is completed. It was observed that, although, keeping the first four of the actuators

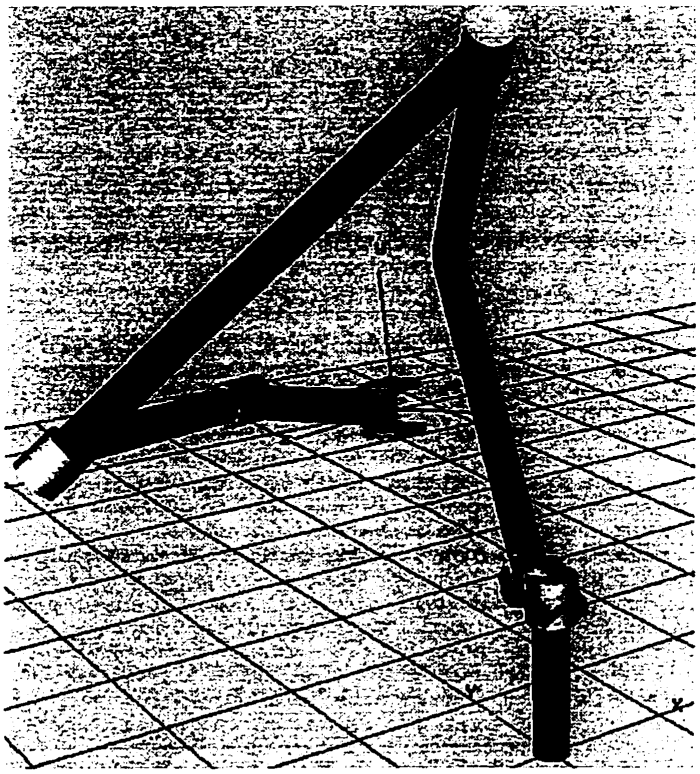

Figure 7.2: Fully isotropic seven-axis manipulator: first candidate manipulator

close to the first axis is advantageous from the point of view of dynamic performance, installation of the four units at a close vicinity proved to be difficult. In particular, since the joint axes 2 and 3 of the candidate manipulator almost intersect at about 11° (Fig. 7.2), one possible solution was the use of a differential gear transmission between actuators 2 and 3. The preliminary design of the candidate manipulator with the differential gear that was implemented for this purpose is shown in Fig. 7.3.

Before leaving the last iterative design loop, it was decided that, by modifying the kinematic structure of the manipulator, the differential gearing system be eliminated. In order to do this, the link length a_2 was preassigned a minimum value that could enclose two of the selected actuators. In turn, one of the constraints, namely $b_2 = 0$, was relaxed from the numerical formulation of the kinematic design. The outcome

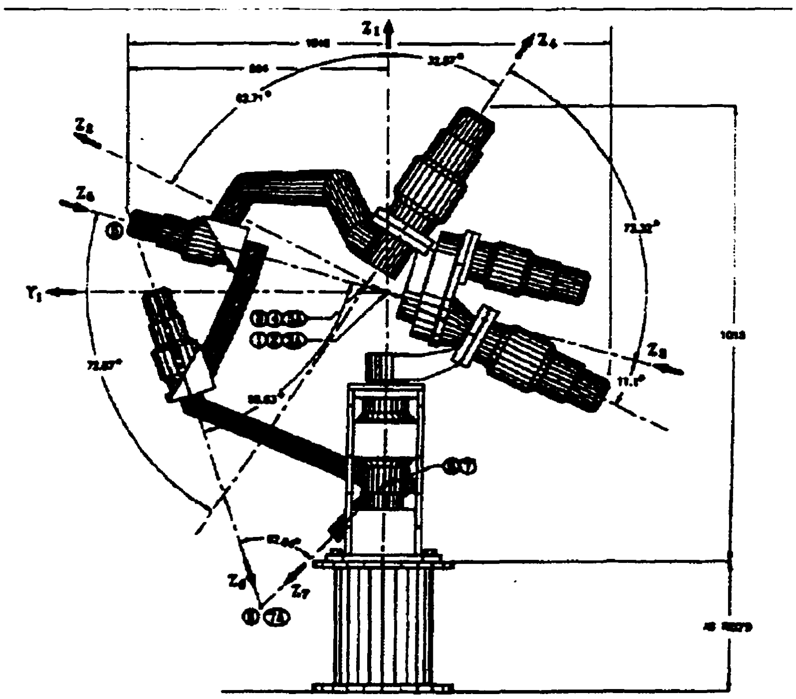

Figure 7.3: Completed preliminary design of the candidate manipulator

of this final modification was our final design, whose three-dimensional skeleton rendering is shown in Fig. 7.4, and whose scaled DH parameters are given in Table 7.3. It is apparent that the first four joints are divided into two separate groups of two joints, that still lie as close as possible to the first axis. This completed the iterative kinematic and overall mechanical design loops, thereby completely defining the architecture of REDIESTRO 1.

7.5 Detailed Mechanical Design

Having completed the preliminary kinematic and mechanical designs of REDIESTRO 1, the detailed mechanical design of the link subassemblies was undertaken. The exact shape of each link, together with the location of the corresponding actuators along each joint axis formed the last design loop, as shown at the bottom of the design flow diagram of Fig. 7.1. Hence, as another outcome of this loop, the offset distance

Link i	a_i (mm)	b_i (mm)	α_i (deg)	θ_i (deg)	$d_{OI}(mm)$	ϕ (deg)
1	0	0	-58.31	0	952.29	0.0
2	231.13	-22.91	-20.0289	-11.01	-114.043	0.0
3	0	36.93	105.26	91.94	-97.0	0.0
4	398.84	0	60.91	113.93	133.93	180.0
5	0	-471.59	59.88	-2.26	-10.9172	180.0
6	135.59	578.21	-75.47	150.25	267.6810	0.0
7	234.44	-145.05	0	63.76	-128.55	180.0
Scale Factor = 0.1926						
Characteristic Length = 220.6505 mm						
$\sum_{i=1}^{7} a_i = 1000$ mm						
Reach at zero configuration = 1218 mm						
Maximum Reach = 2190.9 mm						

Table 7.3: Scaled parameters of REDIESTRO 1

from the origin of frame i along the ith joint axis to a reference point attached to the actuator, denoted by I, should be determined. This *motor-insertion offset distance* is denoted by d_{OI}. The location of the actuator reference point is taken as the centre of the output shaft and level with the face mounting flange, as shown in Figures E.1 to E.4. The orientation of the axis of the ith actuator inserted with respect to the ith joint axis is also given (angle ϕ_i). This angle determines whether the output shaft of the actuator inserted in the link points along the positive or the negative z-axis. Furthermore, in this loop, with the aid of RVS, the Robotic Visualisation System developed at CIM, a step-by-step design of each link-and-actuator assembly was completed, while monitoring many different issues, such as collisions among links and actuators, feasibility, constructibility, minimization of the moment arms as seen by the previous actuator, etc. Figs. 7.5 and 7.6 are the RVS renderings of REDIESTRO 1 at the isotropic and at the maximum-reach configurations, respectively. In Appendix D, the three-dimensional CAD drawings of the robot and the link subassemblies are included along with the detailed mechanical drawings of the each link. The electromechanical specifications of the actuators are provided in Section E.1. As the design of the manipulator was finalized, the detailed CAD drawings of the components were made with the use of AutoCAD®. Furthermore, the solid modelling capabilities

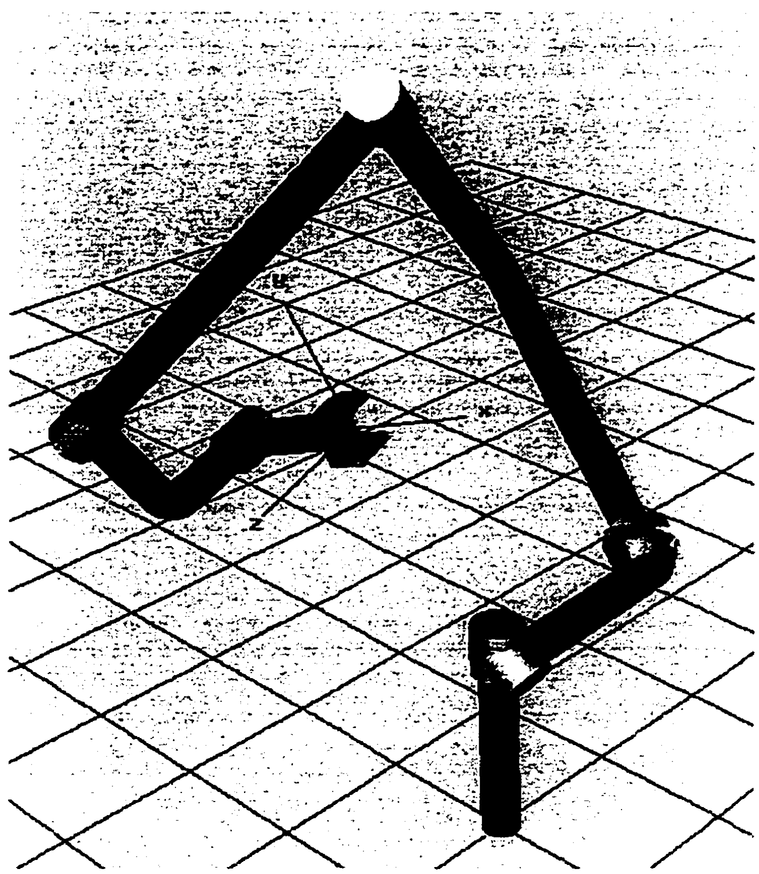

Figure 7.4: Skeleton rendering of REDIESTRO 1 at the isotropic configuration

of AutoCAD® were utilized to obtain the inertial parameters of each link, defined in its local coordinate frame. By completing the detailed drawings for each link, a three-dimensional solid model of the corresponding link-actuator subassembly was then made, and the inertial parameters were estimated. Table 7.4 contains the inertial parameters of the links, namely, the mass, mass-center location and moments of inertia. Moreover, photographs of REDIESTRO 1 are shown in Fig. 7.7-a and -b.

7.6 Heuristic Design Rules

In this section, the heuristic design rules that were developed during the course of this design are briefly outlined. To date, most robotic manipulators have been designed

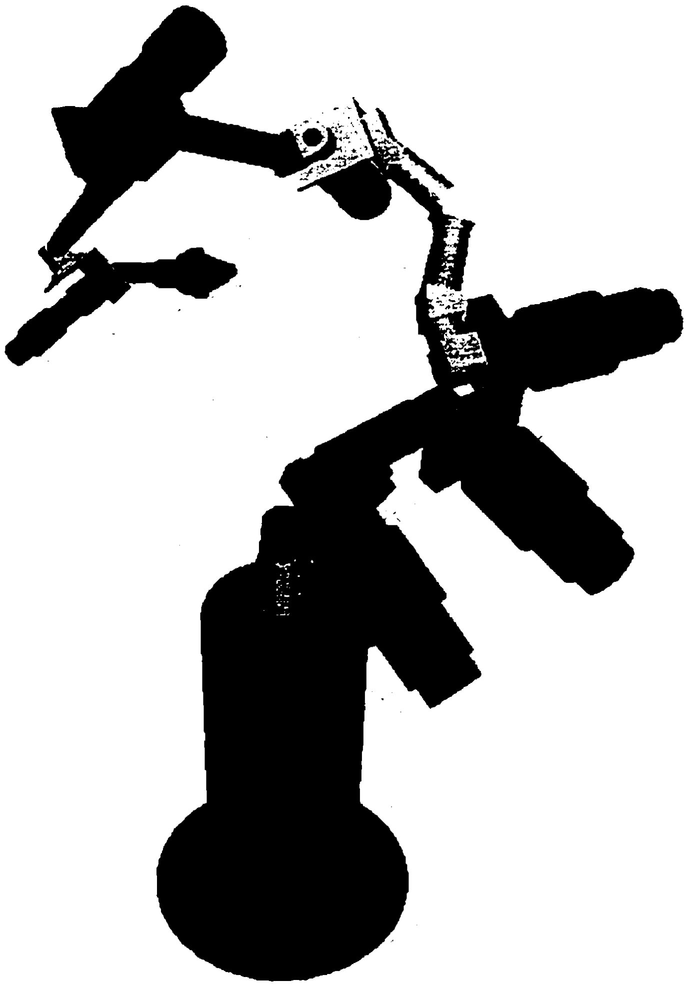

Figure 7.5: REDIESTRO 1 at the isotropic configuration

with conventional orthogonal architectures. By exploring other general architectures, it is possible to design manipulators for particular or general applications, while considering several kinematic, static or functional design issues. It is concluded that the Jacobian matrix can be used effectively to address design considerations such as synthesis of the kinematic chain, numerical conditioning, singularities of the workspace, extreme reach and workspace volume. Depending on the characteristics of the manipulator and tasks to be performed, priority can be placed on fulfilling one or more of the foregoing demands. For the design of REDIESTRO 1, we are mainly concerned

Figure 7.6: REDIESTRO 1 at the fully stretched configuration

with the kinematic conditioning of the kinetostatic transformations. In this regard, we aimed at the design of an isotropic seven-revolute joint manipulator. Thus, the highest design priority was given to the realization of an isotropic Jacobian matrix. Other design considerations such as structural requirements, collision and functionality of the link-actuator subassemblies, workspace, extreme reach of the manipulator, and constructibility of the links are variables that were prioritized and satisfied accordingly. For instance, the second-priority task for the design of REDIESTRO 1 was concerned with structural considerations, namely, concentration of the first four joints near the first axis to minimize the static and inertial loads imposed on the proximal drives. It was concluded that predetermined lower and higher bounds had to be placed on the distance between the second and third axes, i.e., on a_2, in order to best enclose the four proximal drive units, while keeping them in close proximity. The location of each actuator along the corresponding joint axis was determined

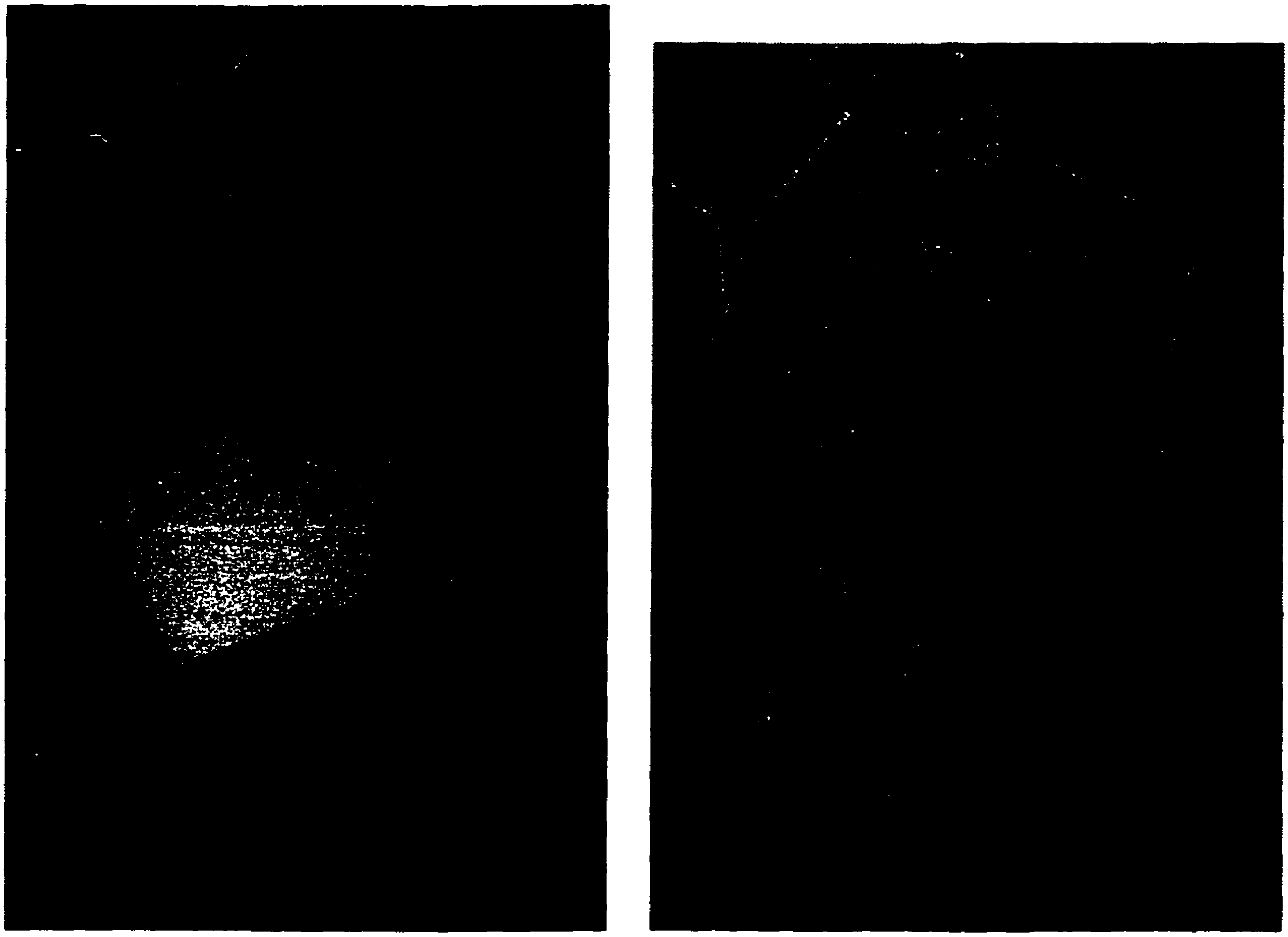

(a) (b)

Figure 7.7: Photographs of REDIESTRO 1: (a) Surface-cleaning setup, (b) Peg-in-hole insertion and removal setup

from the considerations below:

- Minimization of the moment arm created with respect to the previous drive.

  When two consecutive joint axes are nonparallel and nonintersecting, the static (dynamic) load imposed by the first drive is affected by the moment arm (radii of gyration), which is in turn affected by the location of the second actuator along its joint axis.

- Creation of collision-free regions around the isotropic configuration.

Parameters		link 1	link 2	link 3	link 4	link 5	link 6	link 7
Mass (kg)		17.313	5.580	28.586	7.390	5.987	2.557	0.2
Center of	x:	4.8e-4	0.1155	-0.0011	0.3071	0.0	-0.0919	0.06345
Gravity	y:	-0.1607	-0.0036	-0.1176	-0.0408	-0.1326	0.03434	0.0
(m)	z:	-0.1186	-0.0618	-0.1170	0.0699	-0.3209	0.49	-0.0034
Moments of	x:	0.89926	0.02573	1.6620	0.09297	0.8284	0.6541	0.000024
Inertia	y:	0.31342	0.13223	0.7860	0.8881	0.7019	0.6714	0.001136
(kg m^2)	z:	0.62745	0.11099	0.9387	0.8753	0.1317	0.0374	0.001135
Products of	xy:	-2.7e-5	-0.0045	0.0001	-0.1203	0.00009	-0.00839	0.0
Inertia	yz:	0.3689	0.0012	0.1221	-0.0204	0.26852	0.04574	0.0
(kg m^2)	zx:	-1.2e-5	-0.0404	0.0003	0.1411	0.00016	-0.12596	0.0
Radii of	x:	0.2279	0.0679	0.2411	0.1121	0.3719	0.5057	0.0110
Gyration	y:	0.1345	0.1539	0.1658	0.3466	0.3424	0.5124	0.0753
(m)	z:	0.1904	0.1410	0.1812	0.3444	0.1483	0.1210	0.0753

Table 7.4: Inertial parameters of REDIESTRO 1 in its local frames

In order to exploit the inherent well-conditioning characteristics of an isotropic manipulator, or to make use of the large singularity-free regions around the isotropic configurations, it is essential to maximise the accessibility of the corresponding region from a structural viewpoint as well. This can be achieved by minimizing the presence of structural obstacles within the region, and by maximising the accessible positive and negative range of motion for each joint about its corresponding isotropic point.

- Functionality and constructibility of the design.

Focusing strictly on the two previous items can result in link shapes and geometries that are not feasible in terms of manufacturing processes and functionality. Hence, in conjunction with the above-mentioned design issues, one has to take into consideration constructibility by making reasonable compromises against other critical aspects.

7.7 Conclusions

In this Chapter an overview of the design, manufacturing and realization of a redundant seven-axis isotropic manipulator, called REDIESTRO 1 (REDundant, Isotropically Enhanced, Seven-Turning-pair RObot), was given. Kinematic design tools developed in the previous Chapters of the thesis were used to produce a family of such designs. Further mechanical design specifications were introduced in order to narrow down the selection set. The preliminary and detailed mechanical design of one representative instance of this family was undertaken, and finally, heuristic design rules were outlined. REDIESTRO 1 was designed, manufactured, and commissioned at McGill's Centre for Intelligent Machines. This manipulator has seven degrees of freedom, its maximum reach is about 2.1909 meters. In the Cartesian workspace of the manipulator, there exists a circle of radius 1.1528 meters centred on the first axis, all of whose points correspond to isotropic postures of the manipulator, i.e., *circle of isotropy*. The robot is equipped with seven harmonic-drive units of actuation, each containing a permanent-magnet DC motor, an incremental encoder, an electromagnetic brake, and a harmonic drive gear-head. REDIESTRO 1 has been serving as a useful redundant experimental robot on which several aspects of the current state of the art in robotics are being tested. To name a few, characterization of the joint flexibility and friction, kinematic and dynamic calibration, trajectory planning, object- and self-collision avoidance, impedance control and hybrid position-and-force control for complex tasks such as surface cleaning and insertion and removal of mating objects.

Chapter 8

Concluding Remarks

8.1 Conclusions

Within the context of kinematic dexterity and singularities, both analysis and design of manipulator architectures were discussed in detail in this thesis, with particular attention being given to the *kinematic design* of redundant manipulators.

In Chapter 1, the workspace and singularities of *regional structures* were considered. Regional structures or spatial three-axis architectures forming the positioning part of most of the existing nonredundant industrial manipulators, they can be regarded as representatives of the existing nonredundant designs. First, a review of the reported contributions made to manipulator singularities was conducted. A novel method for the determination of the Cartesian singularities of the forward kinematic map was then introduced. This method, that determines the resolvent of two polynomials, is based on the notion of *nonminimal* transfer-function realization for single-input/single-output (SISO) linear dynamical systems, and can be applied to general n-axis manipulators. Having determined the resolvent of the manipulator characteristic polynomial and its derivative with respect to one of the joint variables, a CAD-based methodology was then devised for the three-dimensional graphical renderings of the Cartesian workspace boundaries. The second part of Chapter 1, is devoted to the characterization of the joint-space *uniqueness domains*, i.e., subregions of the manipulator joint-space that contain unique inverse kinematic solutions. Algebraic expressions were provided that define the boundaries of the uniqueness domains[1]. In this regard, singular- vs. nonsingular-*posture changing*-manipulators were discussed, where, with the aid of a theorem, it is proven that *special manipulators* cannot change solution branch without crossing singularities. Furthermore, in confirming with the conjecture made by Burdick (1992), an example of a *nongeneric* regional structure that *can* change solution branch without crossing singularities is introduced. In the last section of Chapter 1, a critical evaluation of the *merits* of nonsingular-posture-changing manipulators over their singular-posture-changing counterparts is provided, while these two classes of regional structures are compared as they follow a given Cartesian-space trajectory. It is thus concluded that, designing regional structures for the ability of singularity-free solution-branching does not necessarily lead to a *better* architecture.

The focus of Chapter 3 is on manipulator *dexterity measures*. A review of the existing indices of merits for the characterization of kinematic performance of manipulators is provided. Invariance properties of these measures are then discussed in detail, whereby the issue of the sensitivity of the performance measures to the end-effector operation point is analyzed through different illustrative examples. Despite the search of some researchers for an *operation-point-insensitive index*, as an *intrinsic*, and thus *faithful* measure for quantifying kinematic performance, we maintain that, if a measure is capable of characterizing the effects of the size of the end-effector and the location of the operation point on the overall manipulator dexterity, why should we deprive our performance characterization form this feature? Moreover, it is believed in some circles that a measure that does depend on the operation point can be rendered one that does not depend on the latter by simply assigning zero values to the four DH parameters of the last link. In other words, an

[1] the method introduced in this thesis is similar to the method proposed independently in (Tsai et al., 1993)

operation-point-sensitive measure is more general in its scope, since it encompasses the range of applications of the operation-point-insensitive measures.

In Chapter 4 the condition numbers of general matrices are discussed in detail, where particular attention is paid to two important features of these numbers as applied to kinematic performance, namely, characterizing *distance* to singularities and *sensitivity* of the associated linear systems, with respect to perturbations. Determined, underdetermined and overdetermined linear systems of equations and their applications in the analysis of manipulator kinematic-performance are also reviewed. The notions of *matrix isotropy* and *kinematic isotropy* are introduced through formal definitions. With the aid of a theorem, the necessary and sufficient conditions for the isotropy of general rectangular matrices are provided. Geometric interpretations of the isotropy of linear transformations are also provided. In the last section of Chapter 4, isotropic manipulators are formally defined followed by a general description of the techniques used in this thesis for the isotropic design of manipulators. Through a simple illustrative example for the isotropic design of planar 2-R manipulators, it is shown that optimizing the condition number amounts to simultaneously decreasing the rms value of the distances from the end-effector operation point to the axes of the manipulator, while increasing the area of the triangle formed by the two joints and the operation point. As a byproduct of the foregoing simple example, it is also shown that, the 2-norm condition number at the isotropic point is not a smooth function of the joint variable θ_2.

Chapter 5 is devoted to the isotropic design of redundant manipulators. First, the isotropic design of seven-axis manipulators is discussed in detail, several examples of such architectures being provided. It is shown that the isotropy condition for seven-axis manipulators leads to an underdetermined system of nonlinear equations, an infinity of architectures satisfying the said system thus being avaliable. Representative examples from the solution set are obtained by formulating a nonlinear optimization problem. Furthermore, a design methodology is introduced whereby additional functional design requirements are incorporated in order to narrow down the design space, thus obtaining a determined system of nonlinear equations.

Next, *anthropomorphic* considerations are incorporated into the design methodology mentioned above. It is shown that anthropomorhic designs can lead to *pseudoredundancy* of the architectures. It is then concluded that, in general, full isotropy and anthropomorphism cannot coexist for seven- and eight-axis manipulators. An illustrative example of a nine-axis architecture that possesses both of the foregoing features is provided. Planar *hyperredundant* manipulators are considered next, the optimum posturing of a 30-axis planar arm being calculated. It is first shown that if the Jacobian matrix associated with hyperredundant manipulators is reformulated as a function of the *absolute*—as opposed to the *relative*—joint variables, then the isotropy condition takes on a very simple form. Additional design requirements for the optimum posture design of this class of redundant manipulators are then outlined, namely, kinematic isotropy, smoothness of the manipulator posture, and the orientation of the last link. The resulting optimum posture resembles a cobra in its familiar ready-to-attack configuration. In the last section of Chapter 5, a comparative analysis of isotropic, versus nonisotropic manipulators is made, the basis of this comparison being on the distribution of the set of singularities of the manipulators throughout their joint-space. In general, comparing two manipulators for any functional purpose is not a well-defined task. The framework in which a fair comparison can find meaning is first defined. The comparison of redundant manipulators in the sense of kinematic dexterity and singularity distributions is then provided through illustrative examples, where it is observed that the joint-space singularity distribution of isotropic architectures are *better* behaved than those associated with the comparable nonisotropic designs.

Some of the main contributions of the thesis are introduced in Chapter 6, where the kinematic conditioning and dexterity of general revolute-jointed manipulators are discussed from a geometric point of view. First, based on a previously reported *measure of isotropy* (Kim and Khosla, 1991), a novel measure of conditioning for general matrices is introduced. It is shown that this measure is a linear approximation to the normalized Frobenius-norm (F-norm) condition number; for quasiisotropic matrices, this measure provides a very close prediction of the condition number. For both rectangular and square matrices, upper and lower bounds are obtained for this measure in terms of the F-norm and the 2-norm condition numbers. Based on this measure of conditioning, a measure of manipulator conditioning is devised that is highly suited for the intended task of manipulator design. Moreover, this performance index is substantially less expensive to compute than other measures of kinematic conditioning, and is amenable to optimization using gradient methods, rather than with purely direct-search methods, which are much slower. Based on a gradient technique for the minimization of this index with respect to the normalizing length and the operation point of the end-effector, a preferred normalizing length and a preferred operation point of the end-effector are obtained. In this regard, the notions of *manipulator layout*, *layout conditioning*, *layout length* and *layout centre* for any serial-type robotic manipulators are introduced. Furthermore, the characteristic layout of manipulators are discussed followed by discussions on the characteristic length and the characteristic point. Several illustrative examples are provided for determining the optimum layout of both redundant and nonredundant industrial manipulators.

In Chapter 7 an overview of the design and manufacturing of a redundant seven-axis manipulator with an isotropic architecture is reported. This manipulator, which is named REDIESTRO 1 (REDundant, Isotropically Enhanced, Seven-Turning-pair RObot) was designed, manufactured and commissioned at the McGill Centre for Intelligent Machines. Since its completion in 1994, REDIESTRO 1 has been serving as an experimental platform for several robotics-related projects both internally in the Department of Mechanical Engineering of McGill University and in collaboration with external research groups. REDIESTRO 1 is currently being employed for the STEAR-5 Phase III[2] Project conducted by Bombardier Inc., Canadair Defence Systems Division (DSD), Concordia University and McGill University. In phase II of STEAR-5, REDIESTRO 1 was used to implement Trajectory Planning and Object Avoidance (TPOA) schemes developed for redundant manipulators. During phase III of the same project, currently under way, hybrid position-and-force and impedance control techniques are being successfully applied to REDIESTRO 1 for tasks such as surface cleaning and insertion and removal of mating objects such as Orbital Replacement Units (ORU) type of objects.

8.2 Suggestions for Further Research

During the development of the research work reported in this thesis, a number of related research areas are identified that could form the basis for future work, namely,

1. To conduct a more elaborate investigation of the *global isotropic* design versus the local methodology discussed in the thesis. Although the singularity distribution of the architectures that are designed for local dexterity were investigated in the thesis, it appeared to the author that the issue of global-versus-local isotropic designs and their relationship can be expanded upon in further detail. The equivalence of local, versus global isotropic designs, was first reported in Gosselin and Angeles (1991), where it was found that, for a planar two-axis example both coincide. It seems that the extension of the aforementioned equivalence to general manipulator architectures remains an open question. It is thus suggested to employ the *homotopy classes* in order to investigate the relationship between local and global design methodologies.

2. To investigate through experiments the role of the kinematic isotropy of redundant manipulators in the framework of *hybrid position*-and-*force*

[2]Strategic TEchnologies in Automation and Robotics

control strategies. The appearance of the isotropy condition in the said framework was recently reported in (Goldenberg, 1996).

3. To device isotropy-based numerical procedures for the calibration of the geometrical parameters of redundant manipulators. The numerical behaviour of most existing calibration methodologies is a crucial concern for the successful implementations of these techniques. Moreover, in many of the existing methodologies, the Jacobian matrix associated with the manipulator is needed. It is thus believed that, by establishing an isotropy-based calibration procedure, one would indeed expect superior convergence and accuracy from the underlying numerical procedures.

References

Angeles, J., 1997, *Fundamentals of Robotic Mechanical Systems*, Springer-Verlag, New York.

Angeles, J., Bulca, F., Arenson, N., and Arenson, M., 1996, "Kinematic sensitivity of redundant robotic manipulators," *Proc. 5th International Symposium on Advances in Robotic Kinematics (ARK)*, Portorož-Bernardin, Slovenia, June 22–26, pp. 17–26.

Angeles, J. and López-Cajún, C. S., 1993, "Kinematic isotropy and the conditioning index of serial robotic manipulators," *The International J. Robotics Research*, Vol. 11, No. 6, pp. 560–571.

Angeles, J., Ranjbaran, F., and Patel, R. V., 1992, "On the design of the kinematic structure of seven-axes redundant manipulators for maximum conditioning," *Proc. IEEE Int. Conf. Robotics Automat.*, Vol. 1, pp. 494–499.

Angeles, J., 1988, "Special loci of the workspace of spherical wrists", *Proc. First International Workshop on Advances in Robot Kinematics*, September 19–21, Ljubljana: 36–45.

Angeles, J. and López-Cajún, C. S., 1988, "The dexterity index of serial-type robotic manipulators", *Proc. ASME 20th Biennial Mechanisms Conference*, Sept. 25–28, Kissimmee, pp. 79–84.

Arenson, N., 1997, *The Real-Time Resolved-Rate Redundancy Resolution Schemes for Robotic Manipulators.* M. Eng. Thesis, Department of Mechanical Engineering, McGill University.

Basavaraj, U. and Duffy, J., 1993, "End-effector motion capabilities of serial manipulators," *The International J. Robotics Research*, Vol. 12, No. 2, pp. 132–145.

Bennett, D. J., Hollerbach, J. M., and Henri, P. D., 1992, "Kinematic calibration by direct estimation of the Jacobian matrix," *Proc. IEEE Int. Conf. Robotics Automat.*, Vol. 1, pp. 351–357.

Berger M. and Gostiaux B., 1988, *Differential Geometry: Manifolds, Curves, and Surfaces*, Springer Verlag, New York.

Borrel, P. and Liégeois, A., 1986, "A Study of manipulator inverse kinematic solutions with applications to trajectory planning and workspace determination," *Proc. IEEE Int. Conf. Robotics Automat.*, Vol. 2, pp. 1180–1185.

Burdick, J. W., 1995, "A classification of 3R regional manipulator singularities and geometries," *Mechanisms and Machine Theory*, Vol. 30, No. 1, pp. 71–89.

Burdick, J. W., 1992, "A recursive method for finding revolute-jointed manipulator singularities," *Proc. IEEE Int. Conf. Robotics Automat.*, Vol. 1, pp. 448–453, Nice.

Burdick, J. W., 1991, "A classification of 3R regional manipulator singularities and geometries," *Proc. IEEE Int. Conf. Robotics Automat.*, Vol. 3, pp. 2670–2675.

Burdick, J. W., 1988, *Kinematic Analysis and Design of Redundant Manipulators*. Ph.D. Thesis, Stanford University, Stanford.

Canadair, DSD, Robotics Group, 1997, STEAR 5 Phase III First Interim Report. Bombardier Inc., Canadair Defence Systems Division (DSD), Montreal, Quebec.

Canadair, DSD, Robotics Group, 1994, STEAR 5 Phase II Final Report, Bombardier Inc., Canadair Defence Systems Division (DSD), Montreal, Quebec.

Ceccarelli M., 1996, "A formulation for the workspace boundary of general N-revolute manipulators," *Mechanisms and Machine Theory*, Vol. 31, No. 5, pp. 637–646.

Ceccarelli, M. and Vinciguerra, A., 1995, "On the workspace of general 4R manipulators," *The International Journal of Robotics Research*, Vol. 14, No. 2, pp. 152–160.

Ceccarelli, M., 1994a, "Determination of the workspace boundary of a general N-revolute manipulator," in Lenarčič J. and Ravani B. (editors), *Advanes in Robot Kinematics and Computational Geometry*, Kluwer, Dordrecht, pp. 39–48.

Ceccarelli, M., 1994b, "Optimal synthesis of three-revolute manipulators," *Meccanica*, Vol. 29, pp. 95–103.

Chen, C. -T., 1984, *Linear System Theory and Design*, Harcourt Brace Jovanovich Inc., The Dryden Press, Saunders College Publishing, USA.

Chirikjian, G. S. and Burdick, J. W, 1994, "A modal approach to hyper-redundant manipulator kinematics,", *Proc. IEEE Trans. Robotics and Automation*, Vol. 10, No., 3, pp. 343–354.

Chirikjian, G. S. and Burdick, J. W, 1993, "Design and experiments with a 30 DOF robot," *Proc. IEEE Int. Conf. Robotics Automat.*, Vol. 1, pp. 113–119, Atlanta.

Denavit J. and Hartenberg, R. S., 1955, "A kinematic notation for lower-pair mechanisms based on matrices," *ASME Journal of Applied Mechanics*, pp. 215–221.

Dotty, K. L., Melchiorri, C., and Bonivento, C., 1992, "A critical review of the current kinematic- and dynamic-manipulability theory," *Proc. 3rd International Workshop on Advances in Robot Kinematics*, pp. 269–273, Ferrara, Italy.

Farrell, J. D., Thompson, J. M., Karlen, J. P., Vold, H. I., Eismann, P. H., 1990, "Modular, configurable, kinematically redundant manipulators," *Proc. Japan-USA Symp. Flexible Automat.*, Kyoto, July 1990, pp. 303–308.

Finkbeiner, D., 1966, *Introduction to Matrices and Linear Transformations*, W. H. Freeman and Company, San Francisco.

Goldenberg, A., 1996, "Hybrid control,", Tutorial on *Proc. IEEE Int. Conf. Robotics Automat.*, April 22–28, Minneapolis.

Golub, G. H. and Van Loan, C. F., 1989, *Matrix Computations*, The John Hopkins University Press, Baltimore.

González–Palacios, M. A., Angeles, J., and Ranjbaran, F., 1993, "The kinematic synthesis of serial manipulators with a prescribed Jacobian," *Proc. IEEE Int. Conf. Robotics Automat.*, Atlanta, Vol. 1, pp. 450–455.

Gosselin, C. and Angeles, J., 1991, "A global performance index for the kinematic optimization of robotic manipulators," *ASME J. Mechanical Design*, Vol. 113, No. 3, pp. 220–226.

Gupta, K. C. and Roth, B., 1982, "Design considerations for manipulator workspace," *ASME Journal of Mechanical Design*, Vol. 704, Oct., pp. 704–711.

Hardy, G. H., Littlewood, J. E., and Polya G., 1934, *Inequalities*, Cambridge University Press, London.

Hayati, S., 1985, "Improving the absolute positioning accuracy of robot manipulators," *Journal of Robotic Systems*, Vol. 2, pp. 397–413.

Hollerbach, J. M., 1985, "Optimum kinematic design for a seven degree of freedom manipulator," in Hanafusa H. and Inoue, H. (editors), *in Robotics Research, the 2nd Int. Symp.*, MIT Press, pp. 215–222.

Householder, A. S., 1964, *The Theory of Matrices in Numerical Analysis*, Dover Publications, Inc., New York.

Hsu, M. S. and Kohli, D., 1987a, "The Jacobian analysis of mechanical manipulators," *Mechanism and Machine Theory*, Vol. 22. No. 3, pp. 265–275.

Hsu, M. S. and Kohli, D., 1987b, "Boundary surfaces and accessibility regions for regional structures of manipulators," *Mechanism and Machine Theory*, Vol. 22. No. 3, pp. 277–289.

Hunt, K. H., 1978, *Kinematic Geometry of Mechanisms*, Clarendon Press, Oxford.

International Federation For the Theory of Machines and Mechanisms (IFToMM), Commision A, Standards for Terminology, 1991, *Terminology for the Theory of Machines and Mechanisms*, Vol. 26, No. 5.

Jacobsen, S. C., Smith, F. M., and Backman, D. K., 1990, "High performance, high dexterity, force reflective teleoperator," *Proceedings, 38th Conference on Remote Systems Technology*, Vol. 2, pp. 180–185.

Kahan, W., 1966, "Numerical linear algebra," *Canadian Math. Bull.*, vol. 9, pp. 757–803.

Kailath, T., 1980, *Linear Systems*, Prentice–Hall, Inc., Englewood Cliffs.

Kim, J.-O. and Khosla, P. K., 1992a, "Framework for task based design of manipulators," *4th Int. Symp. on Robotics and Manufacturing, (ISRAM'92)*, Vol. 4, pp 27–32.

Kim, J.-O. and Khosla, P. K., 1992b,"A multi-population genetic algorithm and its application to design of manipulators," *IEEE/RSJ Int. Workshop on Intelligent Robots and Systems (IROS'92)*, 1992.

Kim, J.-O. and Khosla, P. K., 1992c, "Task based synthesis of optimal manipulator configurations," *1992 Japan-USA Symposium on Flexible Automation - A Pacific Rim Conference- ISCIE, San Francisco.*

Kim, J.-O. and Khosla, P. K., 1991, "Dexterity measures for design and control of manipulators," *IEEE/RSJ Int. Workshop on Intelligent Robots and Systems* (IROS'91), pp. 758–763.

Klein, C. A. and Miklos, T. A., 1991, "Spatial robotic isotropy," *Int. J. Robotics Res.*, Vol, 10, no. 4, pp. 426–437.

Klein, C. and Blaho, B., 1987, "Dexterity measures for the design and control of kinematically redundant manipulators," *Int. J. of Robotics Res.*, Vol. 6, No. 2, pp 72–83.

Kohli, D. and Spanos J., 1985a, "Workspace analysis of mechanical manipulators using polynomial discriminants," *ASME Journal of Mechanisms, Transmissions and Automation in Design*, Vol. 107, pp. 209–215.

Kohli, D. and Spanos J., 1985b, "Workspace analysis of regional structures of manipulators," *ASME Journal of Mechanisms, Transmissions and Automation in Design*, Vol. 107, pp. 216–225.

Kumar, A. and Waldron, K. J., 1981, "The workspaces of a mechanical manipulator," *ASME Journal of Mechanical Design*, Vol. 103, July pp. 665–672.

Lee, T. W. and Yang, D. C. H., 1983, "On the evaluation of manipulator workspace," *ASME Journal of Mechanisms, Transmissions and Automation in Design*, Vol. 105, March, pp. 70–77.

Leigh, D. C., 1968, *Nonlinear Continuum Mechanics*, McGraw-Hill Book Co., New York.

Li, Z., 1990, "Geometrical considerations of robot kinematics," *Int. J. of Robotics and Automation*, Vol. 5, No. 3, pp. 139–145.

Lin, C.-C. and Tsai, L.-W., 1991, "The workspace of three-dof, four-jointed spherical wrist mechanisms," *Proc. IEEE Int. Conf. Robotics Automat.*, Vol. 2, pp. 1548–1553.

Maton, R. and Roth, B., 1996, "The effects of actuation scheme on the kinematic performance of manipulators," *Proceedings of The 1996 ASME Design Engineering Technical Conferences and Computer in Engineering Conference*, 96-DET/MECH-1147.

Mavroidis, C. and Roth, B., 1992, "Structural parameters which reduce the number of manipulator configurations," *ASME Biennial Mechanisms Conference*, September 13–16, Vol. 45, pp. 359–366.

Mirsky, L., 1956, "The norms of adjugate and inverse matrices," *Arch. Math.*, Vol. 7, pp. 276–277

Mitrinovic, D. S., 1970, *Analytic Inequalities*, Springer-Verlag, New York.

Neumark, S., 1965, *Solution of Cubic & Quartic Equations*, Pergamon Press, London.

Oblak, D. and Kohli, D., 1988, "Boundary surfaces, limit surfaces, crossable and noncrossable surfaces in workspace of mechanical manipulators," *ASME Journal of Mechanisms, Transmissions and Automation in Design*, Vol. 110, pp. 389–396.

O'Malley, C. D. and Saunders, C. M., 1983, *Leonardo on the Human Body*, Dover Publications, Inc., New York

Ou, Y.-J. and Tsai, L.-W, 1994, "Design of a three-dof tendon-driven manipulator with the characteristic of equal maximum tensions," in Lenarčič J. and Ravani B. (editors), *Advanes in Robot Kinematics and Computational Geometry*, Kluwer, Dordrecht, pp. 369–378.

Ou, Y.-J. and Tsai, L.-W, 1993, "Kinematic synthesis of tendon-driven manipulators with isotropic transmission characteristics," *ASME J. Mechanical Design*, Vol. 115, No. 4, pp. 884–891.

Paden, B. and Sastry, S., 1988, "Optimal kinematic design of 6R manipulators," *Int. J. of Robotics Res.*, Vol. 7, No. 2, pp. 43–61.

Pai, D. K. and Leu, M., 1992, "Genericity and singularities of robot manipulators," *IEEE Trans. Robotics and Automation*, Vol. 8, No., 5, pp. 545–559.

Pai, D. K. and Leu, M., 1989, "Generic singularities of robot manipulators," *Proc. IEEE Int. Conf. Robotics Automat.*, Vol. 1, pp. 738–744.

Park, F. and Brockett, R. W., 1994, "Kinetic dexterity of robotic mechanisms," *Int. J. of Robotics Res.*, Vol. 13, No. 1, pp. 1–15.

Park, F., 1991, *The Optimal Kinematic Design of Mechanisms*. Ph.D. Thesis, Division of Applied Sciences, Harvard University, Cambridge (MA).

Pieper, D. L., 1968, *The Kinematics of Manipulators Under Computer Control*, Ph.D. Thesis, Stanford University, Stanford, (CA).

Ranjbaran, F., Angeles, J. and Kecskeméthy, A., 1996, "On the kinematic conditioning of robotic manipulators," *Proc. IEEE Int. Conf. Robotics Automat.*, Minneapolis, Vol. 4, pp. 3167–3172.

Ranjbaran, F., Angeles, J., González-Palacios, M. A., and Patel, R. V., 1995, "The mechanical design of a seven-axes manipulator with kinematic isotropy," *Journal of Robotics and Intelligent Systems*, Vol. 13, pp. 1–21.

Ranjbaran, F., Angeles, J., 1994, "On positioning singularities of 3-revolute robotic manipulators", *Proc. 12th Symposium on Engineering Applications of Mechanics*, Montreal, June 1994, pp. 273–282.

Ranjbaran, F., Angeles, J., and Patel, R. V., 1992, "The determination of the Cartesian workspace of general three-axes manipulators", *Proc. 3rd International Workshop on Advances in Robot Kinematics*, sept. 7–9, pp. 318–325, Ferrara, Italy

Rice, J., 1966, "A theory of condition," *SIAM J. Num., Anal.* Vol. 2, No. 3, 287–310.

Roth, B., 1975, "Performance evaluation of manipulators from a kinematic viewpoint," NBS Special Publication: Performance Evaluation of Programmable Robots and Manipulators, pp. 39–61

Salisbury, J. K. and Craig, J. J., 1982, "Articulated hands: Force control and kinematic issues," *Int. J. of Robotics Res.*, Vol. 1, No. 1, pp. 4–17.

Salmon, G., 1964, *Higher Algebra*, 5th Edition (1885), reprinted:1964, Chelsea Publishing Co., New York.

Sarcos Research Corporation, 1993, *Dextrous Teleoperation System Manual*, Utah.

Seraji, H., Long, M., and Lee, T. S., 1993, "Motion control of 7-dof arms: The configuration control approach,", *IEEE Trans. Robotics and Automation*, Vol. 9, No., 2, pp. 125–139.

Seyfferth, W., Maghzal, A. J., and Angeles, J. 1995, "Nonlinear Modeling ans parameter identification of Harmonic Drive robotic transmissions," *Proc. IEEE Int. Conf. Robotics Automat.*, Vol. 3, pp. 3027–3032.

Shadpey, F., Ranjbaran, F., Patel, R. V. and Angeles, J. 1996, "A compact cylinder-cylinder collision avoidance scheme for redundant manipulators," *Proc. Sixth International Symposium of Robotics and Manufacturing (ISRAM '96)*, Vol. 6, pp. 769–774, Montpellier, France.

Shigley, J. E. and Uicker, J. J. ., 1995, *Theory of Machines and Mechanisms*, 2nd Edition, McGraw-Hill Inc.

Singh, J. R. and Rastegar, J., 1995, "Optimal synthesis of robot manipulators based on global kinematic parameters," *Mechanism and Machine Theory*, Vol. 30, No. 4, pp. 569–580.

Smith, D. R. and Lipkin, H., 1993, "Higher order singularities of regional manipulators," *Proc. IEEE Int. Conf. Robotics Automat.*, Vol. 1, pp. 194–199.

Smith, D. R., 1990, *Design of Solvable 6R Manipulators*, Ph.D. Thesis, Georgia Institue of Technology, Atlanta.

Smith, F. M., Backman, D. K., and Jacobsen, S. C., 1992, "Telerobotic manipulator for hazardous environment," *Journal of Robotic Systems*, Vol. 9, No. 2, pp. 251–260.

Spanos, J. and Kohli, D., 1985, "Workspace analysis of regional structures of manipulators," *ASME Journal of Mechanisms, Transmissions and Automation in Design*, Vol. 107, pp. 216–222.

Strang, G., 1988, *Linear algebra and its applications*, Harcourt Brace Jovanovich, Publishers, San Diego.

Takano, M., 1985, "A new efficient solution for inverse kinematics problem (synthesis) of a robot with any type of configuration", *Journal of the Faculty of Engineering, The University of Tokyo (B), Vol. XXXVIII, No. 2, pp. 107-134.*

Tandirci, M., Angeles, J., and Ranjbaran, F., 1992, "The characteristic point and the characteristic length of robotic manipulators", *ASME Biennial Mechanisms Conference*, September 13–16, Scottsdale, Arizona, Vol. 45, pp. 203–208.

Tarantola, A., 1987, *Inverse Problem Theory*, Elsevier, New York, USA.

Tsai, K. Y., Arnold, J., and Kohli, D., 1993, "Generic maps of mechanical manipulators," *Mechanism and Machine Theory*, Vol. 28. No. 1, pp. 53–64.

Tsai, Y. C. and Soni, A. H., 1983, "An algorithm for the workspace of a general N-R robot," *ASME Journal of Mechanisms, Transmissions and Automation in Design*, Vol. 105, pp. 52-57.

Tsai, Y. C. and Soni, A. H., 1981, "Accessible region and synthesis of robot arms," *ASME Journal of Mechanisms, Transmissions and Automation in Design*, Vol. 103, pp. 803–811.

Vinogradov, I. B., Kobrinski, A. E., Stepanenko Y. E., and Tives, L. T., 1971, "Details of kinematics of manipulators with the method of volumes," (in Russian), *Mekhanika Mashin.*, No. 27–28, pp. 5–16.

Watkins, D. S., 1991, *Fundamentals of Matrix Computations*, John Wiley & Sons.

Toronto, ONtario.

Wenger, P., 1996, "Singularity analysis and categorization of generic 3-R regional manipulators," in Lenarčič J. and Parenti-Castelli V. (editors), *Recent Advanes in Robot Kinematics*, Kluwer, Dordrecht, pp. 109–118.

Wenger, P., 1992, "A new general formalism for the Kknematic analysis of all nonredundant manipulators," *Proc. IEEE Int. Conf. Robotics Automat.*, Vol. 1, pp. 442–447, Nice, France.

Whitney, D. E., 1972, "The mathematics of coordinated control of prosthetic arms and manipulators," *ASME J. of Dyn. Syst., Meas. and Control*, Vol. 94, pp. 303–309.

Williams, O., Angeles, J., and Bulca, B. 1993, "Design philosophy of an isotropic six-axis serial manipulator," *Robotics and Computer-Aided Manufacturing*, Vol. 10, No. 4, pp. 275–286.

Yang, D. C. and Lai, Z. C., 1985, "On the conditioning of robotic manipulators-service angle," *ASME J. of Mech., Trans. and Automation in Design*, Vol. 107, pp. 262–270.

Yoshikawa, T., 1985, "Manipulability of robotic mechanisms," *Int. J. of Robotics Res.*, Vol. 4, No. 2, pp. 3–9.

Yoshikawa, T., 1983, "'Analysis and control of robot manipulators with redundancy", *Preprints 1st Int. Symp. Robotics Res*, Aug. 28–Sept. 2, Bretton Woods, N. H.

Appendix A

Jacobian Determinant of the 3-axis Manipulators

The architecture-dependent coeeficients of the trigonometric functions appearing in eq. (2.16), are given below:

$$
\begin{aligned}
m_1 &= 0.5a_3^2 b_2 \mu_1 \mu_2 \qquad\qquad (A.1)\\
m_2 &= -a_1 a_3 b_3 \lambda_2 \mu_1 \mu_2\\
m_3 &= 0.5a_3 \mu_1 \mu_2 [a_2(b_2 + b_3) - a_1 b_3 \lambda_1 \mu_2^2]\\
m_4 &= 0.5a_3 \mu_1 \mu_2 [a_2(b_2 - b_3) - a_1 b_3 \lambda_1 \mu_2^2]\\
m_5 &= 0.25a_3^2 b_2 \mu_1 \mu_2 (1 + \lambda_2)\\
m_6 &= 0.25a_3^2 b_2 \mu_1 \mu_2 (1 - \lambda_2)\\
n_1 &= 0.5a_3^2 (a_2 \lambda_2 \mu_1 + a_1 \lambda_1 \mu_2)\\
n_2 &= -a_1 a_2 a_3 \mu_1\\
n_3 &= -0.5a_1 a_3^2 \mu_1 \mu_2^2\\
n_4 &= 0.5a_3 (a_1 a_2 \lambda_1 \mu_2 + b_2 b_3 \mu_1 \mu_2^2 - a_2^2 \mu_1)\\
n_5 &= 0.5a_3 (a_1 a_2 \lambda_1 \mu_2 + b_2 b_3 \mu_1 \mu_2^2 + a_2^2 \mu_1)\\
n_6 &= 0.25a_3^2 [a_1 \lambda_1 \mu_2 (1 + \lambda_2) - a_2 \mu_1 (1 + \lambda_2)]
\end{aligned}
$$

$$n_7 = 0.25a_3^2[a_1\lambda_1\mu_2(1-\lambda_2) + a_2\mu_1(1-\lambda_2)]$$

with

$$\lambda_i \equiv \cos\alpha_i, \quad \mu_i \equiv \sin\alpha_i \tag{A.2}$$

Moreover, detailed expressions for $f_1(\theta_2, \theta_3) \equiv \xi^2$ and $f_2(\theta_2, \theta_3) \equiv z$ appearing in eq. 2.20 are gven next,

$$\begin{aligned} \xi^2 &= (a_1 + a_2c_2 + a_3c_2c_3 + b_3\mu_2s_2 - a_3\lambda_2s_2s_3)^2 \\ &+ (b_2\mu_1 + b_3\lambda_2\mu_1 + b_3c_2\lambda_1\mu_2 - a_2\lambda_1s_2 - a_3\lambda_1c_3s_2 - a_3\lambda_1\lambda_2c_2s_3 + a_3\mu_1\mu_2s_3)^2 \end{aligned} \tag{A.3}$$

and

$$z = b_1 + b_2\lambda_1 + b_3(\lambda_1\lambda_2 - c_2\mu_1\mu_2) + a_2\mu_1s_2 + a_3\mu_1c_3s_2 + a_3(c_2\lambda_2\mu_1 + \lambda_1\mu_2)s_3 \tag{A.4}$$

with

$$c_i \equiv \cos\theta_i, \quad s_i \equiv \sin\theta_i \tag{A.5}$$

Appendix B

On The Smoothness of the 2-Norm Condition Number

We show here that the 2-norm condition number is not a smooth function at the isotropic point. This characteristic is general and not limited to 2×2 matrices. By means of the symbolic expressions obtained in Chapter 4, the proof can be provided using the Jacobian matrix of a planar 2-R manipulator. It will be shown that κ_2 is not a smooth function of θ_2 at the isotropic configuration θ_2^*, by making apparent that its derivative $d\kappa_2 / d\theta_2$ is undefined at θ_2^*. To this end, we differentiate eq. (4.44), while making use of chain rule, i.e.,

$$\left.\frac{d\,\kappa_2}{d\,\theta_2}\right|_{\theta_2^*} = \left.\left(\frac{\partial\,\kappa_2}{\partial\tau}\,\tau' + \frac{\partial\,\kappa_2}{\partial\delta}\,\delta'\right)\right|_{\theta_2^*} \tag{B.1}$$

But, from eqs. (4.40), and (4.41), we have,

$$\tau' = 2\,\delta' = \pm 1 \tag{B.2}$$

Moreover, the terms involving partial derivatives in eq. (B.1) are obtained by differentiating eq. (4.44), while making use of eq. (4.36), as,

$$\frac{\partial\kappa_2}{\partial\tau} = \frac{\kappa_2}{\sqrt{\kappa_F^2 - 1}} \tag{B.3}$$

and

$$\frac{\partial \kappa_2}{\partial \delta} = \frac{-1}{2\,\delta}\,(\frac{1}{\sqrt{\kappa_F^2 - 1}} + \kappa_2) \tag{B.4}$$

Substituting the foregoing equations in eq. (B.1), yields

$$\frac{d\,\kappa_2}{d\,\theta_2} = \frac{\tau'\,\delta\,\kappa_2 - \sqrt{\delta}\,\delta' - \sqrt{\delta\,(\kappa_F^2 - 1)}\,\kappa_2\,\delta'}{2\,\delta\,\sqrt{\delta\,(\kappa_F^2 - 1)}} \tag{B.5}$$

It can be readily verified that the foregoing expression evaluated at θ_2^*, is of an indeterminate form, i.e, with $\theta_2 = \pm 3\pi/4$, we have $\tau = 1$, $\tau' = \pm 1$, $\delta = 1/4$, $\delta' = \pm 1/2$, and $\kappa_2 = \kappa_F = 1$, and thus, $d\,\kappa_2/d\,\theta_2|_{\theta_2^*}$ takes on the form 0/0.

In order to shed more light on the behaviour of κ_2, we will obtain the *left* and the *right* derivatives of κ_2 at θ_2^*, denoted respectively by

$$\left.\frac{d\,\kappa_2}{d\,\theta_2}\right|_{(\theta_2^*)^+} \quad \text{and} \quad \left.\frac{d\,\kappa_2}{d\,\theta_2}\right|_{(\theta_2^*)^-},$$

We will next show that the indeterminacy of the derivative of κ_2 is inherited from that of the derivatives of the eigenvalues at the isotropic point. The derivative of κ_2 can be obtained directly using λ_{max} and λ_{min}, i.e., by differentiating eq. 4.16, i.e.,

$$\frac{d\,\kappa_2}{d\,\theta_2} = \frac{1}{2\,\kappa_2\,\lambda_{min}}\,(\lambda'_{max} - \kappa_2^2\,\lambda'_{min}) \tag{B.6}$$

or, once evaluated at θ_2^*, as

$$\left.\frac{d\,\kappa_2}{d\,\theta_2}\right|_{\theta_2^*} = \frac{1}{4}\,(\lambda'_{max} - \lambda'_{min})|_{\theta_2^*} \tag{B.7}$$

Furthermore, λ'_{max} and λ'_{min} are determined from eq. (4.43) as,

$$\lambda'_{max} = \frac{\tau'\,\sqrt{\tau^2 - 4\,\delta} + \tau\,\tau' - 2\,\delta'}{2\,\sqrt{\tau^2 - 4\,\delta}} \quad \text{and} \quad \lambda'_{min} = \frac{\tau'\,\sqrt{\tau^2 - 4\,\delta} - \tau\,\tau' + 2\,\delta'}{2\,\sqrt{\tau^2 - 4\,\delta}} \tag{B.8}$$

Both of the foregoing expressions evaluated at θ_2^* will be of the indeterminate form (0/0). Hence, we obtain the left and the right derivatives of λ_{max} and λ_{min} at θ_2^*, respectively, from,

$$\left.\frac{d\,\lambda_{max}}{d\,\theta_2}\right|_{(\theta_2^*)^+} = \lim_{h\to 0^+} \frac{\lambda_{max}(\theta_2^* + h) - \lambda_{max}(\theta_2^*)}{h} \tag{B.9}$$

$$\left.\frac{d\,\lambda_{max}}{d\,\theta_2}\right|_{(\theta_2^*)^-} = \lim_{h\to 0^-} \frac{\lambda_{max}(\theta_2^* + h) - \lambda_{max}(\theta_2^*)}{h} \tag{B.10}$$

and,

$$\left.\frac{d\,\lambda_{min}}{d\,\theta_2}\right|_{(\theta_2^*)^+} = \lim_{h\to 0^+} \frac{\lambda_{min}(\theta_2^* + h) - \lambda_{min}(\theta_2^*)}{h} \tag{B.11}$$

$$\left.\frac{d\,\lambda_{min}}{d\,\theta_2}\right|_{(\theta_2^*)^-} = \lim_{h\to 0^-} \frac{\lambda_{min}(\theta_2^* + h) - \lambda_{min}(\theta_2^*)}{h} \tag{B.12}$$

In the foregoing expressions we have assumed that the limits exist. The evaluation of these limits is rather tedious, and we will present only the detailed procedure for obtaining the left and the right derivatives of λ_{max}. One of the two isotropic configurations, namely, $\theta_2^* = 3\,\pi/4$, is considered, the second one following similarly. Using eqs. (4.30), (4.31), (4.40), (4.41), and the first of eq. (4.43) in conjunction with eqs. (B.9) and (B.10), and after some trigonometric simplifications we obtain

$$\left.\frac{d\,\lambda_{max}}{d\,\theta_2}\right|_{(\frac{3\pi}{4})^+} = \lim_{h\to 0^+} \frac{1 - (\cos h + \sin h)}{2\,h} + \lim_{h\to 0^+} \frac{\sqrt{1 + \sin h\,\cos h} - (\cos h + \sin h)}{h}$$

$$\left.\frac{d\,\lambda_{max}}{d\,\theta_2}\right|_{(\frac{3\pi}{4})^-} = \lim_{h\to 0^-} \frac{1 - (\cos h + \sin h)}{2\,h} - \lim_{h\to 0^-} \frac{\sqrt{1 + \sin h\,\cos h} - (\cos h + \sin h)}{h}$$

Multiplying both numerator and denominator of the right hand-side of each of the foregoing equations, respectively, by $1 + (\cos h + \sin h)$ and by the square root $\sqrt{1 + \sin h\,\cos h + \cos h + \sin h}$, it follows that,

$$\left.\frac{d\,\lambda_{max}}{d\,\theta_2}\right|_{(\frac{3\pi}{4})^+} = \lim_{h\to 0^+} \frac{-\sin h\,\cos h}{h\,(1 + \sin h + \cos h)} + \lim_{h\to 0^+} \frac{|\,\sin h\,\cos h\,|}{h\sqrt{1 + \sin h + \cos h + \sin h\,\cos h}}$$

$$\left.\frac{d\,\lambda_{max}}{d\,\theta_2}\right|_{(\frac{3\pi}{4})^-} = \lim_{h\to 0^-} \frac{-\sin h\,\cos h}{h\,(1 + \sin h + \cos h)} + \lim_{h\to 0^-} \frac{|\,\sin h\,\cos h\,|}{h\sqrt{1 + \sin h + \cos h + \sin h\,\cos h}}$$

or,

$$\left.\frac{d\,\lambda_{max}}{d\,\theta_2}\right|_{(\frac{3\pi}{4})^+} = \lim_{h\to 0^+}(\frac{\sin h}{h})\frac{-\cos h}{(1+\sin h+\cos h)} + \lim_{h\to 0^+}(\frac{\sin h}{h})\frac{\cos h}{\sqrt{1+\sin h+\cos h+\sin h\,\cos h}}$$

$$\left.\frac{d\,\lambda_{max}}{d\,\theta_2}\right|_{(\frac{3\pi}{4})^-} = \lim_{h\to 0^-}(\frac{\sin h}{h})\frac{-\cos h}{(1+\sin h+\cos h)} - \lim_{h\to 0^-}(\frac{\sin h}{h})\frac{\cos h}{\sqrt{1+\sin h+\cos h+\sin h\,\cos h}}$$

Moreover, recalling that

$$\lim_{h\to 0^+}\frac{\sin h}{h} = \lim_{h\to 0^-}\frac{\sin h}{h} = 1$$

we then have

$$\left.\frac{d\,\lambda_{max}}{d\,\theta_2}\right|_{(\frac{3\pi}{4})^+} = \frac{-1+\sqrt{2}}{2} \tag{B.13}$$

$$\left.\frac{d\,\lambda_{max}}{d\,\theta_2}\right|_{(\frac{3\pi}{4})^-} = \frac{-1-\sqrt{2}}{2} \tag{B.14}$$

This proves that κ_2 is not a smooth function of θ_2 at the isotropic configuration, as the left and the right derivatives of the function at that point are finite but not equal.

Appendix C

Derivation of the Identity Used for the Determination of $\mathbf{p}_{\mathcal{L}}$

The derivation of the identities used in Chapter 6 is included here, while determining the position vector of the layout centre $\mathbf{p}_{\mathcal{L}}$. It is required to prove the identity given below:

$$\mathrm{tr}(\mathbf{B}\,\mathbf{A}\,\mathbf{B}^T) = \mathbf{b}^T\,\mathbf{b}\,\mathrm{tr}(\mathbf{A}) - \frac{1}{2}\mathbf{b}^T\,(\mathbf{A} + \mathbf{A}^T)\,\mathbf{b} \tag{C.1}$$

where

$$\mathbf{b} \equiv \mathrm{vect}(\mathbf{B}) = -\mathrm{vect}(\mathbf{B}^T)$$

and the operator vect$(\cdot)$ represents the *axial vector* of its matrix argument, as defined in Leigh (1968).

Let,

$$\mathbf{B} \equiv \begin{bmatrix} 0 & -b_z & b_y \\ b_z & 0 & -b_x \\ -b_y & b_x & 0 \end{bmatrix} \quad \text{and} \quad \mathbf{A} = \begin{bmatrix} a_{11} & a_{12} & a_{13} \\ a_{21} & a_{22} & a_{23} \\ a_{31} & a_{32} & a_{33} \end{bmatrix}$$

then

$$\mathbf{b} = \begin{bmatrix} b_x \\ b_y \\ b_z \end{bmatrix} \tag{C.2}$$

Now, expanding the matrix product appearing in the left-hand side of eq. (C.1), and after some algebraic manipulations, we can obtain the relation given below:

$$\begin{aligned}\operatorname{tr}(\mathbf{B}\,\mathbf{A}\,\mathbf{B}^T) = {} & (b_x^2 + b_y^2 + b_z^2)\,(a_{11} + a_{22} + a_{33}) \\ & - b_x\,b_y\,(a_{12} + a_{21}) \\ & - b_x\,b_z\,(a_{13} + a_{31}) \\ & - b_y\,b_z\,(a_{23} + a_{32}) \\ & - (a_{11}\,b_x^2 + a_{22}\,b_y^2 + a_{33}\,b_z^2)\end{aligned} \tag{C.3}$$

It is apparent that the foregoing expression can be rewritten as

$$\operatorname{tr}(\mathbf{B}\,\mathbf{A}\,\mathbf{B}^T) = \mathbf{b}^T\,\mathbf{b}\,\operatorname{tr}(\mathbf{A}) - \frac{1}{2}\mathbf{b}^T\,(\mathbf{A} + \mathbf{A}^T)\,\mathbf{b}$$

thus proving eq. (C.1).

Appendix D

Mechanical Drawings of REDIESTRO 1

D.1 Link Subassembly Drawings

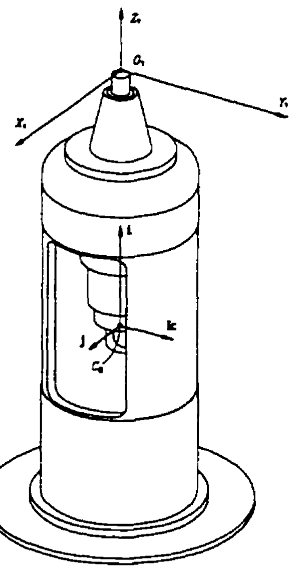

Figure D.1: Base subassembly drawing

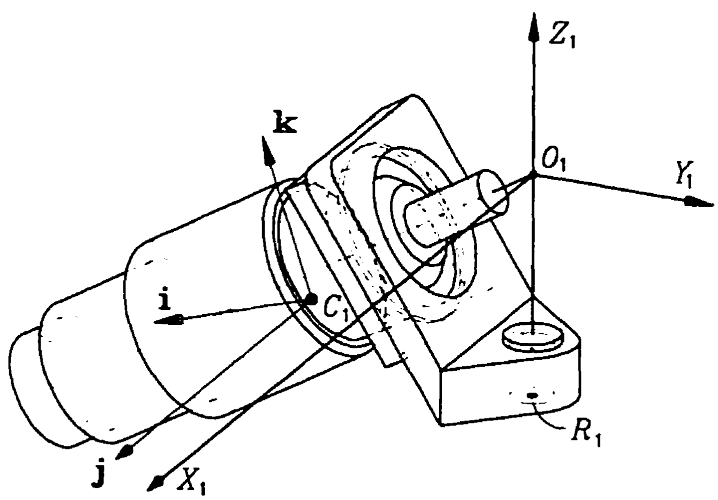

Figure D.2: Link 1 subassembly drawing

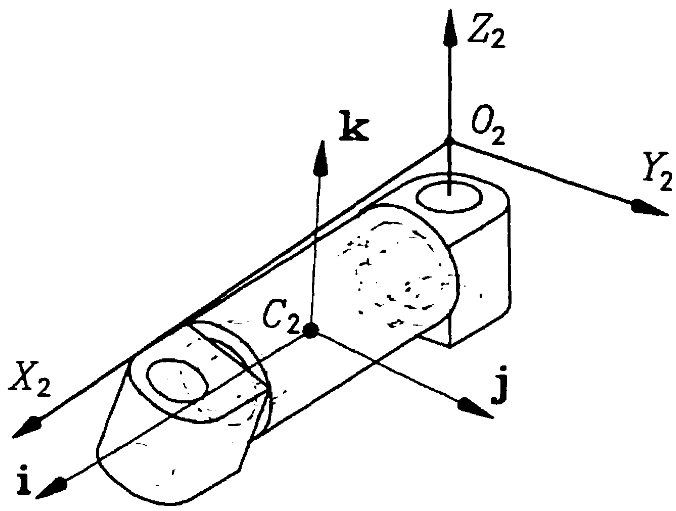

Figure D.3: Link 2 subassembly drawing

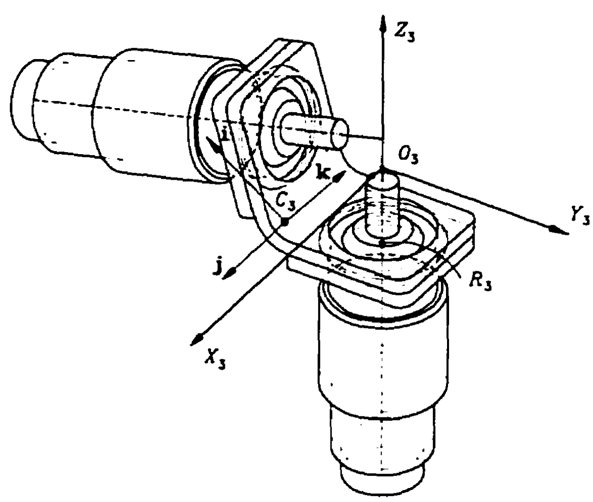

Figure D.4: Link 3 subassembly drawing

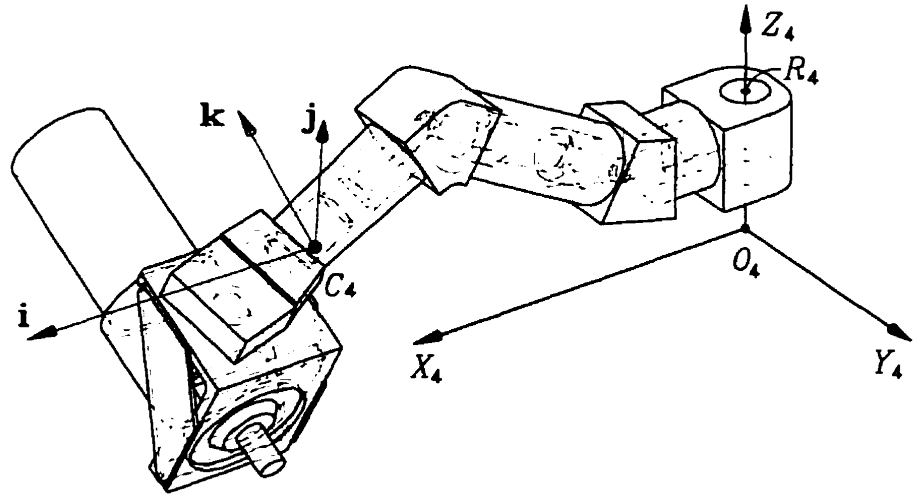

Figure D.5: Link 4 subassembly drawing

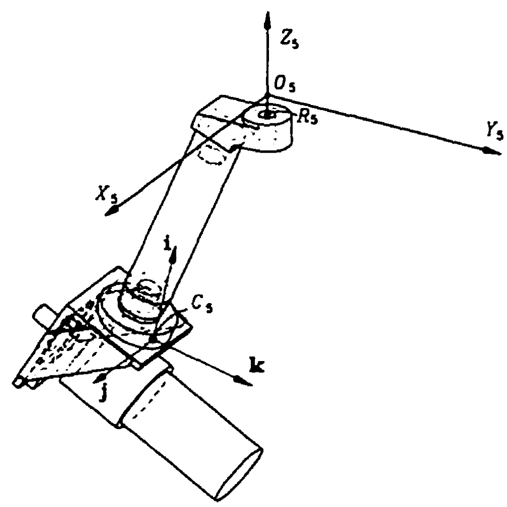

Figure D.6: Link 5 subassembly drawing

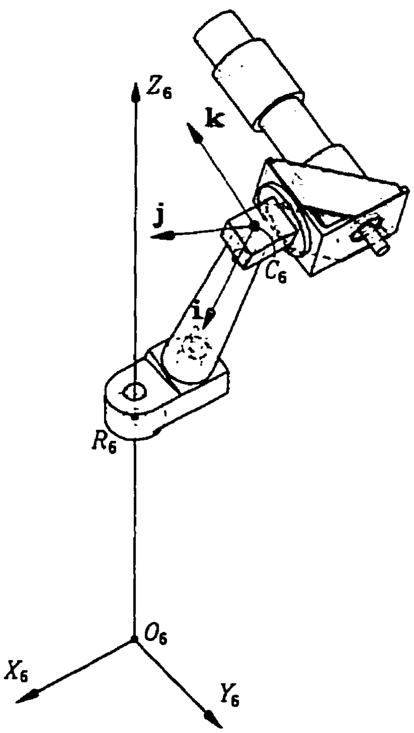

Figure D.7: Link 6 subassembly drawing

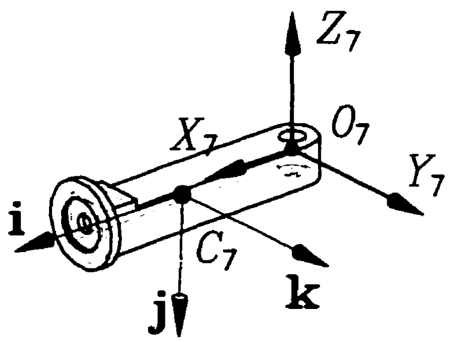

Figure D.8: Link 7 subassembly drawing

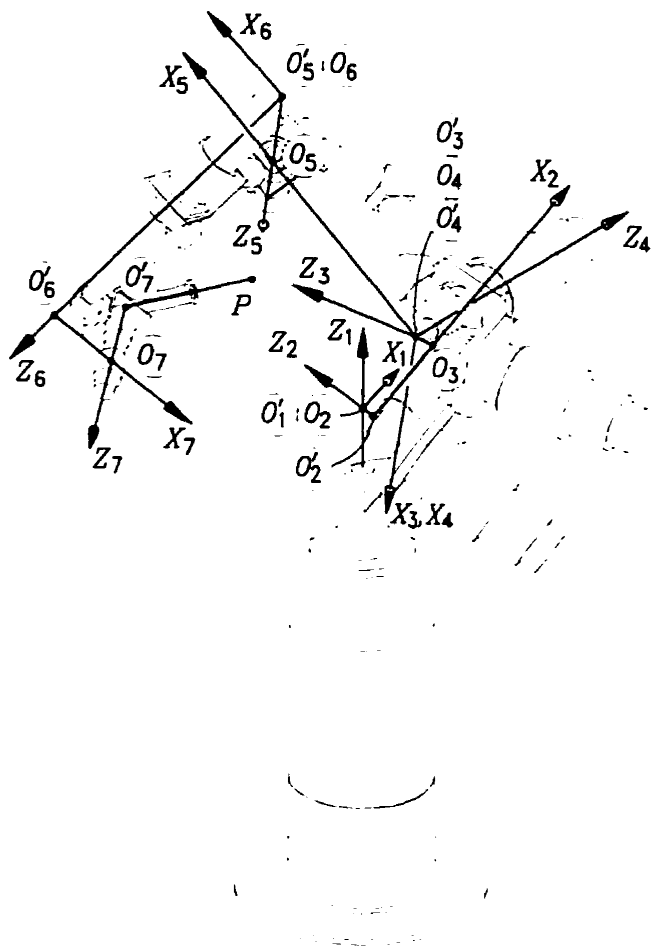

Figure D.9: Manipulator assembly drawing

D.2 Detailed Drawings

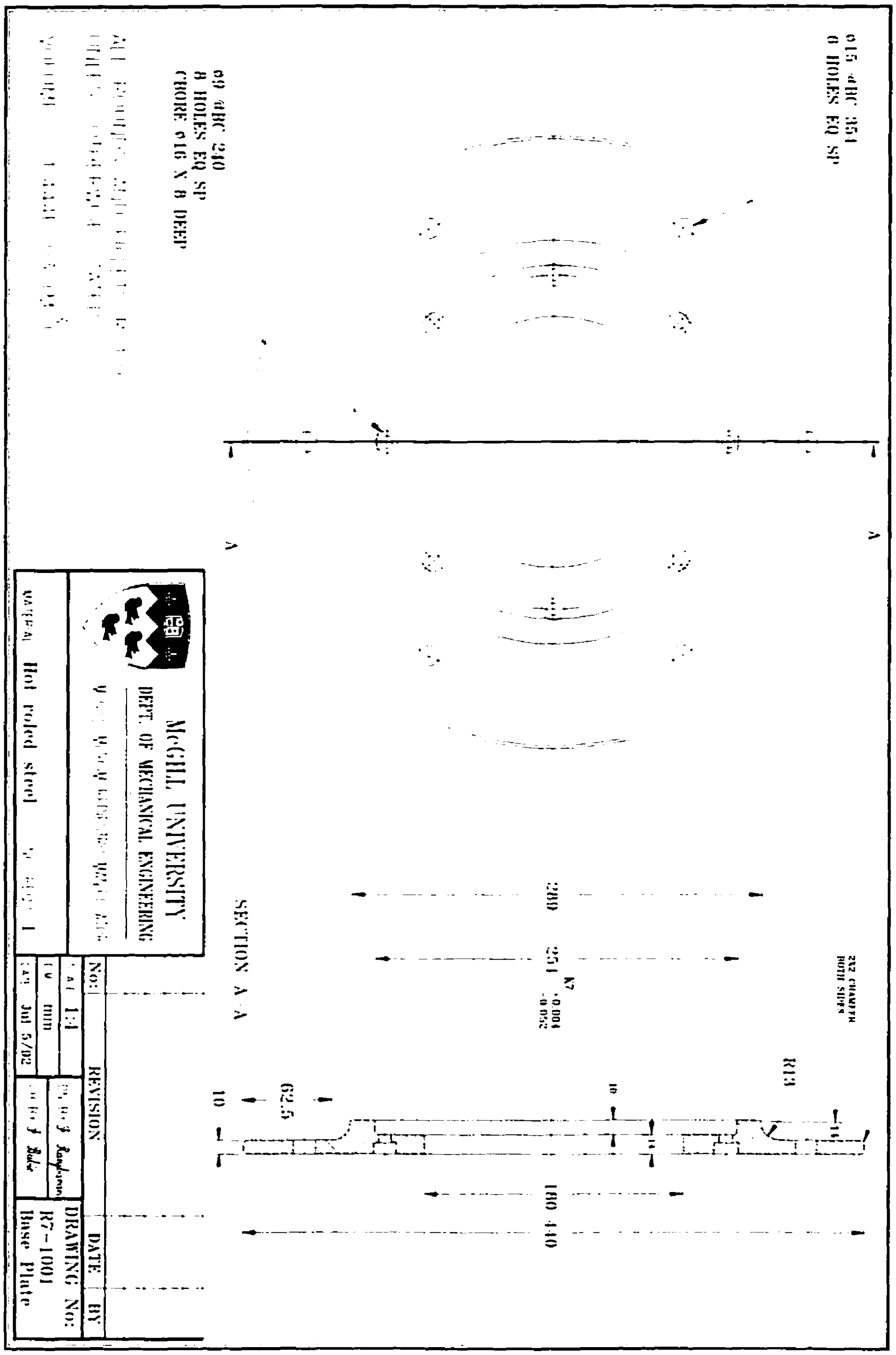

Figure D.10: Base-flange detailed drawing

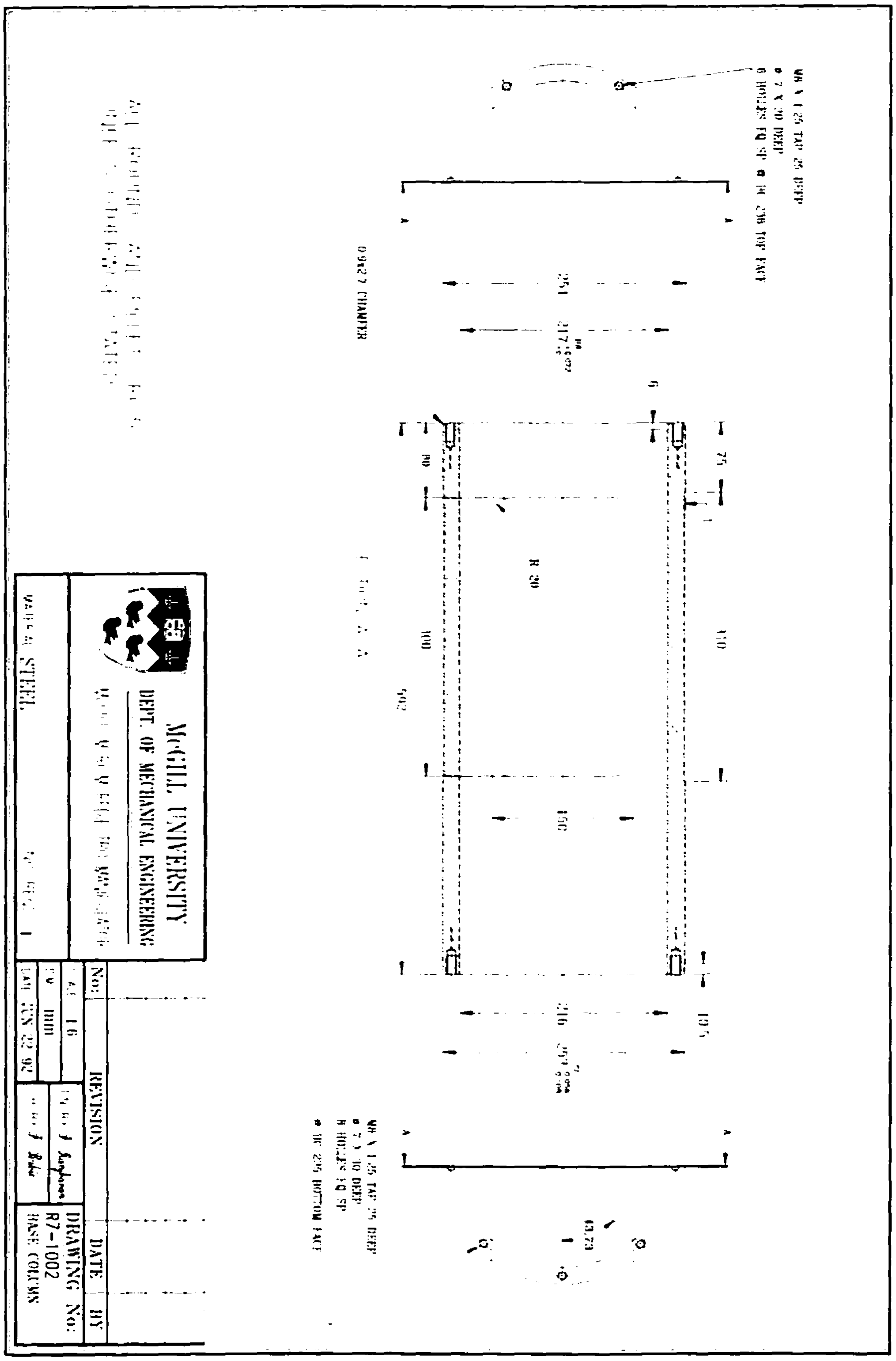

Figure D.11: Base-trunk detailed drawing

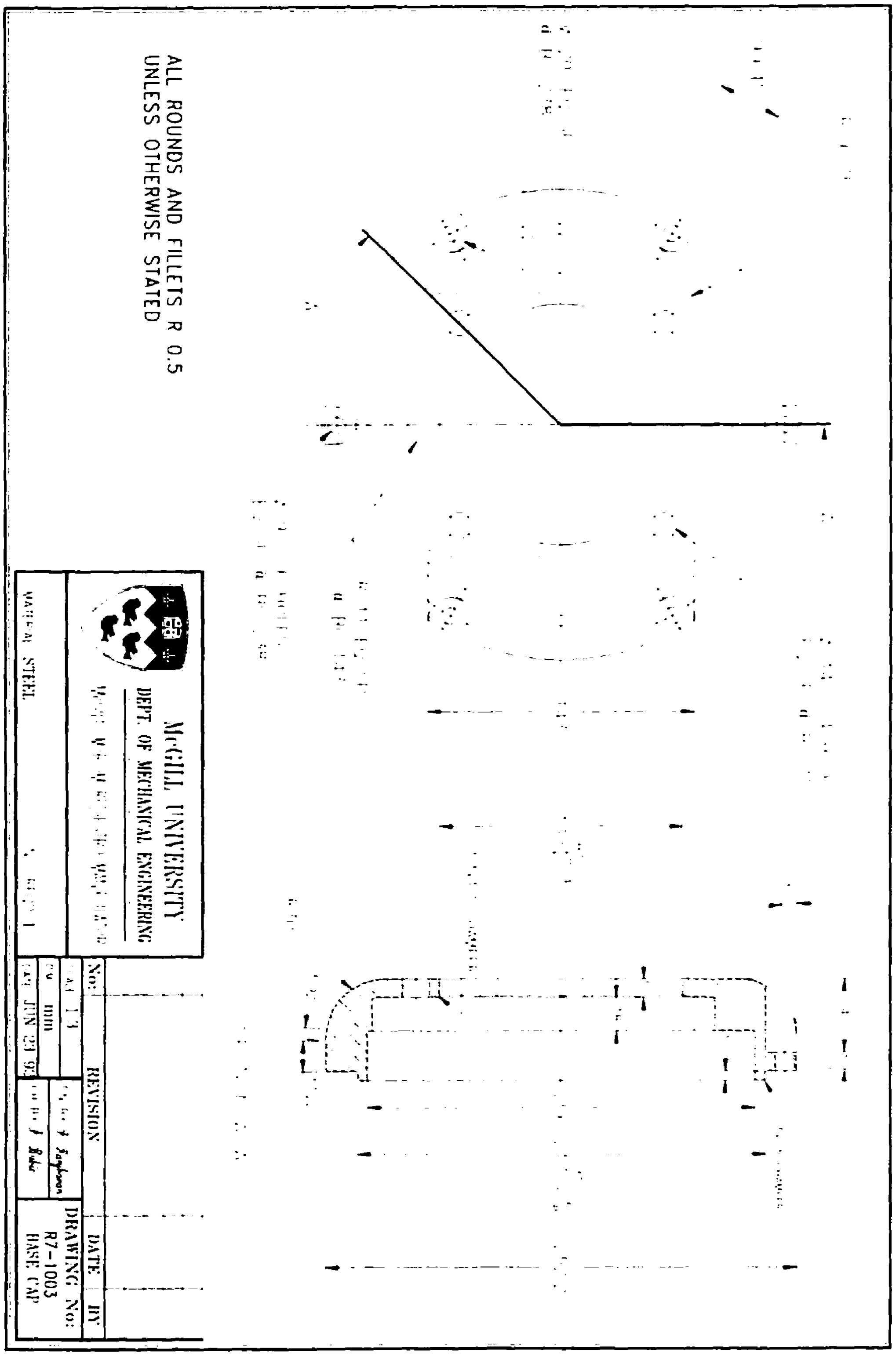

Figure D.12: Base-cap detailed drawing

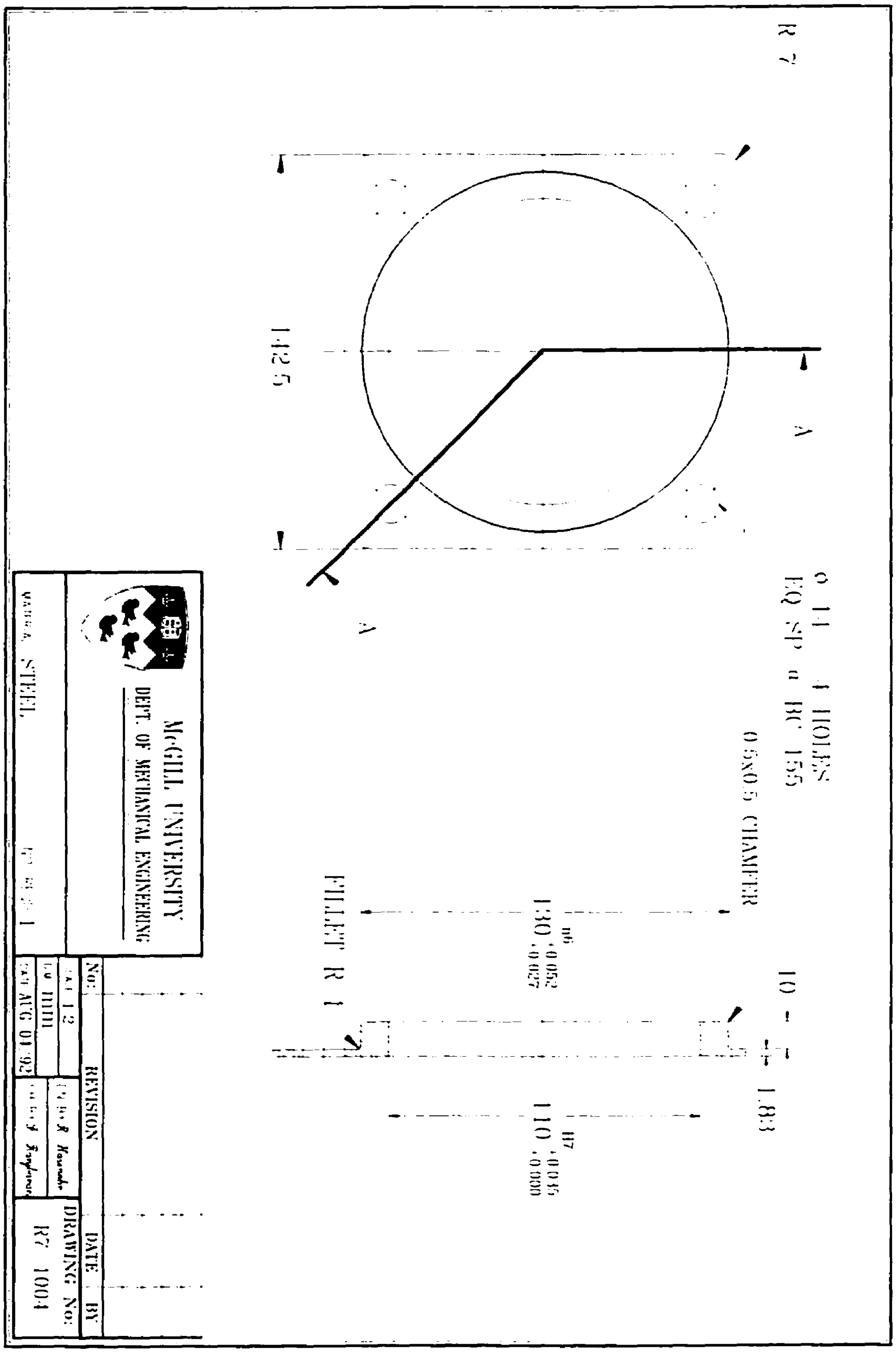

Figure D.13: Base-spacer detailed drawing

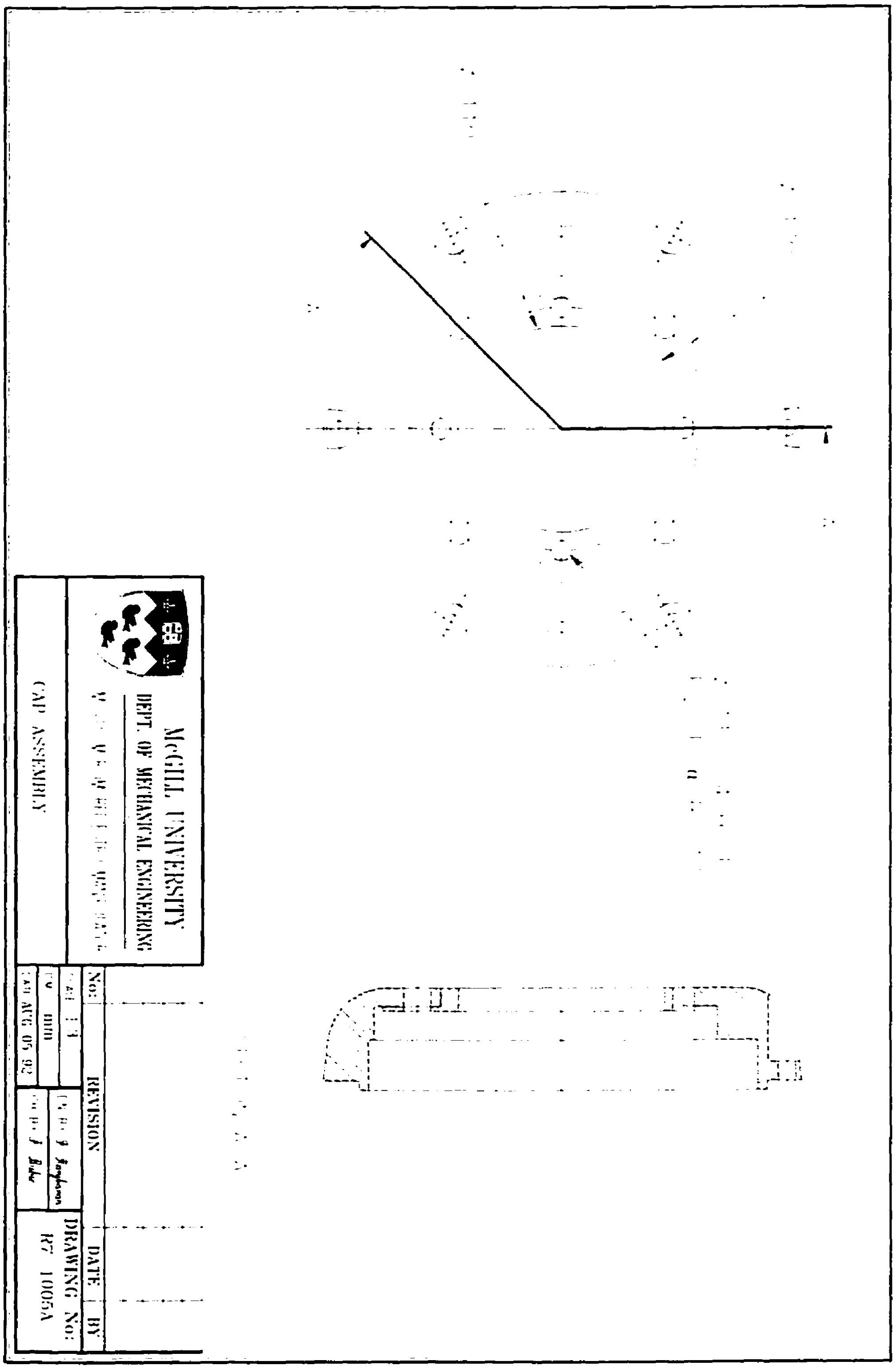

Figure D.14: Base-spacer-cap detailed drawing

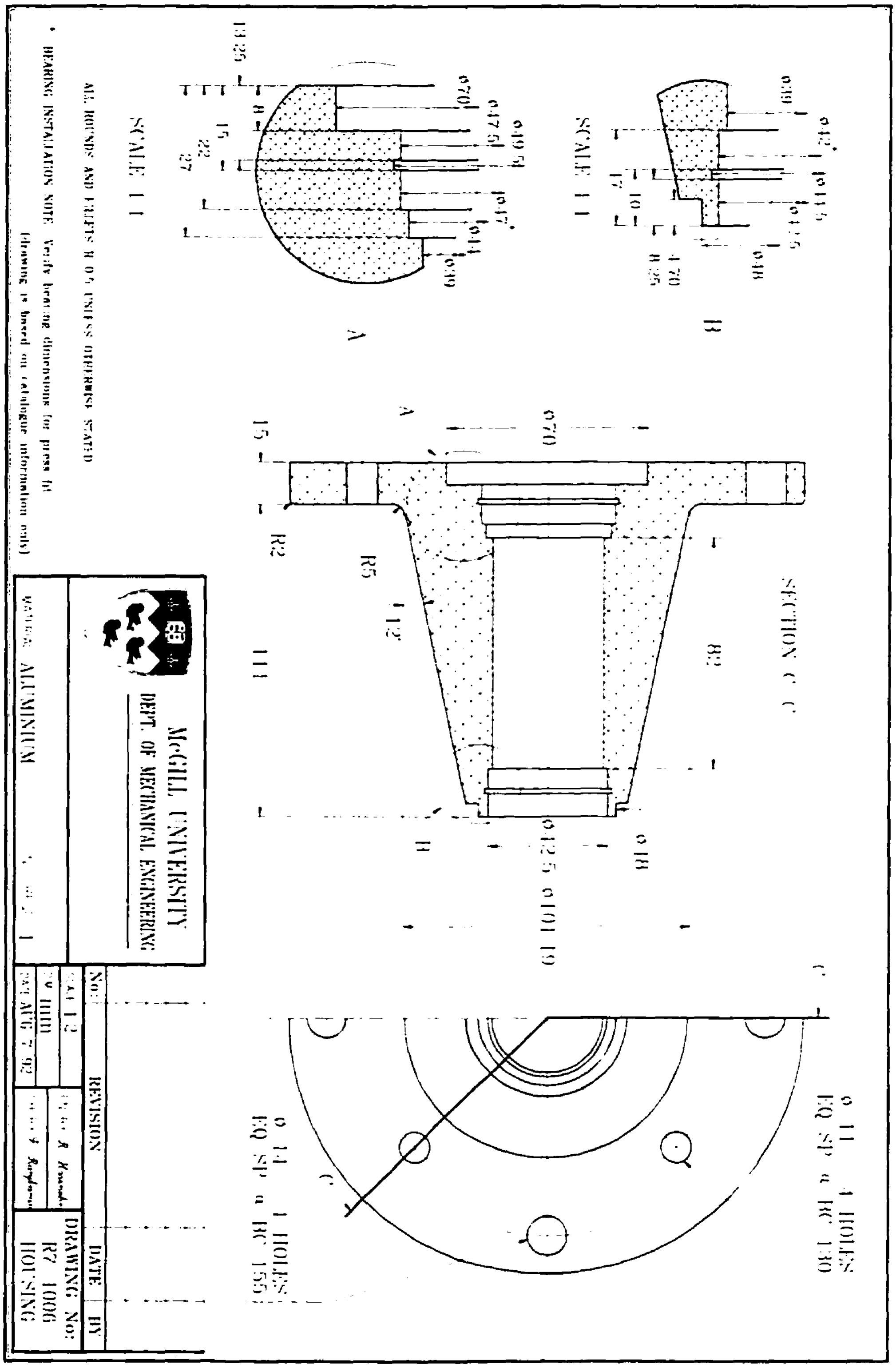

Figure D.15: Base-conical bearing housing detailed drawing

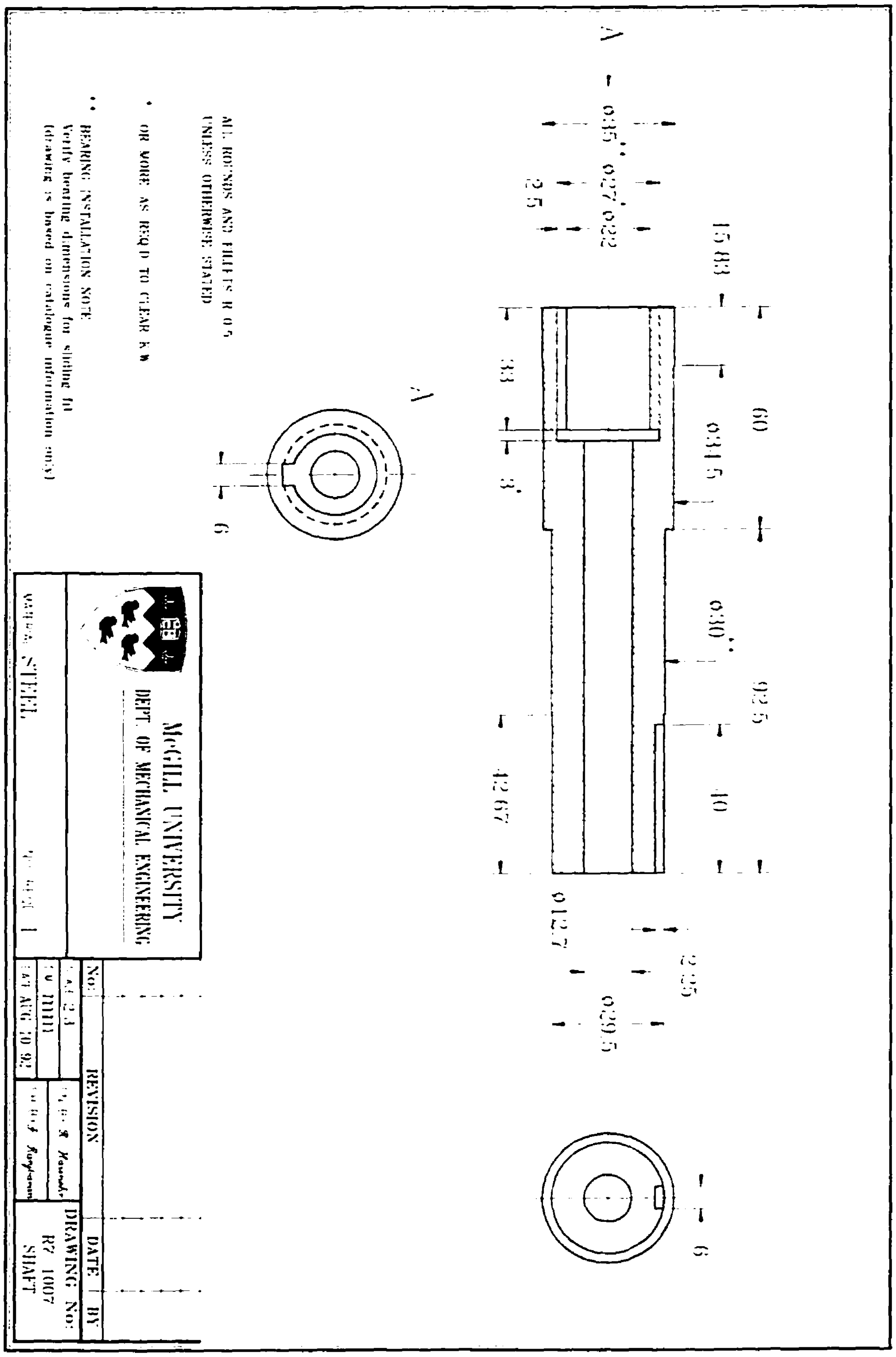

Figure D.16: Link 1: Main drive shaft detailed drawing

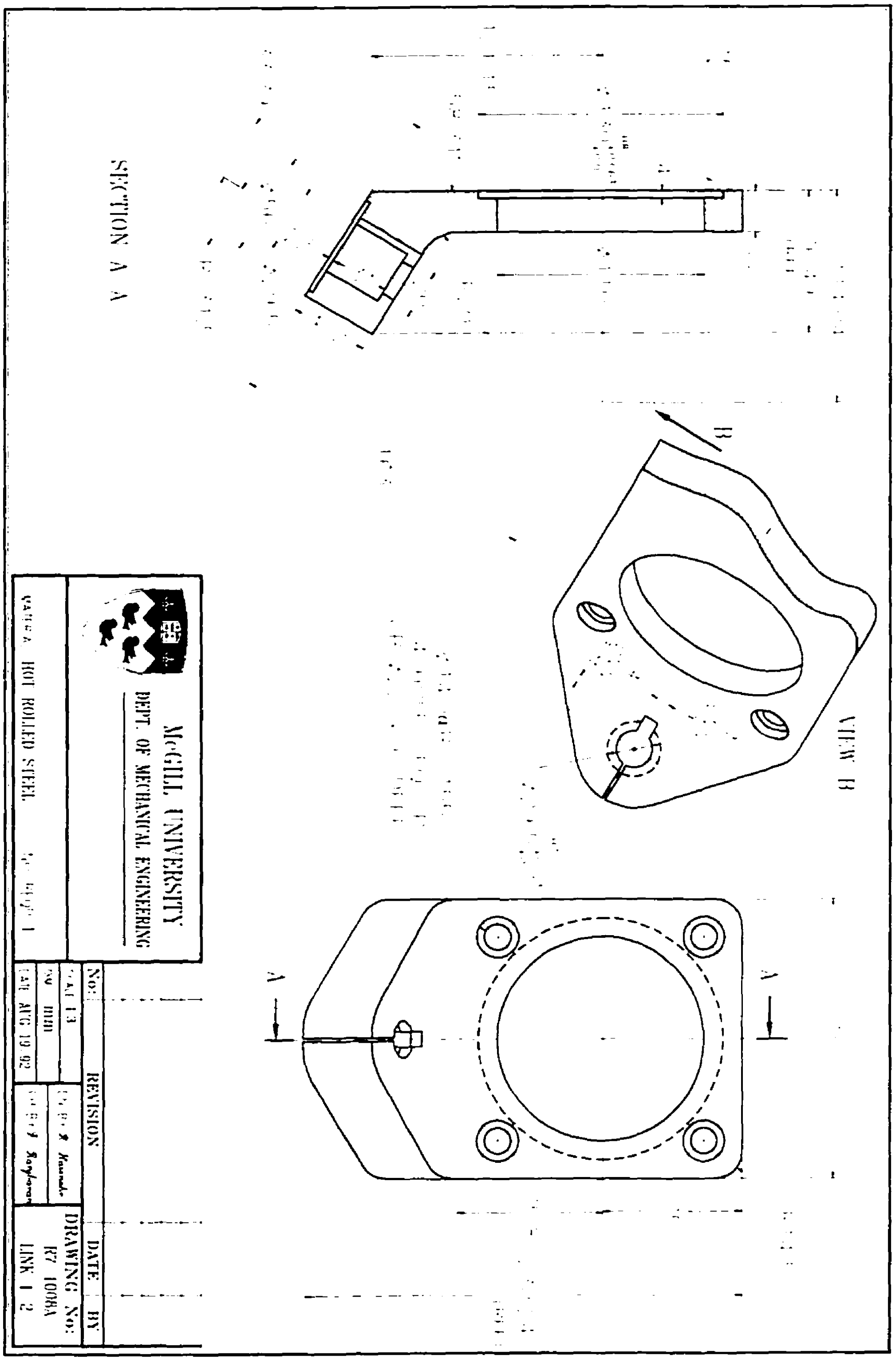

Figure D.17: Link 1 main link-flange detailed drawing A

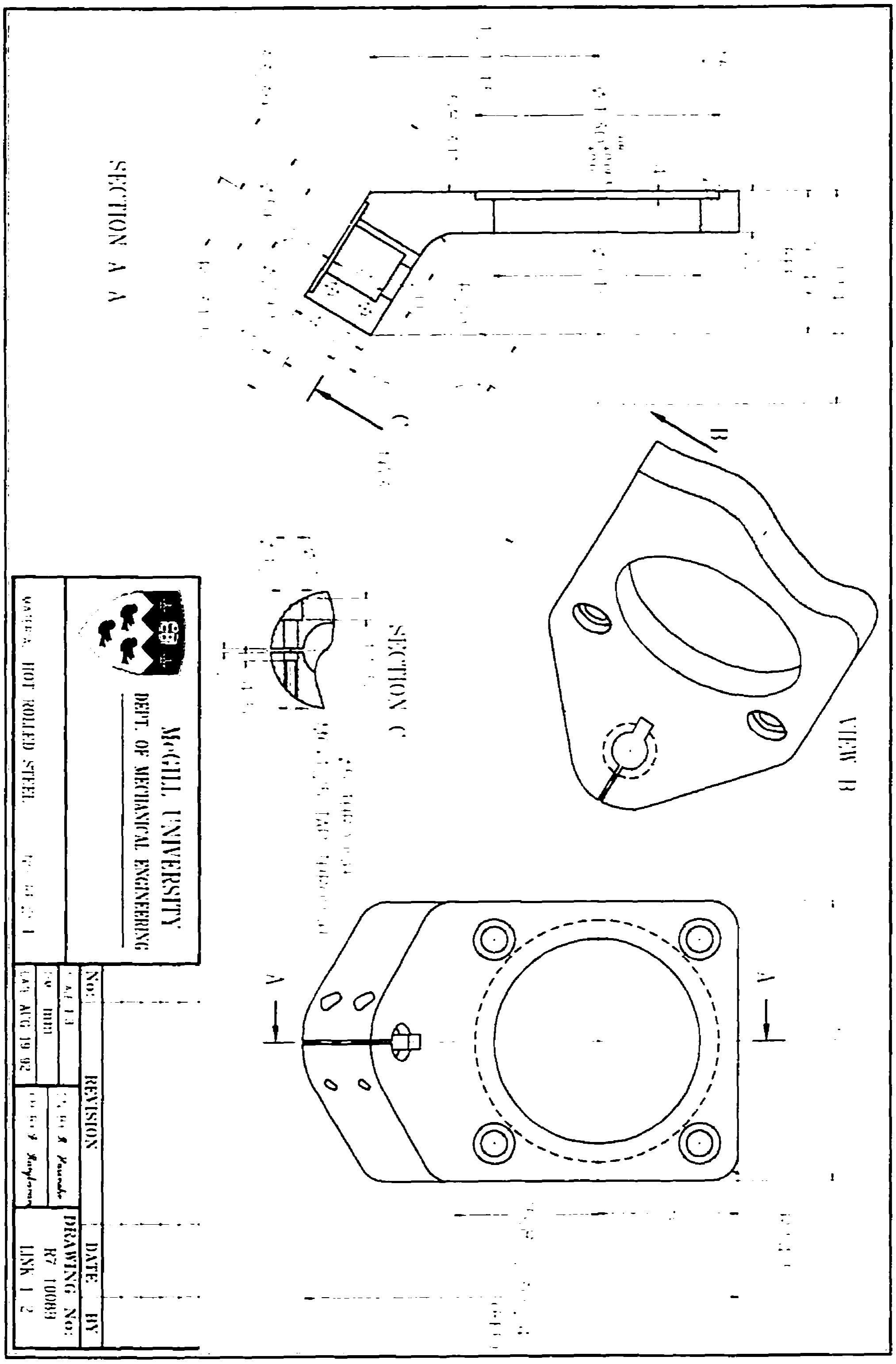

Figure D.18: Link 1 main link-flange detailed drawing B

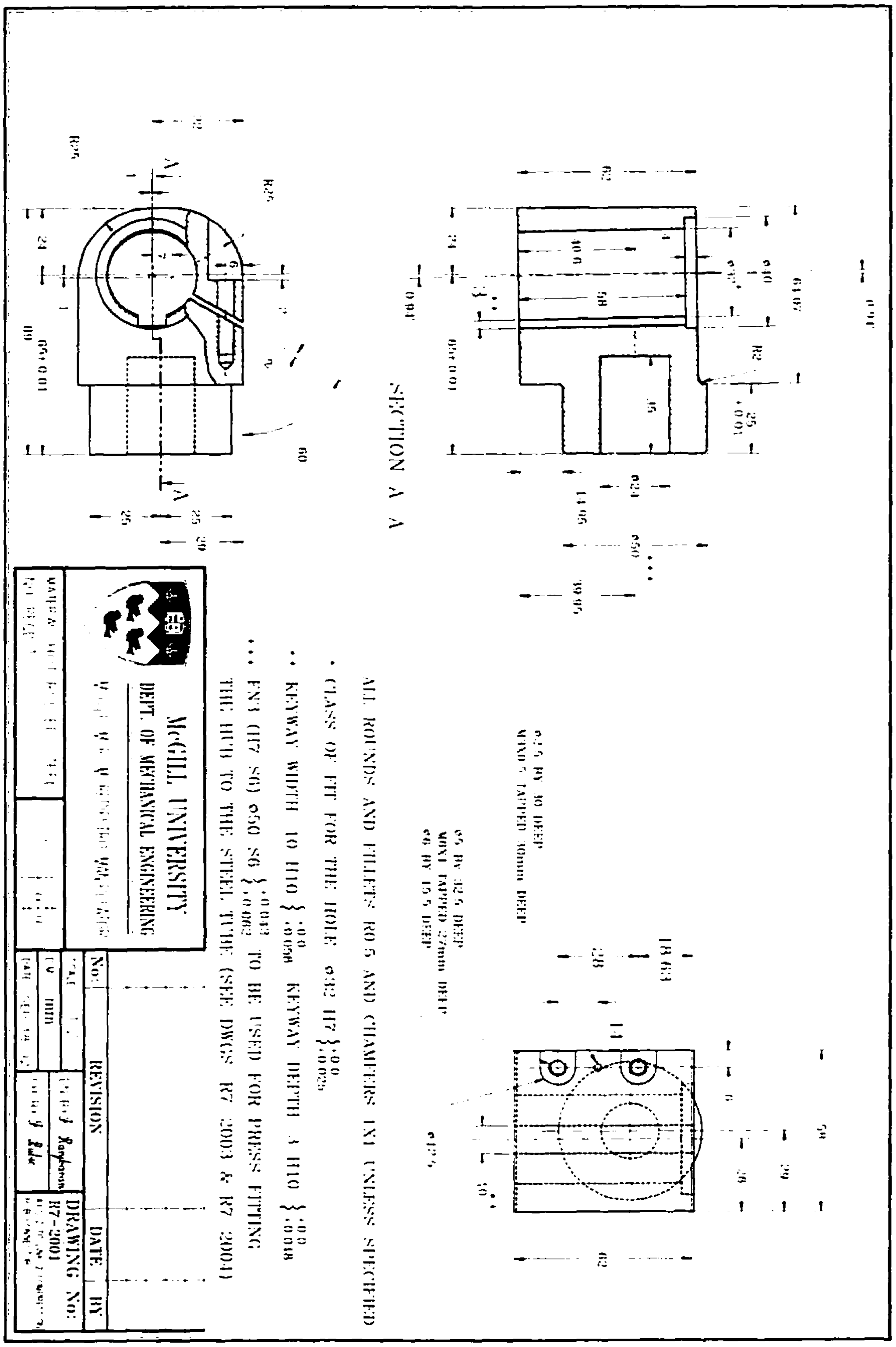

Figure D.19: link 2, motor 2 hub detailed drawing

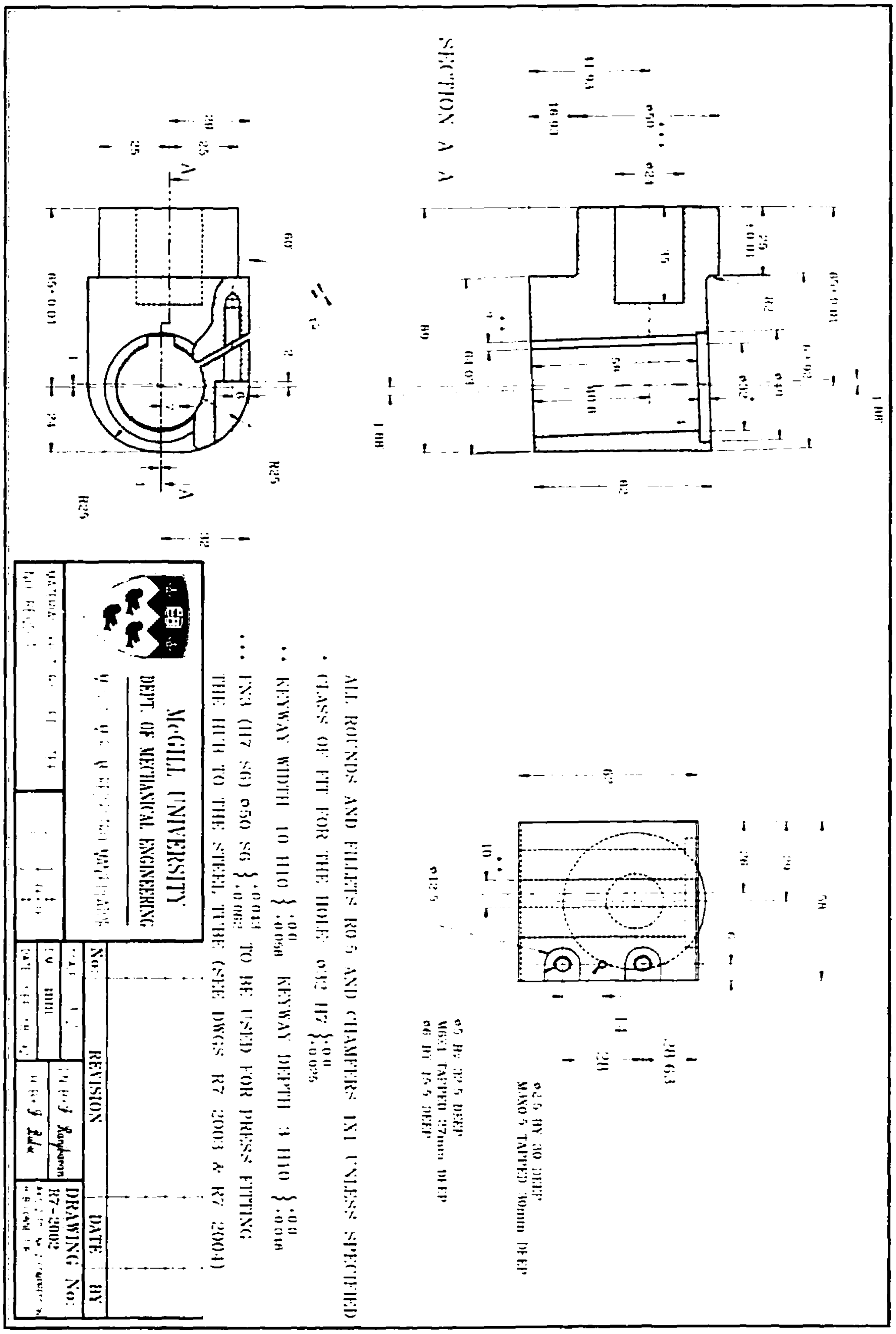

Figure D.20: Link 2, motor 3 hub detailed drawing

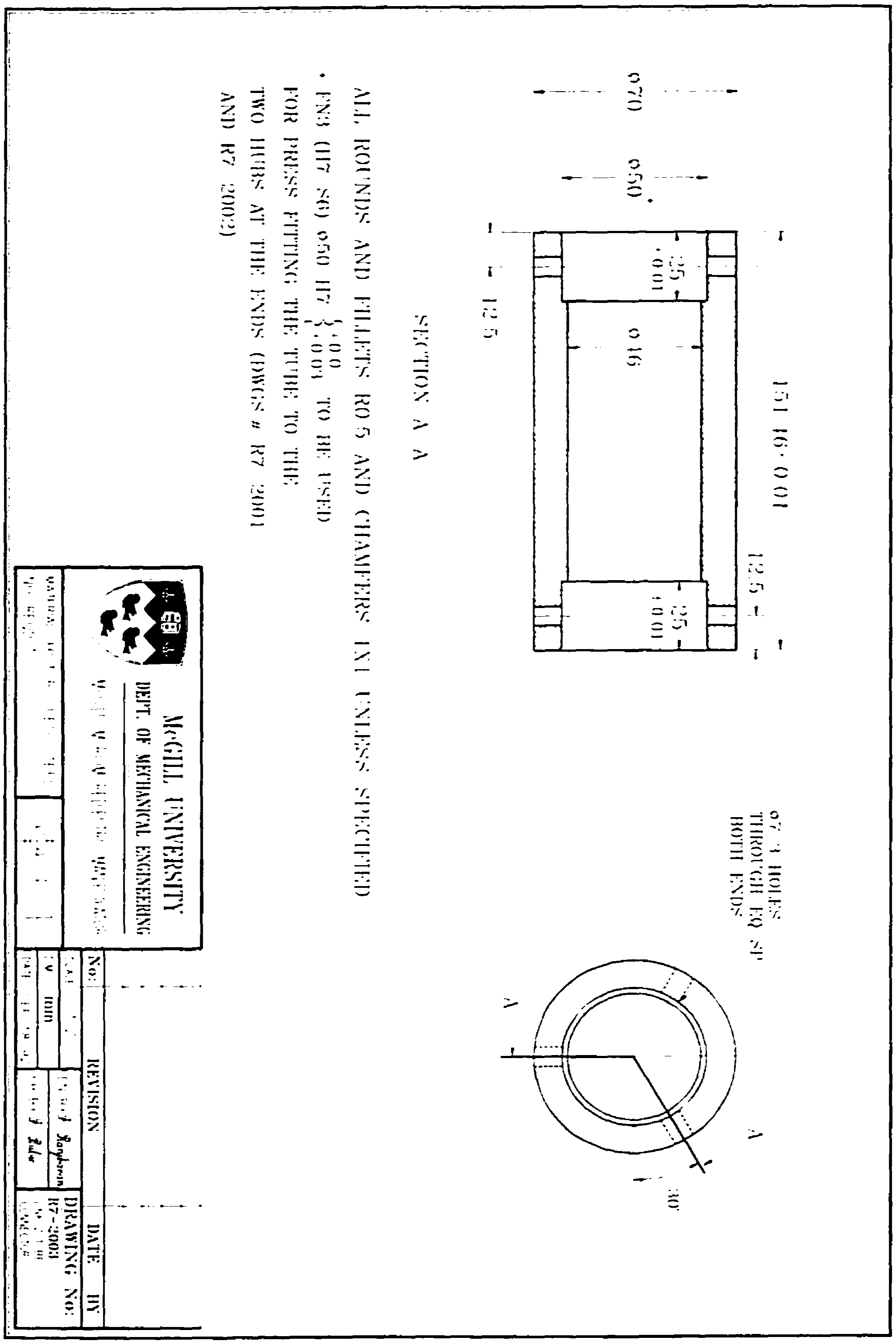

Figure D.21: Link 2, main body detailed drawing

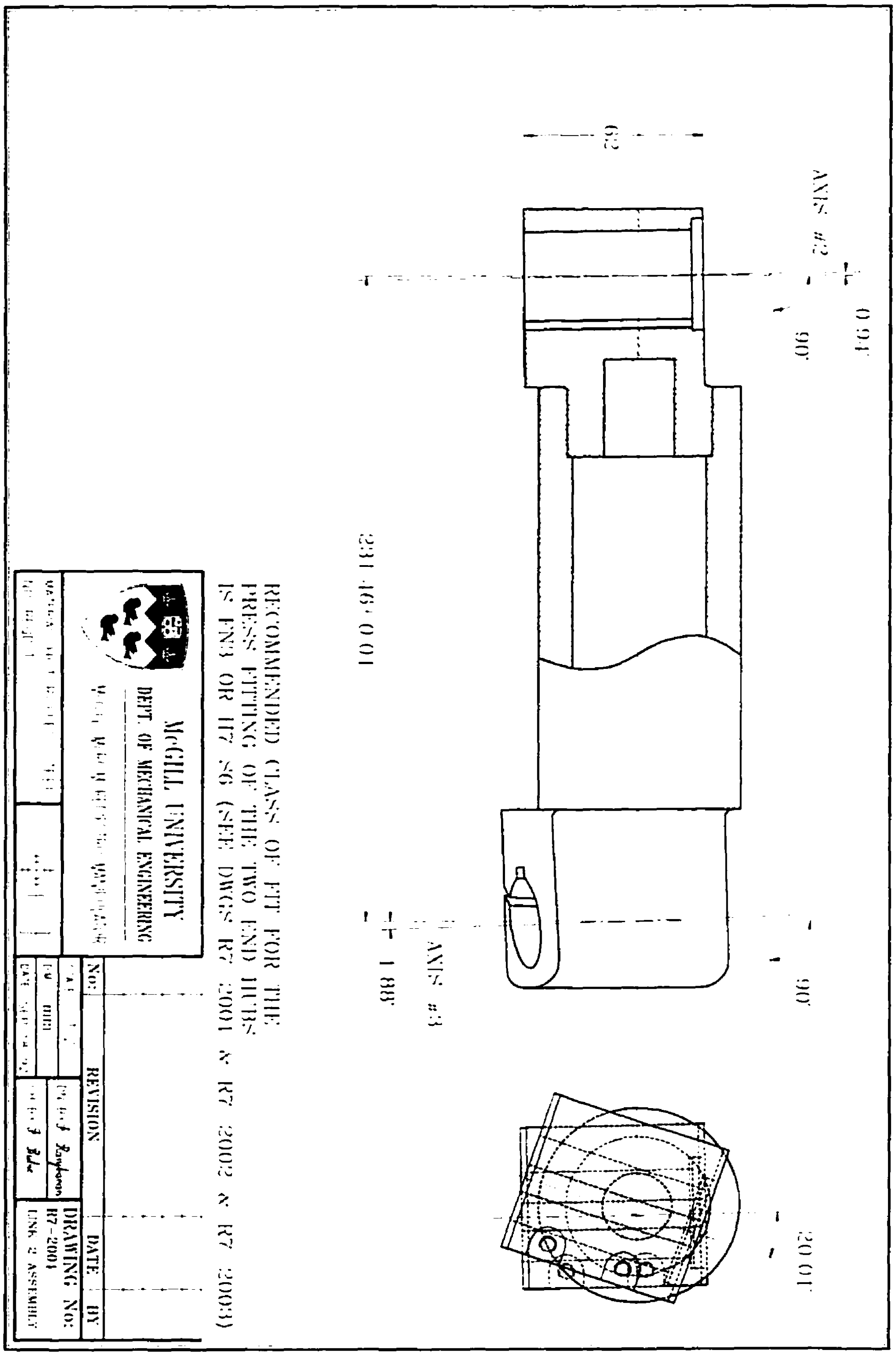

Figure D.22: Link 2, assembly drawing

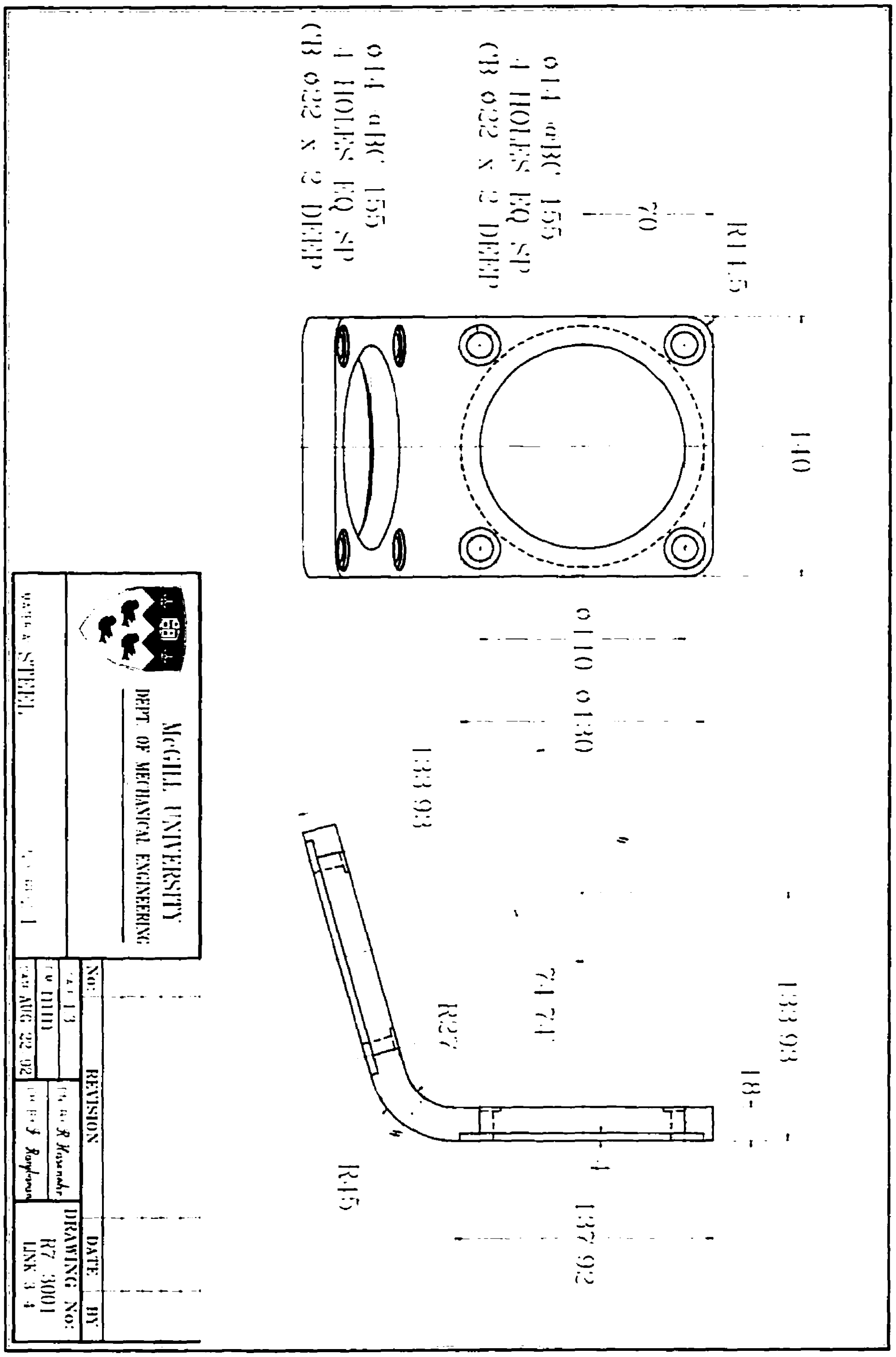

Figure D.23: Link 3, detailed drawing

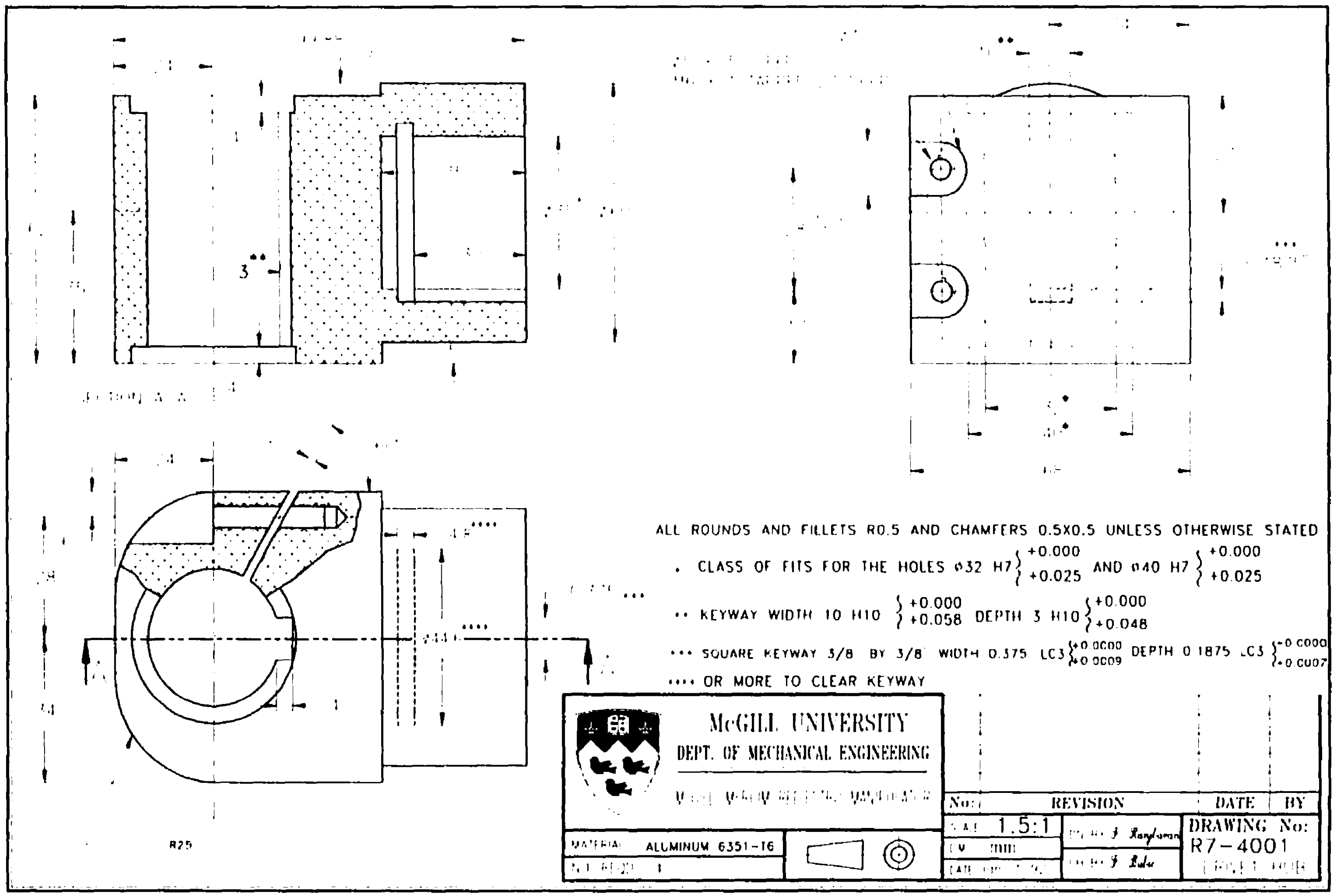

Figure D.24: Link 4, Motor 3 hub detailed drawing

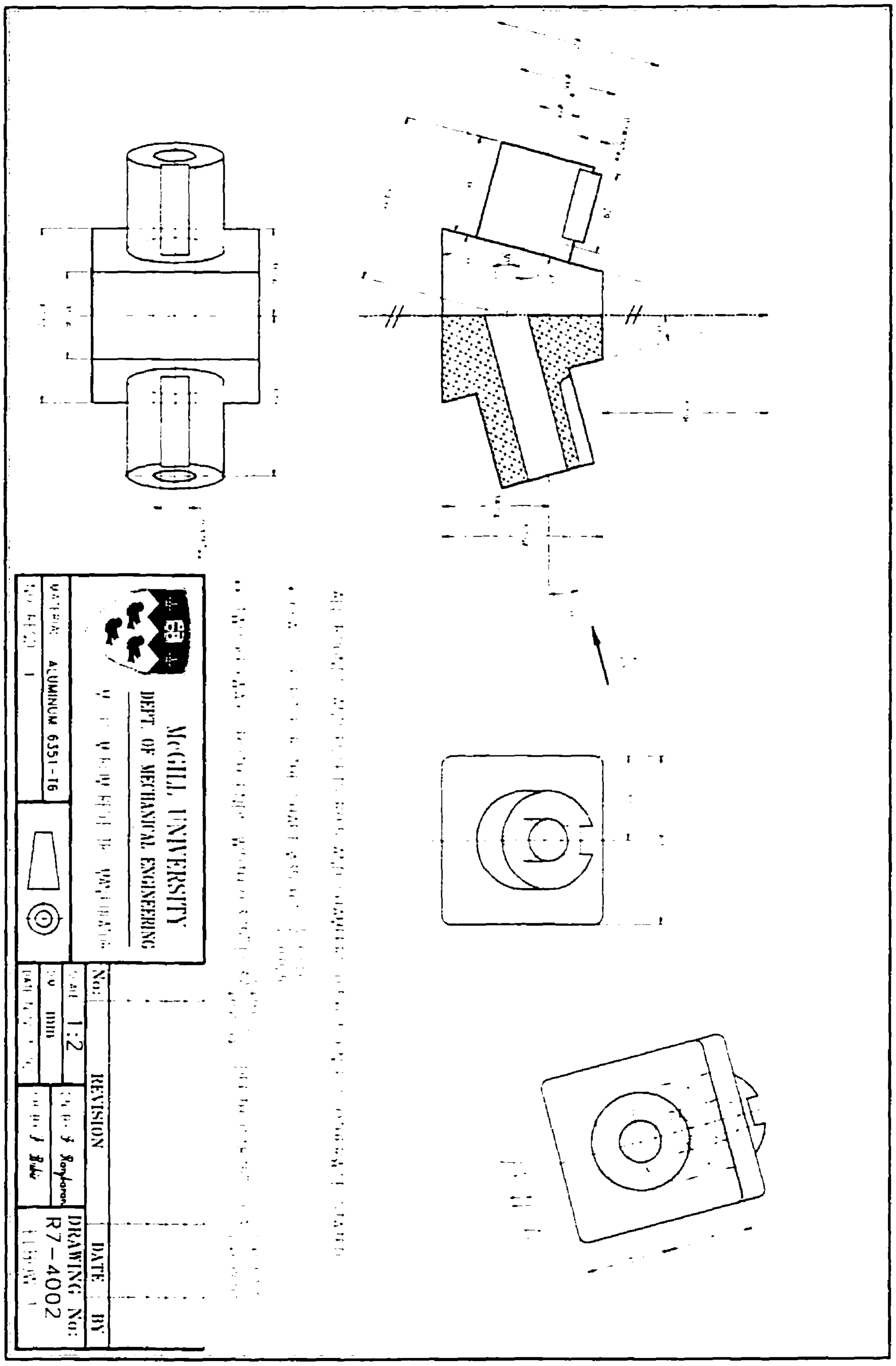

Figure D.25: Link 4, hub-to-shoulder connector detailed drawing

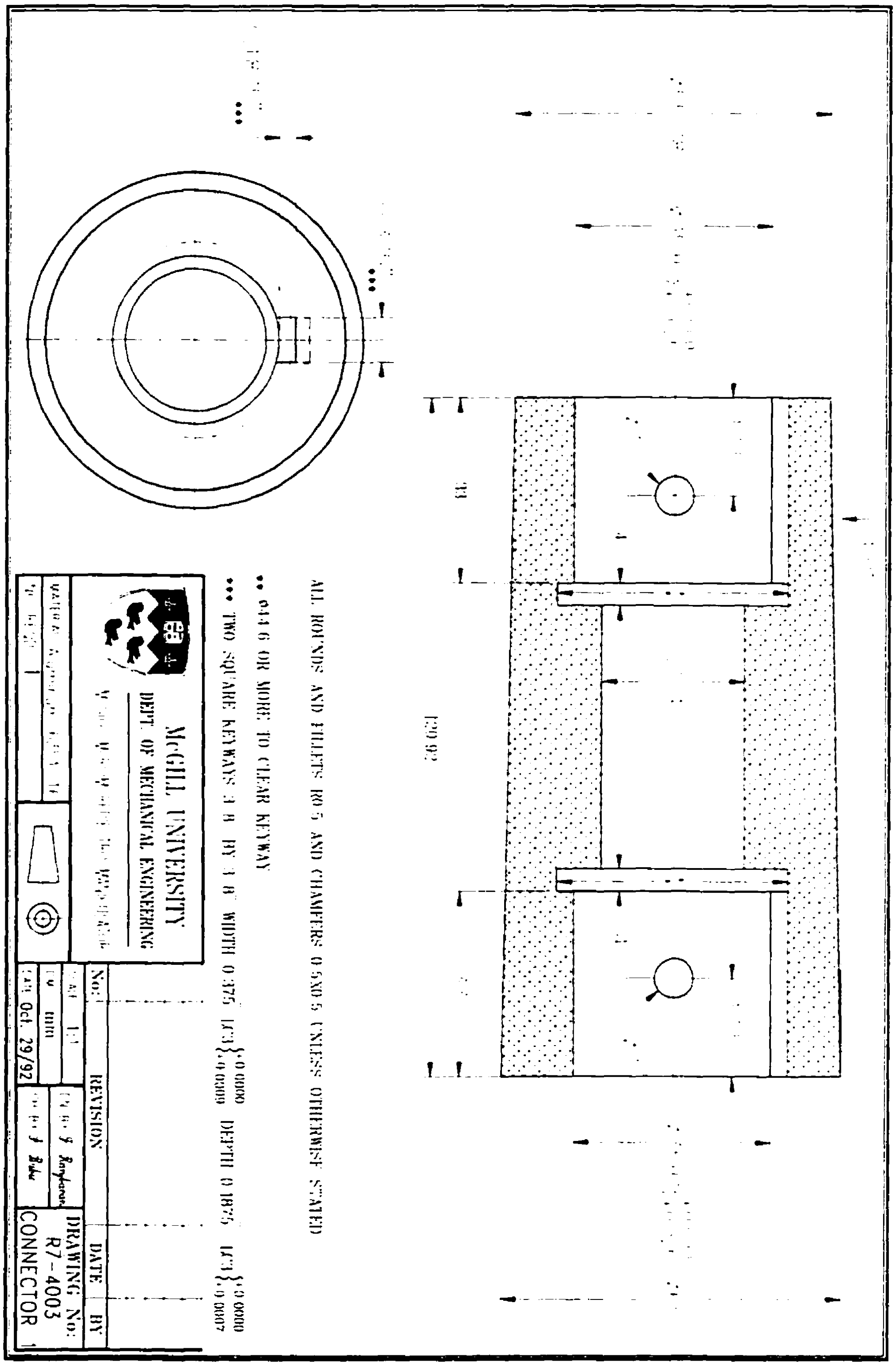

Figure D.26: Link 4, shoulder detailed drawing

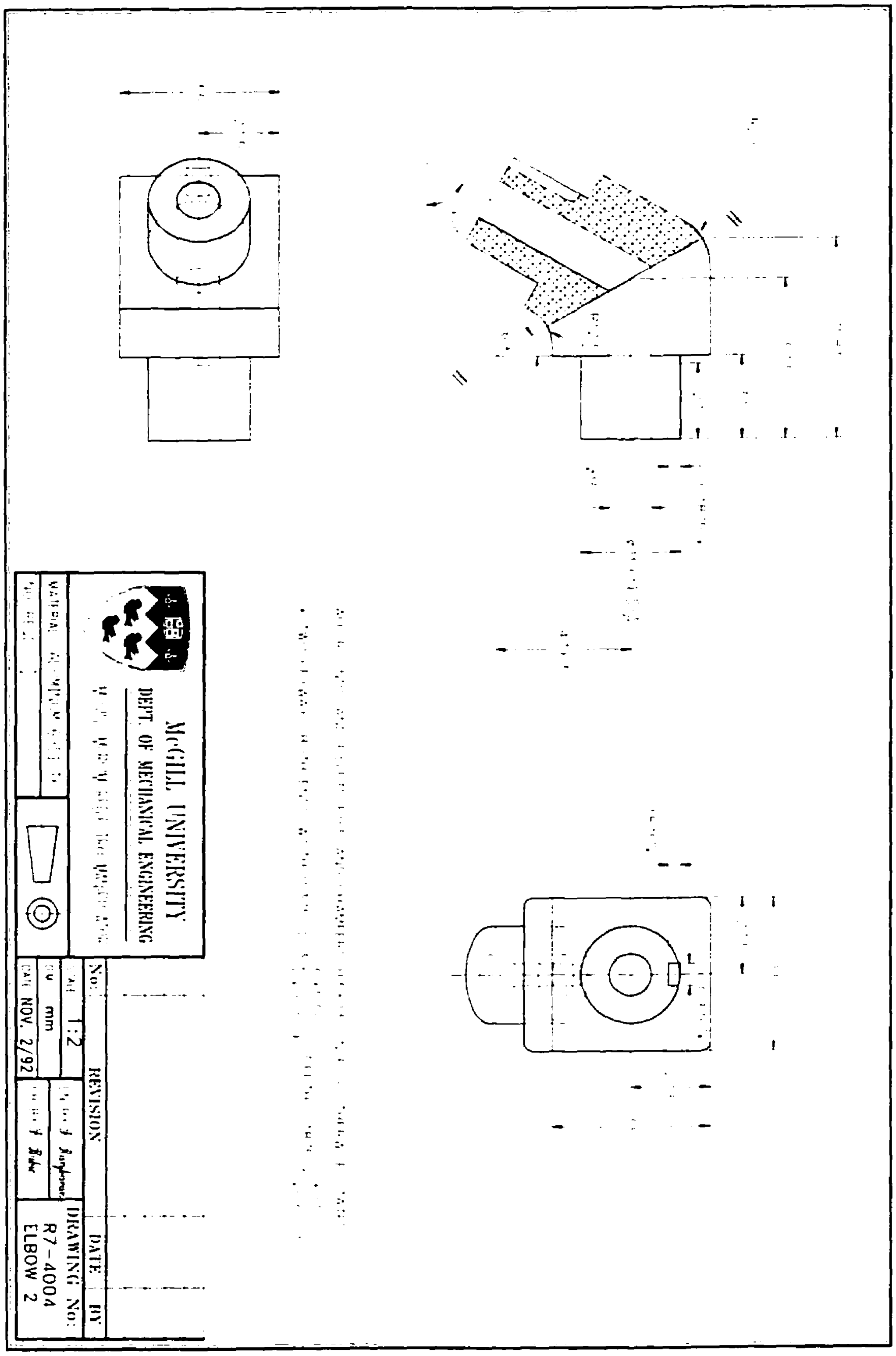

Figure D.27: Link 4, shoulder-to-elbow detailed drawing

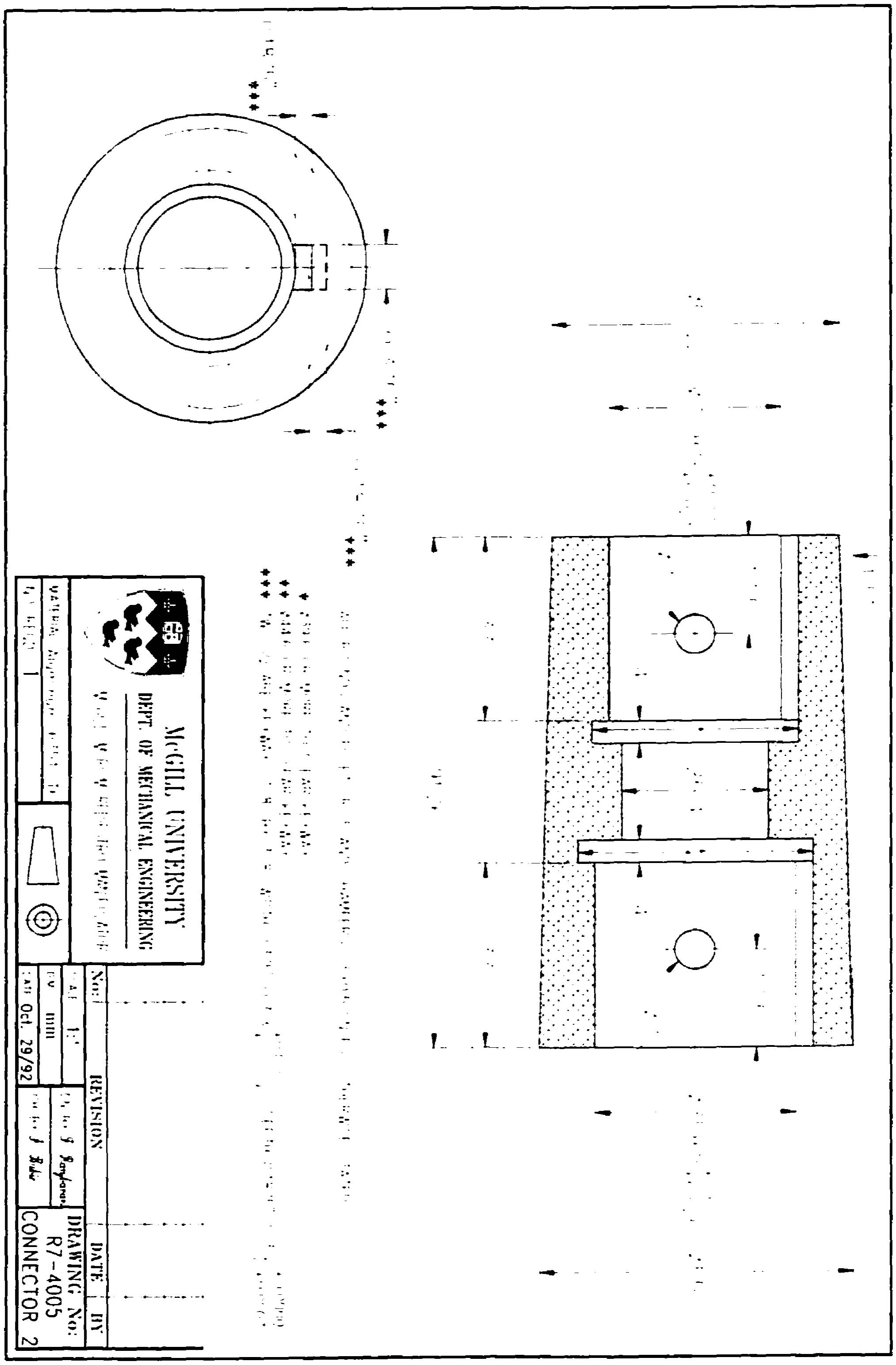

Figure D.28: Link 4, shoulder detailed drawing

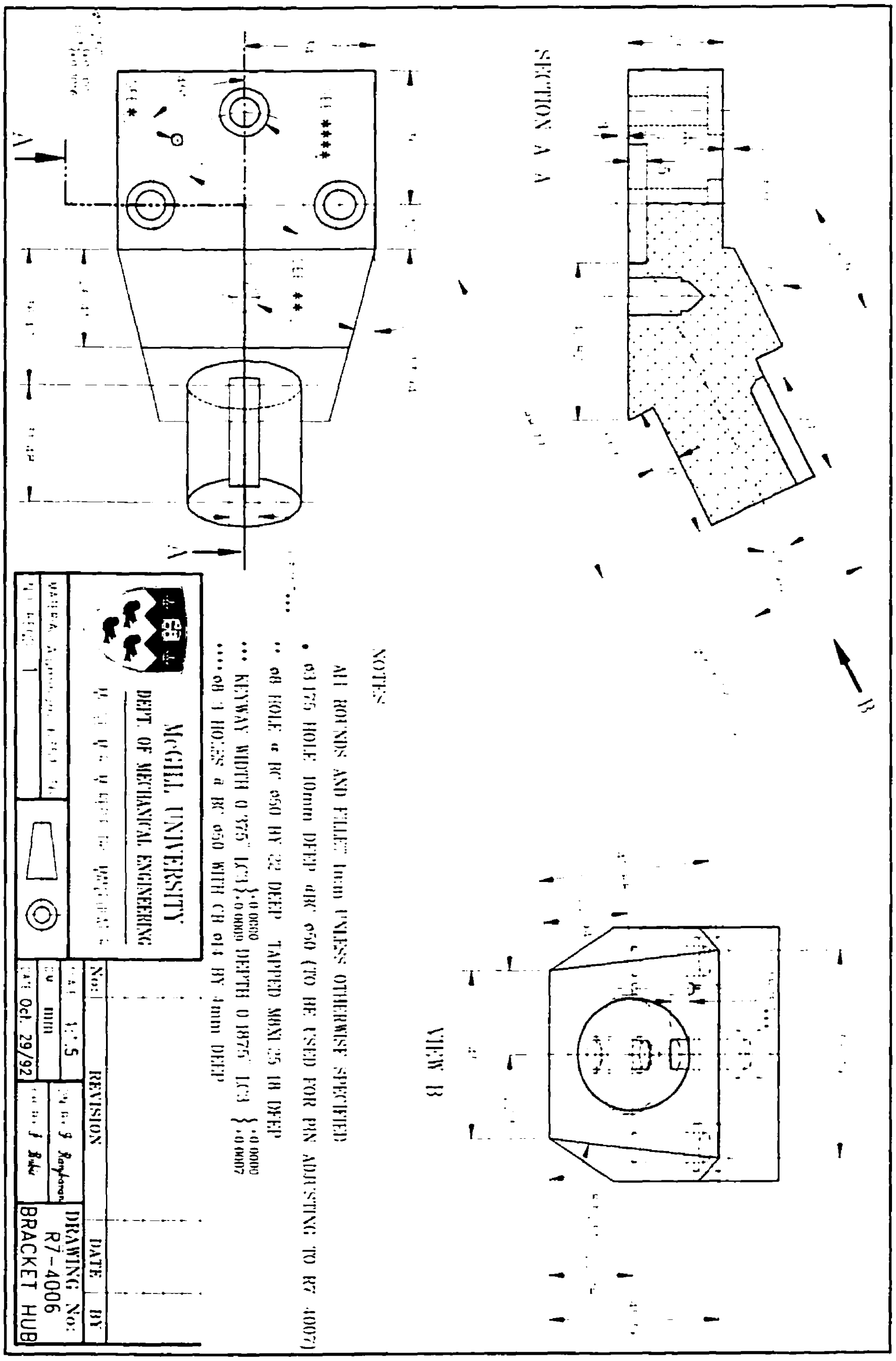

Figure D.29: Link 4, mounting block detailed drawing

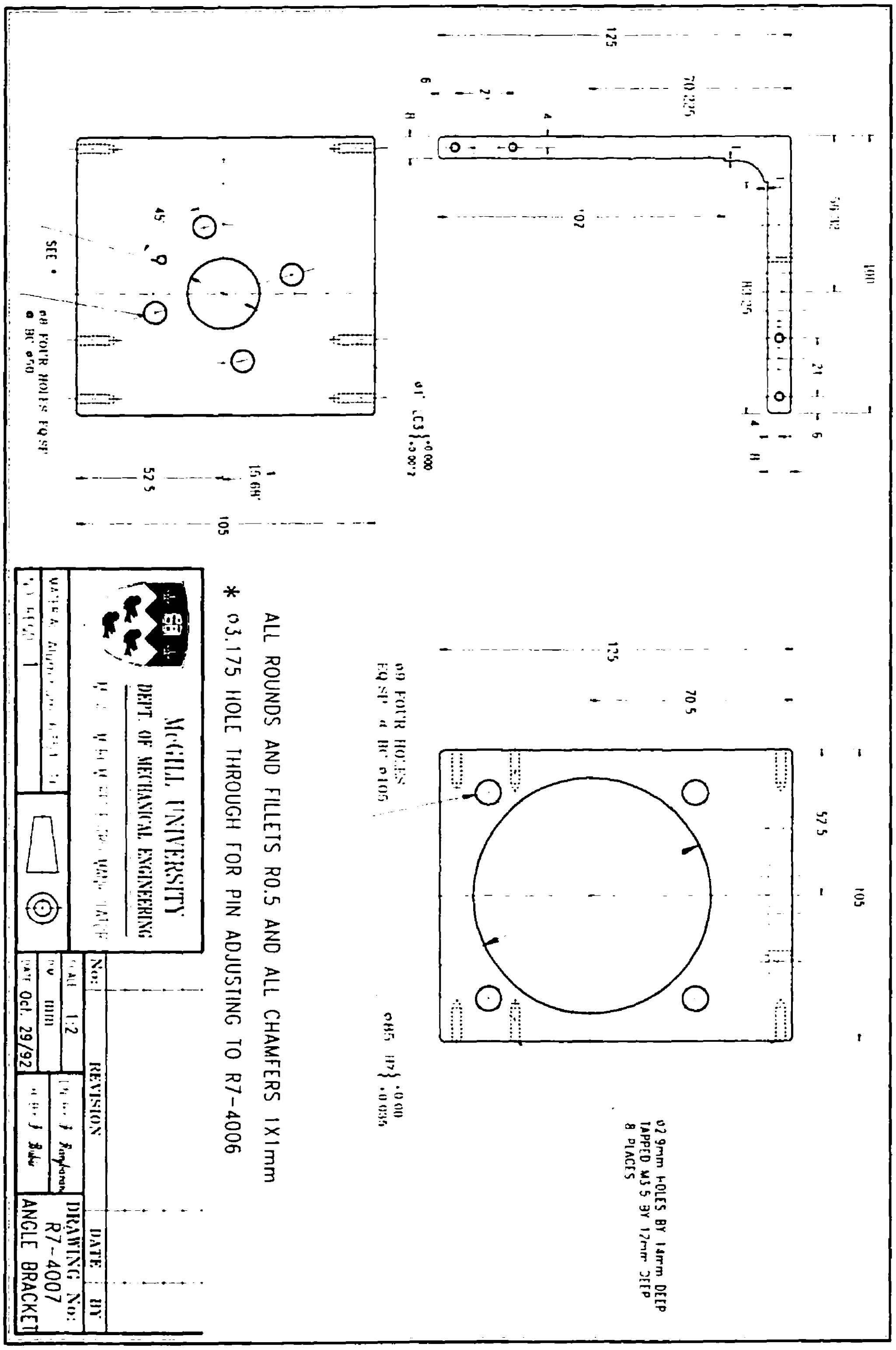

Figure D.30: Link 4, motor 4 bracket detailed drawing

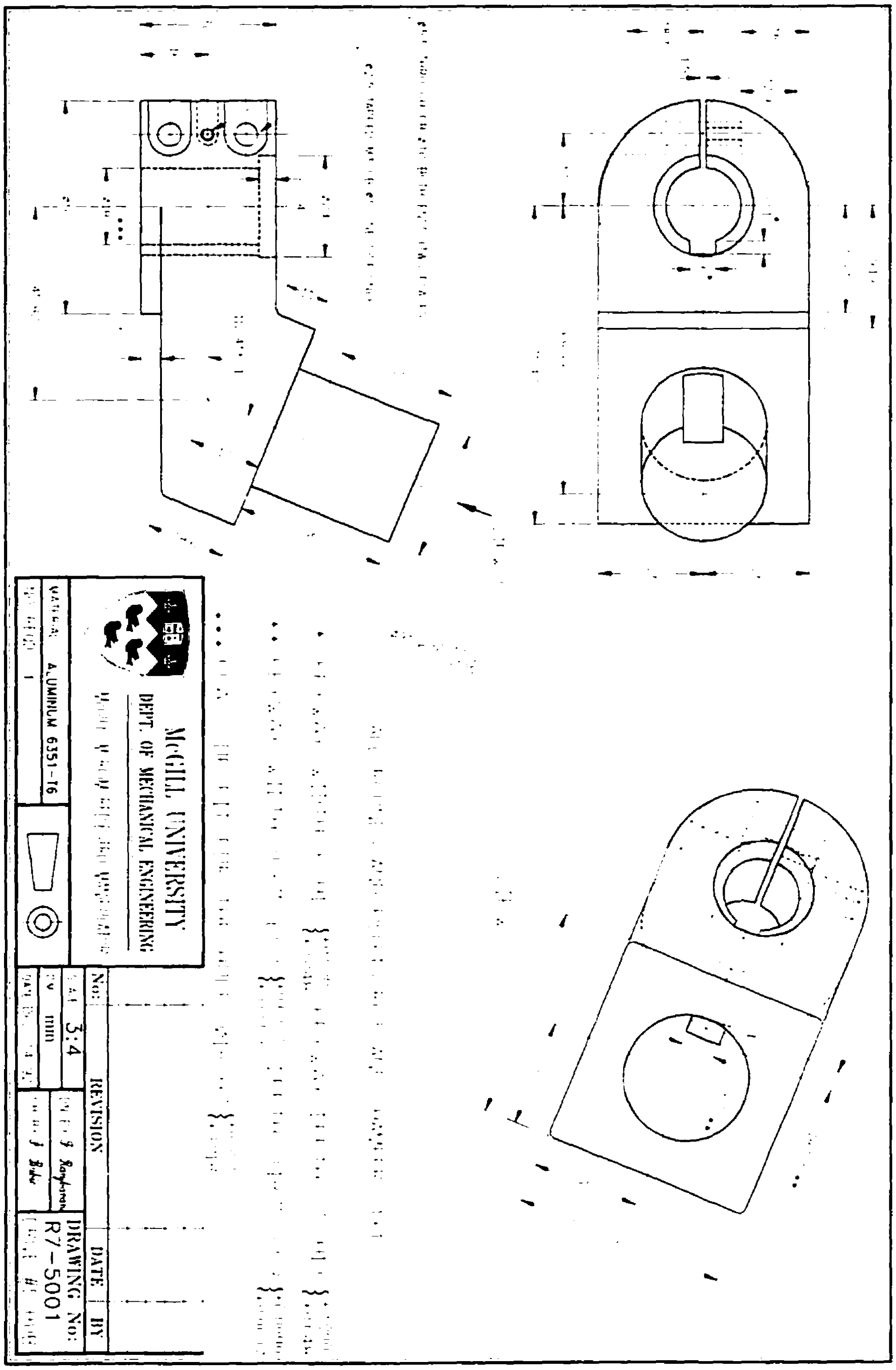

Figure D.31: Link 5, motor 4 hub detailed drawing

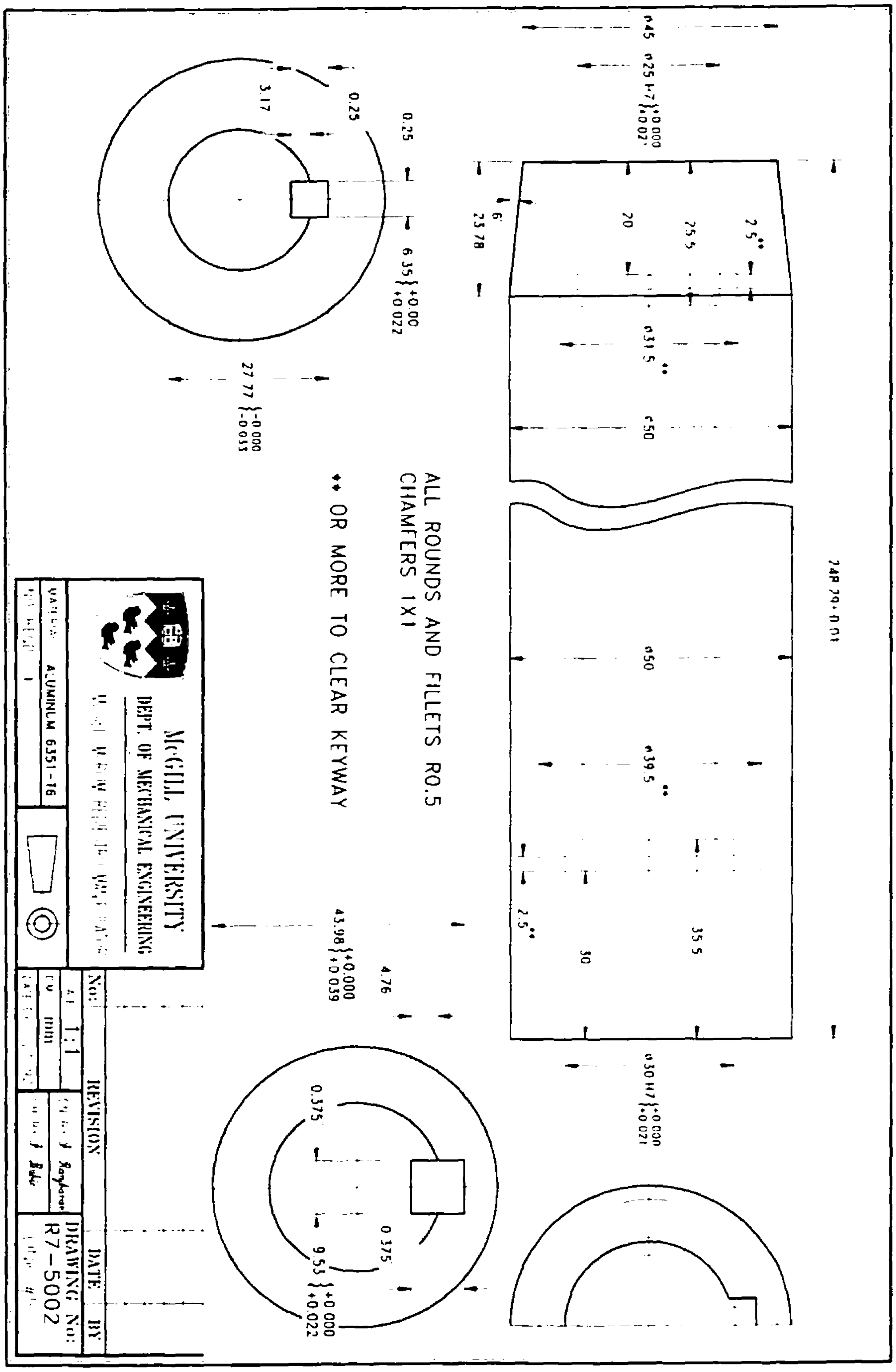

Figure D.32: Link 5, main arm detailed drawing

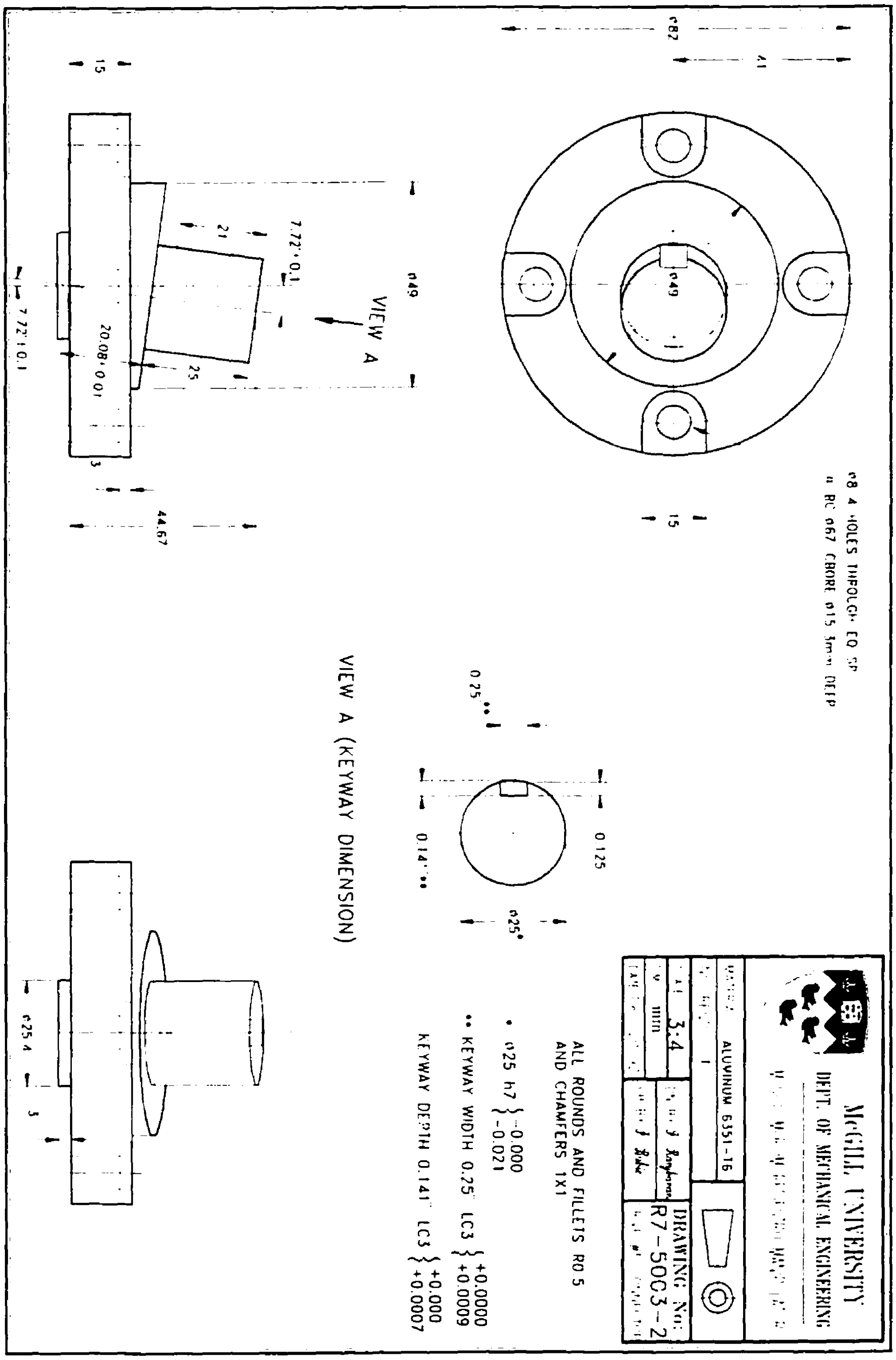

Figure D.33: Link 5, mounting block detailed drawing

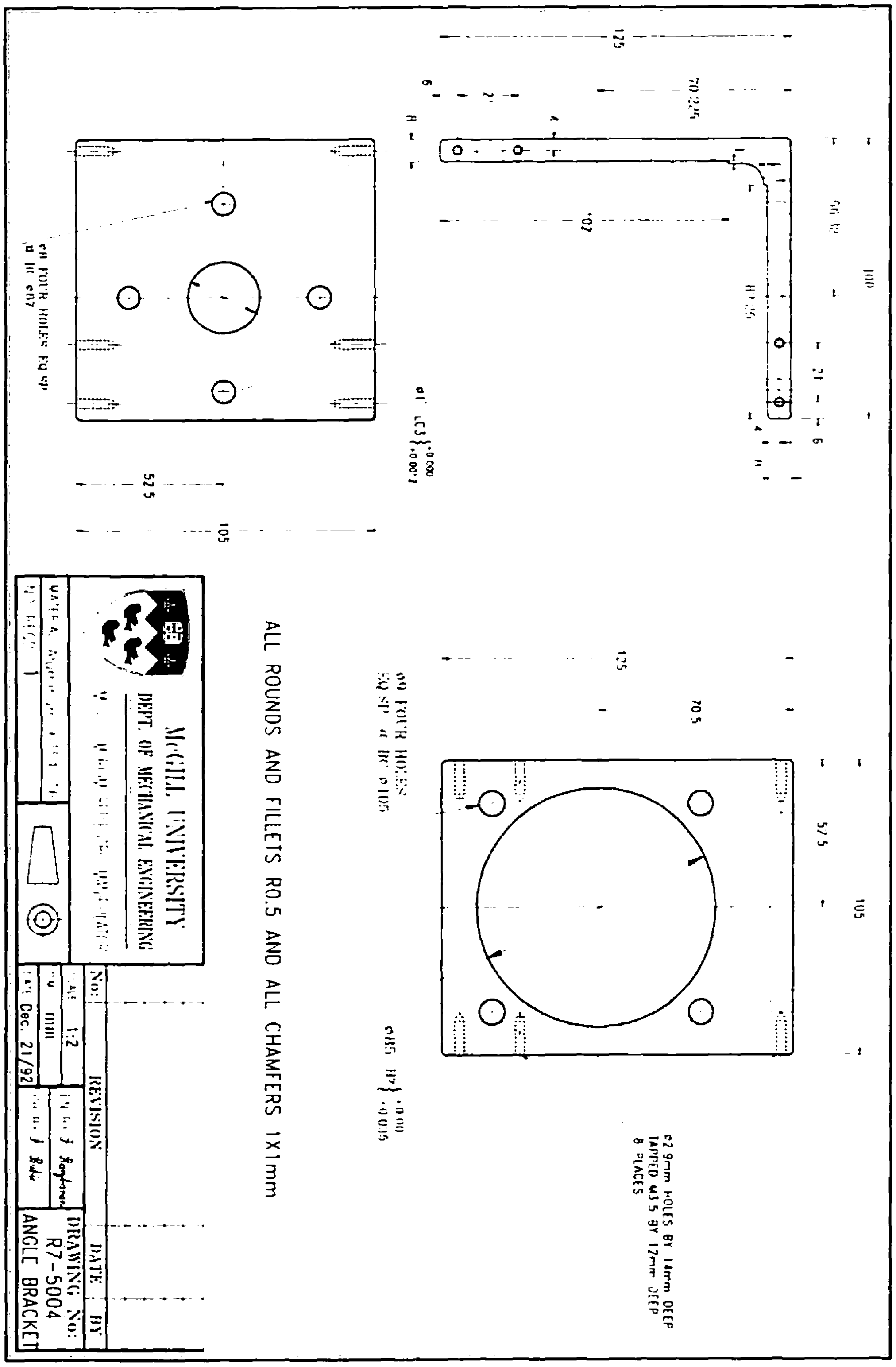

Figure D.34: Link 5, motor 6 bracket detailed drawing

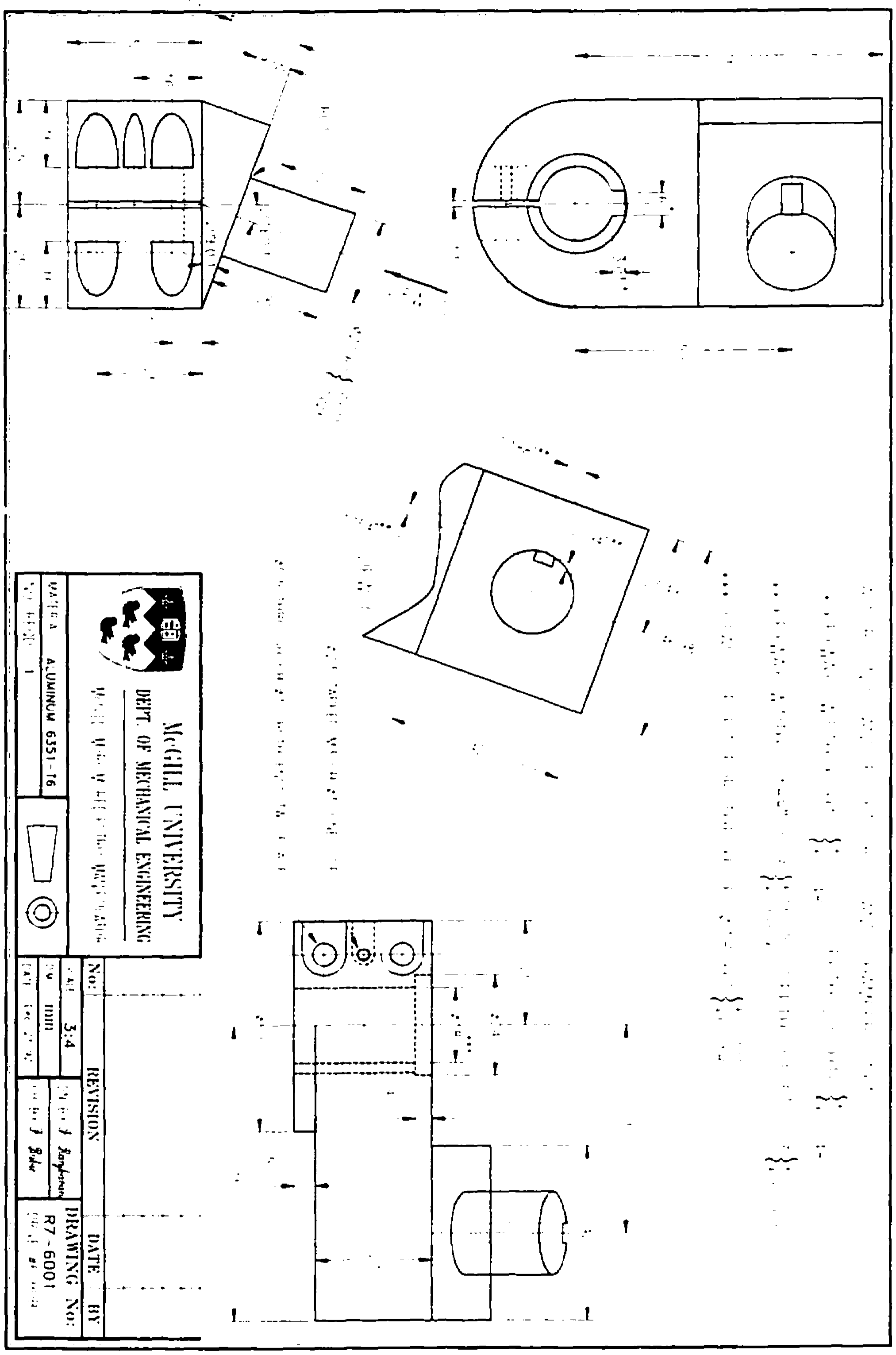

Figure D.35: Link 6, motor 5 hub detailed drawing

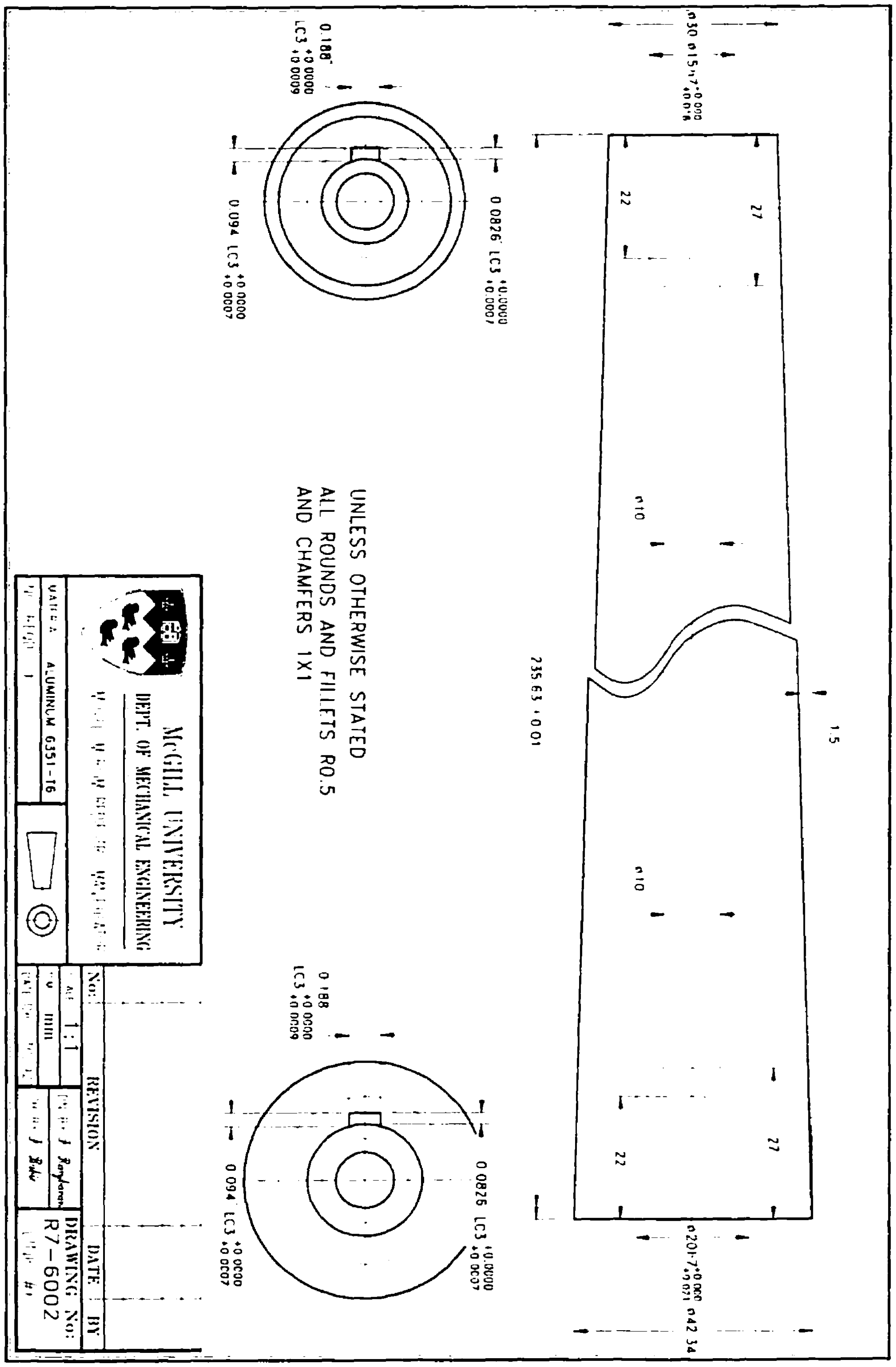

Figure D.36: Link 6, main arm detailed drawing

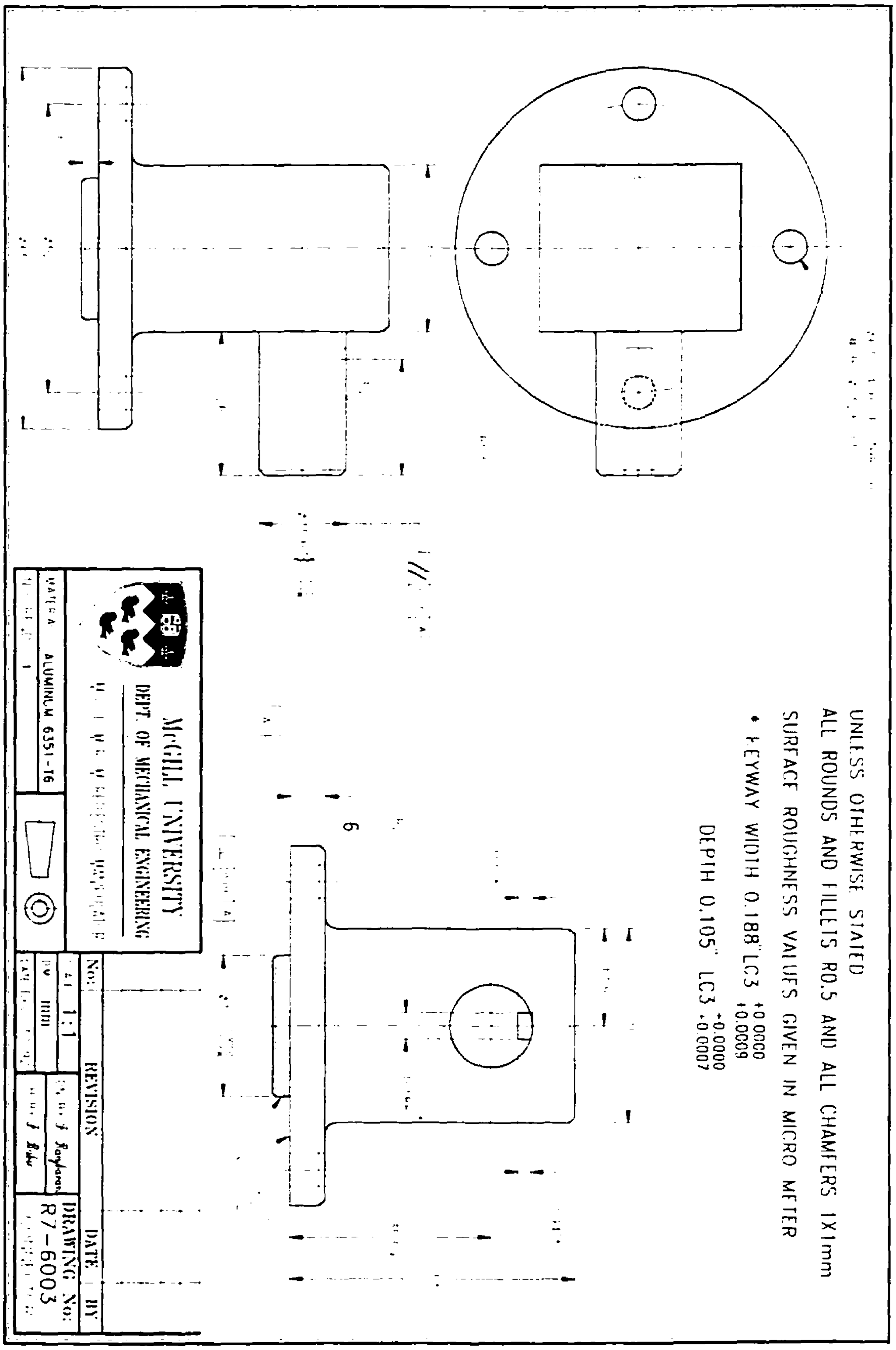

Figure D.37: Link 6, mounting block detailed drawing

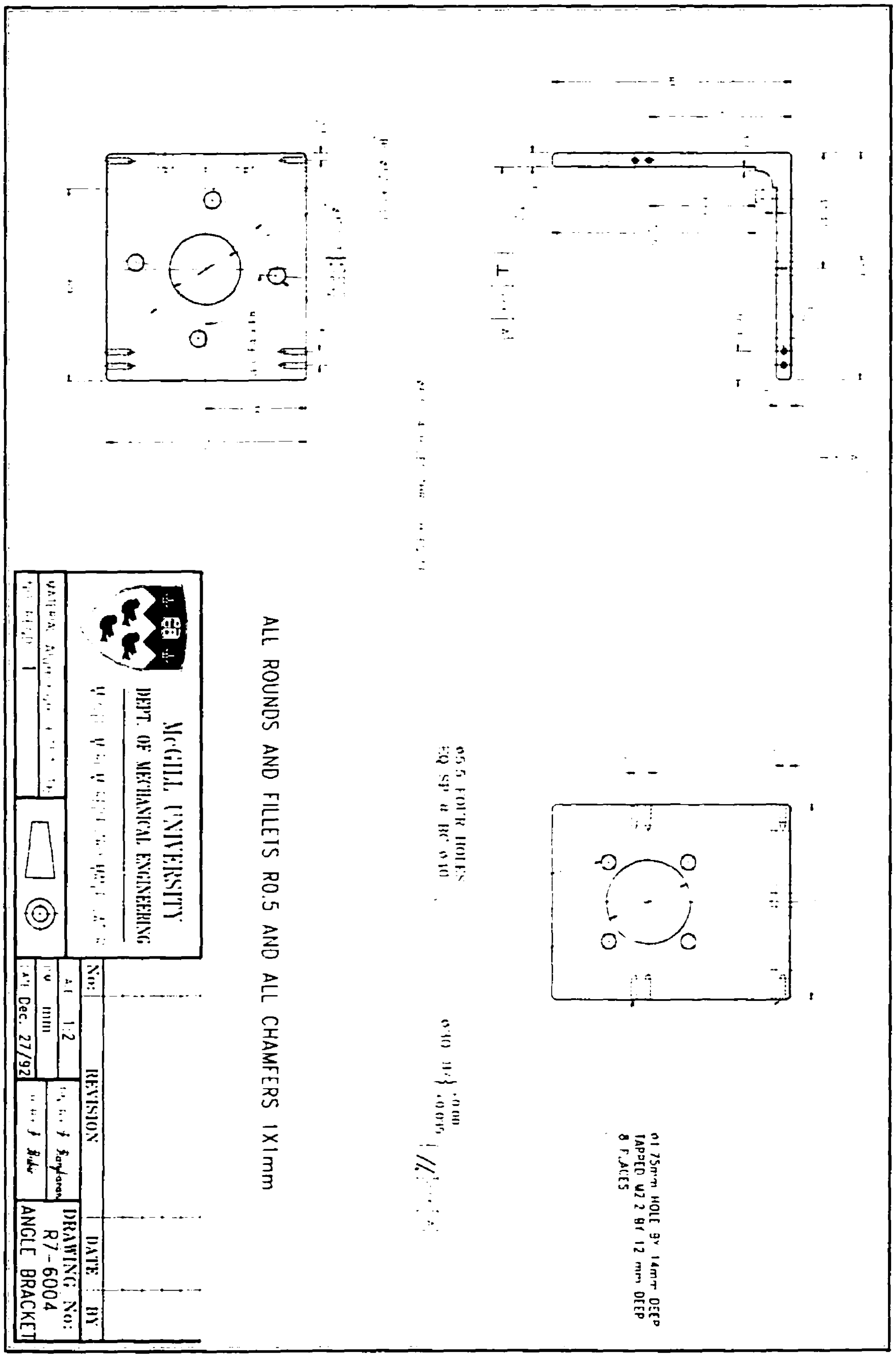

Figure D.38: Link 6, motor 6 bracket detailed drawing

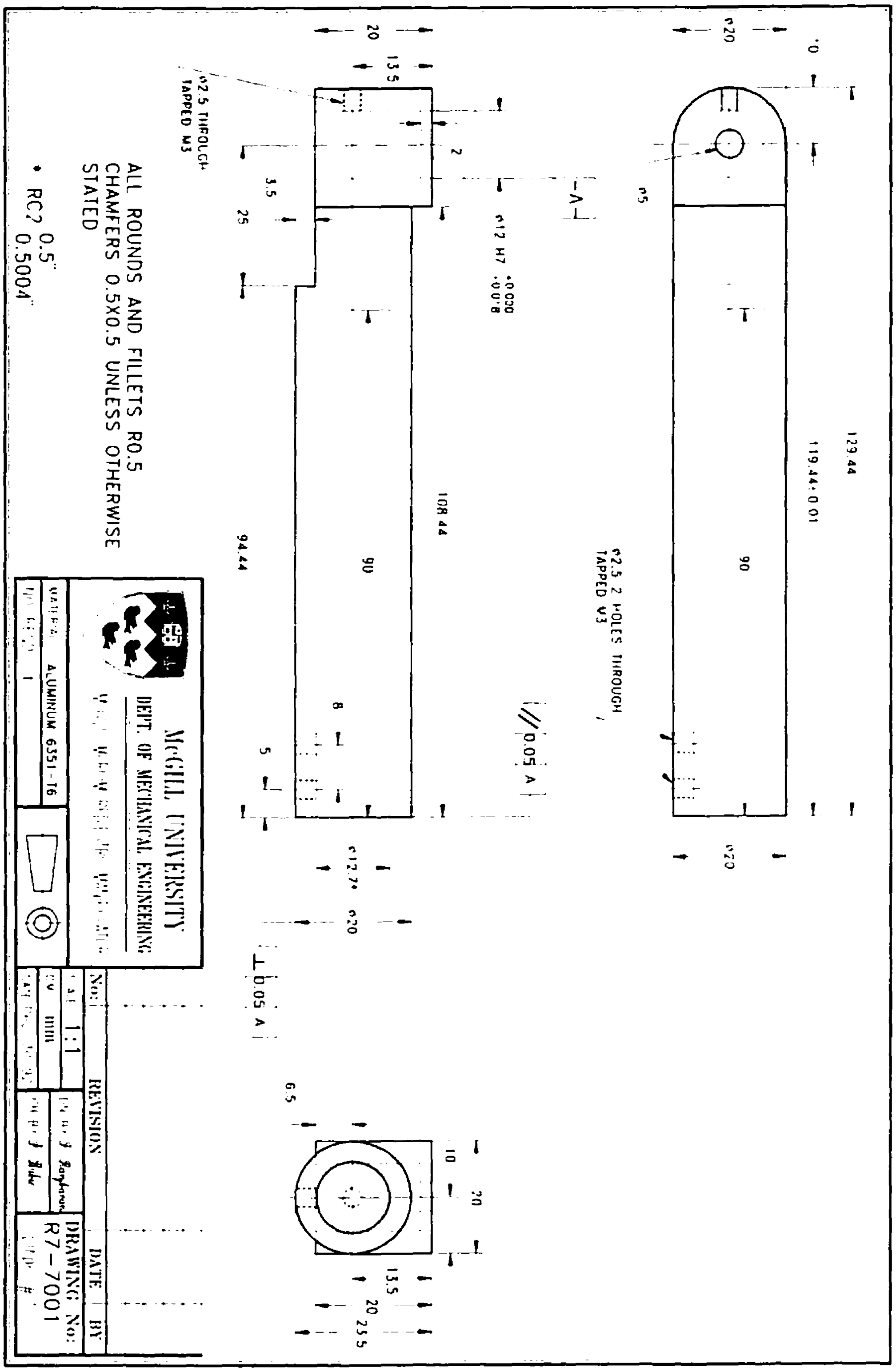

Figure D.39: Link 7, end-effector main shaft detailed drawing

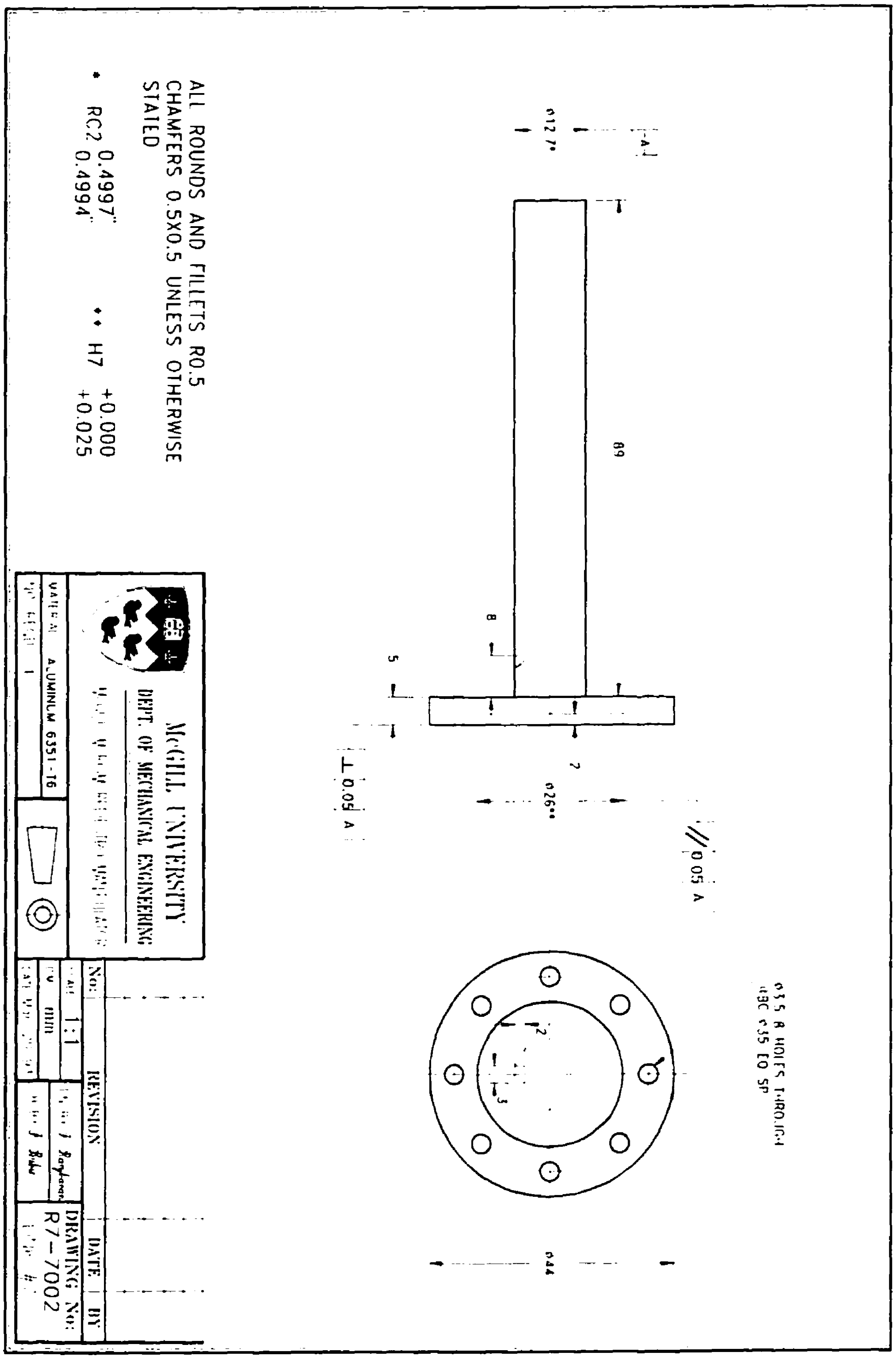

Figure D.40: Link 7, end-effector tool shaft detailed drawing

Appendix E

Electromechanical Specifications of the Actuators

E.1 Actuators of REDIESTRO

In this Section the electromechanical specifications of the actuators of REDIESTRO 1 are recorded. In Section E.1.2, the mechanical drawings of each actuator unit is provided, and in Section E.1.1 the electromechanical specification of each unit is tabulated.

E.1.1 Electromechanical Specifications of the Actuators

The Actuators that are used for REDIESTRO 1 are from Harmonic Drive Systems Inc., each including a DC-motor, harmonic drive, incremental encoder and electromagnetic brake. For the specification of each unit letter "B" stands for brakes, "E" denoting encoder while "AL" stands for 5V line drive encoder. The number between "E" and "AL" is the encoder resolution divided by 10. Moreover, "sp" stands for special configuration. REDIESTRO 1 power transformer are also from Harmonic Drive Systems Inc. Encoders are able to be used as quadrature, thus, allowing a maximum resolution equal to four times the nominal pulse per revolution specidied for each unit, (Table E.2)

Remarks regarding the specification of the actuators:

- The mass of each unit given in Table E.2 is the mass of the DC motor plus the gear-head plus the encoder, while the mass of the brakes are included in brackets.

- The inertia given here is the sum of motor and harmonic drive gear-head converted to the output side of the actuator. These are provided in the manufacturers' catalogue in Kgf-cm sec^2. To convert to Kg m^2, multiply by 9.806/100.

- The torque constants are referred to the output side as well.

Model Number	Serial Number
RH-25-1507-BE-100AL-sp	104477
RH-32-1212-BE-036AL-sp	104480
RH-32-1212-BE-036AL-sp	104478
RH-32-1212-BE-036AL-sp	104479
RH-20-1903-BE-100AL-sp	104470
RH-20-1903-BE-100AL-sp	104471
RH-14-3002-BE-100AL-sp	104614

Table E.1: REDIESTRO 1, Actuators model

Model Number	Joint	Gear Red.	Encoder Res. P/rev	Max. Torque Nm	Rated Torque Nm	Mass (+Brake) Kg	Inertia (Encoder) Kg m^2
RH-25-1507	1	200	200	147	42	4.7 (6.2)	9.3157+(0.0275)=9.3432
RH-32-1212	2	260	360	314	97	8.7 (11.5)	50.7951+(0.0464)=50.8415
RH-32-1212	3	260	360	314	97	8.7 (11.5)	50.7951+(0.0464)=50.8415
RH-32-1212	4	260	360	314	97	8.7 (11.5)	50.7951+(0.0464)=50.8415
RH-20-1903	5	160	1000	78	17	3.1 (4.1)	2.3534+(0.0176)=2.3710
RH-20-1903	6	160	1000	78	17	3.1 (4.1)	2.3534+(0.0176)=2.3710
RH-14-3002	7	100	1000	19.6	5.9	0.78	0.0816+(0.005)=0.0866

Table E.2: REDIESTRO 1, Actuators mechanical specification

The Amplifiers that are used for REDIESTRO 1 are made by Copley Control Corporation, with their specifications being provided in Table E.5.

Model Number	Joint	Torque Const. Nm/A (Load Side)	Max. Current A
RH-25-1507	1	40/200=0.2	4.9
RH-32-1212	2, 3 and 4	55/260=0.211	8.1
RH-20-1903	5 and 6	32/160=0.2	3.1
RH-14-3002	7	5.76/100=0.0576	4.1

Table E.3: REDIESTRO 1, Actuators electrical specification

Joints	Model Number
1	PT1-10004
2, 3 and 4	PT1-10007
5 and 6	PT1-10002
7	PT1-03803

Table E.4: REDIESTRO 1, power transformer model

Model Number	Joint	High Volt. Supply VDC	Output Voltage V	Peak Power Output	Max. Cont. Current A
303B	1	16 to 90	$V_h - 0.26l_o$	±90V at ±12A	6
303B-1	2, 3 and 4	16 to 90	$V_h - 0.26l_o$	±90V at ±12A	6
303B-1	5 and 6	16 to 90	$V_h - 0.26l_o$	±90V at ±12A	6
303	7	16 to 80	$V_h - 0.26l_o$	±75V at ±12A	6

Table E.5: REDIESTRO 1, Amplifiers model and pecifications. Where V_h is high voltage applied and l_o is current into motor or load. -1 stands for high inductance load.

E.1.2 Actuator Drawings

The mechanical drawings of the actuators are given in Figs. E.1 to E.4.

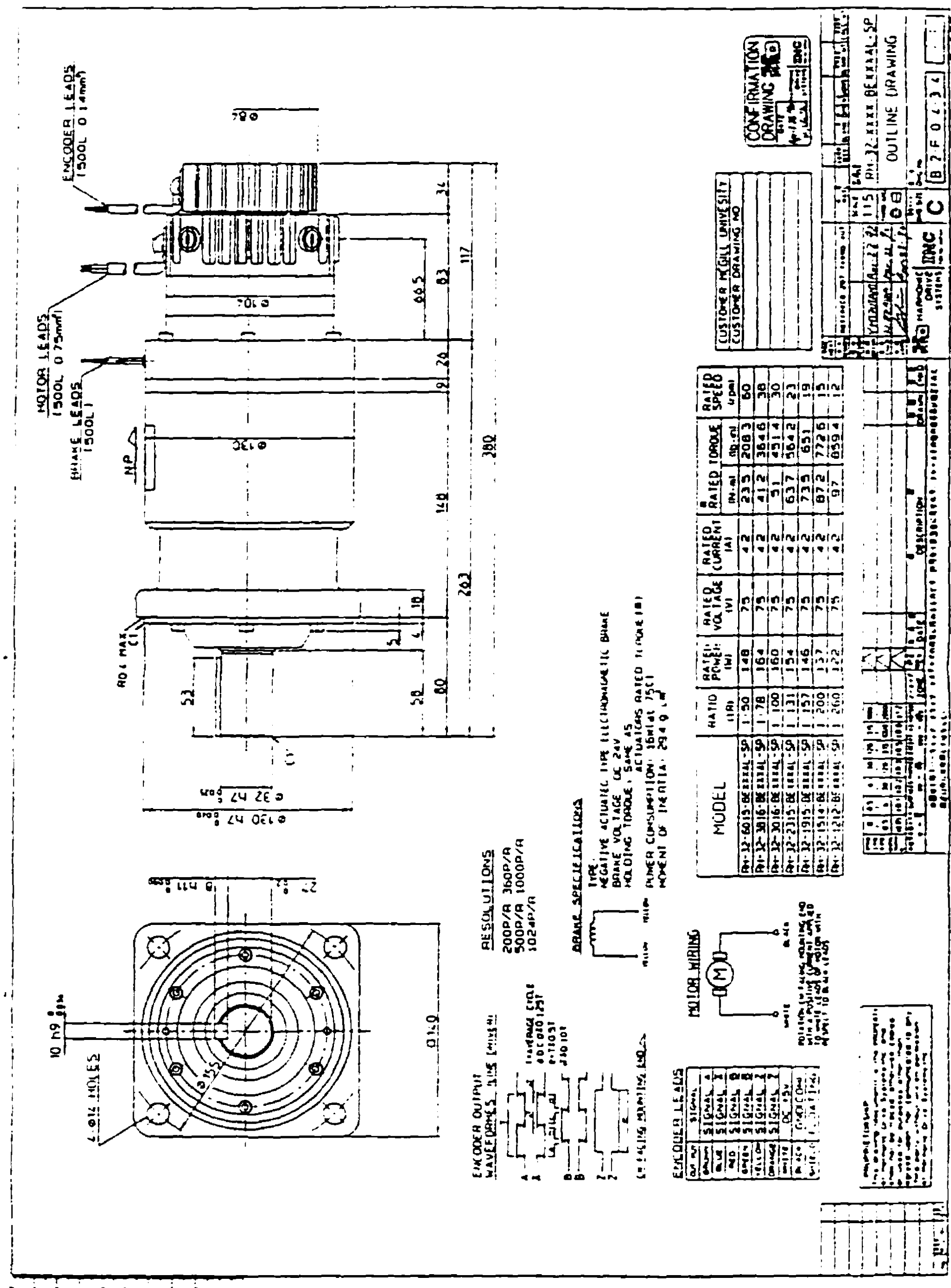

Figure E.1: Mechanical specification of Rh-32 (joints 2,3 and 4)

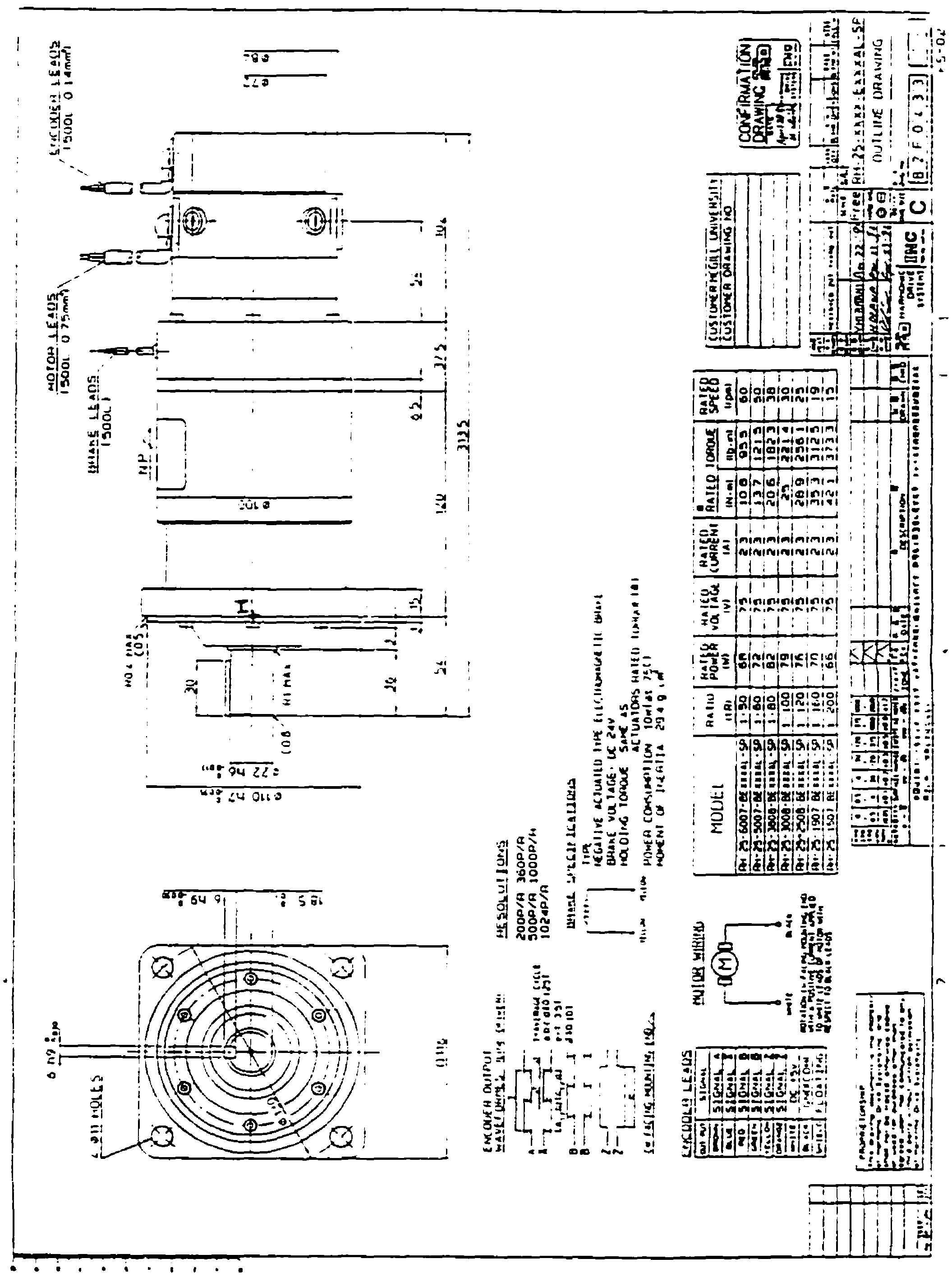

Figure E.2: Mechanical specification of Rh-25 (joint 1)

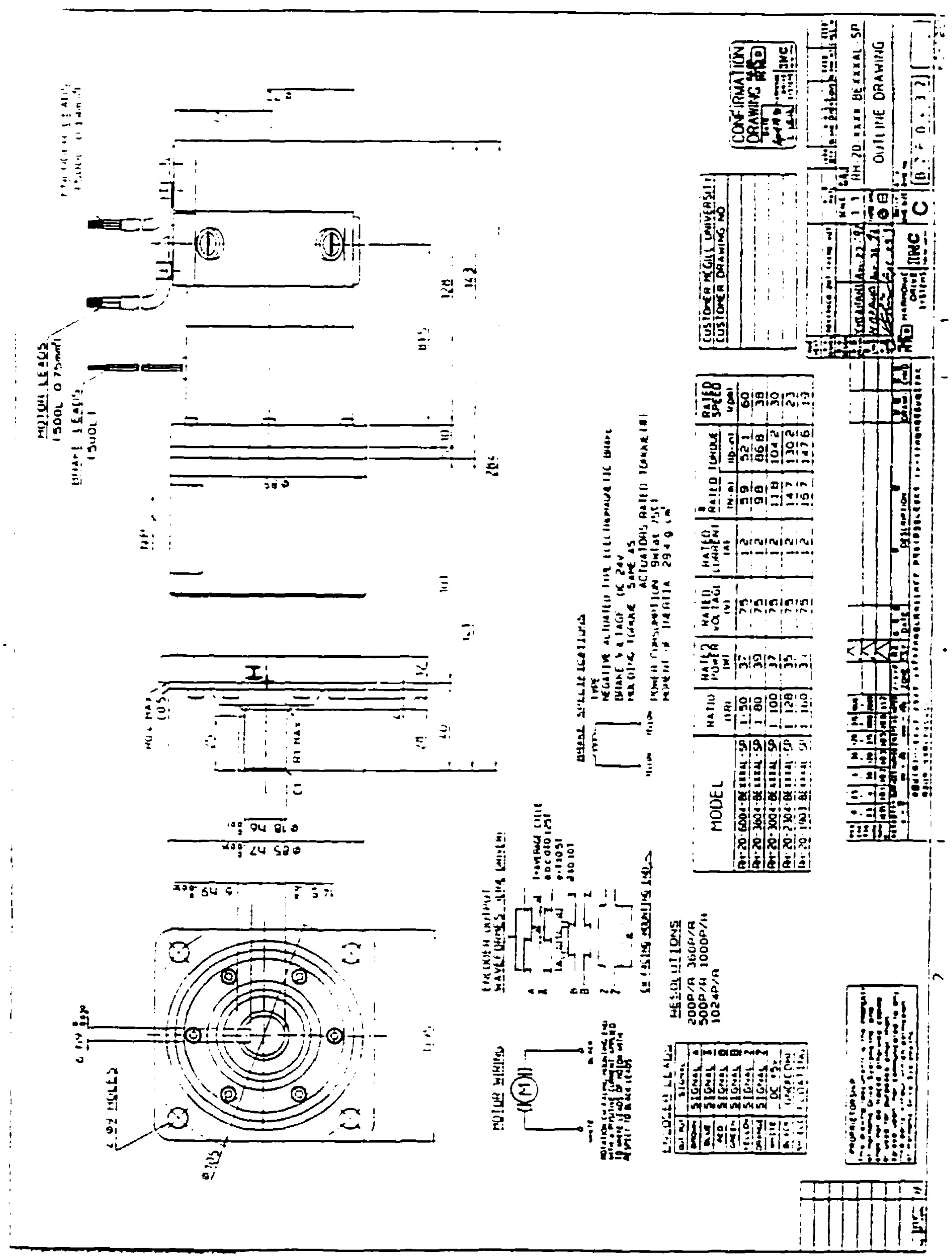

Figure E.3: Mechanical specification of Rh-20 (joint 5, and 6)

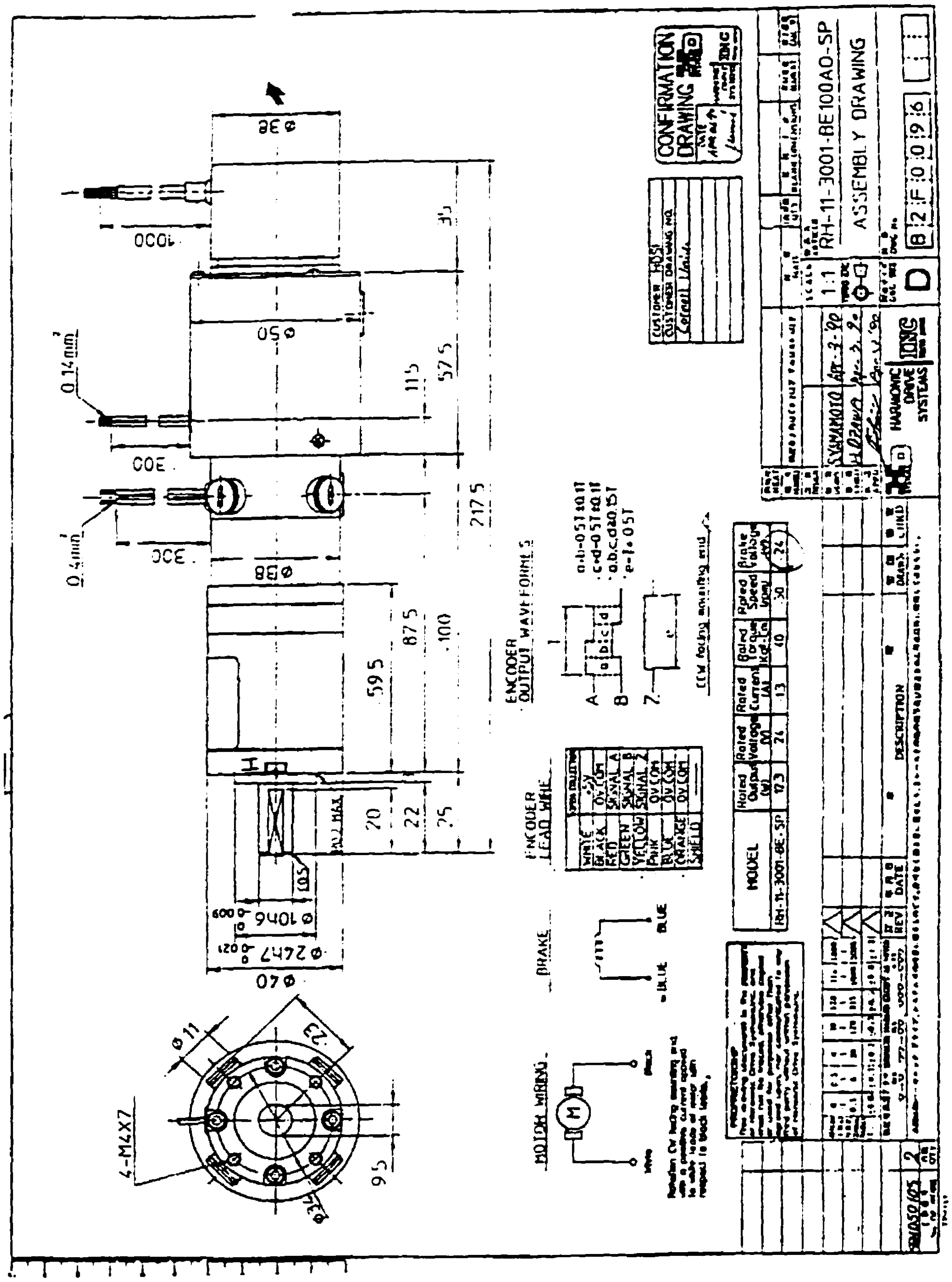

Figure E.4: Mechanical specification of Rh-14 (joint 7)

IMAGE EVALUATION TEST TARGET (QA-3)

150mm

6″

APPLIED IMAGE . Inc
1653 East Main Street
Rochester, NY 14609 USA
Phone: 716/482-0300
Fax: 716/288-5989